Tampere University

TONI PAKKALA

Assessment of the Climate Change Effects on Finnish Concrete Facades and Balconies

Tampere University Dissertations 204

Tampere University Dissertations 204

TONI PAKKALA

Assessment of the Climate Change Effects on Finnish Concrete Facades and Balconies

ACADEMIC DISSERTATION
To be presented, with the permission of
the Faculty of Built Environment
of Tampere University,
for public discussion in the auditorium RG202
of the Rakennustalo building, Korkeakoulunkatu 5, Tampere,
on 14 February 2020, at 12 o'clock.

ACADEMIC DISSERTATION
Tampere University, Faculty of Built Environment
Finland

Responsible supervisor and Custos	Adjunct Professor Jukka Lahdensivu Tampere University Finland	
Supervisor	Professor Matti Pentti Tampere University Finland	
Pre-examiners	Associate Professor Emilio Bastidas-Arteaga University of Nantes France	Ph.D. Sudip Talukdar British Columbia Institute of Technology Canada
Opponent	Professor Tore Kvande NTNU Trondheim Norway	

The originality of this thesis has been checked using the Turnitin OriginalityCheck service.

Cover design: Roihu Inc.

ISBN 978-952-03-1422-4 (print)
ISBN 978-952-03-1423-1 (pdf)
ISSN 2489-9860 (print)
ISSN 2490-0028 (pdf)
http://urn.fi/URN:ISBN:978-952-03-1423-1

PunaMusta Oy – Yliopistopaino
Tampere 2020

Abstract

Although Finnish building stock is young, a significant share of Finland's national property consists of buildings. A major part of that stock is now aged between 30 and 60 years and their outdoor facing structures are reaching or have already reached their renovation date. The value of renovation has increased steadily since the 1990s and is now surpassing the value of new construction. Thus, maintenance and safeguarding the service life of the existing building stock is recognised as having a major effect on the national wealth. At the same time, the quality of, for example, the concrete facades and balconies built that time has found to be poor, mainly because majority of them were built during the time when quality requirements were not even at the level of need of the current climate.

The goal of this research is to determine what needs to be done in the building stock to adapt to climate change. The research is limited to outdoor exposed concrete facades and balconies because of their significant role in the Finnish building stock, and because the current condition and deterioration mechanisms and their rates have been extensively studied before. However, the aim is that most of the findings can be utilised also in new construction, regardless of the construction material.

This thesis discusses the effect of climate change by two ways: its effect on the intensity of selected climatic factors and their effect on the deterioration rate of the best-known deterioration mechanisms of concrete, i.e. corrosion of reinforcement and freeze-thaw damage. The results show that climate change is going to intensify especially wind-driven rain (WDR) load, which is a significant part of almost all of the most critical deterioration mechanisms. However, the effect is highly dependent on the location and the direction of orientation of the structure. The highest deterioration rates have been shown to be in coastal areas and southern areas and in structures facing southern directions. The geographical dependence is significant because a considerable share of Finnish existing building stock is located in the coastal area or southern Finland where the climatic load is and will be the most severe. On the other hand, the deterioration rate is and will be low in Lapland and so is the share of buildings. However, results imply that even with insufficient quality, the concrete structures can have a decent service life and the structures can be effectively protected against climatic factors, for example, by sheltering. The results of this study can be used to target both the actual methods used in renovation and preventative maintenance methods.

Keywords: concrete, climate change, deterioration, freeze-thaw damage, outdoor climate, reinforcement corrosion

Preface

This research is a part of a long continuum of research projects related to durability of existing Finnish concrete facades and balconies. While the earlier research has focused on the state of those structures at present, this study looks towards the oh-so-unpredictable future. The research was completed at the Unit of Civil Engineering at Tampere University but the timeframe has been such long that even the name of the university has changed during the process, name of the department multiple times. The studies presented in this thesis started at Tampere University of Technology somewhere around 2012. However, the most important thing is that the same great people around me, both colleagues and friends, have been there for the whole time.

I consider myself very lucky because…

…I got Adjunct Professor Jukka Lahdensivu and Professor Matti Pentti as supervisors. Jukka is the greatest reason I started this long journey, believed in it and what is the most important, we have this research group full of people pulling together and supporting each other. Matti is probably the greatest reason I ended up to work as a research assistant at the department and found the joy of an academic work. I am very thankful that both of them have persistently answered all of my, sometimes silly questions to help me better understand the field.

…Associate Professor Emilio Bastidas-Arteaga and PhD Sudip Talukdar were willing to pre-examine this thesis and did it in very observant way. Their valuable comments made the final version more explicit and probably a bit easier to approach.

…D.Sc. Harry Edelman provided me a funding for a while which was a nice experiment between otherwise unfunded studies. In addition, Harry really inspired me to look outside the box.

…I have had such a great colleague and a friend as D.Sc. Arto Köliö supporting and coworking over a decade now. In addition to all of the support you have given, you also made it concrete that finishing doctoral studies is possible.

…I have worked with the great people of “Renovation and Service-life Engineering of Structures” research team. To name some of you, B.Sc. Jussa Pikkuvirta did most of my actual work when I was busy finishing this, B.Sc. Antti-Matti Lemberg helped extremely lot with the calculations, M.Sc. Petri Annila and M.Sc. Tero Marttila have been there always ready to help for over a decade and D.Sc. Kimmo Hilliaho showed a great example of persistence during his doctoral studies. Outside the group, I want to thank PhD

Mihkel Kiviste who helped a lot by sharing his experience when Arto and I took baby steps with academic writing and M.Sc. Anssi Laukkarinen who is a great example of an endlessly knowledge-thirsty researcher.

…I had a possibility to utilise the work of students who needed a good topic for their Bachelor's thesis. Some of them had great impact on this research.

…I got guidance from Finnish Meteorological Institute, especially from PhD Kimmo Ruosteenoja, whenever I needed. Without their data, this work would have not been possible.

…even though I did not have funding for the actual work for most of the time, few foundations supported the work during the process by giving me personal grants and thus, an additional push to work extra hours. I would like to give acknowledgements to Kerttu ja Jukka Vuorinen fund, Kiinko Real Estate Education Foundation, the Confederation of Finnish Construction Industries RT and Yrjö and Senja Koivunen fund.

…I have made numerous friends at the department over the unit borders, especially relating to different team sports, which have kept me in shape, both physically and mentally.

…friends have given me always something else to think about. Special thanks go to the Sauna group and the Q-group for a forgetable many nights and trips full of laughs and bad jokes over the years.

…I was born in a family where three older brothers were already old enough to look after me and never stopped to do so. My life has been almost too easy because I have always had clear footsteps to follow and if their paths sometimes led to crossroads or opposite directions, it was easy to pick the one I knew would work for me. Well well, this one led here, not bad! Additional thanks to my sisters-in-law who have always been ready to welcome the little brother for a visit.

…minulla on vanhemmat, jotka ovat aina kannustaneet väsymättä eteenpäin ja kouluttautumaan, vaikka se tarkoitti vääjäämättä sitä, että viimeinenkin toivo tilaa jatkavasta peräkammarinpojasta haihtui.

…I found something far more important from this University than any degrees, my wife. Thank you, Heidi, for all the support, understanding, warmth, love and the home you have given during this long, long process. I love you!

Tampere 13.12.2019

Toni Pakkala

Contents

Terminology

Building stock	All buildings standing at a given time
Capillarity	Property of porous material to transfer liquid water by capillary suction pressure
Carbonation	Neutralisation reaction of concrete by carbon dioxide in the surrounding air penetrating the concrete cover leaving the reinforcement susceptible to corrosion
Carbonation-induced corrosion	Corrosion initiated by carbonation of concrete cover
Climatic load	Climatic factors affecting deterioration mechanisms and rate
Corrosion	Degradation of metal due to its electrochemical dissolution in an electrolyte
Corrosion rate	The rate of metal loss due to corrosion, expressed in this study as corrosion current density [µA/cm²]
Degradation/Deterioration	A process reducing the performance level of a structure over time due to environmental influences
Freeze-thaw damage / Freeze-thaw attack	Damage that occurs when water-saturated concrete is subjected to cycles of freezing and thawing
Frost damage	Damage to concrete when it freezes during the setting process

Initiation phase	The first phase of service life in which favourable conditions for actual deterioration are developed due to, for example, climatic loads i.e. carbonation reaches reinforcement or first cracks form due to freeze-thaw cycles
Propagation phase	The second phase of service life from the start of the deterioration process to the actual deterioration affecting service life, for example loss of strength
Protective pore ratio	Share of all pores not filled with capillary water of total concrete porosity
Residential buildings	Domestic buildings intended for residential use including detached and attached houses and blocks of flats
Service-life of structure	The period of time after installation during which a structure meets or exceeds the performance requirements given to it
Thin-section analysis	Examination of the microstructure of concrete using an optical microscope. A translucent slide approx. 25 µm thick is made from a concrete core sample for the examination
Wind-driven rain	Driving rain that hits vertical surfaces due to wind

List of Symbols and Abbreviations

θ	wall orientation relative to north [°]
BES	precast concrete element system widely used in Finland since 1970s
CFD	Computational Fluid Dynamics
C_R	roughness coefficient
C_s	CO_2-consentration [kg/m³]
C_T	topography coefficient
D	hourly mean wind direction from north [°]
FMI	Finnish Meteorological Institute
FPC	freezing point crossing
I_θ	driving rain exposure index [l/m²]
I_A	airfield annual index [l/m²]
I_{WA}	wall annual index [l/m²]
IPCC	Intergovernmental Panel on Climate Change
k	carbonation coefficient [mm/ √ (years)]
k_c	execution transfer parameter
k_e	environmental function
N	number of years of available data
NDT	non-destructive testing
O	obstruction factor
r	hourly rainfall total [mm]
r_i	average annual corrosion rate during year i
$R_{NAC}^{-}1$	inverse effective carbonation resistance, dry concrete [(mm²/years)/(kg/m³)]
SB model	wind-driven rain model by Straube and Burnett
t	time [years]
t_o	time of reference [years]
t_{prop}	age when critical corrosion depth is achieved [years]
TUT	Tampere University of Technology
v	hourly mean wind speed [m/s]
w	weather exponent
W	wall factor
WDR	wind-driven rain
x	carbonation depth [mm]
x_c	carbonation penetration [mm]
x_{corr}	corrosion penetration depth [mm]

List of Publications

I. Köliö A., Pakkala T. A., Lahdensivu J., Kiviste M. 2014. Durability demands related to carbonation induced corrosion for Finnish concrete buildings in changing climate. *Engineering Structures*, 62-63 (2014). Pp. 42–52.

II. Pakkala, T. A., Köliö, A. Lahdensivu J., Kiviste M. 2014. Durability demands related to frost attack for Finnish concrete buildings in changing climate. *Building and Environment*, 82 (2014). Pp. 27–41.

III. Pakkala, T. A., Lemberg, A.-M., Lahdensivu, J., Pentti, M. 2016. Climate change effect on wind-driven rain on facades. *Nordic Concrete Research*, Publication 54 1/2016. Pp. 31–49.

IV. Pakkala, T. A., Köliö, A., Lahdensivu, J., Pentti, M. 2019. Predicted corrosion rate on outdoor exposed concrete structures. *International Journal of Building Pathology and Adaptation*, 37 (5). Pp. 679–698.

V. Pakkala, T. A., Lahdensivu, J. Huuhka, P., Kivioja, H., Lemberg, A.-M. 2019. Freeze-thaw Damage Dependence on Wind-driven Rain of Outdoor Exposed Concrete – A Case Study. *Nordic Concrete Research*, Publication no. 61 2/2019, <Accepted manuscript 27th Nov 2019>

Author's Contribution

In Article I, the author planned the research work together with all the co-authors. The research material was gathered by Jukka Lahdensivu, the literature review was prepared and written by Mihkel Kiviste, the required calculations and simulations were carried out by the correspinding author Arto Köliö and the climate change parameters were prepared by the author. The interpretation of the results was done in cooperation with all the researchers.

In Article II, the author planned the research work together with all the co-authors. The research material was gathered by Jukka Lahdensivu, the literature review was prepared and written by Mihkel Kiviste and the climate change parameters and calculations were prepared by the author who acted as the corresponding author. The interpretation of the results was done in cooperation with all the researchers.

In article III, the author planned the research work together with Jukka Lahdensivu. The literature review was prepared by the author and the calculations by Antti-Matti Lemberg and the author. The author wrote the article as the corresponding author. The co-authors commented on the manuscript.

In article IV, the author planned the research work together with Arto Köliö and Jukka Lahdensivu. The corrosion prediction model and its backgound information were provided by Arto Köliö, while the data and the calculations based on the model were done collaboratively by Arto Köliö and the author. The literature review and analysis of the results were done by the author. The co-authors commented on the manuscript.

In article V, the author planned the outline of research work with Jukka Lahdensivu and the author planned the research methods. The data collection done with consideration of condition investigation reports was carried out by Petteri Huuhka and case study calculations were done by Henna Kivioja. The climate data related calculations were done collaboratively by Antti-Matti Lemberg and the author. The literature review and analysis of the results were done by the author. The co-authors commented on the manuscript.

Article I was included in a dissertation (Köliö 2016) prior this one. Articles II-V have not been included in a dissertation before this one.

1 Introduction

The Finnish building stock is quite young compared to many other European countries, although many have gone through the same phases during the last century such as rebuilding after the World Wars and urbanisation leading people from the countryside to growth centres. The oldest buildings still standing are medieval churches made of stone and brick masonry. However, masonry was for a long time a sign of wealth, and common residential buildings were traditionally made of wooden structures such as logs walls. The oldest residental wooden structures have been subjected to many threats such as the harsh climate, conflagrations in the closed wooden city districts and urbanisation when many new apartments were needed quickly. Thus, they have been more widely replaced and rebuilt than masonry structures.

At the same time, the fairly young building stock has resulted in its comprehensive documentation (Huuhka 2016). Based on the database of Statistics Finland (2019), there were 1,523,196 buildings and free-time residences in Finland in 2017. Only 5% of them were built before 1920. When considering only residential buildings, 12% of the amount and 8% of the floor area were built before 1940. 70% of all residential buildings and 80% of their floor area have been built since 1960, see Figure 1 and Figure 2.

Balconies arrived with the concrete element building boom of the late 1960s. There are 75,000 balconies in buildings built before 1960, while the total number of balconies is 1.3 million, 1.1 million of which are in apartment building blocks. Thus, 95% of all existing balconies in Finland have been built since the 1950s. Nowadays other balcony structures, such as metal balconies, exist alongside concrete balconies but almost all balconies built between 1960–1990 were concrete balconies with precast side panels, slabs and parapets. (Riihimäki et al. 2018)

Although the stock is young, based on the biannual State of the Built Environment report (ROTI 2019) 45% of Finland's national property consists of buildings. A major part of that stock is now aged between 30 and 60 years, i.e. close to the age of refurbishment of both the envelope and interior service equipments. Based on the report, the value of the buildings stock is €500 billion of which the share of residential buildings is 64%. In 2017, the value of new construction was €13.9 billion while the value of renovation was €13 billion, of which the share of residential buildings were 58%. The value of renovation has increased steadily since the 1990s and is now surpassing the value of new

construction (Riihimäki et al. 2018). Thus, maintenance and safeguarding the service life of the existing building stock is recognised as having a major effect on the national wealth. (ROTI 2019)

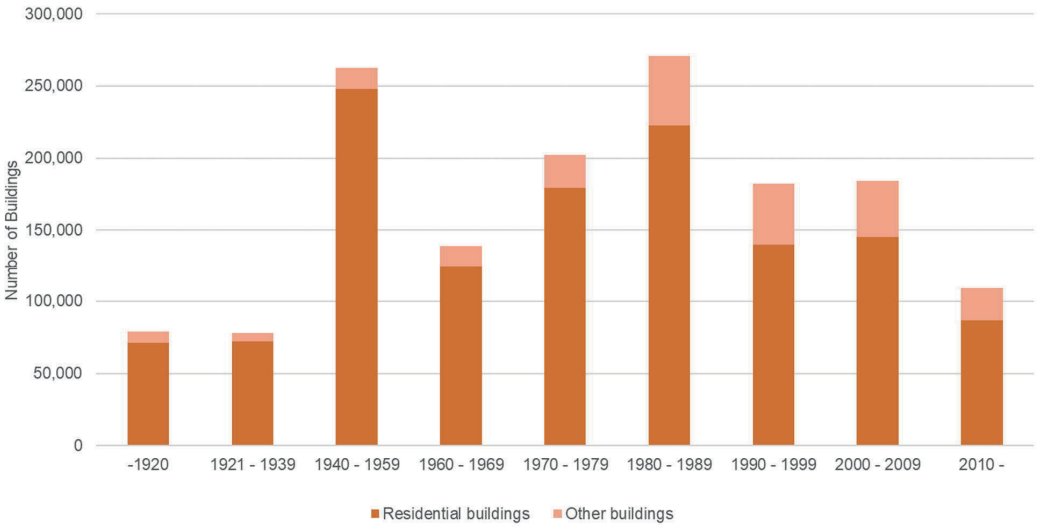

Figure 1 Number of buildings in Finland categorised by the construction year (adapted from Statistics Finland 2019). Note: the 1920s and 1930s are grouped together, and so are 1940s and 1950s.

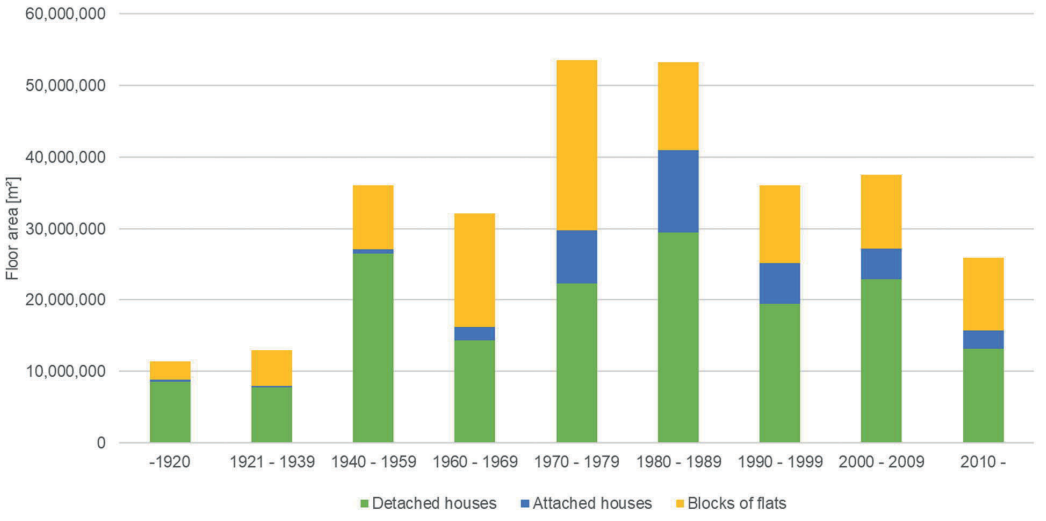

Figure 2 The floor area of residential buildings in Finland categorised by the construction year (adapted from Statistics Finland 2019). Note: the 1920s and 1930s are grouped together, and so are 1940s and 1950s.

The renovation need of residential buildings is calculated to be €9.4 billion during 2016–2025 and is expected to increase by 17% during the following ten-year period (ROTI 2019). 89% of all residential buildings are detached houses and only 5% block of flats. However, in floor area, 55% are detached houses and 33% block of flats (Statistics Finland 2019). The share of the population living in them is almost equal. Huuhka (2016) estimated in her studies that the relevance and volume of high-rise multifamily housing is increasing due to demographic changes in Finland that show a tendency of population concentration from rural areas to community centres and cities. This change is also connected to the ageing of the population. Thus, national housing policies are putting an emphasis on the population concentration.

Finland can be divided in four areas based on both the density of residential buildings and the climatic conditions: the coastal area, southern Finland, inland and Lapland (northern Finland). Although the area of Lapland is almost 30% of Finland, only 3% of the population lives there and 5% of buildings are located there. In the other three areas live 38%, 29% and 30% of all population, respectively. The same shares in floor area of residential buildings are 35%, 30% and 31%, respectively. Figure 3 shows the areas based on the boundaries of municipalities together with the shares of blocks of flats. The shares of other residential building types are shown in Appendix I. As can be seen in the Figure 3, the boundary of the coastal area is not a uniform distance from the coastline, but is based on the boundaries of municipalities, which have coastline. According to Kuismanen (2008), in Finland the warming effect of sea stretches more than 20 km inland and the strong wind zone on average 15 km. Depending on the geography, strong winds can exceed 70 km inland at most (Koistinen & Turtiainen 2006).

1.1 Finnish facades and balconies

In 2017, 1.4 million m² of facades were built on block of flats, 1.3 million m² on detached houses and 0.2 million m² on attached houses. Together they constitute 37% of all new construction. Even though the construction of small houses has decreased significantly in the past ten years, the share of wooden facades is still 35% of all facades. The second largest facade material is metal (22%), mostly due to industrial buildings, supermarkets, warehouses, etc. The average annual area of built concrete facades has remained at around 1 million m² since 2000, which makes up approx. 12% of all facades. The share of both rendering and brick wall are a bit lower, approx. 10%. (Riihimäki et al. 2018)

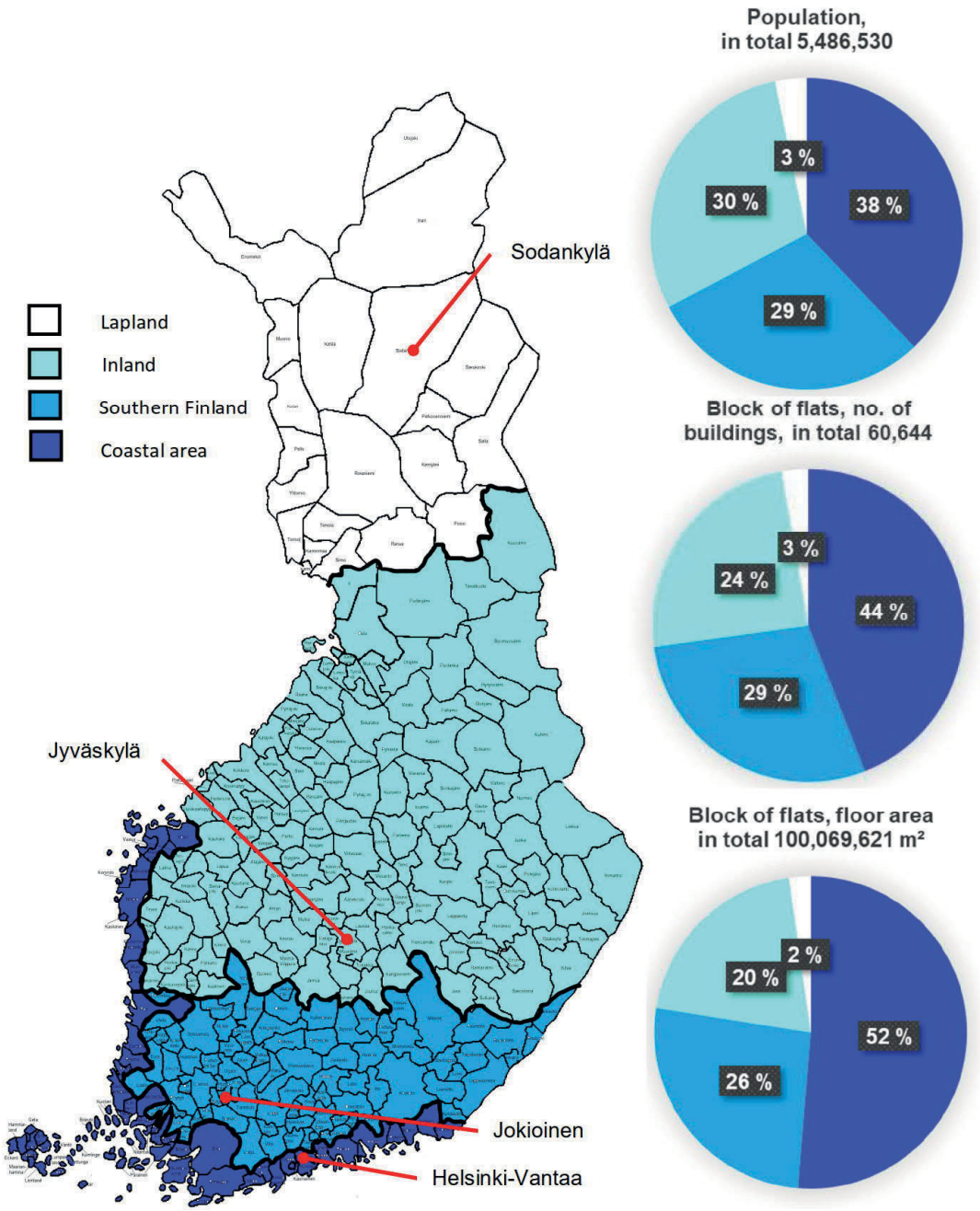

Figure 3 Finland can be divided into four main areas based on climate and concentrations of population and residential buildings (Statistics Finland 2019). The cities marked on the map are weather stations of Finnish Meteorological Institute whose data has been used in this study.

In blocks of flats, the share of concrete is 28%, brick 37%, rendering 18% and wood 6%. The share of concrete is increasing and the share of brick is decreasing significantly, having been almost 60% in 2005. The huge share of brick can be explained by brick tiles used as a surface layer for precast concrete elements. The reason is due the reporting methods used in Finland according to which only the visible surface is usually reported, so the numbers are not completely reliable. The use of solid masonry walls or cavity walls in blocks of flats is rare, so their share can be added almost fully in the share of concrete facades. (Riihimäki et al. 2018)

The calculated renovation need of facades, excluding painting and coating, is approx. 4.7 million m² and is increasing annually by 3.5–4%. The estimated actual number of renovated facades was 3.6 million m², but the annual variation is great. The share of renovation of wooden facades is 67%. The amount of renovation operations used on concrete buildings is approx. 0.6–0.8 million m² including mortar replacements and covering methods such as external thermal insulation with rendering (ETICS), rear-ventilated rainscreen facades and new concrete finishing. In 2017, the amount of painting and coating used as a maintenance or renovation method was approx. 9.6 million m² of which the share of concrete, ETICS and rear-ventilated facades was 28% (2.7 million m²) and the rest includes the painting of wooden facades.

1.2 Objectives and scope of the study

As previously stated, an enormous share of Finnish national wealth consists of the existing building stock, but a significant share of it is reaching or has already reached its renovation date. Thus, the current state and renovation strategies of the existing building stock have a major economic impact. While there is need to study how to reach eligible service life or sometimes how to extend it, the effect of climate change must also be taken into account as much as it needs to be taken into account in new construction. The goal of this research is to determine what needs to be done in the building stock to adapt to climate change.

The research is limited to outdoor exposed concrete facades and balconies because of their significant role in the Finnish building stock, and because the current condition and deterioration mechanisms and their rates have been extensively studied before. However, the aim is that most of the findings can be utilised also in new construction, regardless of the construction material.

The following questions will be addressed in the research:

- How do the different climate change scenarios affect climatic conditions critical to the degradation of concrete structures such as rain intensity, wind strength, wind direction and freeze-thaw cycles in different areas of Finland?

- How does climate change affect the progress of the main deterioration mechanisms?

- How is climate change affecting different parts of buildings and structural elements, i.e. which parts are most vulnerable and need special attention?
- Is there a need for requirements to be set or defined for renovation or new structural solutions when climate change is taken into account?

The articles constituting this dissertation can be divided in two sections. Articles I, II and IV present modelling-based predictions of how the best-known deterioration mechanisms in outdoor exposed Finnish concrete structures will progress in the future climate. Articles III and V focus on WDR load as a best-known factor affecting the outdoor exposed durability of concrete. More precisely, Article III shows how the WDR load will change in the future climate. Article V concludes with the connection of WDR with the actual freeze-thaw deterioration of concrete.

2 Effect of climate exposure on concrete facades and balconies

2.1 Typical structures

Finnish concrete facade and balcony structures have principally been precast concrete element structures since the late 1960s. Industrial growth, urbanisation and thus the rapid need for new apartments in the growth cities led to the development of Concrete Element System (BES) that was introduced in 1970. (SBK 1970). Before BES, precast concrete elements were increasingly being used, but were often manufactured on-site. After the development of BES, the manufacture of concrete elements became concentrated in factories. Since then, precast concrete elements have dominated structural elements in the construction of blocks of flats. The system defines both inner and envelope structures. For structures facing the outdoor climate, it defines facade elements and balcony slabs, parapets and side panels. In addition to the details of an element, the system has standardised floor height etc.

The durability-related properties of BES elements have changed as knowledge and experience of them have increased. Durability-wise, the most important properties are concrete grade, the cover depth of the reinforcement and freeze-thaw durability properties. The changes in requirements for durability properties since 1965 are shown in Table 1 as they have been presented in Finnish Concrete Codes.

Durability properties were not extensively taken into account in the guidelines or codes until the mid-1970s when the temperatures of heat treatment were restricted followed by the recommendation to use air-entrainment to produce freeze-thaw durable concrete and increase concrete cover. Since the 1990s, the improvement in concrete grade has enhanced durability properties, due to denser and better-quality concrete. However, in the mid-1990s it was also recognised that a higher grade

than C32/40 can expose the concrete surface to cracking, which may reduce durability properties. (Lahdensivu 2014)

Table 1 Development of requirements related to durability properties presented in Finnish Concrete Codes. (Lahdensivu 2014)

Period	Concrete grade/cube strength [MPa]	Minimum concrete cover of an outdoor exposed structure [mm]	Freeze-thaw durability (minimum requirement)
1965 – 1977	C20/25	20	-
1978 – 1979	C20/25	25	Protective pore ratio 0.15 (recommendation)
1980 – 1989	C20/25	25	Protective pore ratio 0.15
1990 – 1992	C25/30	25	Protective pore ratio 0.20
1993 – 2003	C32/40	25	Protective pore ratio 0.20
2004 – present	C32/40	25	Spacing factor $\leqslant$ 0.27

The typical structures and location of the reinforcements of a typical concrete facade element and balcony structures are shown in Figure 4 and Figure 5. The surface of balcony structures has often been painted to protect it from climatic loads, although a plain concrete surface has also been widely used. In facades, a wide variety of different surface treatments have been used, mostly for aesthetical reasons. Based on Lahdensivu (2012), the most popular surface layers or finishings in buildings built between 1965–1995 have been exposed aggregate, brushed painted, painted plain concrete, uncoated plain concrete, ceramic tile, brick tile and white concrete. The most popular until the 1980s were the three first-mentioned, while brick tile and white concrete have been preferred since the 1980s.

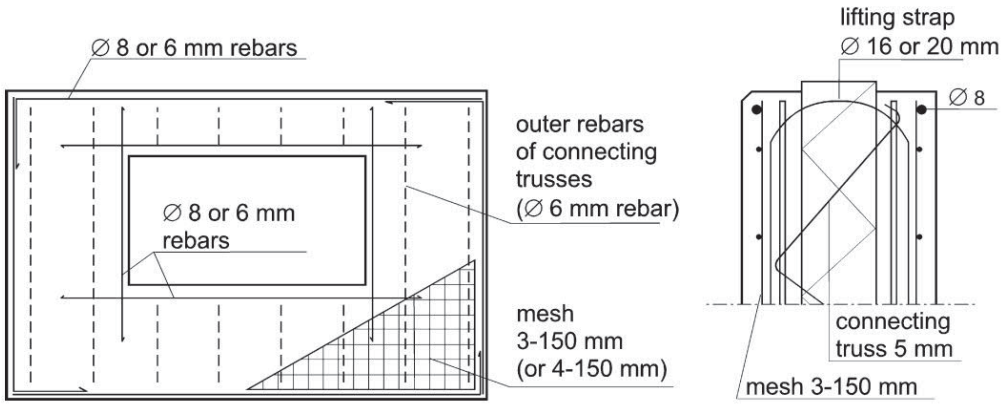

Figure 4 Typical facade precast element panel. (Pentti et al. 1998)

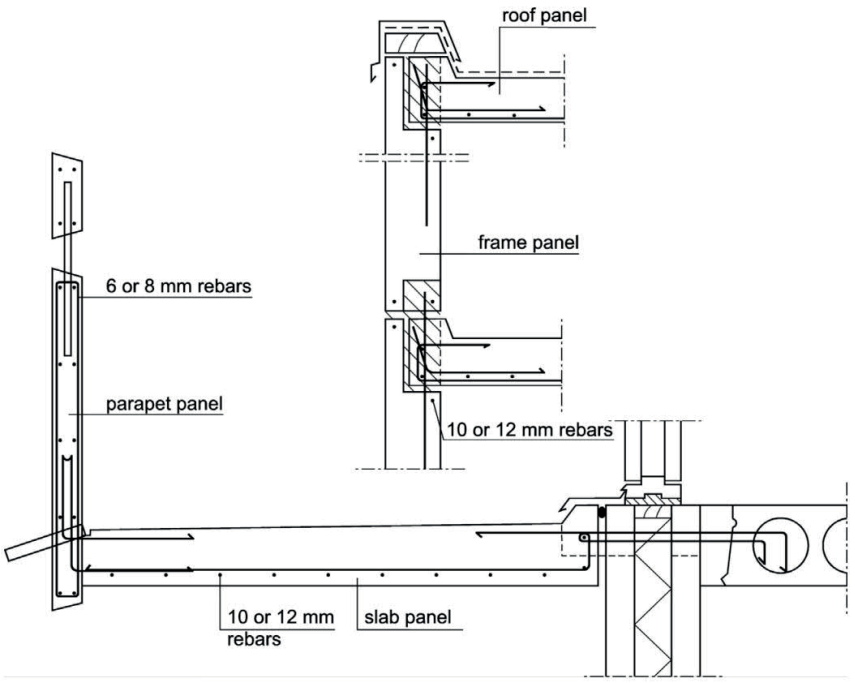

Figure 5 Cross-sections of typical precast balcony elements and their joints to the building frame. (Pentti 1994)

2.2 Degradation of concrete

2.2.1 Main causes of degradation

The degradation of concrete structures is caused by the simultaneous influence of environmental, structural and material factors. Concrete structures exposed to the Nordic outdoor climate are subject to several parallel degradation mechanisms, whose progress depends on many factors related to the structure in question, type of exposure and materials. However, in addition to harsh environmental stress, the occurrence of degradation requires the inadequate performance of structures and poor durability properties of materials. In the absence of any of them, there will be no damage to the concrete structure. When all of them are present, degradation eventually results in cracking or spalling of concrete that might reduce the bearing capacity or bonding reliability of the structures. The structures and material properties can be influenced during the design and building processes. To achieve a durable result, both are controlled by the guidelines and requirements in force, but the environmental load is a variable factor, although it can also be controlled by sheltering, for example.

Harsh climate conditions increase the requirements for durable materials. The main reasons for facade and balcony degradation in the Finnish climate are the freeze-thaw damage of concrete and corrosion of reinforcements induced by carbonation of the surrounding concrete. (Pentti et al. 1998, Lahdensivu 2012). The presence of chlorides in facade structures is very rare (Lahdensivu 2012). A common denominator in every mechanism is water in varying forms. It can either work as a passage for harmful substances, such as chlorides, cause damage by phase changes (freeze-thaw), increase the electrical conductivity of reinforcements or cause dissolution of substances in concrete (Nilsson 2003).

2.2.2 Freeze-thaw attack

Freeze-thaw attack due to a high moisture load is a common reason for the deterioration of concrete structures in the Nordic outdoor climate. Freeze-thaw attack needs free water in pore structures to occur. When water freezes, it expands by approx. 9% creating hydraulic pressure in the pore structure, which can lead to internal damage. To prevent the damage, there must be enough air-filled pores in the pore system through which the overpressure can escape.

Kuosa & Vesikari (2000) presented that there are more than 15 different theories or explanations for freeze-thaw attack on porous materials, which indicates that freeze-thaw attack is a complex process. Most of them complement each other and especially the idea of hydraulic pressure as the main reason for the cracking. Some of the best-known theories are shown in Table 2.

.

Table 2. Some of the best-known theories for freeze-thaw damage of concrete.

Theory	Content
Hydraulic pressure (Powers 1949)	Freezing water expands creating hydraulic pressure within the pore structure. The unfrozen water is forced out of the pore causing localised internal tensions in the material, which may result in cracking.
Volume changes in microscopic ice crystals (Powers & Helmuth 1953)	Complements the hydraulic pressure theory. During the freezing process, small ice crystals grow in capillary pores. The growth of the crystals causes a pressure in the pore structure, which may result in cracking.
Saturation pressure of supercooled water (Litvan 1972)	The pore water does not freeze immediately as the temperature drops under 0 °C. The freezing begins in bigger capillary pores while water in the smallest gel pores starts to freeze under -20 °C. Thus, the unfrozen water is supercooled and its saturation pressure is higher than that of ice, which causes drying of the paste. Cracking may occur, for example, when the rate of freezing is too high.
Critical degree of water saturation (Fagerlund 1977)	Above a critical degree of water saturation, porous and brittle material may suffer damage while freezing. If the actual water saturation is below the critical level, no damage can occur.
Osmotic pressure (Pigeon & Pleau 1995)	Complements the hydraulic pressure and ice crystals theories by taking into account the migration of dissolved chemicals (e.g. Na_2O, K_2O) in pore water. The dissolved chemicals lower the freezing temperature of pore water and increase the concentration of salts in the unfrozen water. The concentration difference between the pore water solutions causes osmotic pressure in the structure, which may result in cracking.
Hydraulic pressure of ice expansion (Penttala 1998)	When temperature decreases, the ice in the pore system shrinks, allowing supercooled pore water to migrate through capillaries to empty spaces where it freezes rapidly. Thereafter, when the temperature increases, the increased amount of ice needs more space than before, which causes pressure in the structure. The pressure is dependent on the thermal coefficient differences between concrete and ice

According to Litvan (1972), the freezing point of pore water depends on the size of the pore. Pigeon & Pleau (1995) presented that, in capillary pores with a radius of more than 0.02 µm, the freezing point of the pore water is -1 – -3 °C. In the smallest capillary pores (radius 0.005 µm), the freezing point is -15 °C. The gel pores are even smaller and, in them, the freezing point is -20 – -40 °C. The range of different size pores is substantial, so it is impossible to give a specific temperature where the freezing of water in capillary pores occurs. However, it is certain that in the capillary pore system, the freezing does not happen as soon as the temperature drops below 0 °C.

The fib Model Code for Service Life Design (International Federation for Structural Concrete 2006) proposes a design model for the service life of concrete structures based on the theory of critical degree of saturation (Fagerlund 1977, Fagerlund 2004). The basis of the model is that there is a critical degree of saturation specific to each concrete type above which concrete is likely to be damaged by freezing. If the actual degree of saturation stays below the critical level, the concrete is not harmed by freeze-thaw cycles. According to this model, service life ends when this critical degree of saturation is achieved, but it does not specify whether a freezing event occurs at the same time and

therefore has to be considered to be on the safe side. The model requires special laboratory tests to be conducted on each specific concrete type in order to be able to calculate the critical degree of saturation, so the application of the model is limited in practice.

The initial freeze-thaw damage occurs as cracking. In outdoor exposed structures, the cracking usually starts from the surface. When the cracking has occurred, more water, dirt and salts can penetrate the surface leading to more cracks going deeper into the structure. However, the first cracks are usually so small, width less than 0.01 mm, that they need a microscope to be found. Severe cracking can be detected in most of the cases using NDT methods, such as visually and by hammering. (Lahdensivu 2013)

Far-advanced freeze-thaw damage leads to a reduction in the strength of concrete, loss of adhesion or crazing or chipping of the surface due to internal expansion. Disintegration of concrete also accelerates the carbonation of concrete and makes it easier for chlorides to penetrate it, which exposes the reinforcement of concrete to corrosion. (Lahdensivu 2012)

Freeze-thaw durability can be increased by improving the concrete grade or by air-entrainment. The former is based on more compact thus less porous concrete. The latter is based on producing protective pores by air-entrainment admixtures. The efficiency of air-entrainment is dependent of a sufficient amount and even distribution of the pores. The most reliable way to estimate the success of air-entrainment is to take a sample and make a thin-section analysis of it based on a standard ASTM C856-18A (2018). In the analysis, the amount and distribution are detected by microscope. The results are shown as a spacing factor, which is the average of half the distance between protective pores. The other less precise method is to study the protective pore ratio, which is the volumetric ratio of protective pores compared to all the pores, without taking a stand on the distribution or size of the protective pores. The method is based on the withdrawn standard SFS 4475 (1988), however it was used until 2004 as the main method to estimate the success of air-entrainment. Nowadays it is used as a supporting method for thin-section analysis.

Pigeon & Pleau (1995) presented that concrete with a spacing factor <0.20 mm can generally be considered freeze-thaw-resistant, but they and a few other studies (e.g. Pigeon et al. 1986, Aïtcin & Mindess 2011) have shown that concrete with ordinary Portland cement is freeze-thaw-resistant if the spacing factor is less than 0.50 mm. Lahdensivu (2012) showed that concrete with a protective pore ratio of 0.20 is considered to be freeze-thaw-resistant in Finnish outdoor conditions, but a ratio of >0.10 has been shown to give some protection against freeze-thaw attack. Koskiahde (2004) presented that a protective pore ratio of 0.20 corresponds to a spacing factor of 0.25 if the pores are quite evenly distributed.

Shang and Song (2008) studied the behaviour of air-entrained concrete under compression with constant confined stress after freeze-thaw cycles. The constant confined stress did not change the failure mode, which was tensile splitting, regardless of the number of freeze-thaw cycles. In addition,

the magnitude of the confined stress used in the tests did not significantly affect the loss of compressive strength. Regardless of the confined stress, the compressive strength decreased 3.7–9.5% after 100 freeze-thaw cycles and by as much as 40.9–49.6% after 400 cycles. In triaxial tensile-compressive-compressive (T-C-C) tests, Shang (2013) discovered that ultimate strength of air-entrained concrete decreased by 8.9–20.3% after 100 cycles and 44.8–59.7% after 400 cycles depending on the triaxial stress levels used. The experimental results showed that the dynamic modulus of elasticity and strength decreased as the freeze-thaw cycle was repeated.

Shang et al. (2014) have also studied the effect of fast freeze-thaw cycles on the mechanical properties air-entrained concrete of different strength grades. The study included testing the effect of number of fast freeze-thaw cycles on the compressive and tensile strengths of wet air-entrained concrete of five different strength grades (C20, C25, C30, C40, C50). The results were also compared to plain concrete with no air-entrainment. The study showed that the strength grade has a major effect on the strength loss of the concrete, especially after 50 fast freeze-thaw cycles. While the C20 concrete had lost 50% of its compressive strength after 300 cycles, the C40 and C50 had lost approximately 10%. The non-air-entrained concrete (C30) degraded before 50 cycles. The study also showed that the tensile and compressive strengths decreased by the same rate during the freeze-thaw cycling. It should be noted that the freezing rate is usually higher than in nature where it is typically 0.5–2 C/h (Pigeon & Pleau 1995).

In addition, Penttala & Al-Neshawy (2002) and Zandi Hanjari et al. (2011) showed the significant influence of freeze-thaw cycles on the compressive strength of wet concrete and the even greater influence on the modulus of elasticity and compressive strain at peak stress. Reduced tensile strength and increased fracture energy were also measured.

The degree of freeze-thaw damage may vary in different parts of facades and balconies depending, for instance, on the moisture load and variation in material properties and thickness of the concrete structure. Freeze-thaw damage due to a high local moisture load may affect only a very limited area. On the other hand, the improper surface treatment of non-freeze-thaw-resistant concrete may result in deterioration across most of the side panel surface and corners of buildings.

2.2.3 Corrosion of reinforcement

The corrosion of steel reinforcement in concrete is an electrochemical phenomenon where cathodic and anodic areas are formed on the steel surface and the pore water of concrete acts as an electrolyte. (Page 1988). The sizes of the cathodic and anodic areas thus play a key role in the corrosion rate.

The pore water of fresh concrete is highly alkaline: its pH is usually over 13 (Page 1988). The high alkalinity forms a dense oxide layer on a steel surface, which efficiently protects the embedded steel

from corrosion. However, if carbon dioxide (CO_2) penetrates the concrete surface, it reacts with calcium hydroxide ($Ca(OH)_2$) forming calcium carbonate ($CaCO_3$), which causes a reduction of alkalinity lowering the pH of the pore water. This reaction is called carbonation. Corrosion due to carbonation is common over steel surfaces with an evenly spaced cathode in anode areas. Chlorides, instead, can form a small but very concentrated anode area on steel, thus leading to high corrosion current in that area and forming pitting corrosion. (Schießl 1988). Both carbonation and chlorides propagate as a front from the surface, decelerating in time. However, the local rate of the front in both mechanisms can be significantly higher, for example because of the cracking. In regard to concrete facades in a non-marine environment, the corrosion of reinforcements is mainly initiated by carbonation (Lahdensivu 2012). Parrott (1996) and Jones et al. (2000) stated that 2/3 of all structural concrete is exposed to environmental conditions that favour carbonation-induced corrosion.

Because concrete protects steel from corrosion as a protective layer for the reinforcement, corrosion does not initiate immediately. This can be taken into account by depicting reinforcement corrosion as a process consisting of two or more consecutive phases as shown in Figure 6 produced by Köliö (2016), referring to studies by Tuutti (1982), Liu & Wayers (1998) and Li (2004). The initiation phase of carbonation-induced corrosion is well-known (Tuutti 1982, Monteiro et al. 2012, Lahdensivu 2012), but information on the propagation phase is more limited (Köliö 2016).

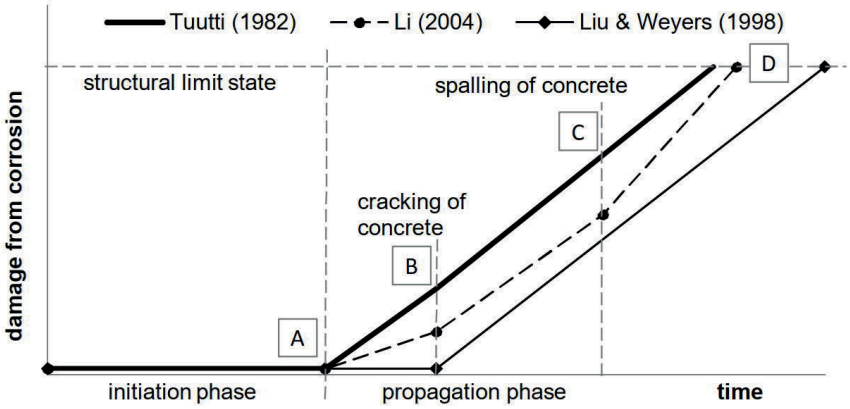

Figure 6 Models for reinforcement corrosion utilising the principle of initiation and propagation. Reprinted from Köliö, Propagation of Carbonation-Induced Reinforcement Corrosion in Existing Concrete Facades Exposed to the Finnish Climate (2016), with permission of the author.

The factors that can limit carbonation, i.e. the initiation phase, are related to the actual properties of the concrete (e.g. the thickness of the concrete cover, high cement content, the pore structure and the water-cement ratio) and external environmental properties (e.g. the amount of atmospheric CO_2 and the sources of moisture). (Broomfield 2007, Parrott 1987)

Point A in Figure 6 is important in the sense of the service life of concrete structures. At that point, carbonation has reached the depth of the steel and the corrosion reaction can start. It is also often referred to as the end of the service life of the structure, although no actual damage has yet occurred. If the propagation phase could also be taken into account, the service life could be effectively utilised (Köliö 2016). The other possibilities for the endpoint of service life calculations are cracking (point B) and spalling (point C) of the concrete and critical deflection or collapse (point D). (Li 2004, Köliö 2016)

Several parameters have been found to affect carbonation rate including material and structural properties and environmental factors. In their studies, Guiglia & Taliano (2013) found that both the environmental factors and the quality of the concrete play key roles in the carbonation process. The latter is explained by the inverse effective carbonation resistance of concrete on the evolution of the carbonation depth in time. Models for the active corrosion of reinforcing steel have been actively developed for chloride-induced corrosion, but models given for carbonation-induced corrosion cases are rarer (Köliö et al. 2014). The reason for this has been assumed to be the easy avoidance of carbonation problems in new construction by increasing concrete cover or concrete quality (Raupach 2006).

The greatest factors affecting corrosion rate are the cover depth, diameter of reinforcement, temperature, oxygen availability and moisture content of concrete (Ahmad 2003). Based on the actual corrosion rate measurements on site, Mattila (2003) presented that the number of rain events correlates noticeably with corrosion rate in Finland. Studies (Tuutti 1982, Andrade & Castillo 2003) have also indicated that drying and wetting cycles have a major effect on corrosion rate. Köliö et al. (2017) concluded that the scatter in the active corrosion rate in outdoor concrete structures could be explained by on-site weather parameters, especially by WDR. In addition, Köliö (2016) presented that, if using cracking as a limiting factor, the service life of structures sheltered from direct rain, such as balcony slab soffits, can be extended by of decades. At the same time, in the cases of the most severe climate loads, especially high amount of WDR and relatively high temperatures, outdoor exposed facades and balcony structures can add 1–6 years to service life.

2.2.4 Other mechanisms causing degradation of concrete

2.2.4.1 Alkali-aggregate reaction

Alkali-aggregate reaction (AAR) is a chemical reaction between the alkali hydroxides in cement and the reactive components in the aggregate particles. The reaction is expansive and a gel reaction product is formed during the reaction. The cracking caused by alkali-aggregate reaction is uneven and thick. The cracking resembles that caused by freeze-thaw attack, which is why they can be confused with each other. The reaction requires three factors to occur: reactive aggregate, high alkalinity and sufficient moisture. Usually it is detected in structures facing high moisture load such as dams and bridges. (Neville 1995)

Since the previous decade, observations of AAR in Finland have been rare in any structures. However, based on the latest research (Lahdensivu et al. 2018) a form of alkali-silica reaction (ASR) has been detected in bridges, facades, balconies and swimming pools. ASR findings have been made in structures all around Finland. It has been shown, that the same types of aggregates are used in Finnish concrete structures as in Sweden, for example, where problems have appeared more extensively. The reasons for relatively slow deterioration are thought to be a relatively steady aggregate and cold climate, which can decelerate the reaction. Although ASR observations in buildings are still very rare, the latest findings refer to the possibility of an increasing amount of ASR damage to structures, which have potentially reactive aggregate and high ambient humidity conditions. (Lahdensivu et al. 2018)

2.2.4.2 Secondary void filling

High moisture stress can expose concrete to secondary void filling. Usually the filling is caused by late ettringite reaction where ettringite mineral crystallises on the walls of air-filled pores. Although, the forming can cause cracking, the harm for concrete structures is more related to freeze-thaw durability while it reduces the volume of the pores. According to Lahdensivu (2012), some degree of secondary void filling is common in both facades and balconies, but is rarely related to any deterioration.

2.3 Observed degradation

The state of existing precast concrete element buildings in Finland is relatively well-known, mainly because of the extensive systematic condition investigation methods. The methods were developed during the late 1980s and early 1990s. A condition investigation usually follows a guideline, which was first published in 1997 and has since been updated several times. The latest version was published in 2019 (Concrete Association of Finland 2019). Lahdensivu et al. (2013) have presented the content of a condition investigation. Usually it includes both the NDT methods (familiarisation with the original plans, visual inspection, hammering, cover depth measuring) and the destructive methods such as drilling concrete core samples. The core samples are investigated more precisely in a laboratory while a portion of the samples is subjected to thin-section analysis and others to, for example, protective pore, tensile strength and carbonation depth measurements.

In the Repair Strategies of Concrete Facades project (BeKo) conducted at Tampere University of Technology (TUT) 2006–2009 (Lahdensivu et al. 2010), an extensive condition investigation database was gathered based on condition investigation reports of 947 concrete buildings built in 1960–1996. Based on the database, Lahdensivu (2012) analysed the deterioration rate of concrete structures in the current climate. The studies showed that the concrete used did not meet the require-

ments in terms of quality. Together with the inadequate requirements until the late 1980s, the deterioration potential of the studied structures is significant. The two major issues have been the cover depth of reinforcement and freeze-thaw durability of the concrete.

2.3.1 Freeze-thaw damage

Freeze-thaw damage can be detected by NDT methods (visually or by hammering) or from drilled cores by tensile strength tests, examining the protective pore ratio or thin-section analysis. The most accurate method is thin-section analysis where not only the number of protective pores can be detected but also the distribution and spacing of the pores together with the actual cracking of concrete. Protective pore ratio is often an adequate method to supplement thin-section analysis, although it gives only the ratio of protective pores compared to total pore volume. Hammering of concrete prevails the dislocation of concrete, i.e. far-advanced damage. Far-advanced freeze-thaw damage, e.g. a netlike cracking or bending of an element, can be seen visually. The latter two are used to direct the sampling, thus all of the methods are used in parallel during a systematic condition investigation. (Lahdensivu et al. 2013)

A protective pore ratio of 0.20 is shown to give effective protection against freeze-thaw damage, a ratio of 0.10 some protection, and a ratio below 0.10 can be considered to make concrete non-freeze-thaw-resistant in the Finnish outdoor climate. The protective pore ratios measured from the concrete core samples have shown that balcony structures in particular lack air-entrainment and are not thus considered to be freeze-thaw-durable in moist conditions, see Figure 7. However, as mentioned in Table 1, air-entrainment was not a requirement at all until the late 1970s. It explains the better protective pore ratio of, for example, brick panel-clad and white concrete compared to exposed aggregate samples, while the former has become more popular since the 1980s. However, if only the samples collected from buildings built after 1988 are studied, the share of $\geqslant 0.20$ protective pore ratios is still less than 50% in both facade panels and balcony side panels. The observations made from thin-section analyses are similar corresponding. (Lahdensivu 2012)

Both visual and the laboratory freeze-thaw damage observations have corresponded to the measured success of air-entrainment. Based on visual observations, 46% of exposed aggregate facades sustained local and 16% widespread damage. In balcony structures, the shares have been 22% and 6%, respectively. The highest shares have been found in side panels. The surfaces with some protection against the absorption of rainwater, such as painted facade and balcony structures and cladded surfaces, had the lowest shares of observed freeze-thaw damage. In addition, white concrete had low observed damage, which is mostly explained by the young age of the buildings at the time of investigation. The share of observed damage by thin-section analyses or tensile strength tests correlates with the visual observations, although the shares are lower. This can be explained by the methodology of the investigations because the practice is not to drill concrete cores from the areas where the damage can be detected already by NDT methods. (Lahdensivu et al. 2013)

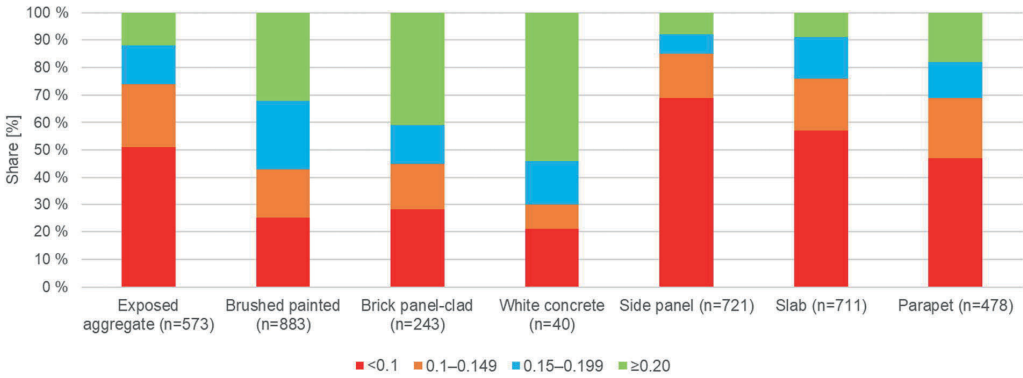

Figure 7 The share of protective pore ratio from drilled concrete cores (reproduced from Lahdensivu, 2012 with the permission of the author).

Table 3 Number of freeze-thaw cycles needed for incipient and frequent frost damage to start revealed by thin-section analyses of exposed aggregate concrete samples of insufficient air-entrainment (protective pore ratio ⩽ 0.10) at different temperatures when rain or sleet has fallen for a maximum of three days before freezing (Lahdensivu 2012)

	Coastal area [number of freeze-thaw cycles]		Inland [number of freeze-thaw cycles]	
Limit temperature	t ⩽ -5 °C	t ⩽ -10 °C	t ⩽ -5 °C	t ⩽ -10 °C
Incipient freeze-thaw damage	307	140	388	189
Frequent freeze-thaw damage	320	146	400	200

Lahdensivu (2012) also calculated the number of freeze-thaw cycles up to three days after rain or sleet needed for incipient or frequent freeze-thaw damage to occur in thin-section analysis, see Table 3. The numbers were calculated by singling out each case where incipient freeze-thaw damage was detected in condition investigations and calculating the number of freeze-thaw cycles after a rain event from the climate data of the nearest weather station the FMI had prepared for the study. The results indicate strongly that the rate of freeze-thaw attack is significantly faster in the coastal area. In that area, 307 cycles correspond to approx. 26 years and in inland, 388 cycles to approx. 37 years in the present climate. When the incipient freeze-thaw damage is detected, the time for damage to improve from incipient to frequent is short in both locations corresponding to approx. one year. The

study also showed that concrete samples with sufficient air-entrainment, i.e. a protective pore ratio of > 0.20, did not show signs of freeze-thaw damage, if the structure had undergone 500 freeze-thaw cycles in a real outdoor environment.

2.3.2 Corrosion damage

The cover depths of mesh and edge bars in facade panels have failed to meet the requirements set at the time they were built. As shown in Table 1, the requirement for a cover depth of at least 20 mm has been in force since 1965 and 25 mm since 1977. According to records, more than 85% of the cover meter based records have reached 20 mm only by an exposed aggregate surface (edge bars and mesh), brushed painted surface (edge bars and mesh), brick panel-cladding (edge bars) and white concrete surface (mesh). However, the share of very small cover depths, under 10 mm, is quite low for all facade panel surfaces, see Table 4. (Lahdensivu 2012)

The cover depths measured from balcony structures have been less adequate than in facades. Almost 25% of cover depths measured by cover meter from side panels and slab soffits and approx. 18% of outer surface of parapets do not exceed 20 mm. In addition, the amount of cover depths under 10 mm is higher than in facades. The balcony structures are often load-bearing, i.e. the reinforcement corrosion can affect the bearing capacity of the structures, while in facades the corrosion of steel has more of an aesthetic effect and can accelerate other deterioration mechanisms due to cracking. (Lahdensivu 2012). In addition, the diameter of reinforcement bars is usually smaller in facade panels than in balcony side panels and slabs, see Figure 4 and Figure 5. Studies (Köliö et al. 2015, Hunkeler & Lammar 2012) have shown that the risk of cracking is elevated when the ratio of cover depth to diameter is below approx. 1.5.

The carbonation rate in existing concrete facades and balconies has varied significantly depending on the surface material or finishing, see Table 4 and Figure 8. Instead, the considerable variability of the rate at any surface or finishing is related to different environmental properties and variability of the material properties (Lahdensivu 2012). The rate, called as a carbonation coefficient has been calculated from the concrete core samples by measuring the carbonation depth and the age of the building at the time of the investigation. Carbonation coefficient is described more in detail in section 4.2.3.1. Facades with a brushed concrete surface showed fast carbonation whereas facades with clinker-clad or brick tiles carbonated very slowly. Differences were also observed in balcony structures where the surface treatment and sheltered location caused fast carbonation in the soffit surfaces of balcony slabs compared to other balcony parts. The carbonation coefficient determined from these facade and balcony surfaces showed high standard deviation in a large set of data consisting of 3,919 sample cores due to scatter in material and environmental factors. As mentioned before, carbonation rate has a significant correlation with the surface treatment and porosity of the surface. Thus, it is slower with clinker-clad where the CO_2 can penetrate only through the joints, and with brick panel-clad where the water-cement ratio is lower in the interface. The very slow carbonation of white concrete is explained by its higher concrete grade. The highest carbonation rate was with

brushed and floated panels, whose surfaces are treated while fresh, i.e. the porosity in the surface is high. (Lahdensivu 2012)

Table 4 The share of cover depths and the carbonation coefficient of different facade surfaces and balcony structures (Lahdensivu, 2012).

Structure		Share by cover depth [%]					Carbonation coefficient, k [mm/a^{0,5}]		
		0…4 mm	5…9 mm	10…14 mm	15…19 mm	No.	Av.	Std. dev.	No.
Facade (edge bars)	Exposed aggregate	0.00	0.34	1.14	5.62	21,167	1.96	1.28	849
	Brushed painted	0.01	1.1	2.55	8.17	36,154	2.71	1.23	1,285
	Brick panel-clad	0.02	3.78	4.32	3.31	9,759	1.47	2.20	427
	White concrete	0.00	0.00	1.61	15.28	2,193	0.61	0.92	58
Balcony	Side panel (outer surf.)	0.06	3.84	5.47	15.10	32,540	2.61	1.52	901
	Slab (soffit)	0.04	3.69	5.65	14.41	42,628	3.08	1.40	884
	Parapet (outer surf.)	0.01	1.9	4.12	11.49	26,636	2.06	1.45	719

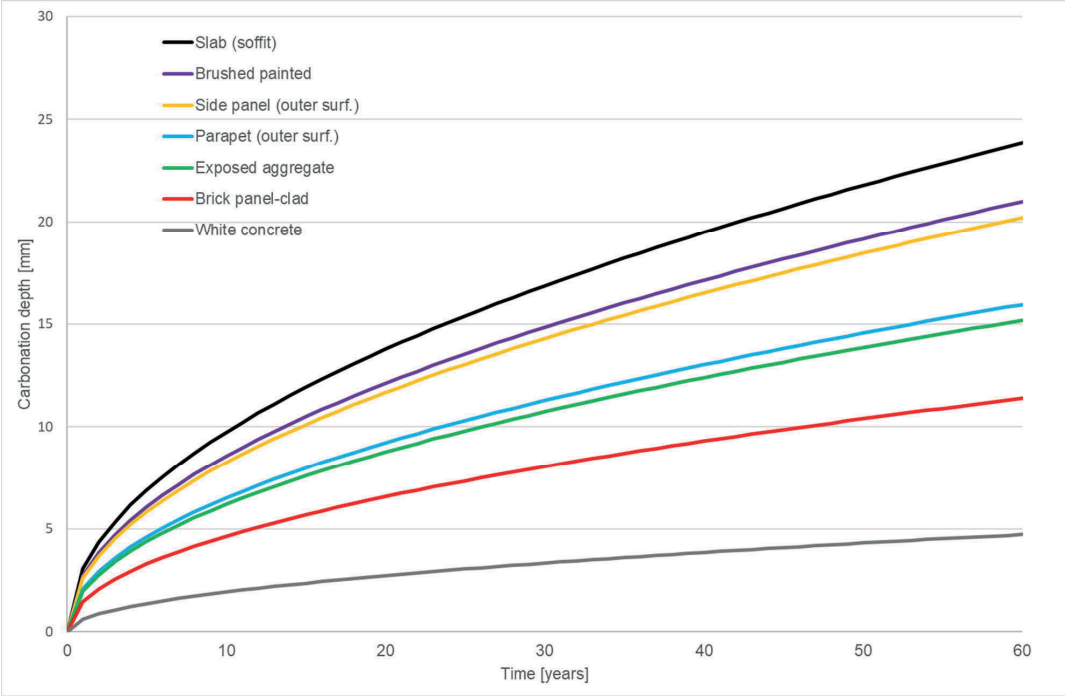

Figure 8 Average carbonation depth of concrete according to surface finishing or structure (reproduced from Lahdensivu, 2012 by the permission of the author).

Visual corrosion damage was detected in 59% of the facades but only in 6% it was widespread. The visual observations correlate with the combination of high carbonation rate, small cover depth and high capillary porosity, so the most extensive corrosion damage in facades was observed in brushed painted, painted plain and exposed aggregate surfaces. The lowest shares were observed in brick panel cladded elements and white concrete. (Lahdensivu 2012)

Visible corrosion in balcony structures has been most extensive in balcony side panels. Of side panels, 51% had local and 15% widespread corrosion damage. Although the carbonation rate is the highest in slab soffits, visible corrosion damage was detected less than in other balcony structures. No corrosion damage was detected in 45% of balcony slabs. The reason for less corrosion damage is the lower moisture load, which increases the carbonation rate while on the other hand, lengthens the propagation phase. (Lahdensivu 2012, Köliö 2016)

Köliö et al. (2017) presented a service life design model. The model is based on regression analysis of time series data on both the environmental conditions and field measurements of the corrosion rate of facade panels and balcony structures at two geographical locations (coastal area and southern Finland) in Finland. The study concluded that the scatter in the active corrosion rate in outdoor concrete structures could be explained by on-site weather parameters, especially by WDR. Model

simulations conducted with 30-year current climate data showed that, despite high temporal scatter due to weather changes, the long-term scale corrosion rate was relatively steady. The corrosion rate was influenced by the geographical location and the direction in which the facade faced. For average critical corrosion penetration of 67.5 µm determined for this structure type (Köliö et al. 2015), the length of the propagation phase differed from 2.0 years (south-facing balcony side panel in southern coastal Finland) to 8.0 years (north-facing facade in northern Finland). With structures sheltered from WDR such as balcony slab soffits, the length of the phase was from 79.8 years in southern coastal Finland to 200 years in northern Finland. (Köliö et al. 2017)

2.4 Summary of Chapter 2

Existing Finnish concrete facade and balcony structures and their degradation mechanisms and rate are known quite extensively. The following conclusions can be drawn based on above examination:

- Since the late 1960s, precast concrete elements have dominated structural elements in the construction of blocks of flats.
- The durability-related properties of the elements have changed as knowledge and experience of them have increased.
- The state of existing precast concrete element buildings in Finland is relatively well-known, mainly because of the extensive systematic condition investigation methods.
- Based on the condition investigation data, the actual properties have lacked quality still in the 1990s, regardless of the development of knowledge and regulations.
- The main causes for degradation of outdoor exposed concrete in Finnish climate have been freeze-thaw attack and carbonation-induced reinforcement corrosion.
- The main reason for freeze-thaw durability problems has been insufficiency or lack of air-entrainment.
- The rate of freeze-thaw attack has been faster in coastal area and observed damage occurred with less freeze-thaw cycles after rain events than in inland. Even with insufficient freeze-thaw durability properties, concrete can withstand a significant number of freeze-thaw cycles without degradation. However, when the incipient cracking is observed, the rate of degradation accelerates remarkably.
- The main reasons for reinforcement corrosion has been inadequate concrete cover and high carbonation rate due to high porosity of concrete. The corrosion damage have been often local in both facades and balconies but widespread damage has been more extensive in balcony structures.

3 Changing climate

3.1 Present climate exposure

3.1.1 Climate conditions in Finland

Köppen-Geiger Climate Classification is a widely used method to present different geographic-related climatic conditions. Kottek et al. (2006) updated the map to represent the current climate and Rubel & Kottek (2010) presented the classification based on the climate at the beginning of the 20th century and the projected 2100 climate. Based on the studies, in the present and former climates the southern coastal region of Finland has been classified as an area of cold and snowy winters, high humidity and long and warm summers (Dfa). The rest of the country has been classified also to have cold and snowy winters and high humidity but short and cold summers (Dfc). Based on the projected 2100 climate, Lapland is still classified as Dfa while the southern Finland and inland is classified as having warm temperate winters, high humidity and cool summers (Cfc). In the present climate, the classification is similar to Sweden excluding the southern parts and the mountains, Norway excluding the coastal areas and the mountains and most of Canada and northern Russia. The projected 2100 classification shifts Finland closer to what is now Central Europe and the British Isles.

However, the Finnish climate is quite steady and mild for its northern latitudes, mostly because of the Gulf Stream that feeds warm currents of air to northern Europe. The Scandinavian Peninsula also shields Finland from the most extreme winds and precipitation compared to Norway, for example. The surface area of Finland is quite large, mostly because of the latitudinal length, which means that there are geography-related differences between the northern and southern parts. The largest differences in climatic conditions are on temperatures, amount and form of precipitation and amount of solar radiation. In addition, most of the storm-class wind speeds are recorded in coastal area and at the tops of the fells in Lapland.

3.1.2 Precipitation and wind-driven rain

Geography has a two-way effect on the amount of annual precipitation in Finland: it is higher in coastal and southern areas than in inland and Lapland and the form of precipitation changes the more northerly the location is. The annual amount of all precipitation and precipitation when the temperature has been over 0 °C, thus including rain and sleet, are shown in the Table 5. The data is based on the 30-year period 1980–2009 (Ruosteenoja et al. 2013a).

Table 5 Average annual precipitation and precipitation when snow is excluded, in four different locations in Finland.

Location	All precipitation [mm/year]	Precipitation while T > 0 °C [mm/year]	Share of precipitation in the form of rain and sleet
Helsinki-Vantaa (Coastal area)	682	589	86%
Jokioinen (Southern Finland)	598	528	88%
Jyväskylä (Inland)	573	489	85%
Sodankylä (Lapland)	479	351	73%

As can be seen in the Table 5, the share of rain and sleet does not vary significantly in the southern part of Finland. However, the amount of precipitation in the form of rain and sleet is 10% higher in the coastal area than in southern Finland, 17% higher than in inland and 40% higher than in Lapland.

As mentioned before, the conditions in Finland are not as harsh as they could be at such latitudes. For example, Rydock et al. (2005) presented the amounts of an average annual precipitation in 1961–1990 at four locations in Norway. They showed that the lowest amount was 763 mm/year in Oslo (inland) and the highest 2,250 mm/year in Bergen (coastal area). The latter is one of the rainiest locations in Europe.

When the wind speed during the rain event is taken into account, the share of wind-driven rain (WDR) on vertical surfaces such as facades is significantly more geographically dependent. Only 0.3% of all precipitation in coastal area comes when the wind is calm. The same shares in southern Finland,

inland and Lapland are 0.5%, 1.2% and 1.1%, respectively. When calm winds and snow are excluded, the average wind speeds during the rain events were 4.7 m/s, 4.1 m/s, 3.3 m/s and 3.1 m/s, respectively. Ruosteenoja et al. (2013a) presented wind roses with all winds and during precipitation in the form of rain or sleet in the coastal area (Helsinki-Vantaa) and inland (Jyväskylä), see Figure 9. As can be seen in the figure, all winds are more evenly distributed while winds during rain and sleet are mainly southern in both the studied locations. During the rain events, the share of high wind speeds is slightly higher than without rain.

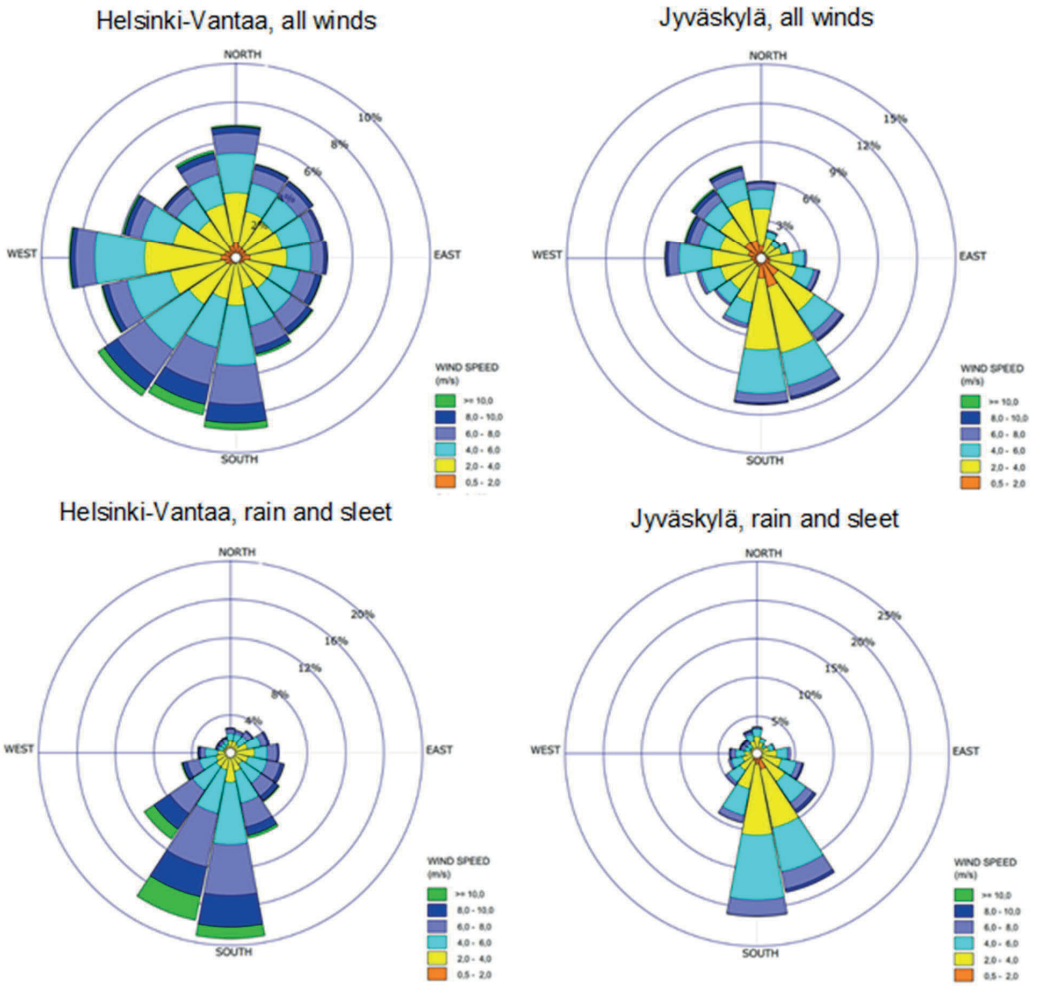

Figure 9 Wind roses in the coastal area (Helsinki-Vantaa) and inland (Jyväskylä) with all winds and winds during rain events. (Ruosteenoja et al. 2013a)

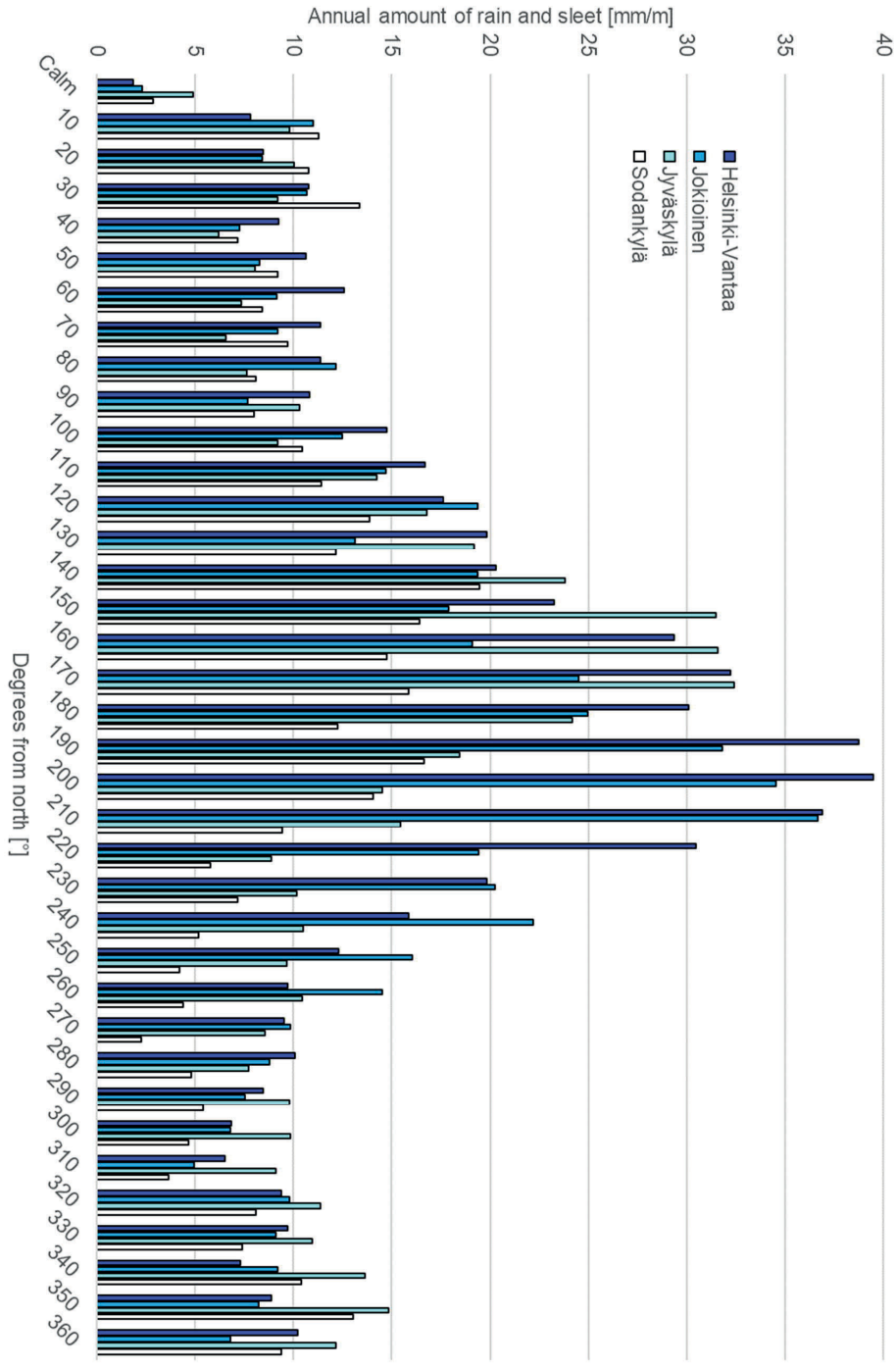

Figure 10 Amount of precipitation in the form of rain and sleet at four locations.

Location-related information on the amount of precipitation in the form of rain and sleet divided up by different wind directions during rain events is shown in Figure 10. The wind directions are shown clockwise as degrees from the north. The numbers are based on the weather data produced by FMI (Ruosteenoja et al. 2013a) including the 30-year period 1980–2009. In the coastal area, southern Finland and inland, significantly higher amounts of precipitation come with southerly winds. The share of precipitation from the wind directions between 140°–220° is 48%, 43% and 41%, respectively. In Lapland, the share is 35% and there are more northerly winds there than in the other locations.

3.1.3 Freeze-thaw cycles

A freeze-thaw cycle can also be referred to as a freezing point crossing (FPC). Usually the limit temperature of 0 °C for a cycle is used because it is the freezing point of free water in normal conditions. However, the freezing point of water can vary for multiple reasons such as varying pressure, dissolved salts and if the water is trapped in small pores in porous materials. When considering porous materials in outdoor climate, the freezing point may be lowered by dissolved salts or the small pore structure. In Table 6, the average annual number of freeze-thaw cycles is shown at four locations. The data is based on the 30-year period 1980–2009 (Ruosteenoja et al. 2013a).

The freeze-thaw cycles are studied because the water can cause degradation of porous materials when expanding during freezing. Thus, the freeze-thaw cycles themselves are not as relevant as the freeze-thaw cycles after a rain event. Table 7 shows freeze-thaw cycles with different limit temperatures up to three days after the rain or sleet event.

The number of annual freeze-thaw cycles between different locations does not vary significantly except in the coastal area where freeze-thaw cycles are rarer. When the limit temperature is set to -5 °C, the number of cycles is reduced by more than 66% at every location. At every location, 70–73% of freeze-thaw cycles with a limit temperature of 0 °C follow rain or sleet events. When the limit temperature is set to -5 °C and -10 °C, on average 64% and 51% of cycles, respectively, follow rain or sleet events. Figure 11 shows the monthly distribution of the annual average of freeze-thaw cycles with different limit temperatures at Helsinki-Vantaa Airport. Most freeze-thaw cycles with a limit temperature of 0 °C occur in spring in March and April when the day temperature rises because of the sun but the night temperature drops below 0 °C. However, with lower limit temperatures the highest number of cycles occurs in winter from December to February. Distributions at other studied locations are shown in Appendix II.

Table 6 Average annual number of freeze-thaw cycles at four locations with varying limit temperatures.

		Number of cycles			
Limit temperature		Helsinki-Vantaa	Jokioinen	Jyväskylä	Sodankylä
0 °C	Average	64	71	71	70
	Min.	52	48	50	49
	Max.	85	99	89	96
-5 °C	Average	17	20	24	24
	Min.	10	12	11	16
	Max.	26	31	33	34
-10 °C	Average	8	9	12	14
	Min.	1	3	4	7
	Max.	13	17	19	22

Table 7 Average annual number of freeze-thaw cycles up to three days after a rain or sleet event at four locations with varying limit temperatures.

		Number of cycles			
Limit temperature		Helsinki-Vantaa	Jokioinen	Jyväskylä	Sodankylä
0 °C	Average	47	51	50	49
	Min.	28	31	30	28
	Max.	66	68	69	71
-5 °C	Average	12	13	14	15
	Min.	4	4	4	7
	Max.	19	21	27	21
-10 °C	Average	4	5	6	7
	Min.	0	1	1	2
	Max.	9	11	11	11

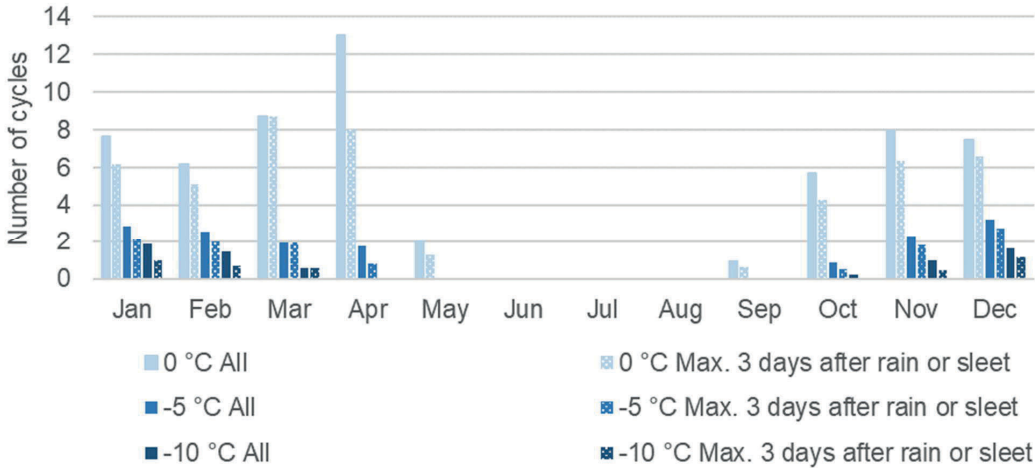

Figure 11 The distribution of annual average freeze-thaw cycles in the coastal area.

3.1.4 Other climatic exposure

Multiple other climatic factors can also cause load on outdoor structures or be part of deterioration mechanisms. The most significant ones considering this study are temperature, relative humidity and solar radiation. Monthly average temperature and relative humidity at four locations are shown in Table 8. The data is based on the 30-year period 1980–2009 (Ruosteenoja et al. 2013a).

Latitude has a major effect on the temperatures, especially in winter. In Lapland, the annual average temperature is under 0 °C and during the winter months (Dec, Jan, Feb) less than 10 °C while in southern Finland and the coastal area the annual temperature is over 5 °C higher during the whole year and over 7 °C higher during the winter. At the same time, relative humidity is lower in Lapland during the cold season. Throughout the year, the highest relative humidity is in southern Finland and inland.

Table 8 Monthly average temperature and humidity at four different locations. (Ruosteenoja et al. 2013a)

	Helsinki-Vantaa		Jokioinen		Jyväskylä		Sodankylä	
Month	T [°C]	[RH%]	T [°C]	[RH%]	T [°C]	[RH%]	T [°C]	[RH%]
Jan	-4.9	87.3	-5.5	89.3	-8.2	88.9	-13.6	84.3
Feb	-5.7	85.1	-6.3	87.1	-8.5	87.0	-12.6	83.1
Mar	-2.0	80.3	-2.5	81.3	-3.9	80.8	-7.5	78.6
Apr	4.0	70.3	3.6	71.8	2.1	71.1	-1.3	70.6
May	10.3	64.2	9.7	65.2	8.8	65.2	5.2	66.9
Jun	14.7	68.5	14.0	68.6	13.8	68.3	11.7	64.0
Jul	17.5	70.3	16.5	72.0	16.3	72.4	14.5	69.1
Aug	15.7	76.6	14.9	76.7	14.0	78.7	11.6	75.6
Sep	10.7	81.2	9.9	82.1	8.8	83.5	6.2	81.5
Oct	5.6	85.1	5.0	87.5	3.6	88.2	0.0	86.6
Nov	0.4	88.1	-0.2	90.6	-2.0	91.1	-7.1	88.3
Dec	-3.0	88.9	-3.7	90.7	-5.9	90.5	-11.8	85.5
Av.	**5.3**	**78.8**	**4.6**	**80.2**	**3.2**	**80.5**	**-0.4**	**77.8**

Table 9 Duration of sunshine and amount of global radiation at four locations. (Pirinen et al. 2012)

	Helsinki-Vantaa		Jokioinen		Jyväskylä		Sodankylä	
Month	Duration of sun-shine [h]	Global radiation [MJ/m²]	Duration of sun-shine [h]	Global radiation [MJ/m²]	Duration of sun-shine [h]	Global radiation [MJ/m²]	Duration of sun-shine [h]	Global radiation [MJ/m²]
Jan	38	31	36	29	29	22	13	6
Feb	74	92	73	91	73	80	61	51
Mar	131	232	130	234	126	214	128	190
Apr	196	398	193	393	187	385	199	388
May	275	583	261	556	256	541	225	499
Jun	266	605	255	582	247	560	261	546
Jul	291	614	266	584	263	558	245	508
Aug	219	445	208	435	199	408	171	358
Sep	143	259	137	252	120	226	105	182
Oct	84	116	78	109	59	90	57	65
Nov	37	35	33	34	25	26	20	12
Dec	26	17	25	16	14	10	1	1

	Helsinki-Vantaa		Jokioinen		Jyväskylä		Sodankylä	
Month	Duration of sunshine [h]	Global radiation [MJ/m²]	Duration of sunshine [h]	Global radiation [MJ/m²]	Duration of sunshine [h]	Global radiation [MJ/m²]	Duration of sunshine [h]	Global radiation [MJ/m²]
Summation	**1780**	**3427**	**1695**	**3315**	**1598**	**3120**	**1486**	**2806**

The amount of sunshine is highly dependent on the time of year. At midsummer, if there are no clouds, the sun can shine for 24 hours without setting in the northern parts of Finland. When the duration of sunshine is measured, it is on average almost the same (within 20 hours) throughout Finland as can be seen in Table 9. Naturally, during the winter there is a great lack of sunshine. In Sodankylä, there is only 1 hour of sunshine in December, in southern areas, a bit over 24 hours. In addition, Table 9 shows average monthly global radiation on a horizontal surface. The annual durations of sunshine and global radiation are both much higher in southern parts than in Lapland. It should be noted, that the direction and angle of sunshine also varies significantly. From the autumn to spring equinoxes, solar radiation is higher from west to south and so is higher on vertical surfaces facing those directions. Throughout the year, the angle of solar radiation is quite low compared to locations closer to the equator. (Pirinen et al. 2012)

3.2 Climate change adaptation studies and projections

3.2.1 Global adaptation studies

Climate change and its effects have been extensively studied all over the globe for decades. After the 1979 World Climate Conference, the United Nations Environment Programme and the World Meteorological Organization announced that they were determined to promote climate change studies. Their efforts led to better knowledge of the major role of carbon dioxide and other greenhouse gases in climate change. In 1988, they established the Intergovernmental Panel on Climate Change (IPCC). The first Workgroup Reports were published in 1990 and the first Assessment Report giving an overview in 1992. (IPCC 1992). So far, a total of five Assessment Reports (in 1992, 1994, 2001, 2007 and 2014) have been published and work on the sixth is underway.

The objective of IPCC's work has been to analyse existing scientifically produced data for national and international decision-making. Since the first Assessment Report, they have included consideration of the climate change effect on human settlements. Most concern has focused on sea level

rise and the effects of extremes of weather on building design and existing buildings in the most vulnerable areas. In addition, every country or union of countries has had possibilities to use the meteorological projection data to assess the impact and adaptation possibilities in their own areas.

In 2013 The European Commission presented the EU Strategy on adaptation to climate change. The strategy focused on three key objectives: to encourage EU Member States to commit to adaptive measures, to promote adaption especially in the most vulnerable sectors (e.g. agriculture, more resilient infrastructure) and to promote better informed decision-making. (European Commission 2013a). Government-driven work has also been done in multiple countries outside the EU, such as in cold countries like Norway (Norwegian Ministry of Climate and Environment 2013) and Canada (Government of Canada 2011).

As a part of the EU strategy, a Working Document considering adapting infrastructure to climate change was published (European Commission 2013a). The projected impacts of climate change and associated threats concerning the construction sector were highlighted as follows: 1) extreme precipitation that may lead to water intrusion and damage to foundations and basements; 2) extreme summer heat events that may lead to material fatigue, accelerated aging and high energy use for cooling; 3) exposure of structures to heavy snowfall; 4) rising sea and river levels that increase the risk of flooding and are likely to increase soil subsidence risks. (European Commission 2013b)

In addition, based on the EU Strategy, adaptation preparedness should be followed in all Member States by horizontal assessment. The latest evaluation was made in 2018 (European Commission 2018a). In Finland, the evaluation notes that at local level 40% of municipalities have a climate strategy and 16 out of 18 regions have published a climate strategy including at least some recognition of adaptation. In addition, the evaluation states that in the water resources, agriculture, land use, energy, health and tourism sectors, the impacts of climate change are relatively well known. (European Commission 2018b), but the evaluation does not mention studies related to infrastructure or construction, nor does it recognise the lack of studies as a knowledge gap.

3.2.2 Adaptation studies and used climate change projections in Finland

The first National Strategy for Adaptation to Climate Change in Finland was published in 2005. Since then it has been updated regularly and the latest version was published in 2014 (Ministry of Agriculture and Forestry 2014). Based on the strategy, Methods for Adaptation and Climate-Durable Planning in the Capital Area was first published in 2012 and updated in 2017 (HSY 2017). Construction-related studies in Finland have been quite rare. Ala-Outinen et al. (2004) produced the first report in Finland considering the impacts climate change might have on the built environment. The study focused on flood risks, ground frost and the depth of ground water but also drew attention to the risks that increasing driving rain may cause for facades. Kuismanen (2008) presented methods for climate conscious architecture for climates in change. Lahdensivu (2010) made estimates of the climate change effects on the durability of facades and balconies. The “Future Envelope Assemblies

and HVAC Solutions" (FRAME) project (Vinha et al. 2013) concluded that future climate conditions in Finland are likely to get worse in terms of the durability of facades and other structures exposed to climate. The project focused on the combined effect of climate change and tightening energy regulations, i.e. how climate change affects the hygrothermal behaviour of the building envelope and, for example, the need for cooling.

The FMI has produced numerous projects related to climate change effect on different sectors. In "The changing climate in Finland: estimates for adaptation studies" (ACCLIM) project (Jylhä et al. 2009), they produced probabilistic estimates of changes in climate over Finland to use in adaptation studies. The estimates were based on the IPCC 2007 climate models. In "Climate Scenarios for Sectoral Research" (SETUKLIM) project (Ruosteenoja 2013b), the FMI updated some of the estimates based on the latest "Coupled Model Intercomparison Project Phase 3" (CMIP3) climate models. In the "Climatological test years in Finland for building physics" (REFI-B) project (Ruosteenoja et al. 2013a), the FMI produced building physics test reference years in the observed and projected future climate to use in calculations for, for example, moisture and energy performance.

The FMI has occasional weather data from the 19th century. They have data in digital form since 1961 from several meteorological stations covering all of Finland. The data consist of temperature, relative humidity, rain intensity, wind speed and direction, solar radiation variables, etc. These observations have been collected at least daily, some of them hourly. In the REFI-B project (Ruosteenoja et al. 2013a), the FMI forecasted the same climate variables as hourly data for four regions (coastal area, southern Finland, inland, Lapland) in three points of time (2030, 2050 and 2100) based on three scenarios produced relating to the IPCC's 4th report (2007). The forecasts are based on an average of 19 different models, which are all based on greenhouse gas emission scenario A2. The A2 scenario involves a situation where greenhouse gases are assumed to increase significantly. (Ruosteenoja et al. 2013a). In addition, the FMI has calculated other significant greenhouse gas emission scenarios A1B (quite large emissions) and B1 (small emissions). All the scenarios have also been updated to be based on the 2013 CMIP3 models (Ruosteenoja et al. 2013b), but the updated data is not as detailed, including the climate variables produced in the REFI-B project.

In models based on 2007 data, the differences between the scenarios start to emerge in 2040, and in updated models in early 2020. The differences related to the used scenario and their effect on annual temperature and precipitation in Finland are shown in Figure 12. In the case of the worst-case scenarios A2 and RCP8.5, the difference between former and updated version is minor.

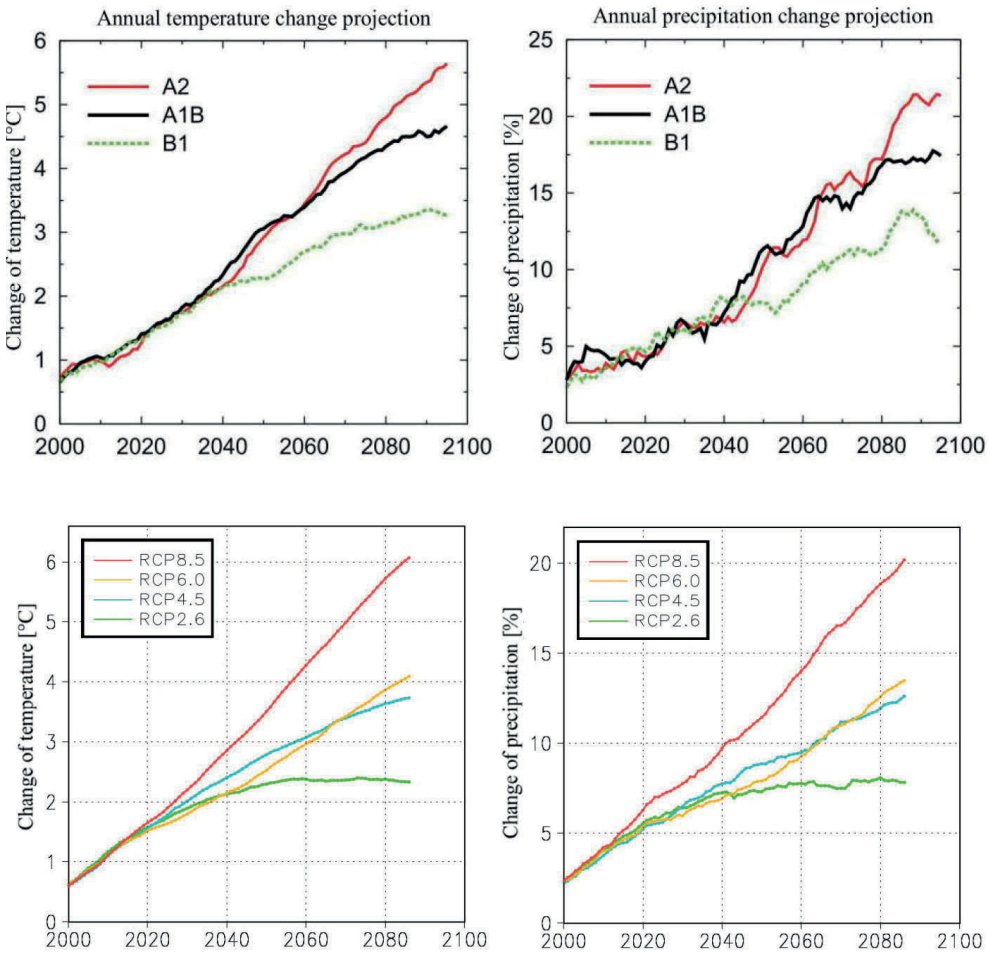

Figure 12 Projections for annual mean temperature and precipitation change in 2000–2100, in relation to the mean of the reference period 1971–2000. The curves depict 11-year running means, averaged over Finland and the responses of 19 global climate models. The upper graphs are reproduced from Jylhä et al. (2009) and the lower from the Ministry of Agriculture and Forestry (2014).

The increase in CO_2 level is highly dependent on the scenario used. According to the REFI-B project, when using A2 scenario the CO_2 level may rise to 840 ppm by the end of the century and to about 540 ppm when using the B1 scenario (Ruosteenoja et al. 2013a). However, the increase is significant compared to the present level which is approx. 410 ppm both in the coastal area and Lapland. The level has increased by 10–20 ppm during last decade (FMI 2019).

3.3 Studies related to assessment of climate change effects on buildings

Climate change itself has been studied worldwide for a long time, but adaptation to climate change in existing buildings has been under scientific research only in very narrow areas. Studies related to the effect of climate change has concentrated mainly building physical problems such as changes in energy need in the cooling and heating of buildings and the energy-efficient performance of buildings (e.g. Dino & Akgül 2019, Gupta & Gregg 2012, Labriet et al. 2015, Li et al. 2012, Mauree et al. 2019, Nik et al. 2012, van Hooff et al. 2016, Vasaturo et al. 2018 and Williams et al. 2012).

Phillipson et al. (2016) stated that it is unlikely that new and yet unknown deterioration mechanisms of building materials due to climate change will be encountered, but the effect of climate change on known deterioration mechanisms and the degradation rate should be under studies. Existing buildings will face a simultaneous need to be conserved and to adapt to changing climate. They propose that there is a strong need for building codes, which take future climate into consideration in the design process.

Auld et al. (2007) presented an extensive review of the climate change effect on the deterioration of different structures and materials in Canada. They listed possible effects of changes in the amount of precipitation, temperature, freeze-thaw cycles, UV-radiation, etc. on different materials (e.g. bricks, concrete and wood), structures (e.g. roofs, facades and pavements) and on heating degree days (HDD). They also presented suggestions for preventing degradation by controlling the climatic load. However, their studies were based on assumptions and experience rather than modelling or test results.

In Norway, a few recent studies have concerned the impact of the climate change on the deterioration of the structures of both new and existing building stock. Kvande & Lisø (2009) studied the climate-adapted design of masonry structures. Lisø's doctoral thesis (2006) focused on generating methods for geographically dependent design in harsh climates. The thesis presented, inter alia, a national map of decay potential in wooden structures based on detailed scenarios for climate change. Based on the methods presented in the thesis, Lisø et al. (2007b) and Almås et al. (2011) later introduced further studies for assessing the effect of climate change on geographically dependent microclimates and GIS-based modelling of the climate change effect on the risk of rot decay in wooden structures, respectively. Based on the former studies, Lisø et al. (2017) proposed a general framework for climate adaptation and moisture-resilient buildings to improve methods for the risk assessment of climate-related strains and geographically dependent climate indices. The need for such a framework was brought up in a Norwegian climate change adaptation plan by the Norwegian Ministry of Climate and Environment in 2013.

Hrabovszky-Horváth (2014) studied the vulnerability of refurbished reinforced concrete buildings to the effects of changing climate in Hungary. According to the study, the Hungarian climate is going to be warmer and drier and the number and intensity of extreme weather events will increase. The study assessed the sensitivity and adaptive capacity of prefabricated reinforced concrete large-panel buildings against the changing climate, and produced estimations of their vulnerability to the increased number of windstorms and extreme rainfall.

The effect of climate change on reinforcement corrosion has been studied quite extensively, but almost all of them have considered new construction. The effect of an increase in CO_2 levels, temperature or both due to climate change on the corrosion of reinforcements has been studied in a few papers. Yoon et al. (2007) studied the effect of CO_2-level increase on the carbonation progress by testing what amount of increase in CO_2 concentration would threaten the durability of concrete. They suggested that adding a tolerance to concrete cover depth should prevent concrete structures from corrosion failure.

Bastidas-Arteaga et al. (2010) used three scenarios of global warming to study the climate change effect on chloride ingress into concrete using a stochastic approach. They concluded that in a continental climate with a reference period of 100 years, the lifetime reduction could be up to 4–6%. In a recent study, Bastidas-Arteaga (2018) presented that reinforced concrete structures exposed to chloride-induced corrosion in oceanic and tropical climates face moderate lifetime reductions ranging between 1.4 and 2.3%, respectively, due to climate change. However, when cyclic load is also taken into account, the reductions are up to 7%.

Recent work has also focused on the assessment of climate change on the durability of concrete structures, especially the corrosion of reinforcements in specific locations. Wang et al. (2012) studied the impact of climate change on corrosion-induced damage in Australia, and Medeiros-Junior (2018) in Brazilia. Talukdar et al. (2012) estimated the effects of climate change on carbonation in Canadian cities and later (Talukdar et al. 2014) globally in different locations. de Lallard et al. (2014) made estimations of the effects of temperature and relative humidity changes in France based on a probabilistic finite element. They studied three different climate change scenarios and six different locations. Based on their study, carbonation is very sensitive to local climate, both temperature and relative humidity, and they concluded that the results highlight the importance of cover thickness over material properties. Based on the results of the former study, Talukdar and Banthia (2013) developed a model of carbonation in concrete infrastructure in the context of global climate change, and concluded that global climate change will affect the progression of and will result in much higher ultimate carbonation depths in the long term.

Stewart et al. (2011, 2012) studied the probabilities of both carbonation- and chloride-induced corrosion due to CO_2, temperature and relative humidity changes until 2100 at two different locations in Australia. In addition, Peng & Stewart have studied the effect of climate change on the carbonation rate and carbonation-induced damage on concrete cover at three different locations in China (2014)

and in Sydney, Australia (2013). They concluded that, in the worst-case, carbonation-induced damage risk may increase in Australia by over 40%, chloride-induced corrosion risk by 3–15% and in China by 45% and 7–20%, respectively. They noted that the results were more sensitive to increase in CO_2 level than to temperature or relative humidity changes. In addition, they also gave suggestions on how to adapt to the increasing risks by proposing an increase in cover depth or concrete grade or adding a coating to concrete surfaces.

Bastidas-Arteaga & Stewart (2015) concluded that, from a cost-benefit perspective, increasing the concrete grade of new reinforced concrete structures is more cost-effective than increasing cover depth, when considering protective measures against the chloride-induced corrosion of reinforcements. Later they made economic assessments of climate change adaption for both new construction (2016a) and existing buildings (2016b). In the first mentioned they presented that the cost-effectiveness of increasing cover depth is actually location-dependent.

In a recent paper, Benítez et al. (2019) compared carbonation models with actual degradation data in Paraguay. They used the best-fitted model to estimate the climate change effect on carbonation-induced initiation time and the propagation time of different strength grade concrete with cover depths of 10 and 25 mm. The results endorsed the effect of quality control, i.e. achieving the minimum concrete cover of 25 mm. In addition, the results showed that climate change does not have a significant effect on the service life of poor-quality reinforced concrete but has a noticeably detrimental effect on good-quality concrete. However, the service life of good-quality reinforced concrete with eligible concrete cover can be decades longer than with lower cover depth.

3.4 Summary of Chapter 3

As summarised, the following observations related to the climate change studies and assessment of the climate change effects on buildings can be highlighted:

- Climate conditions in Finland are quite steady and mild for the latitudes and compared to its neighbouring countries.
- The amount of precipitation is highest in the coastal area. Except in the northern parts of Finland, significantly high share of precipitation come with southerly winds.
- The number of annual freeze-thaw cycles in total and after rain or sleet are more or less at the same level throughout Finland. The number of cycles with limit temperature of 0 °C is the highest in March and April when the days are warm and the nights still cold. Lower limit temperatures emphasize the role of winter months (December to February).
- Climate change and its effects have been extensively studied all over the globe for decades. In addition, studies related to adaptation of buildings and infrastructure have been extensively studied. However, they have mainly considered new construction and their building physical

problems. Studies related to the effect of climate change on existing building stock and especially deterioration mechanisms and its rate have been rare.

- The climate change studies are based on the greenhouse gas development based projections made by global collaboration led by the Intergovernmental Panel on Climate Change (IPCC). Based on IPCC's work, the Finnish Meteorological Institute has produced probabilistic estimates of changes in climate over Finland to use in adaptation studies.

4 Research material and methods

4.1 Research material

4.1.1 Condition investigation database

The extensive condition investigation data produced in the BeKo project (Lahdensivu et al. 2010) at TUT has been utilised in this study in many ways. The database consists of 422 condition investigation reports including results from 947 precast concrete element buildings built in 1960–1996. The condition investigations were made in 1992–2006. The data gathered from the reports included:

- Basic information of the studied buildings, e.g. building year, year of the investigation, height, size, location, surface type of structures, thickness of the outer concrete layer or the balcony structure, type and thickness of heat insulation
- Visual observations, e.g. cracking, spalling, scaling of coating
- Information related to reinforcement, e.g. diameter, cover depth and signs of corrosion of reinforcement, carbonation depth, amount of chlorides
- Information related to concrete, e.g. type and size of aggregates, type of cement, compaction, protective pore ratio, degree of capillary saturation, degree of freeze-thaw damage, secondary void fillings
- Type and condition of fixing of facade panels and suspension method of balcony structures
- Harmful substances of coating and joint materials, e.g. asbestos, lead, polychlorinated biphenyl (PCB).

The height level of observations and taken samples and the direction in which the studied structure was facing was tabulated, if mentioned in the report.

The whole database was used in the studies as background data on the state and deterioration rate of Finnish precast concrete element buildings in the present climate. In Articles I and II, only the results of the buildings built 1990–1996 were studied to estimate the reinforcement corrosion and freeze-thaw durability-related risks in the buildings built according to the present requirements of the Finnish Concrete Codes. The number of buildings from the era in the database is 72. Their average age at time of the investigation was 11 years.

Some of the data, 244 condition investigation reports including 472 precast concrete element buildings, was reanalysed in Article V to collect more specific data on far-advanced freeze-thaw deterioration detected visually or by hammering. The reanalysis was needed to collect the directions in which the damaged structure was facing. The information was not part of the original database, mainly because of poor original description of it in the reports. In addition, in Article V a condition investigation report of a building was used as a case study. Lapland was excluded from the study because of a lack of investigated buildings.

4.1.2 Climate data

The climate data used in all the articles was produced by the FMI, mostly in the REFI-B project (Ruosteenoja et al. 2013a). The FMI made a database for 1980–2009 presenting the present climate in all the articles. The database included at least observations collected every three hours from four weather stations representing the four geographical areas shown in Figure 3: Helsinki-Vantaa (the coastal area), Jokioinen (southern Finland), Jyväskylä (inland) and Sodankylä (Lapland). In some cases, observations of rainfall were collected less than every three hours but rain events were observed more frequently and, based on them, the start and end points of the rain event were estimated. The three-hour data was also linearly interpolated as hourly data. The database consists of the following variables: temperature, relative humidity, wind speed and direction, direct and diffuse solar radiation and precipitation.

Based on the observed data and climate change scenario A2 (see Chapter 3.2.2), the FMI made hourly projections of the same variables for three 30-year time periods: 2030 (period 2015–2044), 2050 (2035–2064) and 2100 (2085–2114). The projections were made for the same locations as the observed data mentioned above. All the projections were used in Articles I and II. In Articles III and IV, only the projections for 2050 and 2100 were used.

In addition, the FMI produced data on freeze-thaw events collected from five locations: Helsinki-Vantaa, Turku (southwest coastal area), Jyväskylä (inland), Oulu (northern inland) and Rovaniemi (Lapland). The maximum and minimum temperatures were collected twice a day during 1960–2009. The data comprised only the annual number of freeze-thaw cycles with different limit temperatures (0 °C, -2 °C, -5°C, -10 °C, -15°C and -20 °C). In Article II, data from Helsinki-Vantaa, Jyväskylä and Rovaniemi were used.

4.2 Research methods

4.2.1 Freeze-thaw related calculations

Lisø et al. (2007a) presented a combination of frost decay exposure index (FDEI) and freezing point crossings (FPC) to characterise the risk of freeze-thaw damage to a porous, mineral material in a given climate. In their studies, the freeze-thaw cycles were considered as temperature crossings over freezing point (0 °C) and the number of cycles was defined as annual average number of days with freezing point crossings.

The FDEI links average annual freezing point crossings (FPC) to the amount of liquid precipitation recorded from the day an FPC has occurred and the preceding two, three or four days. When the FDEI and FPC are shown in the same diagram, the risk of frost decay can be estimated by analysing their relation. For example, if the amount of FPCs is high but the amount of precipitation before the crossings is low, i.e. FDEI is low, the risk of frost decay is relatively low, but if they both are high, the risk is considerable.

Because the limit temperature of 0 °C is considered not to be adequate for the freezing point crossings (see Chapter 2.2.2) of porous material such as concrete, freeze-thaw cycles with limit temperatures of -5 °C and -10 °C were also calculated in this study. In addition, freeze-thaw attack needs pore water to be realised. Thus, the climate database was used to calculate the freeze-thaw events up to three days after a rain event and the amounts of precipitation before rain events, both as annual average amount and average amount prior to a single event.

4.2.2 Modelling wind-driven rain

The share of annual precipitation, which hits a vertical surface by the effect of wind is called wind-driven rain (WDR). A widely used method for modelling WDR is using a standardised airfield annual index I_A (SFS-EN ISO 15927-3 2009). It gives an estimation of the amount of precipitation on vertical surface from different directions at a height of 10 m above ground level at an open place (in the middle of the airfield). The I_A can be calculated with the following Equation 1:

$$I_A = \frac{2}{9} \frac{\sum v r^{\frac{8}{9}} \cos(D-\theta)}{N} \qquad (1)$$

, where v is hourly mean wind speed [m/s], r is hourly rainfall total [mm], D is hourly mean wind direction from north [°], θ is wall orientation relative to north [°], N is the number of years for which data is available and the summation is taken over all hours for which $\cos(D-\theta)$ is positive.

The standard requires hourly data and also has some limitations as the standard does not apply in mountainous areas, areas where at least 25% of WDR comes with severe storms and areas where

a significant share of rain is in the form of snow. The weather data used in this study was collected in 1980–2009 every three hours and interpolated as hourly data. The interpolation causes reduction of rain intensity and wind speeds, otherwise the mentioned limitations are met, apart from the requirement of significant snowfall amount. The standard does not specify how much is 'significant', so the rain events under 0 °C are excluded to meet the requirements better.

The standard SFS-EN ISO 15927-3 (2009) also shows a factor I_{WA} (Wall annual index), which can be used to convert the amount of precipitation collected by a free-standing driving-rain gauge in flat open country to present the amounts of precipitation that impact on a real wall:

$$I_{WA} = I_A C_R C_T O W \quad (2)$$

, where I_A is the airfield annual index, C_R is a terrain roughness coefficient, C_T is a topography coefficient, O is an obstruction factor and W is a wall factor.

The roughness coefficient depends on the height above the ground and the roughness of the terrain in the direction from which the wind is coming, i.e. is there an open sea, farmland, a suburban area or an urban area in the upwind direction. The topography coefficient takes into account the increase of mean wind speed over isolated hills and escarpments near the building subjected to the study. Obstruction factor depends on the horizontal distance to the nearest obstacle, which is at least as high as the wall subjected to the study. The wall factor is, in the case of flat roof multi-storey building, 0.5 for the top 2.5 m of the wall and 0.2 for remainder.

The I_{WA} was used in Articles III and V. In the former, it was used to estimate the amount of WDR in different parts of the facades in a typical Finnish residential block at different geographical locations. In the latter, it was used to estimate the total amount of WDR during the existence of an actual case building located in southern Finland. The result was also used to estimate the amount of WDR needed for freeze-thaw damage to occur in a building where the air-entrainment was insufficient.

The wall annual index is a highly simplified simulation for assessing WDR against building facades. There are other methods to model the WDR as mentioned by, for example, Blocken and Carmeliet (2004, 2010), a semi-empirical SB model by Straube and Burnett (2000) and a Computational Fluid Dynamics (CFD) model by Blocken and Carmeliet (2002, 2007) based on the studies of Choi (1994). They all take into account more precisely the distribution of the WDR in different areas of the facades. However, the SB model has major disadvantages such as lack of coefficients taking into account surrounding obstructions. The CFD model is the most advanced but also needs significantly more demanding computing. (Blocken et al. 2010)

Although the wall annual index is a simplified method, it gives adequate results for comparing, for example, different geographical effects on the amount of wind-driven rain on facades. Compared to CFD modelling, it underestimates the amount of WDR near the top of the facade but overestimates the amount on the top 2.5 metres with high buildings and low rain intensity. The higher the rain intensity, the more it underestimates the amount of WDR. The underestimation increases near the edges of the building. (Blocken et al. 2010)

4.2.3 Modelling climate change effect on reinforcement corrosion

4.2.3.1 Initiation phase

Because carbonation is controlled by the diffusion of carbon dioxide inside concrete, it is commonly modelled with a square root relationship with time (Tuutti 1982), see Equation 3, derived from the differential equation of diffusion (Broomfield 2007). The rate of carbonation, including the effect of both internal and external factors, is in this model denoted by the factor *k* (carbonation coefficient) [mm• years$^{-1/2}$].

$$x = k \cdot \sqrt{t} \tag{3}$$

, where *x* is the carbonation depth [mm] and *t* is time [years].

The model has since been developed further to specify the effect of multiple factors (DuraCrete 2000) and to include the influence of prevailing weather in the fib Model Code (International Federation for Structural Concrete 2006). Later the original model was improved by statistical methods (Ann et al. 2010). Empirical measurements such as by Tuutti (1982) and Huopainen (1997) have indicated that the model tends to overestimate the degree of carbonation, especially in cases where the concrete is exposed to rain. However, Köliö et al. (2014) and Lahdensivu et al. (2019) have shown that Equation 3 fits rather well with the measurements of the actual carbonation of Finnish facades and balconies. The improved methods fit better with better-grade concrete used in Finnish facades and balconies. Equation 3 was used in Article I to estimate the initiation time of reinforcement corrosion.

The square root equation has also been developed to separate the influence of different individual internal and external factors on carbonation (Neves et al. 2012) and further on to isolate the influence of specific factors in the fib Model Code (International Federation for Structural Concrete 2006), see Equation 4. However, Lollini et al. (2012) stated that the estimation of the probability density function of concrete cover in particular was found to be a substantial source of error. The equation for carbonation penetration in the fib Model Code is:

$$x_c = \sqrt{2 \cdot k_e \cdot k_c \cdot R_{NAC}^{-1} \cdot C_s} \cdot \sqrt{t} \cdot \left(\frac{t_0}{t}\right)^w \tag{4}$$

, where k_e is an environmental function, k_c is an execution transfer parameter, R_{NAC}^{-1} is the inverse effective carbonation resistance of dry concrete [(mm²/years)/(kg/m³)], C_s is CO_2 concentration [kg/m³], t is time [years], t_0 is time of reference [years] and w is a weather exponent. In Article I, Equation 4 was used to study the effect of increased CO_2 level and precipitation. The material-related parameters, see Table 10, were based on actual measurements in condition investigations.

Table 10 Parameters used in Equation 4. (Article I)

k_e	k_c	R_{NAC}^{-1}	t_0	w	C_s
0.466	1	28.500	0.0767	varied	varied

The weather parameter in the used fib Model does not take into account the distribution nor the duration of rain events. It only takes into account the number of rainy days and probability of WDR and thus, does not consider the difference between the seasonal rains and small amounts constantly.

Both of the methods above are used in this study with the assumption that the concrete used in present and future climate has the same properties. In addition, the chancing CO_2 concentration is not taken into account but the constant CO_2 concentration of the projected 2050 and 2100 levels has been used. The results should be thus considered to be in a safe side and to present as a kind of a worst-case situation.

4.2.3.2 Propagation phase

The influence of the amount of precipitation on the behaviour of reinforcement corrosion has been observed in earlier studies by Mattila (2003), Mattila & Pentti (2004) and Köliö et al. (2017). In his research, Mattila measured the corrosion current in measurement devices embedded in existing concrete facades. High corrosion current was observed during a year when annual precipitation was exceptionally high and vice versa. He proposed in his studies a rough estimate that corrosion is fast in Finnish climate conditions when annual precipitation is over 480 mm/year. Based on the studies, Article I presented an equation for a rough estimation of the penetration depth of corrosion during the active corrosion phase:

$$x_{corr} = \sum_{i=1}^{t_{prop}} r_i \qquad (5)$$

, where x_{corr} is corrosion penetration depth, r_i is average annual corrosion rate during year i (1 µm/a if annual precipitation < 480 mm and 10 µm/a if annual precipitation ≥ 480 mm) and t_{prop} is the age in years when critical corrosion depth is achieved.

In addition, a Delphin Oracle method shown in fib Model Code (International Federation for Structural Concrete 2006) was used in Article I to estimate the effect of increase of temperature on propagation time.

Köliö (2016) presented a corrosion propagation model for carbonation-induced corrosion for concrete facades exposed to the Finnish climate. In a study (Köliö et al. 2017), measured long-term corrosion rate data was combined with actual climate data at different geographical locations to explore the individual and combined effect of weather parameters on the rate of reinforcement corrosion on already-carbonated concrete facade and balcony structures. Based on the studies, they presented a service life design model to correlate the critical weather parameters directly with corrosion rate inside the mentioned structures.

In Article IV, corrosion rates were simulated using the propagation model mentioned above and presented in Köliö et al. (2017). The model relates the corrosion rate of reinforcement inside carbonated concrete to the weather exposure of the structure. The model is based on a multi-linear regression model based on a time-series analysis of long-term corrosion rate measurements and weather data. The corrosion rate was measured in facade panels and balcony structures at two geographical locations: the coastal area and southern Finland. The regression equation, see Equation 6, and coefficients were determined by fitting the data with the least-squares method. Weather parameters taken into account are ambient temperature (T), ambient relative humidity (RH), WDR (I_{WA}) and solar radiation (RAD).

$$I_{corr} = \beta_0 + \beta_1 \cdot x_1 + (\beta_2 \cdot x_2 + \beta_3 \cdot x_3 + \beta_4 \cdot x_4) + v \quad (6)$$

, where I_{corr} is corrosion current density, β_0 is interception term, $\beta_{1\text{-}4}$, $x_{1\text{-}4}$ are coefficients and parameters of variable weather parameters (T, RH, I_{WA} and RAD) and v is error term. The background and the validation of the model is introduced in detail in Köliö at al. (2017) and the used parameters in Article IV.

4.3 Summary of the used methods

A summary of the methods used in this study is presented in Figure 13 as a flowchart.

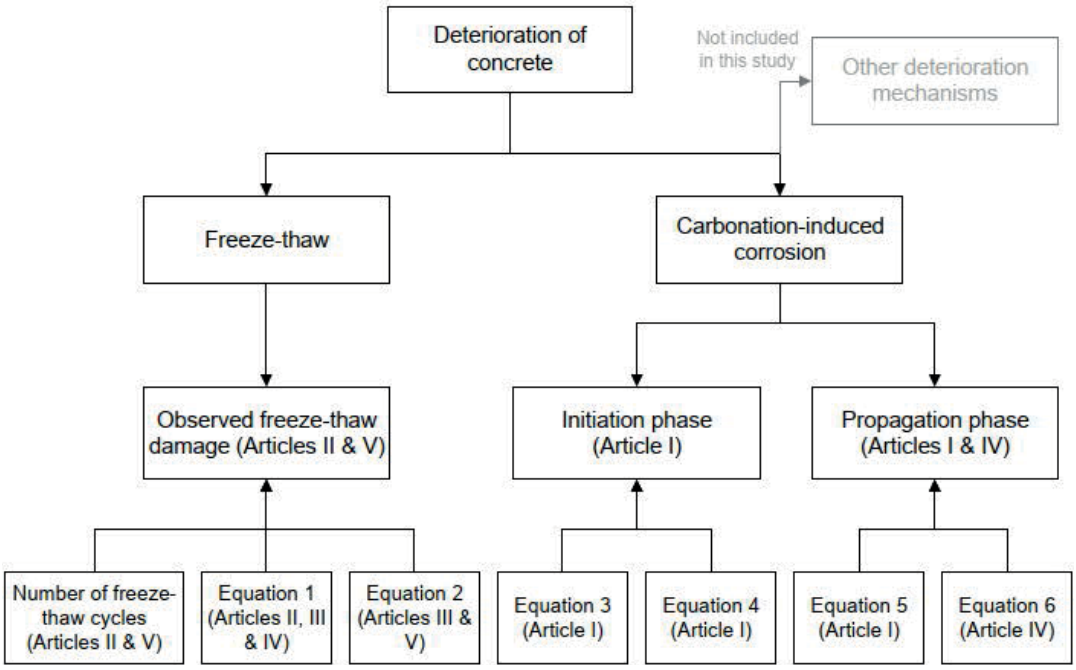

Figure 13 A flowchart of the used methods and their connection to the studied deterioration mechanisms.

4.4 Reliability of the research methods

Research methods have been chosen to give an extensive overview corresponding as good as possible to both Nordic climate conditions and the most common deterioration mechanisms of Nordic concrete structures. In addition, they have been chosen to be accessible within reasonable limits. However, there are multiple error sources in the studies. Most of them are related to climate projections. Only a climate change scenario has been used. The scenario is based on a situation where CO_2 levels increase heavily until the end of the century, so it is a kind of a worst-case scenario. However, it can be taken as a safety factor. Thus, in most of the results, the climate change-based results can be considered a maximum load and studies of present conditions as a minimum load. On the other hand, while the more optimistic scenarios would probably forecast a smaller increase in precipitation, for example, a smaller increase in temperature might lead to a larger number of freeze-thaw cycles in coastal areas.

The models used to estimate the climatic conditions or progress of deterioration do not represent the actual situation at the site. This and former studies have shown that every structure and micro-climate around it are different, even when located close to each other. Therefore, the models are used to compare similar simplified structures and conditions together.

The results should therefore not be taken as a fact of specific location, structure, deterioration rate or climatic condition, but they can be used to make generalised conclusions about the climate change effect on deterioration rate, geographical location dependence, etc. Some of the results mainly considering the climatic conditions can also be generalised to be used as an assistive instrument, for example in the planning process, regardless of the used material.

5 Main results and discussion

5.1 Connection between climatic load and deterioration of concrete in the present climate

5.1.1 Wind-driven rain

Figure 14 and Table 11 show airfield annual index I_A representing the amount of WDR on structures facing different directions. WDR on north-facing facades is significantly lower than on southern-facing ones. In addition, the amount of WDR from the north and northwest does not differ geographically significantly, so the WDR load from northern directions is low and quite similar in all the studied locations.

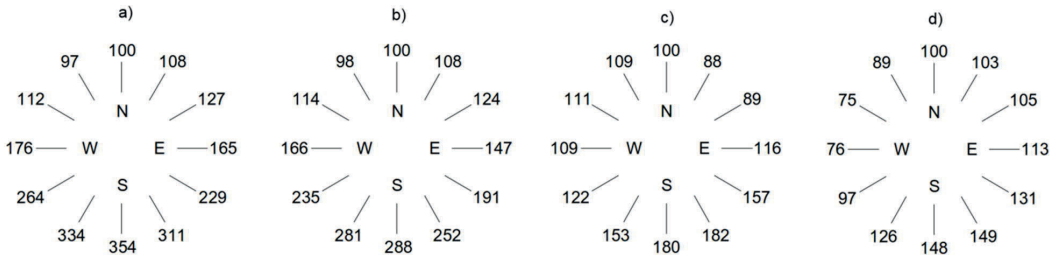

Figure 14 Relative amount of I_A compared to I_A from the north in the present climate from different wind directions in a) the coastal area, b) southern Finland, c) inland and d) Lapland. The reference value 100 is tied to the I_A of each location and thus is not mutually comparable with each other. (Article III)

Table 11 The airfield annual index I_A from different wind directions in the coastal area, southern Finland, inland and Lapland. (Article III)

	Airfield annual index I_A [l/m²]			
Wind direction	Helsinki-Vantaa (coastal area)	Jokioinen (southern Finland)	Jyväskylä (inland)	Sodankylä (Lapland)
North	70	63	67	54
Northeast	81	73	57	56
East	115	93	77	61
Southeast	189	142	115	76
South	247	183	120	79
Southwest	212	166	91	60
West	123	105	72	41
Northwest	70	66	74	44

In the coastal area, in the present climate the I_A is on average 24%, 64% and 135% higher than in southern Finland, inland and Lapland, respectively, while the amount of precipitation is only 12%, 20% and 68% higher. The difference is a consequence of higher wind speed in coastal areas. In the coastal area, 74% of precipitation hits a vertical wall while in southern Finland the share is 66%, in inland 54% and in Lapland 53%. (Article III)

Depending on facade orientation, in the present climate the I_A is 8–36% higher in the coastal area than in southern Finland. The highest difference is from southern directions and the lowest from northern. Compared to the coastal area, the I_A in inland and Lapland is significantly lower from southern directions in the present climate, i.e. 2.3 and 3.5 times lower, respectively, from the south-west direction. (Article III)

In addition, in Article III the WDR stress level on typical 4- and 8-storey blocks of flats in typical Finnish suburbs were studied using the wall annual index I_{WA}, see Equation 2. The results indicated that the highest WDR load in Lapland at the top corner of south-facing facade is almost at the same level as the lowest WDR load in lower parts of the facade in the coastal area, although the latter had another building in front of it reducing the WDR by the obstruction factor. The lower parts of facades inland and in Lapland face less than 10 mm of WDR annually while the top parts of a building in the open coastal area can face over 70 mm of WDR.

5.1.2 Freeze-thaw durability

The success of air-entrainment in the different facade types and balcony structures of buildings built according to present requirements in Finnish Concrete Codes were studied in Article II. The study showed that, although the share of detected damage is very low, air-entrainment has not met the requirements set by the Concrete Codes at the time, see Figure 15 and Figure 16. Only around 50% of facade panels and 60% of balcony structures met the requirements. In addition, the total failure of air-entrainment has been extensive in all of the studied structures, especially in balcony side panels, which are a load-bearing structure and cannot be replaced without tearing apart the entire structure. The low amount of detected failure can be explained by the young age, on average 11 years, of the buildings at the time of the condition investigations.

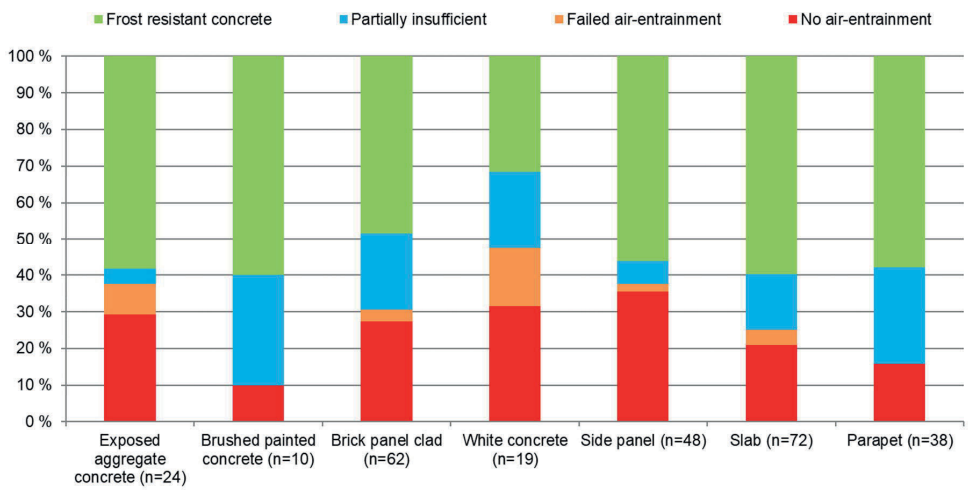

Figure 15 Use of air-entrained concrete in different facade panel types and balcony structures according to the database. The buildings were built between 1990 and 1996. (Article II)

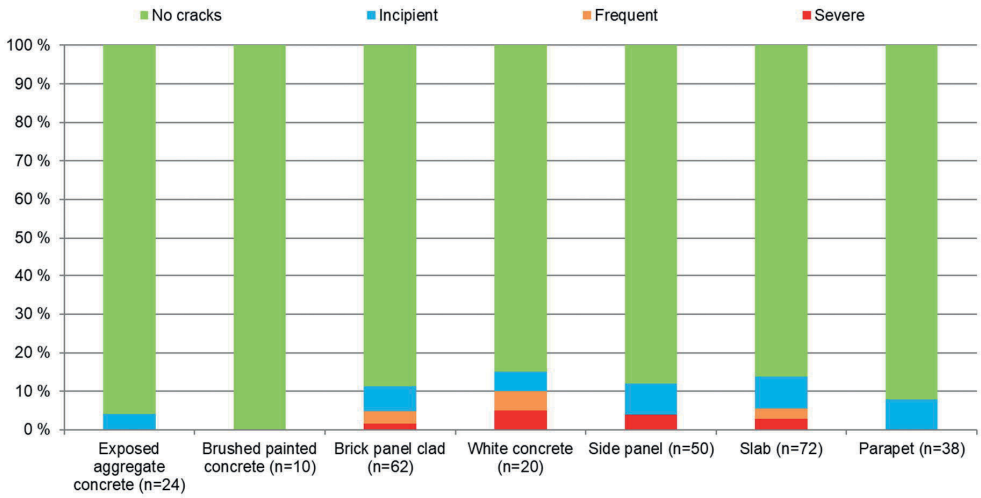

Figure 16 Share of frost damage type indicated by the cracking of concrete of different facade panel types according to thin-section analyses. The buildings were built between 1990 and 1996. (Article II)

The correlation between freeze-thaw damage observed visually or by hammering and WDR load in the present climate was studied in Article V. Based on the condition investigation reports, 81% of far-advanced freeze-thaw damage was located in west-, south-west-, south- and south-east-facing facades. Based on the geographical location, the shares are 88%, 83% and 70% in the coastal area, southern Finland and inland, respectively. In balconies, the share is 84%. However, with balconies it must be taken into account that most of them are located on western and southern facades to maximise the daylight and evening sun. In addition, airfield annual index I_A itself and the amount of it for up to three days before a freezing point crossing were studied. The shares of I_A from west- to southeast directions has been 65% and I_A prior to freeze-thaw events 78%. Both the share of damage and WDR are also location-dependent, hence in coastal area the shares are higher than in inland. Figure 17 and Figure 18 present the findings graphically. As can be seen in the figures, the amount of WDR before freeze-thaw events has a significant relation to freeze-thaw damage observations. (Article V)

An actual case building located in southern Finland with insufficient air-entrainment was studied in Article V. In the case building, far-advanced freeze-thaw damage was recorded in facades and balcony structures in southeast- and southwest-facing facades. Since the building was erected, the total amount of I_A from the same directions was 192 and 207 mm, respectively. In addition, the wall annual index I_{WA} was calculated and implied that freeze-thaw damage has occurred in locations where the amount of I_{WA} was at least 21 mm. (Article V)

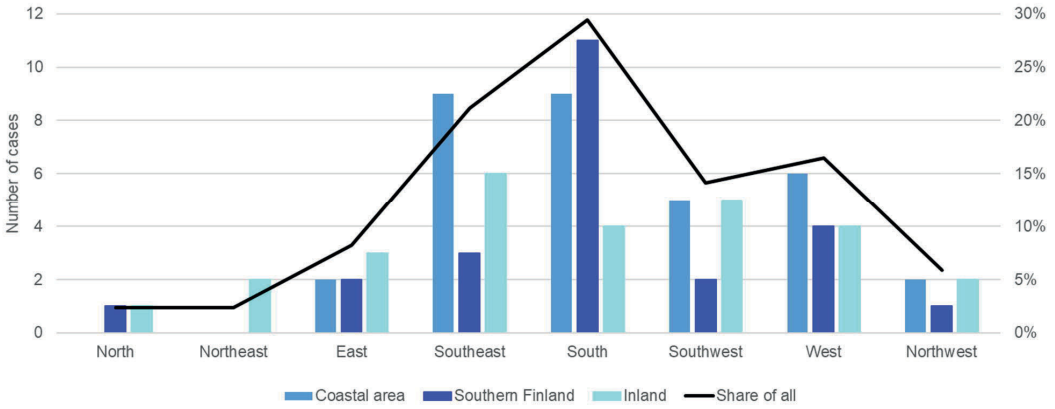

Figure 17 Far-advanced freeze-thaw damage observed in facades facing different directions based on condition investigation data.

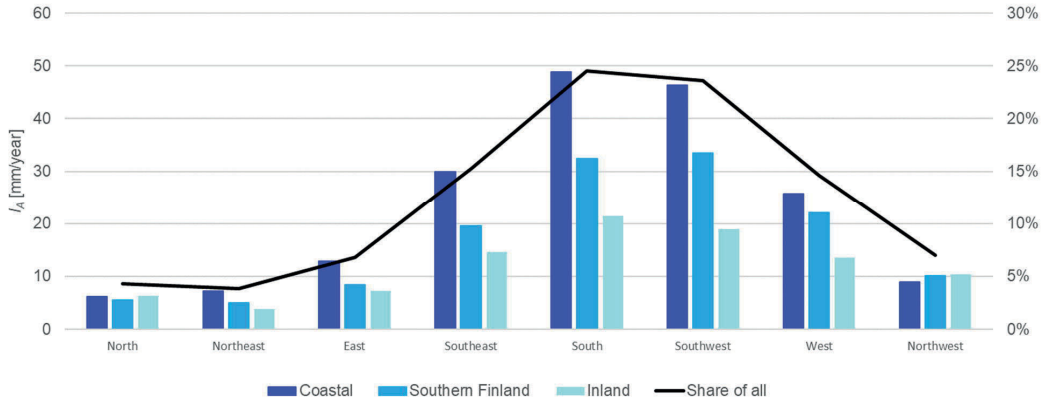

Figure 18 Airfield annual index for up to three days before freezing point crossings with a limit temperature of -5 °C from different directions at the three locations studied.

Both findings of the research imply that even rough estimations of WDR load on facades and balconies could be used to predict the rate of freeze-thaw attack.

5.1.3 Reinforcement corrosion

The initiation of corrosion of reinforcements in facades and balconies in buildings built in 1990–1996 was presented in Article I. The calculations are based on Equation 3. The results indicated that on average 50-year initiation time is achieved by white concrete and brick panel cladding, even with a 10-mm cover depth. Brushed painted concrete needs a sufficient concrete cover. The reason is that the brushing surface treatment leaves the concrete surface more open to carbonation. On average, balcony structures always achieve the 50-year initiation time if the cover depth is > 15 mm except

slab soffit where > 25 mm cover depth is always needed. This is mainly due to an upside-down casting direction, where the soffit surface is floated fresh and thus has poorer compaction. Secondly, the lower surface of the balcony slab is sheltered from the rain, which keeps the surface and pore structure of the concrete dry, allowing easier carbonation. As can be seen Figure 5, the main reinforcement is located in the lower part of the prefabricated balcony slab, so the fast carbonation of the lower surface exposes the reinforcement to the early start of the propagation phase. (Article I)

The modelled corrosion rates of carbonated facade and balcony concrete structures were calculated (Article IV) to compare the effect of season, location and orientation of the structure on the corrosion rate. The calculations were based on the corrosion propagation model by Köliö et al. (2017), see equation 6. The model is based on actual corrosion measurement data combined with actual weather data. According to the study, all the studied factors significantly influenced the corrosion rate. Almost throughout the year, the corrosion rate is the highest in the coastal area followed by southern Finland, inland and Lapland, respectively. Only during the summer months does the order change occasionally. The most significant differences between the locations can be seen in late autumn and winter where the difference in WDR significantly affects the model. The same phenomenon can be seen when the orientation of the structure is examined. The north-facing structures get significantly less WDR load, which can be seen directly in the modelled corrosion rates. Figure 19 and Figure 20 present the difference between the monthly averages of modelled corrosion rate in a carbonated concrete facade based on present climate data.

In southern Finland and inland areas, the monthly changes in corrosion rate are minor. The reason for the low corrosion rate in winter compared to the coastal area is the low temperature and the fact that the form of precipitation is mostly snow. In Lapland, no corrosion can occur in January and February because the temperature stays below 0°C the whole time.

The side panels achieved the highest modelled corrosion rate and balcony slab soffits the lowest. A simple reason for that is once again the amount of WDR and the drying conditions of the structure. The corrosion rate is higher than for facades because side panels are as exposed to WDR as facades, but there is no drying effect of the conduction of interior heat. On the other hand, the slab soffits are sheltered from the direct WDR and the corrosion rate is thus the lowest. Figure 21 presents the difference between the monthly averages of modelled corrosion rates in carbonated side panels and slab concrete based on present climate data. It should be noted that the values of the vertical axis differ from the prior ones, so the results suggest that while the initiation time of a slab soffit is low, the propagation time is long but with side panels it is the opposite.

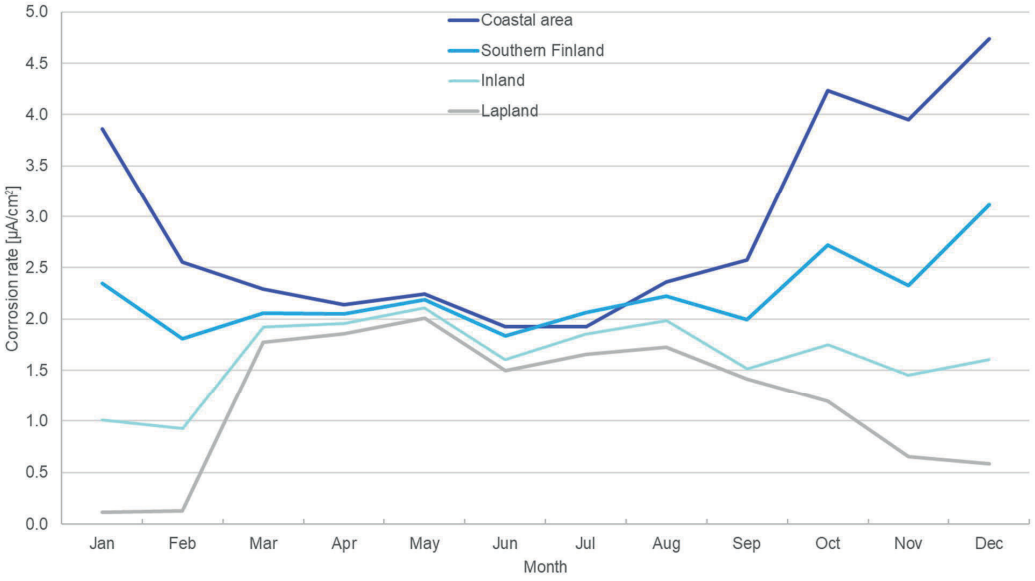

Figure 19 Monthly average of the modelled corrosion rate in carbonated concrete on a south-facing facade.

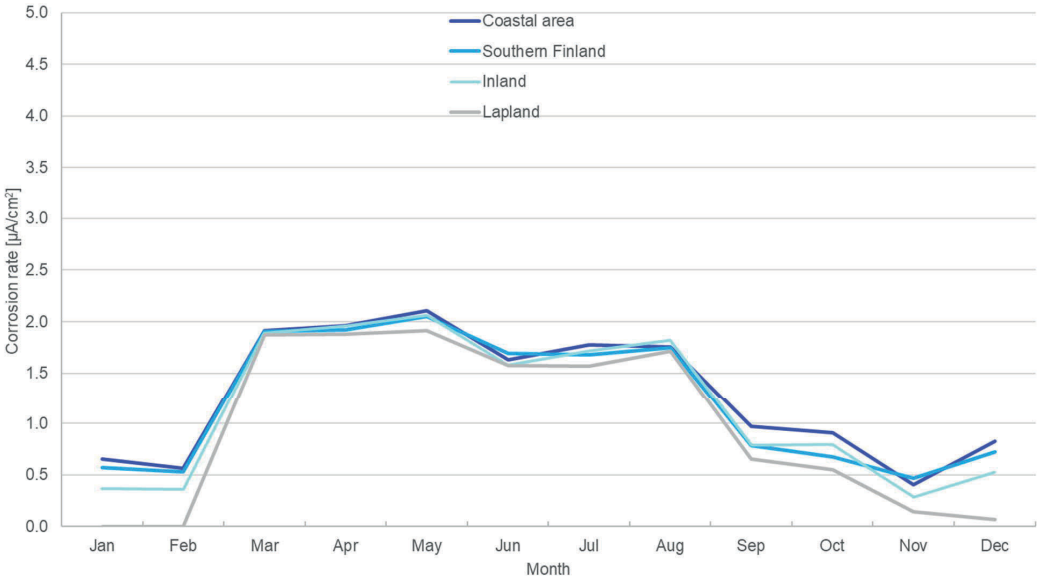

Figure 20 Monthly average of the modelled corrosion rate in carbonated concrete on a north-facing facade.

Figure 21 Monthly average of the modelled corrosion rate in carbonated concrete on south-facing balcony side panels and slab soffits. **Note:** vertical axis differs from prior figures.

The corrosion rates of reinforcements in carbonated concrete in facades and balconies facing the cardinal points are shown in Appendix III.

5.2 Effect of climate change on climatic load

5.2.1 Wind-driven rain

Figure 22 presents the amount of airfield annual index-based simulation of WDR hitting facades facing various directions in the coastal area in present and projected future climates. The numbers at all the studied locations are shown in Appendix IV. As can be seen, the southern facades will face significantly higher amounts of WDR and stress level increases from every direction. (Article II)

The relative increase from different directions compared to the present climate is shown in Figure 23. The I_A will increase on average by 34% in the coastal area, 31% in southern Finland, 44% in inland and 54% in Lapland by the end of the century. At the same time, the amount of precipitation increases 34%, 33%, 47% and 58%, respectively, which indicates that the wind speed during the rain events is not increasing significantly in any location. In the coastal area and southern Finland, the increase of I_A concentrates southern, western and northern winds. In inland and Lapland, the I_A will increase quite evenly from all directions. As a result, southwest-, south- and southeast-facing facades will continue to face the most rain events in the future climate. (Article III)

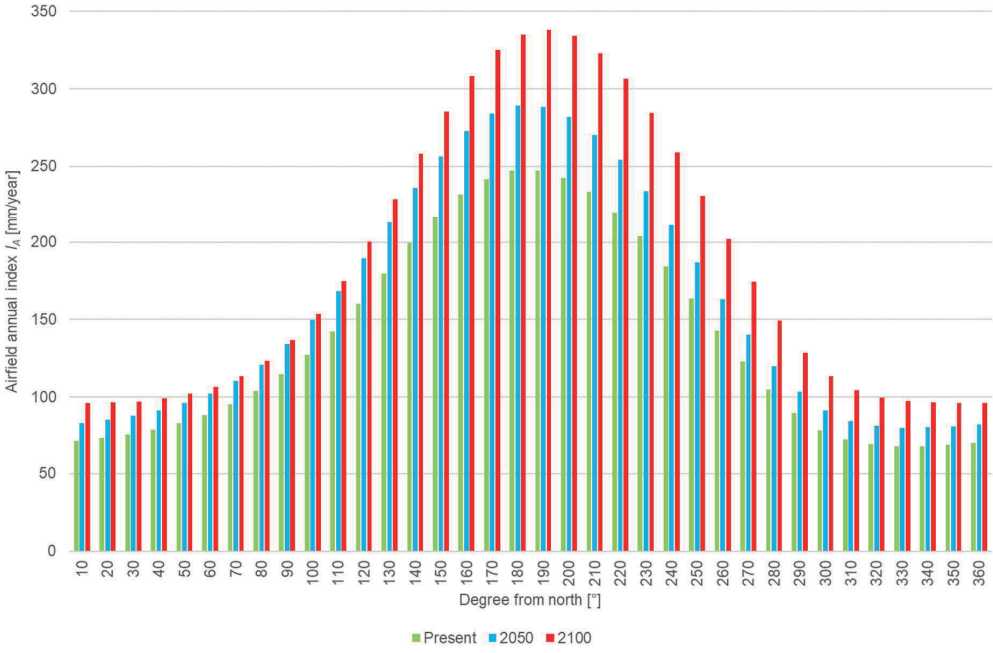

Figure 22 Airfield annual index vs. wind direction of present and future (2050, 2100) climates in the southern coastal area. (Article II)

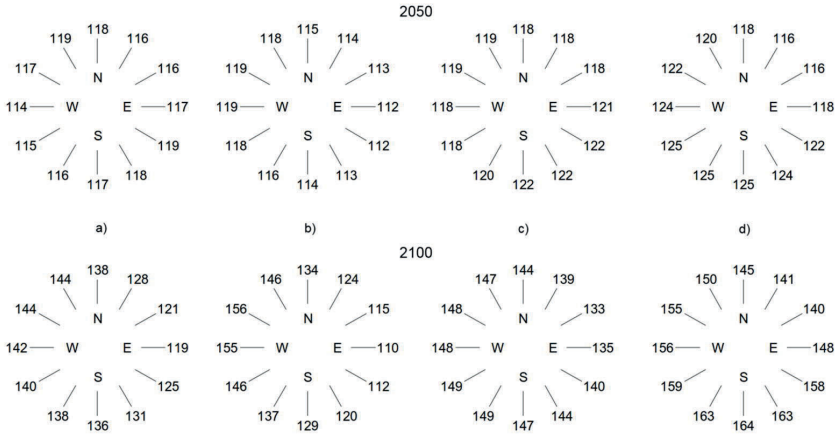

Figure 23 Relative change of I_A at 2050 and 2100 projected climates compared to the present climate from different wind directions in a) the coastal area, b) southern Finland, c) inland and d) Lapland. The reference value 100 is tied up to the I_A in the present climate and thus is not mutually comparable. (Article III)

In addition, the WDR load level on typical 4- and 8-storey apartment buildings in typical Finnish suburbs was studied in Article III using the wall annual index I_{WA}, see Equation 2. The results indicated that at the most stressed point at the top corner of facade I_{WA} is increasing while at the other parts of the facade the increase is not that notable. For example, in the coastal area the increase at the top part of the facade is 15–25 mm/year reaching a maximum value of 95 mm while at lower parts the increase is 5–10 mm/year. Even in the coastal area, the I_{WA} is at present almost negligible at lower parts of the northern facade and most of the eastern and western facades. Even by 2100, the lower parts of the northern and eastern facades will face very small amounts of WDR. At the most stressed parts, i.e. at the top corners of all the facades, the I_{WA} stress level will increase quite evenly in the future climates. In all studied climate projections, I_{WA} on the southern facade in Lapland and on eastern and western facades in inland is quite similar to the northern facade in the coastal area.

5.2.2 Freeze-thaw cycles

The number of freeze-thaw cycles were presented in Article II. In Figure 24, the freeze-thaw cycles with a limit temperature of -5 °C are shown in four different location and divided by the wind direction during the rain events prior to the cycle.

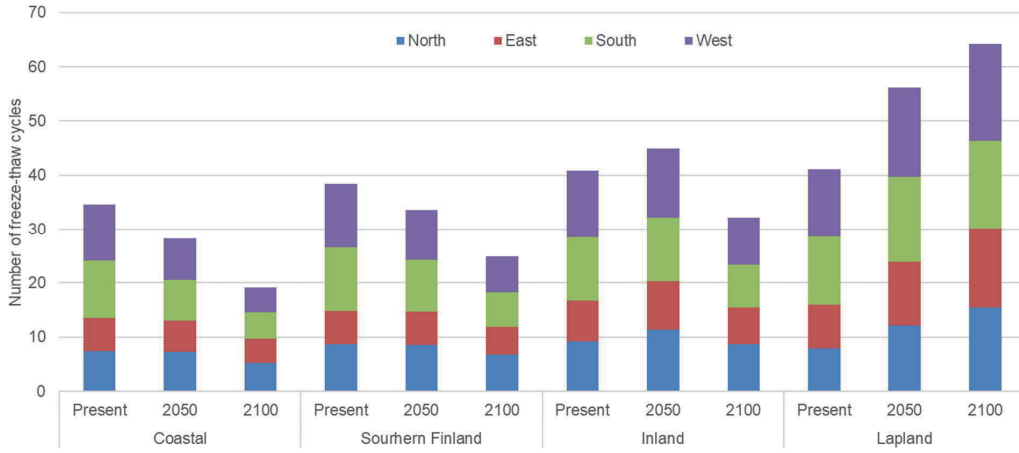

Figure 24 Number of freeze-thaw cycles (-5 °C) up to three days before rain or sleet. The direction shows the wind direction during the rain or sleet events.

The number of freeze-thaw cycles decreases in the coastal area and in southern Finland. In inland, the number of cycles increases at first and decreases when approaching the end of the century. In Lapland, the increase is remarkable.

5.3 Climate change effect on the corrosion of reinforcement

Equation 4 was used to study the effect of increased CO_2 and precipitation on the initiation phase of reinforcement corrosion, i.e. the length of time carbonation took to reach the reinforcement. The used parameters are shown in Table 10. The results are shown in Figure 25.

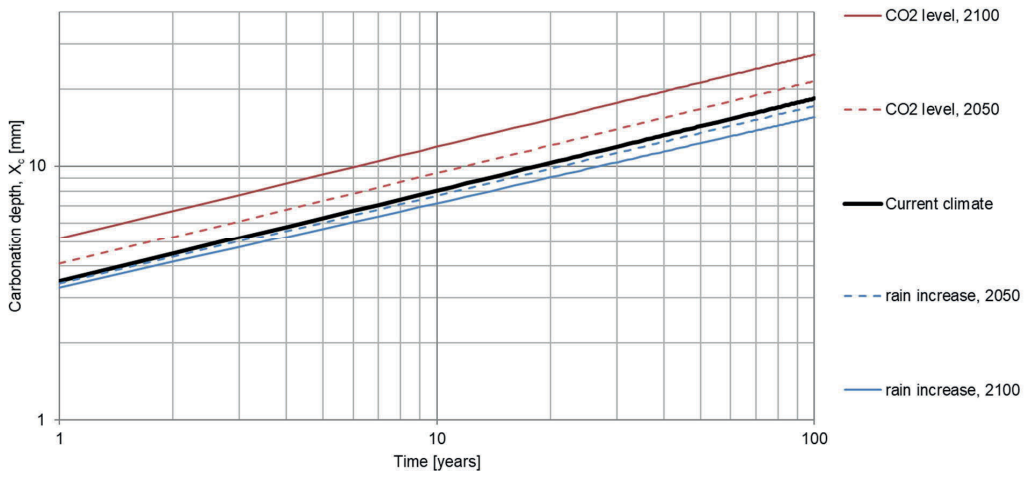

Figure 25 The influence of CO_2 level and increase in precipitation on corrosion initiation by carbonation. It should be noted that the horizontal axis is logarithmic, (Article I)

Increased CO_2 has an accelerating effect on carbonation, and increased precipitation a decelerating one. Based on the method used, increased CO_2 has a greater effect. The increase in rain and sleet will reduce carbonation by 5.7% until 2050 and by 15.4% until 2100. The increase in carbonation by CO_2 level is 17.0% until 2050 and 48.2% until 2100. (Article I)

The amount of WDR has been shown to have a major effect on corrosion rate. In Article I, Equation 3 was used for a rough estimation of the effect of increase in precipitation on the propagation phase, i.e. a crack initiation. The results are presented in Table 12. In addition, the fib Model Code (International Federation for Structural Concrete 2006)-based method for the length of propagation time was studied. The model represents the temperature relationship of active corrosion using a reference propagation time modified by a temperature-related factor. Figure 26 shows the influence of the increase in air temperature induced by climate change.

Table 12 The length (in years) of active corrosion phase in carbonated concrete in respect of crack initiation in different parts of Finland. (Article I)

Climate	Coastal area	Southern Finland	Inland	Lapland
Present	5.7	6.1	8.2	37.5
2050	5.3	5.5	7.4	37.5
2100	5.3	5.1	6.1	19.7

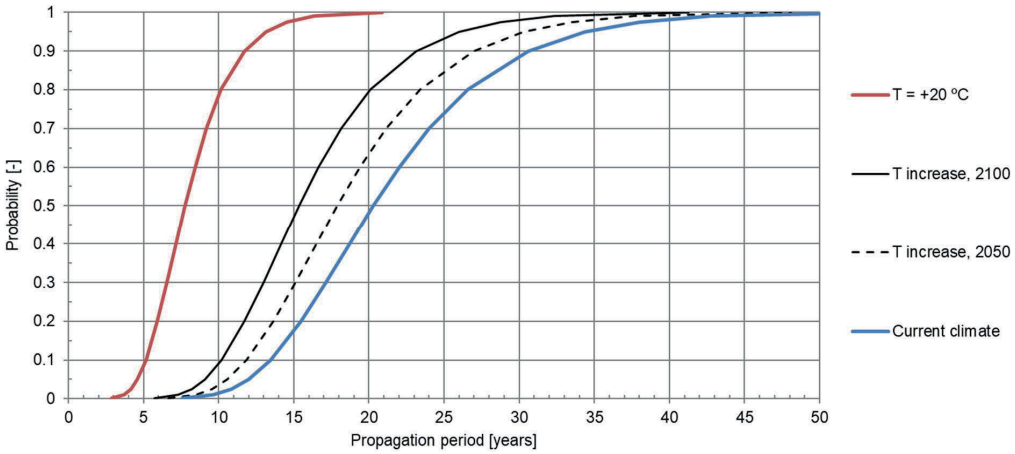

Figure 26 The effect of increase in temperature on the active corrosion of reinforcement in carbonated concrete according to fib 34 (International Federation for Structural Concrete 2006). (Article I)

As can be seen in Table 12, the most significant effect is in inland and Lapland where the propagation time will shorten by 26% and 47%, respectively, by the end of the century. As indicated in Figure 26, the temperature has a major effect on propagation time, but actual corrosion rate measurement-based studies (Mattila & Pentti 2004, Article I, Köliö et al. 2017) have shown that temperature does not have as significant effect as the model suggests, and actual propagation in colder conditions is closer to the +20 °C curve. (Article I)

As mentioned in Chapters 4.2.3.2 and 5.1.3, Köliö et al. (2017) and Köliö's (2016) studies strongly implied that the WDR amount has the greatest effect on the rate of the propagation phase of reinforcement corrosion. The regression-based model Köliö et al. (2017) presented was used in Article IV to estimate the effects of geographical location, direction of orientation of the structures and changing climate on the corrosion rate of facades, balcony side panels and balcony slabs. Some of the results are shown in Table 13 and Figure 27 and Figure 28. More results are shown in Appendix III.

Table 13 presents the average corrosion rates in carbonated concrete facades at all four studied locations, in the directions of the cardinal points and collated as four seasons. Winter consists of the months January, February and December, spring March, April and May, summer June, July and August and autumn September, October and November. Colour highlights are used to classify values as follows: red as very high (⩾3.00 µA/cm²), orange as high (2.00–2.99 µA/cm²), green as moderate (1.00–1.99 µA/cm²) and blue as low (<1.00 µA/cm²) corrosion rate values. Figure 27 shows the monthly average of the modelled corrosion rate in carbonated concrete in the coastal area on south-facing facades and Figure 28 the monthly corrosion rates in the carbonated concrete of south-facing balcony side panels in the coastal area in the 2100 climate. More monthly corrosion rate graphs are presented in Appendix V. (Article IV)

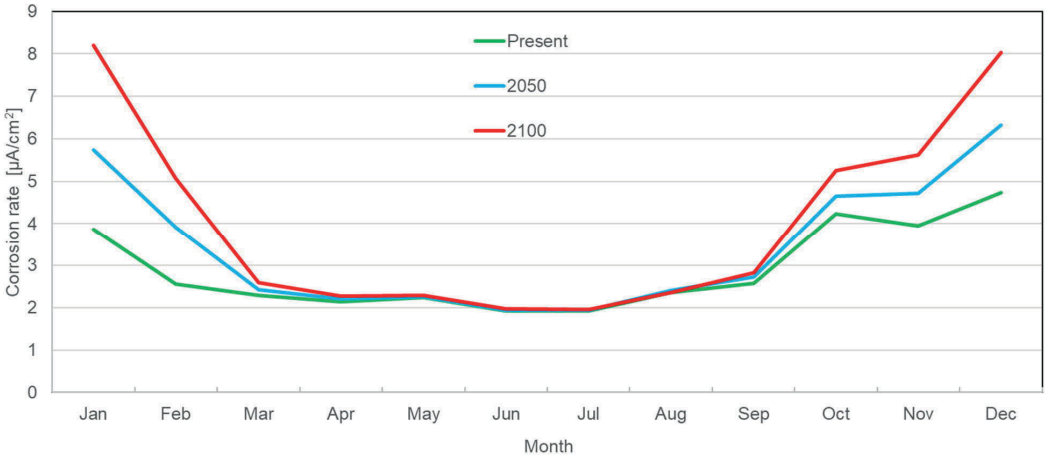

Figure 27 Monthly average of the modelled corrosion rate in carbonated concrete in the coastal area on south-facing facades. (Article IV)

Table 13 An average of the modelled corrosion rate [μA/cm²] of facade reinforcement at four geographical locations (C = coastal, S = southern Finland, I = inland, L = Lapland) in the present climate and in projected future climates. (Article IV)

		North			East			South			West		
		Present	2050	2100	Present	2050	2100	Present	2050	2100	Present	2050	2100
Winter	C	1.24	1.32	1.72	1.44	1.94	2.48	2.42	4.02	5.28	1.73	2.23	2.85
	S	1.00	1.25	1.60	1.10	1.44	1.88	2.07	2.81	3.70	1.63	2.03	2.69
	I	0.87	1.15	1.55	0.94	1.41	1.98	1.29	2.01	2.96	1.04	1.39	1.88
	L	0.62	0.84	1.21	0.59	0.90	1.39	0.67	1.22	2.02	0.65	0.95	1.38
Spring	C	1.90	1.84	1.88	1.84	1.97	2.00	2.10	2.14	2.18	1.93	1.75	1.80
	S	1.89	1.84	1.87	1.81	1.91	1.93	2.02	2.04	2.07	1.87	1.73	1.77
	I	1.87	1.85	1.92	1.66	1.80	1.83	1.89	1.91	1.79	1.86	1.72	1.78
	L	1.79	1.83	1.91	1.66	1.82	1.91	1.79	1.84	1.90	1.70	1.60	1.66
Summer	C	1.50	1.47	1.48	1.62	1.67	1.56	2.29	2.35	2.38	1.64	1.60	1.77
	S	1.40	1.37	1.39	1.50	1.52	1.39	2.10	2.12	2.12	1.62	1.60	1.81
	I	1.44	1.42	1.44	1.45	1.50	1.42	1.78	1.81	1.83	1.45	1.39	1.49
	L	1.31	1.32	1.35	1.34	1.39	1.39	1.60	1.61	1.66	1.26	1.19	1.24
Autumn	C	0.71	0.98	1.28	1.64	2.12	2.13	4.31	5.23	6.30	1.84	2.19	2.92
	S	0.62	0.84	1.05	1.11	1.38	1.39	2.72	3.30	3.84	1.51	1.93	2.68
	I	0.53	0.83	1.22	0.90	1.27	1.59	1.60	2.20	2.93	0.77	1.09	1.56
	L	0.25	0.46	0.81	0.41	0.71	1.11	0.81	1.27	1.97	0.34	0.59	0.92

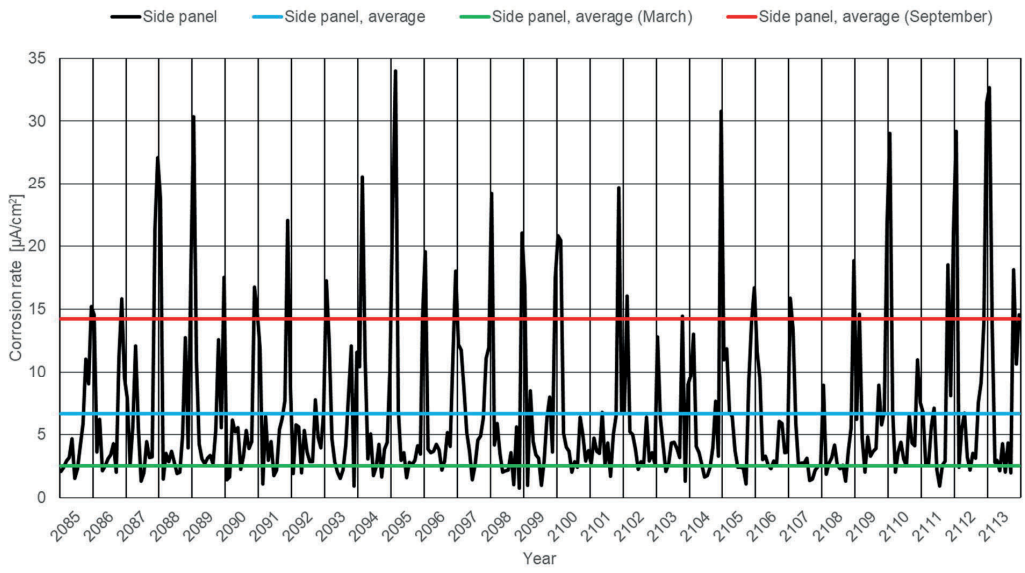

Figure 28 Monthly corrosion rates in the carbonated concrete of south-facing balcony side panels in the coastal area in the 2100 climate. (Article IV)

The results indicate that, in all studied climates, winter and late autumn are the most critical seasons for corrosion rate, not just because of the amount of WDR but also because the amount of solar radiation is and will be low. Thus, conditions for structures to dry are weak, i.e., low solar radiation and high outdoor relative humidity. Based on the future climate scenarios, the relative amount of WDR increases the most in winter and late autumn because a greater share of precipitation will be in the form of rain and sleet instead of snow. The same observation can be seen throughout the studied locations, but first in the southern coastal area because the increasing average temperature reaches the 0°C limit during winter sooner than in northern parts. (Article (IV)

On south-facing facades, the conditions for active corrosion will be quite similar in 2050 in southern Finland and in 2100 in inland compared to present conditions in the coastal area. In Lapland, conditions will reach present conditions in inland in 2050 and present conditions in southern Finland in 2100. On north-facing facades, the corrosion rate will remain almost at the present level at every location and stay significantly lower than south-facing facades. The main reason for both is the significantly lower amount of the WDR from northerly directions, both in present and future climates. (Article (IV)

Even in Lapland at 2100, significantly high corrosion rates can occur in south-facing side panels. In southern Finland, the corrosion rates are already high in south-facing panels in every season and will also be high in east- and west-facing panels in 2100. In the coastal area in the present climate, the corrosion rates are relatively low in winter and autumn, but will increase significantly in the 2100

climate. In coastal area in 2100, the corrosion rate in side panels will be very high throughout the year and in panels facing in every direction. Article (IV)

The corrosion rates in balcony slab soffits are fractions of the values in facades and side panels in every studied case because the soffit is sheltered from WDR. In addition, this indicates the quite minor effect of the RH of outdoor air on reinforcement corrosion in carbonated concrete. There will be an increase in corrosion rates until 2100, however, only the highest corrosion rates in the coastal area will reach the lowest rates in all studied facade cases. (Article IV)

The monthly corrosion studies presented that peaks may be high in the present climate but, in most of the cases, the time period of a peak is not very long. However, while the corrosion rate peaks will be significantly higher in the future climate for facades and side panels, the time period of high corrosion rates will extend due to an increase in the moderate corrosion rates of the present climate in late winter and early autumn. The longer high corrosion rate periods may have a major effect on the propagation phase of reinforcement corrosion. (Article (IV)

5.4 Climate change effect on the freeze-thaw attack

Based on the Lahdensivu's (2012) studies, more freeze-thaw cycles were needed in inland than in the coastal area for freeze-thaw damage to occur, see Table 3. The duration to reach such a number of cycles in present and future climates was calculated from climate data in Article II. The results are presented in Table 14. Based on the results, outdoor conditions where concrete freezes wet will ease considerably already by 2030 in coastal Finland. The inland outdoor climate will remain at the present level and conditions will get even harder with increasing amounts of rain and sleet almost to the end of century. The complete failure of the air-entrainment of fresh concrete (protective pore ratio <0.10) will surely lead to frost damage in concrete structures before the end of the eligible service life of the structure (usually at least 50 years). On the other hand, the results also show that in practice, concrete structures without freeze-thaw resistance still have an initiation time of decades. (Article II)

However, not only the freeze-thaw cycles after a rain event are noteworthy but also the amount of WDR before the cycle plays a significant role. Figure 24 shows that the number of freeze-thaw cycles is decreasing significantly in the coastal area and southern Finland, changing not by much in inland and increasing in Lapland. Figure 29 and Figure 30 present the changes in average amounts of WDR before the events annually and per crossing, respectively. The numbers are comparable with the frost decay exposure index (FDEI) presented in Chapter 4.2.1 but airfield annual index I_A is used instead of driving rain exposure index I_θ (Rydock et al. 2005).

Table 14 Time that it takes in the present and different future climates for incipient frost damage to show in thin-section analyses with different temperature thresholds and rain or sleet up to 2 days before threshold exceedance (in the case of no air-entrainment). (Article II)

Climate at the year of construction	Coastal area [years]		Inland [years]	
	t ⩽ -5 °C	t ⩽ -10 °C	t ⩽ -5 °C	t ⩽ -10 °C
2000	26	35	37	45
2030	40	61	40	58
2050	50	78	41	59
2100	79	350	53	90

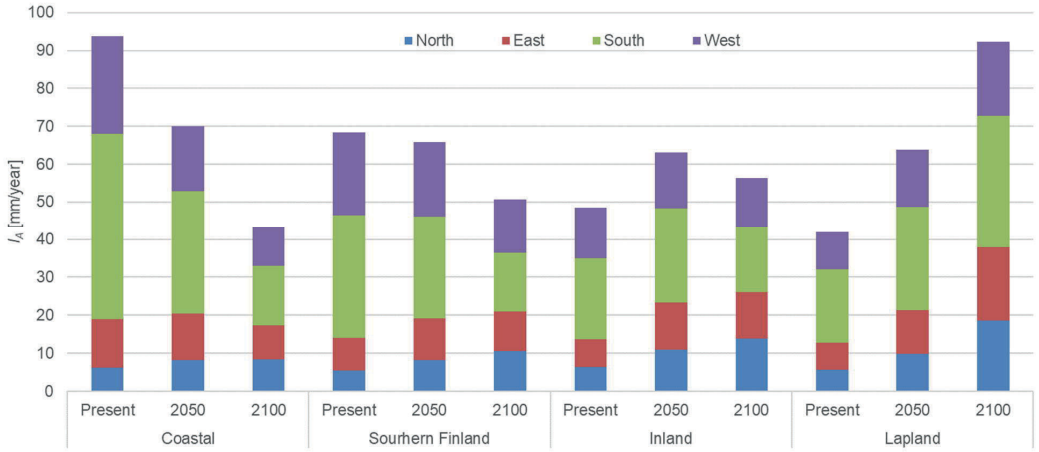

Figure 29 Annual average amount of I_A up to three days before FPC. The direction shows the wind direction during the rain or sleet events.

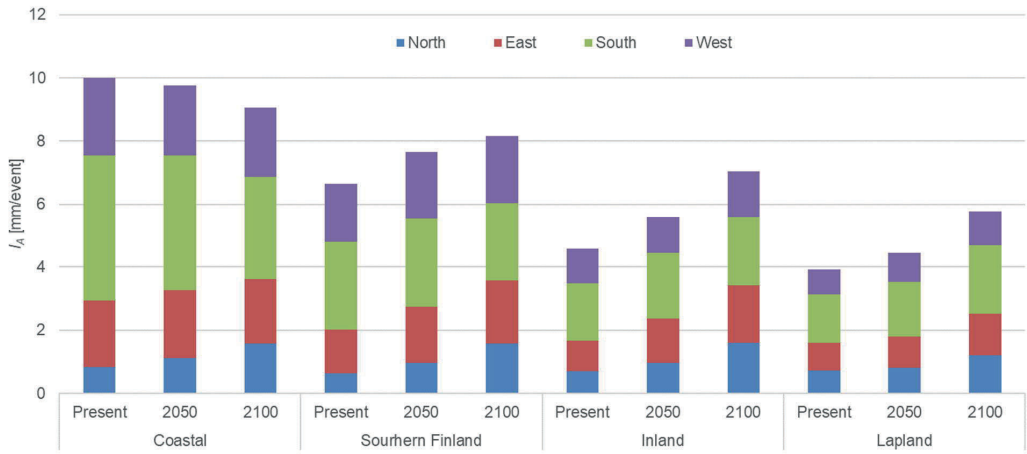

Figure 30 Average amount of I_A up to three days before an FPC (-5 °C). The direction shows the wind direction during the rain or sleet events.

As can be seen, the annual level of WDR prior to freeze-thaw cycles is still decreasing significantly in the coastal area and by the end of the century in southern Finland. In inland and Lapland, the level is increasing. If the wind direction during the rain events is taken into account, the level of WDR load before crossings is becoming more evenly distributed. For example, in coastal area and southern Finland, conditions on south-facing structures are getting easier and staying quite the same in other directions while, in inland and Lapland, the conditions are getting harsher for north-facing structures and staying quite the same in other directions. When studying average WDR load before a single crossing, the load is actually becoming heavier in all locations except in the coastal area where it is going to stay almost at the current level.

The results imply that the intensity of freeze-thaw attack is not decreasing as much as it seems to if only the number of freeze-thaw cycles after rain event is taken into account. In addition, the intensity might be more evenly distributed in the future climate and not as focused on south- and west-facing structures as it is in the present climate. On the other hand, although the number of freeze-thaw cycles is increasing significantly in Lapland, the intensity of a cycle is not as high as in other parts of Finland.

6 Conclusions

6.1 The outcomes of the research

The relevance of the study was indicated in two ways: the amount and state of existing buildings and the quality of concrete structures in buildings built according to requirements corresponding to present requirements. The majority of existing Finnish blocks of flats building stock was built during the time when quality requirements were not even at the level of need of the current climate. Thus, they are in state of renovation need or close to it. In addition, there has been significant lack of quality in both the success of air-entrainment and cover depths, which also exposes younger buildings to worsening climate conditions. However, the study has also shown that, even with insufficient quality, the concrete structures have a significantly longer service life than service-life calculation methods presented in Finnish Concrete Codes predict. For example, insufficiently air-entrained concrete may have a service life of decades in the present climate before incipient freeze-thaw damage occurs.

The research has confirmed that climate change is going to intensify most of the critical climate conditions for the studied concrete facade and balcony structures. The most critical increase in climate load will be in WDR, which will be significant because free water and humidity in pore structures are included in almost all the deterioration mechanisms. According to the climate change scenario A2 used in this study, the increase in the average amount of WDR until the end of the century will be 31%–54%. The lowest increase is in southern Finland and the highest in Lapland.

The climate load is highly concentrated from certain directions, mainly based on the west to south-east wind direction during rain events. Thus, southern-facing structures have at present and will have in the future climate much higher climatic loads. In the coastal area, a south-facing structure faces 3.5 times higher WDR load than north-facing ones. The same number in southern Finland, inland and Lapland is 2.9, 1.8 and 1.5, respectively. Higher WDR load greatly affects the intensity of freeze-

thaw attack and the propagation phase of reinforcement corrosion. For example, 81% of far-advanced freeze-thaw damage has occurred in west- to southeast-facing facades in the present climate. At the same time, the share of WDR before freeze-thaw cycles has been 78%. Both of the shares are highest in the coastal area and decrease in the northern and inland locations. The results imply that even the rough estimations of both the amount of WDR and especially WDR before freeze-thaw cycles could be used to estimate the rate and intensity of freeze-thaw attack.

Based on the used scenario, climate change will reduce the number of freeze-thaw cycles closely after exposed to wind-driven rain or sleet in coastal area and southern Finland until the end of the century. In inland, the number of freeze-thaw cycles increases until 2050, then falls until the end of the century. In Lapland, the number of freeze-thaw cycles after rain or sleet increases significantly. Almost the same pattern can be expected with the average annual amount of rain or sleet before the freeze-thaw cycles. However, the study also showed that the intensity of a freeze-thaw cycle, i.e. amount of WDR before a cycle, is not decreasing significantly even in the coastal area and is actually increasing in all other parts. The intensity of a freeze-thaw cycles is also lowest in Lapland although the amount of FPCs is the highest. The amount of WDR itself is increasing quite evenly from different wind directions, except in coastal and southern Finland where the increase is far greater from western than eastern winds.

In addition, based on a model used in a study, the propagation phase of reinforcement is highly related to the direction in which the facade is facing. North-facing facades are more protected from WDR, so the corrosion rate is significantly lower than in south-facing facades. The balcony side panels have the highest corrosion rate because of their weaker ability to dry during the most intense WDR season in autumn and early winter. At the same time, balcony slab soffits are sheltered from direct WDR and thus, their corrosion rate is remarkably low. Climate change will increase the corrosion rate significantly, especially during the periods when the conditions for structures to dry are weak, i.e. in autumn and early winter when the amount of solar radiation is low and relative humidity outdoor is high. At the same time, the relative amount of WDR is increasing the most in winter and late autumn because a greater share of precipitation is in the form of rain and sleet instead of snow.

Geographical location has at the very least the same or even a greater effect on deterioration rates than the direction in which structure is facing. For example, in the present climate, it has taken significantly less time for freeze-thaw damage to occur in the coastal area than inland. The effect was also shown to be considerable in corrosion rates, which are highest in the coastal area and the lowest in Lapland. Once again, the amount of WDR has the greatest effect on both. The amount of WDR in the form of rain and sleet is 24%, 64% and 135% higher than in southern Finland, inland and Lapland, respectively. The amount of precipitation is only 12%, 20% and 68% higher, respectively. The difference is due to the higher wind speed in coastal areas. Until the end of the century, the difference will slightly flatten out because the increase is on average 34% in coastal area, 31% in southern Finland, 44% in inland and 54% in Lapland. The geographical dependence is significant

because, as can be seen in Figure 3, a considerable share of Finnish existing building stock is located in the coastal area or southern Finland where the climatic load is and will be the most severe. On the other hand, the share of buildings in Lapland is very low.

The effect of climate change on carbonation, i.e. the initiation time of reinforcement corrosion, was studied less extensively. A model used in the study predicted that the increase in CO_2 levels will increase carbonation depth by 17% in the 2050 climate and 48% in the 2100 climate. However, at the same time the increase in rain and sleet will reduce carbonation by 5.7% and 15%, respectively. If the results are combined with the results of concentrated WDR from certain directions, it can be concluded that the CO_2-level increase will significantly affect structures with less WDR, such as balcony slabs and north-facing structures. On the other hand, the higher amount of WDR in the coastal area and southern-facing structures can even out the effect of CO_2-level increase. Based on the research, reinforcement corrosion is a mixture of either the long initiation time and short propagation time of facades and side panels or short initiation time and very long propagation time of slab soffits. While corrosion-induced service life consists mostly of initiation time, the total service life of slab soffits can be considered to be shortening, and the service life of other structures to remain quite the same.

It should be noted that buildings built after the research material presented in these studies should have a higher concrete grade and lower water-cement ratio and thus better resistance to the presented deterioration mechanisms of lower grade concrete with a relatively high water-cement ratio. However, the existing building stock is a major part of a Finnish national property. The research has shown that concrete that meets the requirements will continue to reach an eligible service life in the future climate. Even the existing concrete structures of low quality can have a reasonable service life, especially when protected from the highest climate load. In addition, the research implied that if the concrete lacks quality, the time from initiation to larger scale deterioration is short both in freeze-thaw- and reinforcement corrosion-induced deterioration mechanisms. Thus, adequately frequent condition investigations will have an even more important role in the future so that the state of the deterioration can be detected and the timing of renovation better planned.

Climate change will bring higher climatic load, not only for concrete but also for all other outdoor facing building materials. Throughout Finland, the increase is the highest in WDR, especially during the times of the year when drying conditions are poor because of lack of solar radiation and high relative humidity. At the same time in modern buildings, the insulation layer is thicker and thus, the outer layer of facades does not dry in winter the same way as in old buildings with less thermal insulation by the conduction of indoor heat. In addition to the effect on deterioration mechanisms and their rate, the increase in WDR and poorer drying conditions may lead to an increase in aesthetical issues, such as algae growth on the surfaces.

The results of this study can be used to target both the actual methods used in renovation and preventative maintenance methods. The climate load is shown to be both geographical and wind

direction-related, which can be taken into account, for example, when selecting the materials or during planning process. Structures or materials with proven durability against the major climatic factors can be targeted at the facades or parts of facades with the highest climate load. The structures can be effectively protected against climatic factors, for example by sheltering the highly loaded top parts of the buildings with eaves, and balconies with eaves and glazing. The climatic load can also be reduced by regional planning, which takes into account the protection given by other buildings, forests, topography, etc. In addition, a shorter maintenance cycle for outdoor exposed structures can be directed at west- to southeast-facing structures. However, it should be noted that every location and building is different and should be managed together with its close environment and the microclimate it produces.

6.2 The need for further research

As mentioned in Chapter 4.4, both the methods and the data used in this study have multiple error sources. However, as a state-of-art study, this thesis can be considered as a basis for further research. One of the main aspect in further research is narrowing down the uncertainties in different parts of this study. Based on the research carried out in this thesis, the main needs for future research are:

The effect of different climate change scenarios

In this study, only one climate change scenario was used. The scenario was based on a kind of worst-case scenario in which the CO_2 level is predicted to increase significantly. The main reason for the need to study other scenarios is that, even though the projected CO_2 level may be lower, the effect on, for example, the number of freeze-thaw cycles or the duration of the initiation time of reinforcement corrosion might not decrease, which might have an increasing effect on climatic load.

The follow-up of current climate and projections

The period of the first projections based on the scenarios used in this study is closing. Thus, it could be studied what has been the actual change. The climate data used in such studies should always be at least a 30-year period as shorter periods are not reliable, but a follow-up could give an overview of what can be expected. In addition, new projections are being studied all the time and thus, they could be used to study how the deterioration rates might change compared to this research.

The modelling of freeze-thaw damage

Modelling methods for freeze-thaw damage are still unreliable and lacking usable methods, especially for existing low-quality concrete. The actual deterioration data used in this research could be

combined more sophisticatedly with the actual climate data to produce a model of the progress of freeze-thaw attack.

Climate change effect on the length of the initiation period

The effect of climate change on the initiation time of reinforcement corrosion was not studied extensively in this research, but the methods for modelling it and the amount of data available on the actual carbonation rate could be combined to produce more precise studies.

The combined effect of different deterioration mechanisms

In practice, deterioration mechanisms do not act independently, but combine with and affect each other. For example, cracking caused by freeze-thaw damage locally accelerates carbonation and, through an increase of water, the corrosion process. On the other hand, cracking caused by reinforcement corrosion increases the water absorption in concrete and thus the risk of freeze-thaw damage. The deterioration rate of a degraded concrete should therefore be studied to estimate the effect on actual service life, especially in a future climate with a higher WDR load.

The climate change effect on the deterioration rate of other outdoor exposed structures and materials

As mentioned in the introduction, there is a vast amount of other facade materials such as wooden structures and renderings, the deterioration mechanisms and rate of which could be studied in the same way as concrete in this research. A common denominator in terms of the climatic load with all materials in use is the increase in WDR.

Different ways to protect from the climate load

There have also been quality problems with renovation methods and materials. Reliable and fault-tolerant renovation materials and systems should be surveyed extensively to ensure their effectiveness in lengthening the service life of existing buildings facing the changing climate.

Cost-effective adaptation

This study does not take a stand on the economical point of view. However, the results can be used also for economical examination to assess the both economically and durability-wise sustainable adaptation to climate change.

References

Ahmad, S. 2003. Reinforcement corrosion in concrete structures, its monitoring and service life prediction – a review. Cement and Concrete Composites, 25, Pp. 459–471.

Aïtcin, P.-C., Mindess, S. 2011. Sustainability of concrete. Oxon: Spon Press. 301 p.

Ala-Outinen, T., Harmaajärvi, I., Kivikoski, H., Kouhia, I., Makkonen, L., Saarelainen, S., Tuhola, M., Törnqvist, J. 2004. Ilmastonmuutoksen vaikutukset rakennettuun ympäristöön [Impacts of climate change on built environment]. VTT Tiedotteita – Research Notes 2227. 83 p. + 6 app. (in Finnish)

Almås, A.J., Lisø, K.R., Hygen, H.O., Øyen, C.F., Thue, J.V. 2011. An approach to impact assessments of buildings in a changing climate, Building Research & Information, 39(3), Pp. 227–238.

Andrade, C., Castillo, A. 2003. Evolution of corrosion rate of reinforcements. Construction and Building Materials, 15, Pp. 141–145.

Ann, K.Y., Pack, S.-W., Hwang, J.-P., Song, H.-W., Kim, S.-H. 2010. Service life prediction of a concrete bridge structure subjected to carbonation. Construction and Building Materials, 24(8), Pp. 1494–1501.

ASTM C856-18a. 2018. Standard Practice for Petrographic Examination of Hardened Concrete, ASTM International, West Conshohocken, PA. 15 p.

Auld, H., Klaassen, J., Comer, N. 2007. Weathering of Building Infrastructure and the Changing Climate: Adaptation Options. 2006 IEEE EIC Climate Change Technology Conference 10-12 May 2006, EICCCC 2006, Pp. 1–11.

Bastidas-Arteaga, E. 2018. Reliability of Reinforced Concrete Structures Subjected to Corrosion-Fatigue and Climate Change. International Journal of Concrete Structures and Materials, Volume 12, Article 10, 13 p.

Bastidas-Arteaga, E., Chateauneuf, A., Sánchez-Silva, M., Bressolette, P., Schoefs, F. 2010. Influence of weather and global warming in chloride ingress into concrete: A stochastic approach. Structural Safety 32(4), Pp. 238–249.

Bastidas-Arteaga, E., Stewart, M.G. 2015. Economic Assessment of Climate Adaptation Strategies for Existing RC Structures Subjected to Chloride-Induced Corrosion. Structure and Infrastructure. Behavioural Science and Public Health Titles, 12(4), Pp.432–449.

Bastidas-Arteaga, E., Stewart, M.G. 2016a. Damage risks and economic assessment of climate adaptation strategies for design of new concrete structures subject to chloride-induced corrosion. Structural Safety 52(PA), Pp. 40–53.

Bastidas-Arteaga, E., Stewart, M.G. 2016b. Economic Assessment of Climate Adaptation Strategies for Existing RC Structures Subjected to Chloride-Induced Corrosion. Structure and Infrastructure Engineering 12(4). Pp. 432–449.

Benítez, P., Rodrigues, F., Talukdar, S., Gavilán, S., Varum, H., Spacone, E. 2019. Analysis of correlation between real degradation data and a carbonation model for concrete structures. Cement and Concrete Composites, 95, Pp. 247-259.

Blocken, B., Carmeliet, J. 2002. Spatial and temporal distribution of driving rain on a low-rise building. Journal of Wind and Structures, 5(5), Pp. 441–462

Blocken, B., Carmeliet, J. 2004. A review of wind-driven rain research in building science. Journal of Wind Engineering and Industrial Aerodynamics, 92(13), Pp. 1079-1130.

Blocken, B., Carmeliet, J. 2007 On the errors associated with the use of hourly data in wind-driven rain calculations on building facades. Atmospheric Environment, 41(11), Pp. 2335–2343.

Blocken, B., Carmeliet, J. 2010. Overview of three state-of-the-art wind-driven rain assessment models and comparison based on model theory. Building and Environment, 45, Pp. 691–703.

Blocken, B., Dezsö, G., van Beeck, J., Carmeliet, J. 2010. Comparison of calculation models for wind-driven rain deposition on building facades. Atmospheric Environment, 44, Pp. 1714–1725.

Broomfield, J. 2007. Corrosion of Steel in Concrete (2nd edition). Taylor & Francis, Oxon. 277 p.

Choi, E.C.C. 1994. Determination of wind-driven rain intensity on building faces. Journal of Wind Engineering and Industrial Aerodynamics, 51, Pp. 55–69.

Concrete Association of Finland. 2019. by 42 Betonijulkisivun kuntotutkimus [Condition assessment manual of a concrete facade]. Vaasa, The Concrete Association of Finland. 136 p. (in Finnish)

de Larrard, T., Bastidas-Arteaga, E., Duprat, F., Schoefs, F. 2014. Effects of climate variations and global warming on the durability of RC structures subjected to carbonation. Civil Engineering and Environmental Systems 31(2). Pp. 153–164.

Dino, I.G., Akgül, C.M. 2019. Impact of climate change on the existing residential building stock in Turkey: An analysis on energy use, greenhouse gas emissions and occupant comfort. Renewable Energy, 141, Pp. 828–846.

DuraCrete. 2000. Probabilistic performance based durability design of concrete structures. The European Union – Brite EuRam III, DuraCrete. Final technical report of duracrete project, document BE95-1347/R17. CUR, Gouda, Nederland.

European Commission. 2013a. The EU Strategy on adaptation to climate change. 4 p.

European Commission. 2013b. SWD Report 137, Adapting infrastructure to climate change. European Commission, Brussels. 37 p.

European Commission. 2018a. SWD Report 460, Adaptation preparedness scoreboard country fiches accompanying the document. European Commission, Brussels. 743 p.

European Commission. 2018b. SWD Report 461, Evaluation of the EU Strategy on adaptation to climate change. European Commission, Brussels. 225 p.

Fagerlund, G. 1977. The critical degree of saturation method of assessing the freeze/thaw resistance of concrete. Tentative RILEM recommendation. Prepared on behalf of RILEM Committee 4 CDC. Materiaux et Constructions, no 58. Pp. 217–229.

Fagerlund, G. 2004. A service life model for internal frost damage in concrete. Lund Institute of Technology, Division of Building Materials. Lund. Report TVBM-3119. 138 p.

FMI. 2019. Greenhouse gases concentrations. Retrieved June 4th 2019, from https://en.ilmatieteenlaitos.fi/ghg-concentrations.

Government of Canada. 2011. Federal Adaptation Policy Framework, Environment Canada. Gatineau, QC.

Guiglia, M., Taliano, M. 2013. Comparison of carbonation depths measured on in-field exposed existing R.C. structures with predictions made using fib Model Code 2010, Cement and Concrete Composites, 38, Pp. 92–108.

Gupta R., Gregg, M. 2012. Using UK climate change projections to adapt existing English homes for a warming climate. Building and Environment, 55, Pp 20–42.

Hrabovszky-Horváth, S. 2014. The assessment of refurbished reinforced concrete buildings in point of the climate change, Advanced Materials Research, 899, Pp. 440–445.

HSY. 2017. Pääkaupunkiseutu sopeutuu ilmastonmuutokseen [Capital area adapts to climate change]. Helsinki Region Environmental Services Authority, Helsinki. 36 p. (in Finnish)

Hunkeler, F., Lammar, L. 2012. Anforderungen an den Karbonatisierungswiederstand von Betonen [Requirements for the carbonation resistance of concrete]. TFB AG: Wildegg.

Huopainen, J. 1997. Betonijulkisivujen karbonatisoituminen – kenttätutkimus (Carbonation of concrete facades – a field study). MSc thesis, Tampere University of Technology. 51 p.

Huuhka, S. 2016. Building 'Post-Growth' – Quantifuying and Characterizing Resources in the Building Stock. Tampere University of Technology. PhD thesis. TUT Publ. 1414. 288 p.

International Federation for Structural Concrete. 2006. fib Bulletin No. 34. Model Code for Service Life Design. Lausanne. 116 p.

IPCC. 1992. Climate Change: The IPCC 1990 and 1992 Assessments. Intergorvernmental Panel on Climate Change. Canada. 168 p.

IPCC. 2007. Climate Change 2007: The physical science basis. Contribution of Working Group I to the Fourth Assessment Report of the Intergovernmental Panel on Climate Change. Cambridge University Press, Cambridge, U.K. 996 p.

Jones, M., Dhir, R., Newlands, M., Abbas, A. 2000. A study of the CEN test method for measurement of the carbonation depth of hardened concrete. Materials and Structures, 33(2), Pp. 135–142.

Jylhä, K., Ruosteenoja, K., Räisänen, J., Venäläinen, A., Tuomenvirta, H., Ruokolainen, L., Saku, S., Seitola, T. 2009. The changing climate in Finland: estimates for adaption studies. ACCLIM project report 2009. Finnish Meteorological Institute. Reports 2009:4. Helsinki. 78 p. 36 app. (in Finnish, extended English abstract)

Koistinen, J., Turtiainen, H. 2006. Helsinki Testbedin neljäs jakso keskittyy merituulen esiintymiseen [The fourth period of Helsinki Testbed focuses on occurrence of sea winds]. Finnish Meteorological Institute. Press release 2.5.2006. [referred 23.7.2019]. Retrieved from: http://ilmatieteenlaitos.fi/tiedote/1146555236. (in Finnish)

Koskiahde, A. 2004. An experimental petrographic classification scheme for the condition assessment of concrete in facade panels and balconies. Materials Characterization, 53, Pp. 327–334.

Kottek, M., Grieser, J., Beck C., Rudolf, B, Rubel, F. 2006. World map of the Köppen-Geiger climate classification updated. Meteorologische Zeitschrift, 15(3), Pp. 259–263.

Kuismanen, K. 2008. Climate-conscious Architecture – Design and Wind Testing Method for Climates in Change. University of Oulu. PhD Thesis. Acta Universitatis Oulu, C Technica 307. 404 p. 9 app.

Kuosa, H., Vesikari, E. 2000. Betonin pakkasenkestävyyden varmistaminen. Osa 1: Perusteet ja käyttöikämitoitus [Ensuring of concrete frost resistance Part 1: Basic data and service life design]. VTT Technical Research Centre of Finland. Research notes 2056. 141 p. (in Finnish)

Kvande T., Lisø K.R. 2009. Climate adapted design of masonry structures. Building and Environment, 44, pp. 2442–2450.

Köliö, A. 2016. Propagation of Carbonation Induced Reinforcement Corrosion in Existing Concrete Facades Exposed to the Finnish Climate. Tampere University of Technology. PhD thesis. TUT Publ. 1399. 147 p.

Köliö, A., Honkanen, M., Lahdensivu, J., Vippola, M., Pentti, M. 2015. Corrosion products of carbonation induced corrosion in existing reinforced concrete facades. Cement and Concrete Research, 78(Part B), Pp. 200-207.

Köliö, A. Pakkala, T.A., Annila, P.J., Lahdensivu, J., Pentti, M. 2014. Possibilities to validate design models for corrosion in carbonated concrete using condition assessment data. Engineering Structures, 75, Pp. 539–549.

Köliö, A., Pakkala, T.A., Hohti, H., Laukkarinen, A., Lahdensivu, J., Mattila, J., Pentti, M. 2017. The corrosion rate in reinforced concrete facades exposed to outdoor environment. Materials and Structures, 50(1), Pp. 1-16.

Labriet, M., Joshi, S.R., Vielle, M., Holden P.B., Edwards, N.R., Kanudia, A. Loulou, R., Babonneau, F. 2015. Worldwide impacts of climate change on energy for heating and cooling. Mitigation and Adaptation Strategies for Global Change, 20(7), Pp. 1111–1136.

Lahdensivu, J. 2010. Julkisivujen ja parvekkeiden kestävyys muuttuvassa ilmastossa [The Durability of Facades and Balconies in a Changing Climate]. Ministry of the

Environment. Department of the Built Environment. The Finnish Environment 17/2010. Helsinki. 64 p. (in Finnish)

Lahdensivu, J. 2012. Durability Properties and Actual Deterioration of Finnish Concrete Facades and Balconies. Tampere University of Technology. PhD thesis. TUT Publ. 1028. 117 p.

Lahdensivu, J. 2014. Betonijulkisivujen ja parvekkeiden säilyvyys suomalaisissa suunnitteluohjeissa [Durability of concrete facades and balconies in Finnish planning guidelines]. Tekniikan Waiheita, 3/14, Pp. 5–21. (in Finnish)

Lahdensivu, J., Kekäläinen, P., Lahdensivu, A. 2019. Alkali-silica reaction in Finnish concrete structures. Nordic Concrete Research, No. 59, Pp. 31–44.

Lahdensivu, J., Lahdensivu, E., Köliö, A. 2019. Case study on the 20 years propagation of carbonation in existing concrete facades and balconies. Nordic Concrete Research, No. 60, Pp. 1–12.

Lahdensivu, J., Varjonen, S., Köliö, A. 2010. Betonijulkisivujen ja -parvekkeiden korjausstrategiat [Repair Strategies of Concrete Facades and Balconies]. Tampere University of Technology, Department of Civil Engineering. Research report 148. (in Finnish)

Lahdensivu, J., Varjonen, S., Pakkala, T., Köliö, A. 2013. Systematic condition assessment of concrete facades and balconies exposed to outdoor climate. International Journal of Sustainable Building Technology & Urban Development, 4(3), Pp. 199–209.

Li, C.Q. 2004. Reliability service life prediction of corrosion affected concrete structures. ASCE Journal of Structural Engineering 2004:130(10). Pp. 1570–1577.

Li D.H.W., Liu Y., Lam J.C. 2012. Impact of climate change on energy use in the built environment in different climate zones – A review. Energy, 42, Pp 103–112.

Lisø, K.R. 2006. Building envelope performance assessments in harsh climates: Methods for geographically dependent design. Trondheim, Norwegian University of Science and Technology. Doctoral Theses at NTNU 185. 187 p.

Lisø, K.R., Kvande, T., Hygen, H.O., Thue, J.V., Harstveit, K. 2007a. A frost decay exposure index for porous, mineral building materials. Building and Environment, 42(10), Pp. 3547–3555.

Lisø, K.R., Kvande, T., Time, B. 2017. Climate Adaptation Framework for Moisture-resilient Buildings in Norway. 11th Nordic Symposium on Building Physics, NSB2017, 11-14 June 2017, Trondheim, Norway. Energy Procedia, 132, Pp. 628–633.

Lisø, K.R., Myhre, L., Kvande, T., Thue, J.V., Nordvik, V. 2007b. A Norwegian perspective on buildings and climate change. Building Research & Information, 35(4), Pp. 437–449.

Litvan, G. 1972. Phase transitions of adsorbates IV – Mechanism of frost action in hardened cement paste. Journal of the American Ceramic Society, 55(1), Pp. 38–42.

Liu, Y., Weyers, R.E. 1998. Modeling the Time-to-Corrosion Cracking in Chloride Contaminated Reinforced Concrete Structures. ACI Materials Journal, 95(6), Pp. 675 – 681.

Lollini, F., Redaelli, E., Bertolini, L. 2012. Analysis of the parameters affecting probabilistic predictions of initiation time for carbonation-induced corrosion of reinforced concrete structures. Materials and Corrosion, 63(12), Pp. 1059-1068.

Mattila, J. 2003. On the durability of cement-based patch repairs on Finnish concrete facades and balconies. Tampere, Tampere University of Technology. Publication 450. 111 p.

Mattila, J., Pentti, M. 2004. Suojaustoimien tehokkuus suomalaisissa betonijulkisivuissa ja parvekkeissa [Performance of Protective Measures in Finnish Concrete Facades and Balconies]. Tampere University of Technology, Research report 123. 69 p. (in Finnish)

Mauree, D., Naboni, E., Coccolo, S., Pereraa, A.T.D., Nik, V.M., Scartezzini, J.-L. 2019. A review of assessment methods for the urban environment and its energy sustainability to guarantee climate adaptation of future cities. Renewable and Sustainable Energy Reviews, 112, Pp. 743–746.

Medeiros-Junior, R. 2018. Impact of climate change on the service life of concrete structures. In Pacheco-Torgal, F., Melchers, R.E., Shi, X., De Belie, N., Van Tittelboom, K., Sáez, A. (editors) Eco-Efficient Repair and Rehabilitation of Concrete Infrastructures. Woodhead Publishing Series in Civil and Structural Engineering, Pp. 43–68.

Ministry of Agriculture and Forestry. 2014. Kansallinen ilmastonmuutokseen sopeutumissuunnitelma 2022 [National adaptation plan to climate change 2022]. Ministry of Agriculture and Forestry, Helsinki. 30 p. 10 app. (in Finnish)

Monteiro, I., Branco, F.A., de Brito, J., Neves, R. 2012. Statistical analysis of the carbonation coefficient in open air concrete structures. Construction and Building Materials, 29, Pp. 263–269.

Neves, R., Branco, F.A., de Brito, J. 2012. A method for the use of accelerated carbonation tests in durability design. Construction and Building Materials, 36, Pp. 585–591.

Neville, A. 1995. Properties of concrete. Essex. Longman Group. 844 p.

Nik V.M., Kalagasidis A.S., Kjellström E. 2012. Assessment of hygrothermal performance and mould growth risk in ventilated attics in respect to possible climate changes in Sweden. Building and Environment, 55, Pp. 96–109.

Nilsson, L.-O. 2003. Durability concept; pore structure and transport processes, In: Advanced Concrete Technology Set, 2003, Pp. 3-29.

Norwegian Ministry of Climate and Environment. 2013. Climate change adaptation in Norway. Meld. St. 33 (2012-2013), Report to the Storting. 108 p.

Page, C.L. 1988. Basic Principles of Corrosion. In: Schiessl, P.(editor). Corrosion of Steel in Concrete. London, Chapman and Hall. Pp. 3–21.

Parrott, L.J. 1987. A review of carbonation in reinforced concrete. Cement and Concrete Association, Slough, UK. 42 p.

Parrott, L. 1996. Some effects of cement and curing upon carbonation and reinforcement corrosion in concrete. Materials and Structures, 29(3), Pp. 164–173.

Peng, L., Stewart M.G. 2013. Deterioration of concrete structures in Australia under a changing climate. From Materials to Structures: Advancement Through Innovation - Proceedings of the 22nd Australasian Conference on the Mechanics of Structures and Materials, ACMSM 2012, Pp. 1015–1020.

Peng, L., Stewart M.G. 2016. Climate change and corrosion damage risks for reinforced concrete infrastructure in China. Structure and Infrastructure Engineering, 12(4), Pp. 499–516.

Penttala, V. 1998. Freezing-induced strains and pressures in wet porous materials and especially in concrete mortars. Advanced Cement Based Materials, 7/1998, Pp. 8–19.

Penttala, V., Al-Neshawy, F. 2002. Stress and strain state of concrete during freezing and thawing cycles, Cement and Concrete Research, 32(9). Pp. 1407–1420.

Pentti M. 1994. Rakennusvaipan korjaaminen [Repair of building envelope]. In: Kaivonen J-A, editor. Rakennusten korjaustekniikka ja talous [Repair techniques and economy of buildings]. Rakennustieto Oy: Saarijärvi; 1994. Pp. 287–358 (in Finnish).

Pentti, M., Mattila, J., Wahlman, J. 1998. Betonijulkisivujen ja –parvekkeiden korjaaminen, osa I: rakenteet, vaurioituminen ja kuntotutkimus [Repair of concrete facades and balconies, part I: structures, degradation and condition investigation]. Tampere, Tampere University of Technology, Structural Engineering. Publication 87. 157 p. (In Finnish)

Phillipson, M.C., Emmanuel, R., Baker, P.H. 2016. The durability of building materials under a changing climate. Wiley Interdisciplinary Reviews: Climate Change, 7(4), Pp. 590–599.

Pigeon, M., Pleau, R. 1995. Durability of concrete in cold climates. London. E & FN Spon. 244 p.

Pigeon, M., Pleau, R., Aïtcin, P.C. 1986. Freeze-thaw durability of concrete with and without silica fume in ASTM C 666 (procedure A) test method: internal cracking versus scaling. Cement, Concrere and Aggregates, 8(2). Pp. 76–85.

Pirinen, P., Simola, H., Aalto, J., Kaukoranta, P., Karlsson, P., Ruuhela, R. 2012. Climatological statistics of Finland 1981–2010. Reports No. 2012:1. Finnish Meteorological Institute. Helsinki. 96 p.

Powers, T. C. 1949. The air requirement of frost-resistant concrete. Chicago: Portland Cement Association, Research and Development laboratories, Development Department. Bulletin 33.

Powers, T. C., Helmuth, R. A. 1953. Theory of volume changes in hardened Portland cement pastes during freezing. In Proceedings of the Highway Research Board, 32, Pp. 285–295.

Raupach, M. 2006. Models for the propagation phase of reinforcement corrosion – an overview. Materials and Corrosion, 57(8), Pp. 605 – 613.

Riihimäki, M., Laitinen, T., Jaakkonen, L. 2018. Julkisivujen markkinat ja seuranta Suomessa [Facade market survey and follow-up in Finland]. Forecon Report FR-03-00256-16, Julkisivuyhdistys ry. 46 p.

ROTI. 2019. Rakennetun omaisuuden tila –raportti (State of the built environment – report). Available 16.5.2019 htttp://www.roti.fi (in Finnish)

Rubel, F, Kottek, M.. 2010. Observed and projected climate shifts 1901–2100 depicted by world maps of the Köppen-Geiger climate classification. Meteorologische Zeitschrift 19(2), Pp. 135–141.

Ruosteenoja, K., Jylhä, K., Mäkelä, H., Hyvönen, R., Pirinen, P., Lehtonen, I. 2013a. Weather data for building physics test years in the observed and projected future climate. Reports No. 2013:1. Finnish Meteorological Institute. Helsinki. 36 p. 9 app. (in Finnish)

Ruosteenoja, K., Räisänen, J., Jylhä, K., Mäkelä, H., Lehtonen, J., Simola, H., Luomaranta, A., Weiher, S. 2013b. Climate change estimates for Finland on the basis of global CMIP3 climate models. Reports No. 2013:4. Finnish Meteorological Institute. Helsinki. 83 p. (in Finnish)

Rydock, J.P., Lisø, K.R., Førland, E.J., Nore, K., Thue, J.V. 2005. A driving rain exposure index for Norway. Building and Environment, 40(11), Pp. 1450–1458.

SBK. 1970. BES – Betonielementtisysteemi, tutkimusraportti [Development of open concrete element system, Research report]. Suomen Betoniteollisuuden Keskusjärjestö ry. (in Finnish)

Schießl, P. (editor). 1988. Corrosion of Steel in Concrete. London, Chapman and Hall. 101 p.

SFS 4475. 1998. Concrete. Frost resistance. Protective pore ratio. Finnish Standards Association SFS. 2 p. (in Finnish) (withdrawn 2.11.2009)

SFS-EN ISO 15927-3. 2009. Hygrothermal performance of buildings. Calculation and presentation of climatic data. Part 3: Calculation of a driving rain index for vertical surfaces from hourly wind and rain data. Finnish Standards Association SFS, Helsinki. 31 p.

Shang, H.-S. 2013. Triaxial T-C-C behavior of air-entrained concrete after freeze-thaw cycles, Cold Regions Science and Technology, 89, Pp. 1-6.

Shang, H.-S., Cao, W.-Q., Wang, B. 2014. Effect of Fast Freeze-thaw Cycles on Mechanical Properties of Ordinary-Air-Entrained Concrete. The Scientific World Journal, 2014, 7 p.

Shang, H-S., Song, Y. 2008. Behavior of air-entrained concrete under the compression with constant confined stress after freeze–thaw cycles, Cement and Concrete Composites, 30(9), Pp. 854–860.

Stewart, M.G., Wang, X., Nguyen, M.N. 2011. Climate change impact and risks of concrete infrastructure deterioration. Engineering Structures, 33(4), Pp. 1326–1337.

Stewart, M.G., Wang, X., Nguyen, M.N. 2012. Climate change adaptation for corrosion control of concrete infrastructure. Structural Safety, 35, Pp. 29–39.

Statistics Finland. 2019. Statistics: Buildings and free-time residences [e-publication]. Helsinki: Statistics Finland [referred: 25.4.2019]. Retrieved from http://www.stat.fi/til/rakke/rakke_2009-05-28_uut_001_en.html

Straube, J.F., Burnett, E.F.P. 2000. Simplified prediction of driving rain on buildings. Proc. of the International Building Physics Conference, Eindhoven, The Netherlands, 18–21 September 2000, Pp. 375-382.

Talukdar, S., Banthia, N. 2013. Carbonation in concrete infrastructure in the context of global climate change: Development of a service lifespan model, Construction and Building Materials, 40, Pp. 775-782.

Talukdar, S., Banthia, N., Grace, J.R., Cohen, S. 2012. Carbonation in concrete infrastructure in the context of global climate change: Part 2, Canadian urban simulations. Cement and Concrete Composites, 34, Pp. 931–935.

Talukdar, S., Banthia, N., Grace, J.R., Cohen, S. 2014. Climate change-induced carbonation of concrete infrastructure. Proceedings of the Institution of Civil Engineers - Construction Materials, 167(3), Pp. 140-150.

Tuutti, K. 1982. Corrosion of steel in concrete. Stockholm. Swedish Cement and Concrete Research Institute. CBI Research 4:82. 304 p.

van Hooff, T., Blocken, B., Timmermans, H.J.P., Hensen J.L.M. 2016. Analysis of the predicted effect of passive climate adaptation measures on energy demand for cooling and heating in a residential building. Energy, 94, Pp. 811–820.

Vasaturo, R., van Hooff, T., Kalkman, I., Blocken, B., van Wesemael, P. 2018. Impact of passive climate adaptation measures and building orientation on the energy demand of a detached lightweight semi-portable building. Building Simulation, 11(6), Pp. 1163–1177.

Vinha, J., Laukkarinen, A., Mäkitalo, M., Nurmi, S., Huttunen, P., Pakkanen, T., Kero, P., Manelius, E., Lahdensivu, J., Köliö, A., Lähdesmäki, K., Piironen, J., Kuhno, V., Pirinen, M., Aaltonen, A., Suonketo, J., Jokisalo, J., Teriö, O., Koskenvesa, A., Palolahti, T. 2013. Effects of Climate Change and Increasing of Thermal Insulation on Moisture

Performance of Envelope Assemblies and Energy Consumption of Buildings. Tampere University of Technology, Department of Civil Engineering, Research report 159. 354 p. + 43 app. (in Finnish)

Wang, X., Stewart, M.G., Nguyen, M. 2012. Impact of climate change on corrosion and damage to concrete infrastructure in Australia. Clim Change, 110, Pp. 941–957.

Williams K., Joynt J.L.R., Payne C., Hopkins D., Smith I. 2012. The conditions for, and challenges of, adapting England's suburbs for climate change. Building and Environment, 55, Pp. 131–140.

Yoon, I.-S., Çopuroğlu, O., Park, K.-B. 2007. Effect of global climatic change on carbonation progress of concrete Atmospheric Environment, 41(34), Pp. 7274–7285.

Zandi Hanjari, K., Utgenannt, P., Lundgren, K. 2011. Experimental study of the material and bond properties of frost-damaged concrete, Cement and Concrete Research, 41(3), Pp. 244–254.

Appendixes

Appendix I: Share of residential buildings in different areas

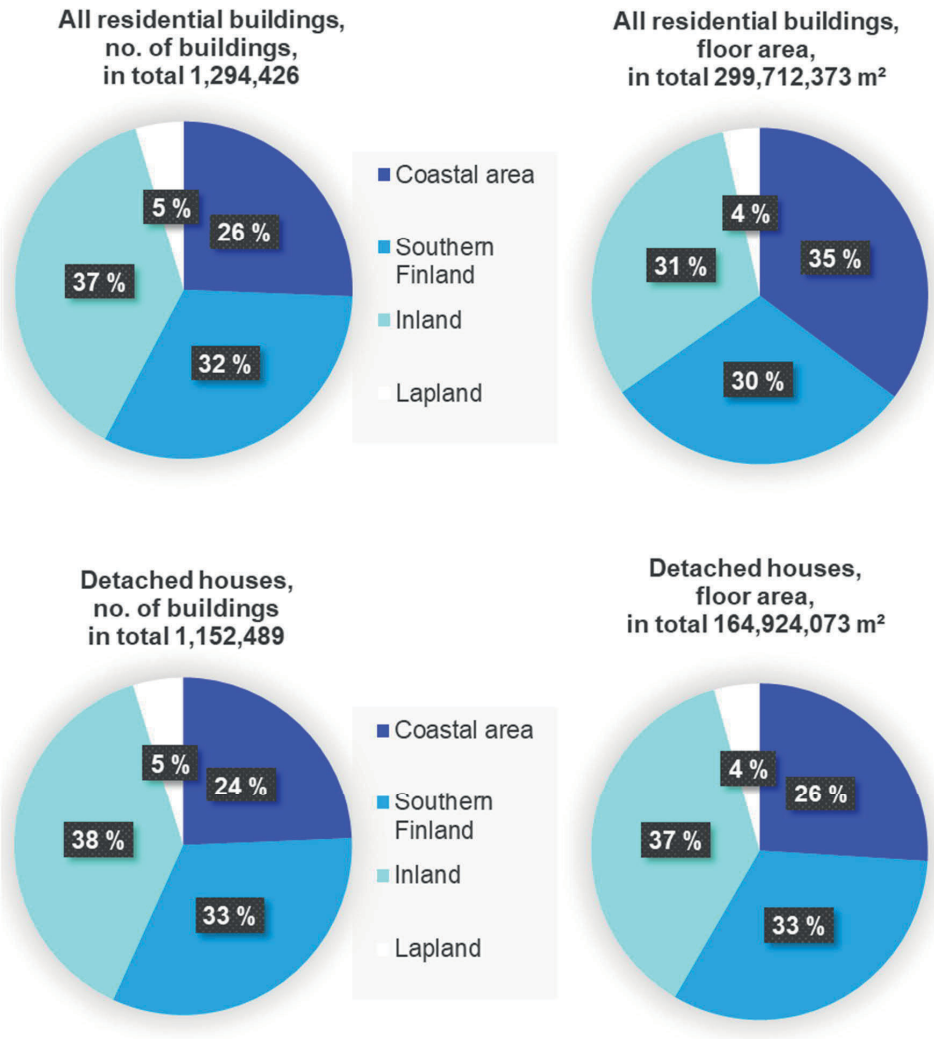

Attached houses,
no. of buildings.
in total 81,293

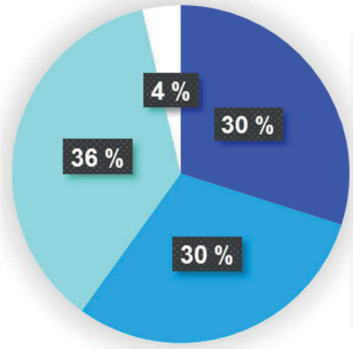

Coastal area
Southern Finland
Inland
Lapland

Attached houses,
floor area,
in total 34,718,679 m²

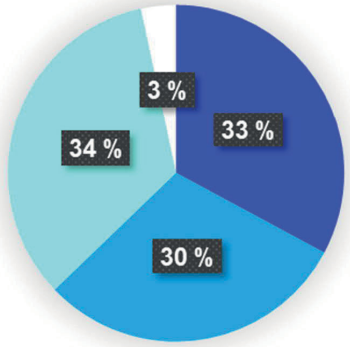

Block of flats,
no. of buildings,
in total 60,644

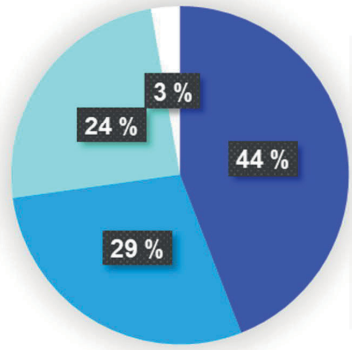

Coastal area
Southern Finland
Inland
Lapland

Block of flats,
floor area,
in total 100,069,621 m²

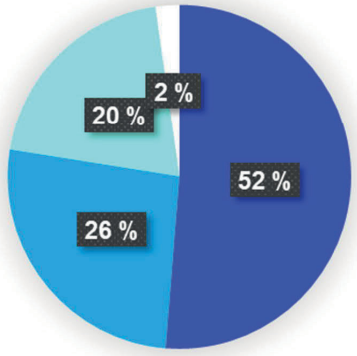

Appendix II: Monthly distribution of freeze-thaw cycles

Coastal area (Helsinki-Vantaa)

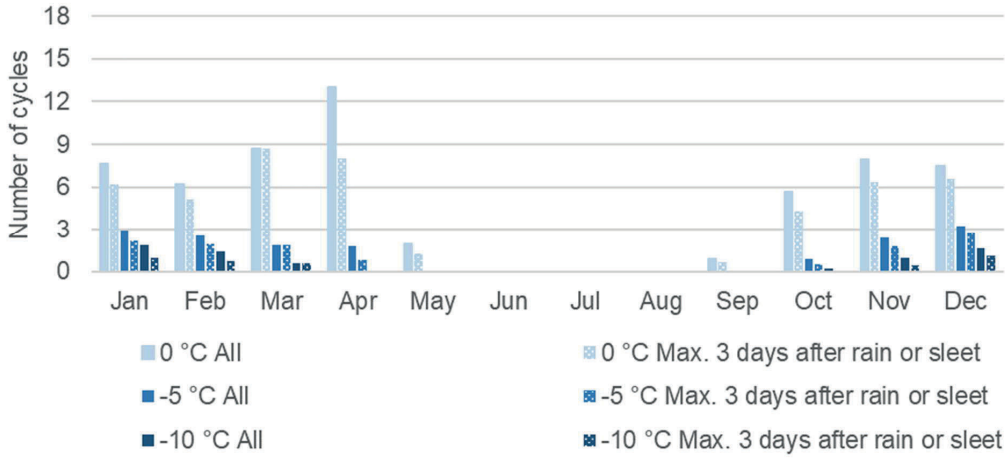

Southern Finland (Jokioinen)

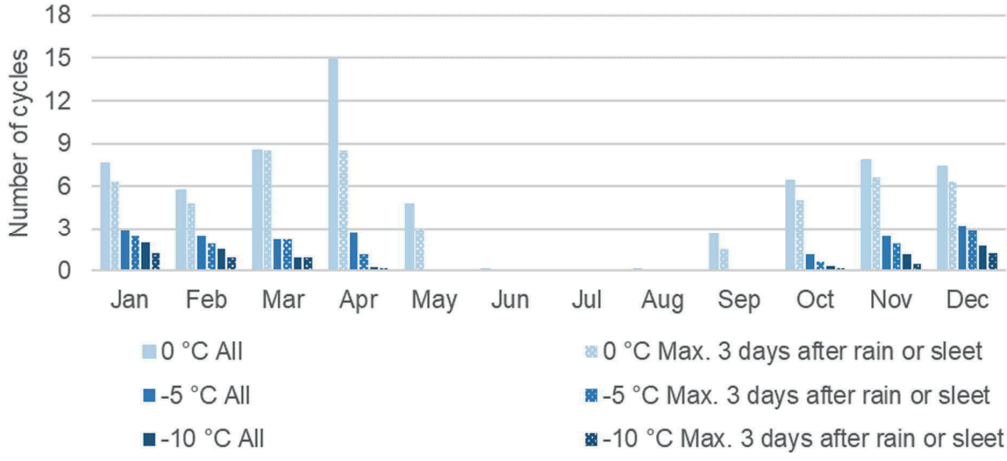

Inland (Jyväskylä)

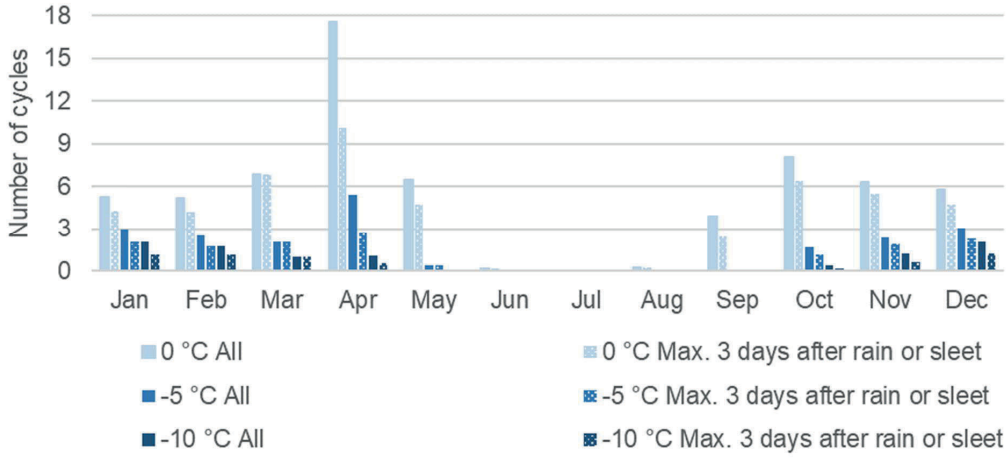

Lapland (Sodankylä)

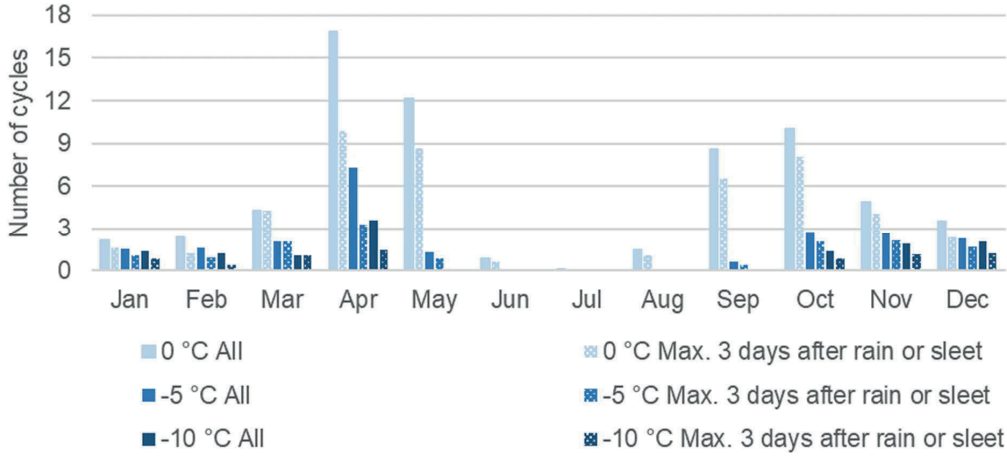

Appendix III: Monthly average corrosion rates of reinforcements in carbonated facade and balcony structures in present and future climates

South-facing facade, present climate

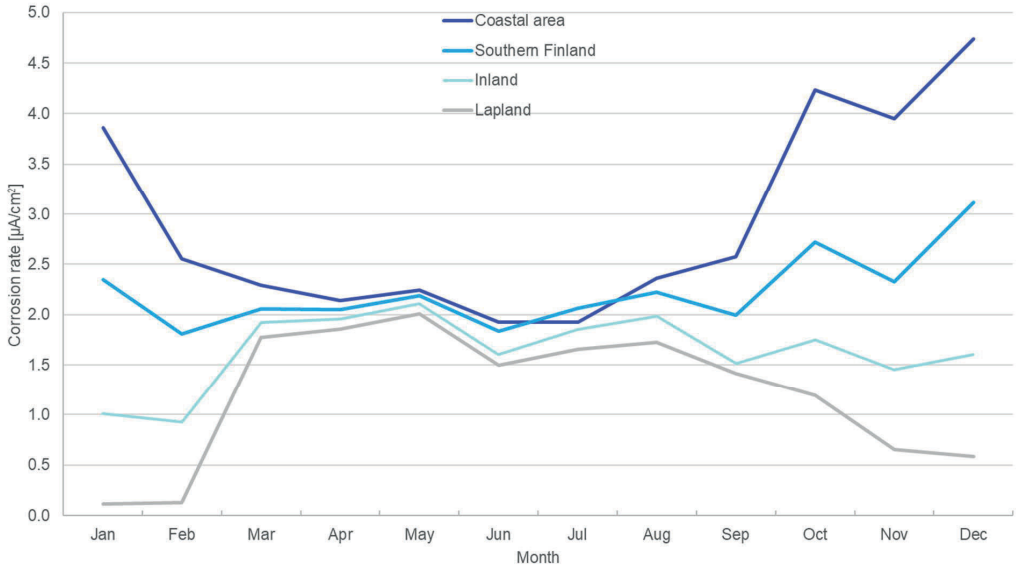

West-facing facade, present climate

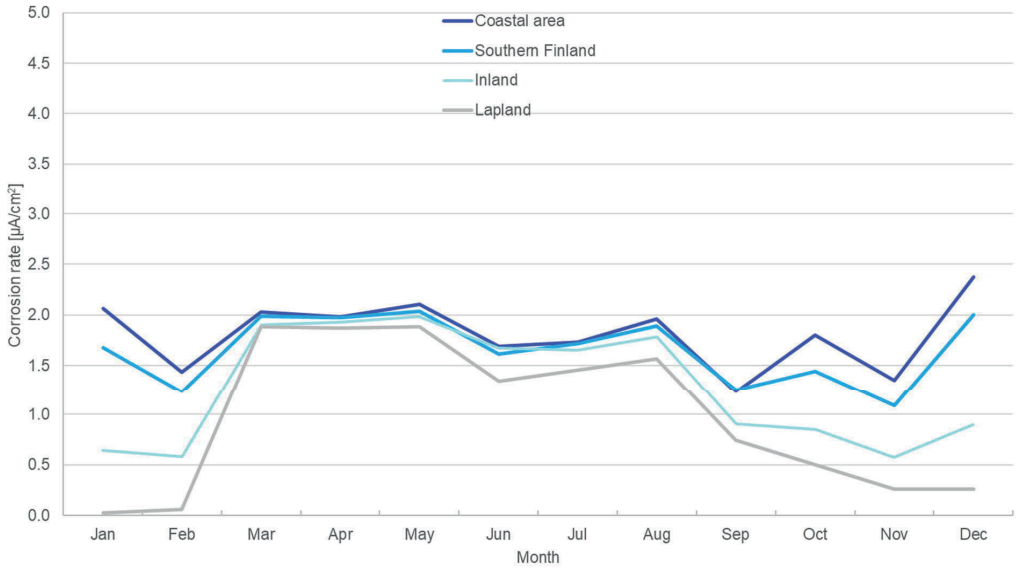

North-facing facade, present climate

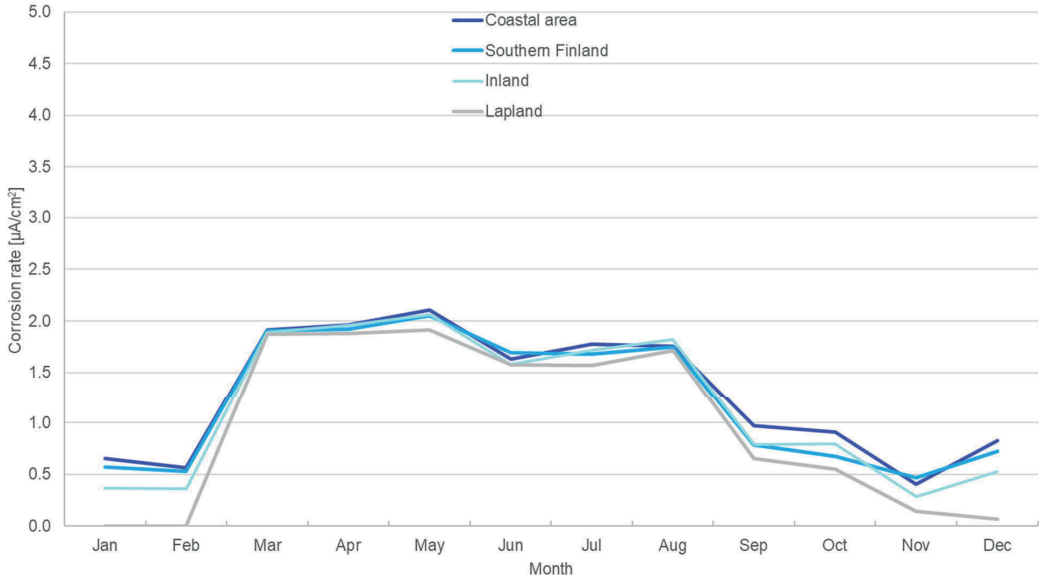

East-facing facade, present climate

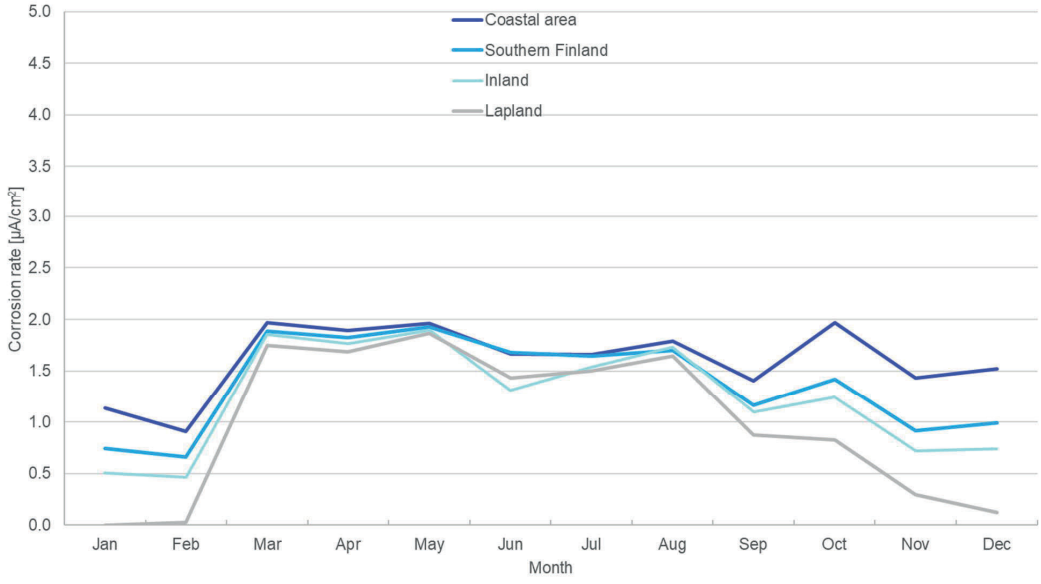

South-facing balcony structures, present climate

West-facing balcony structures, present climate

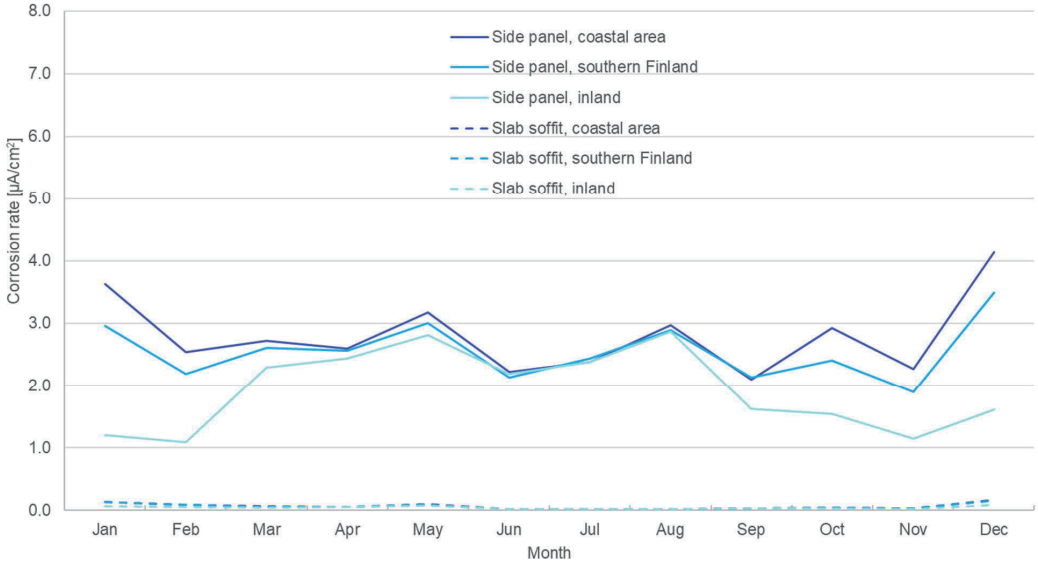

North-facing balcony structures, present climate

North-facing balcony structures, present climate

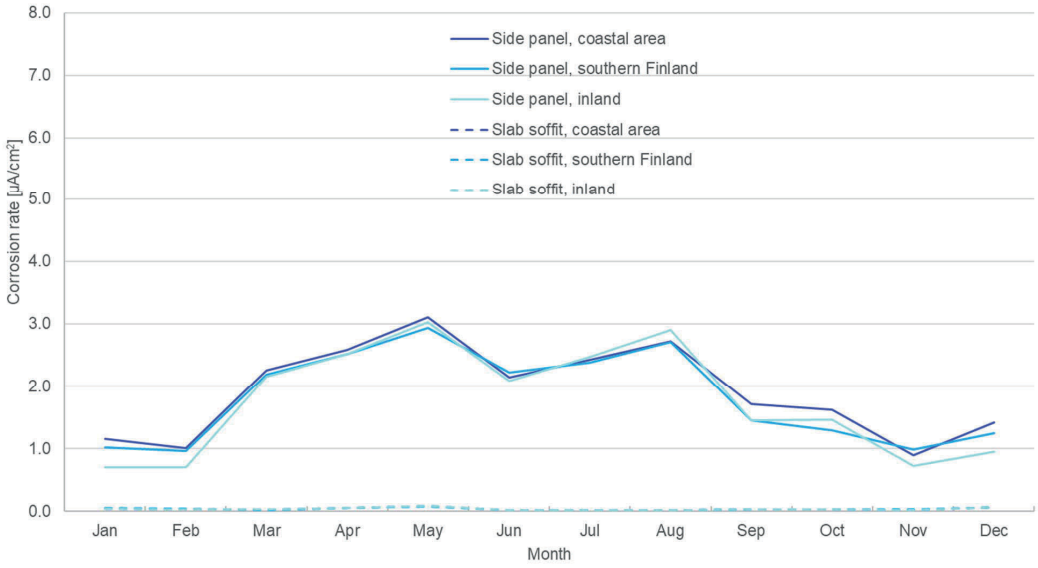

South-facing facade, projected future climates (**note:** the vertical axis)

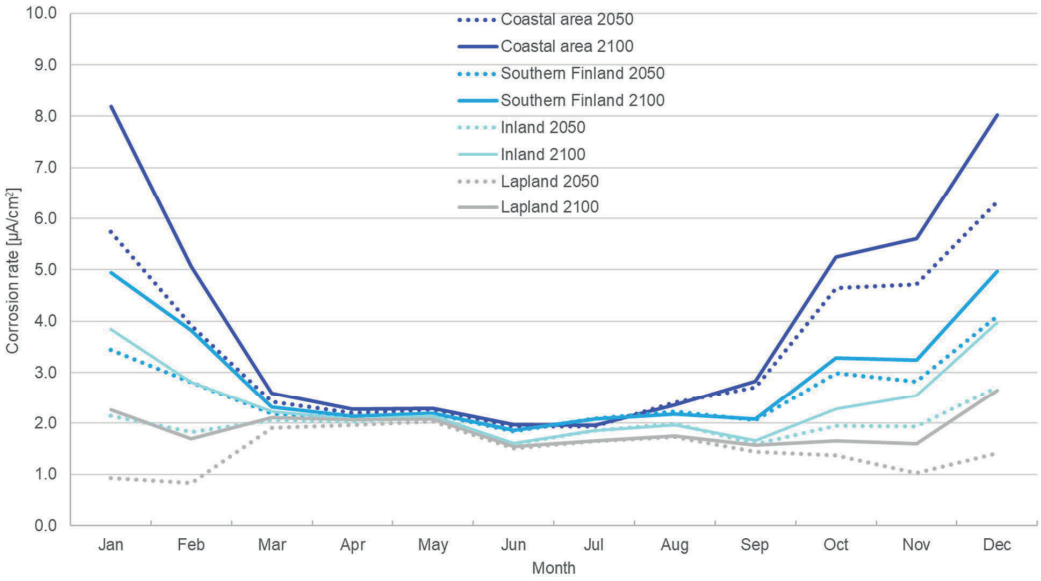

West-facing facade, projected future climates

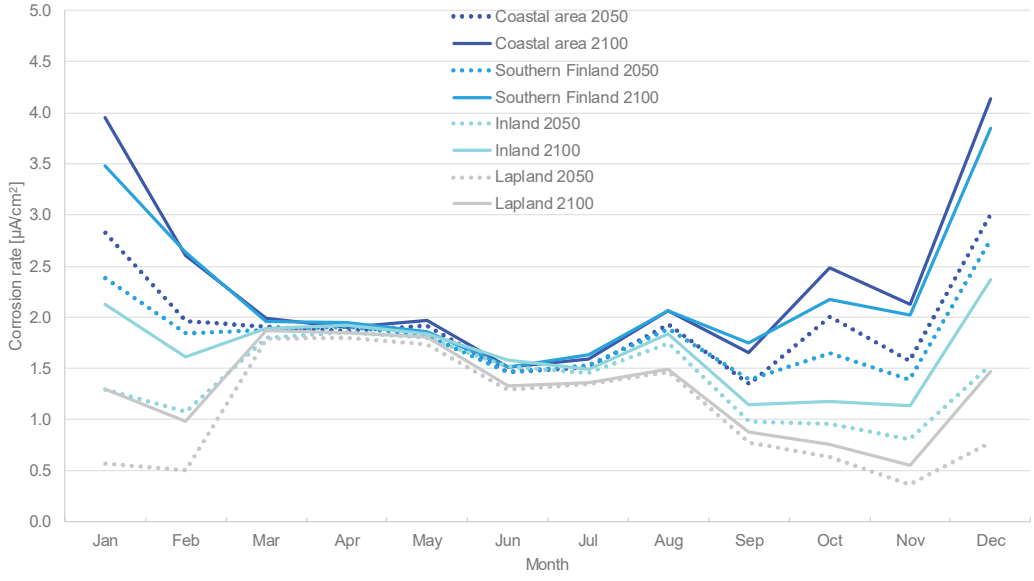

North-facing facade, projected future climates

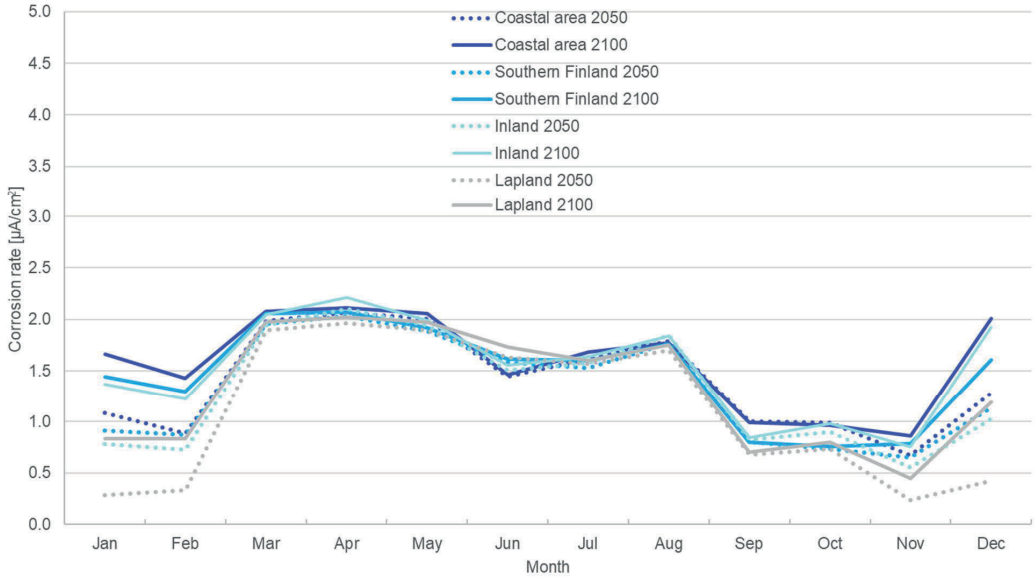

East-facing facade, projected future climates

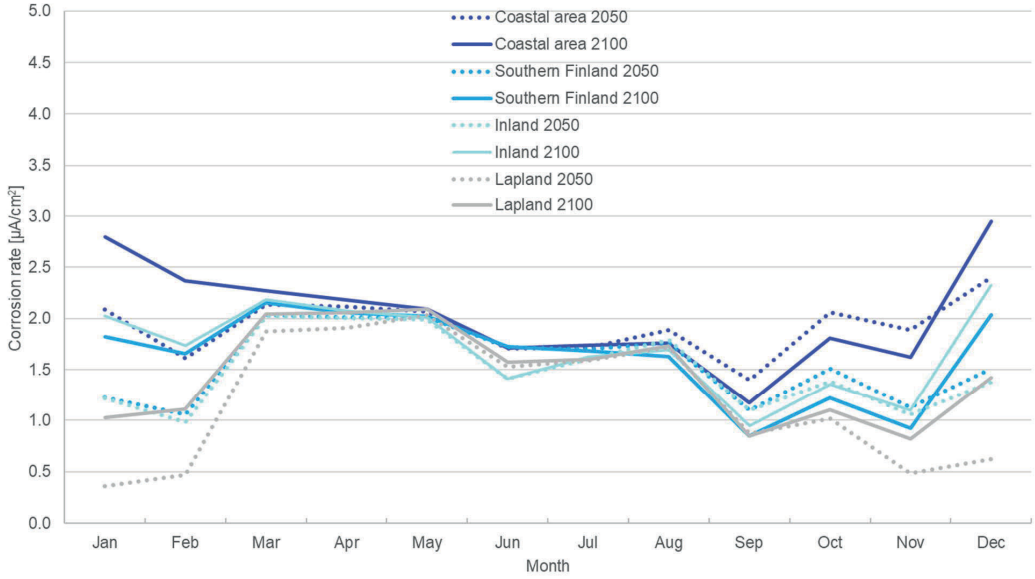

South-facing balcony structures, projected 2100 climate (**note:** the vertical axis)

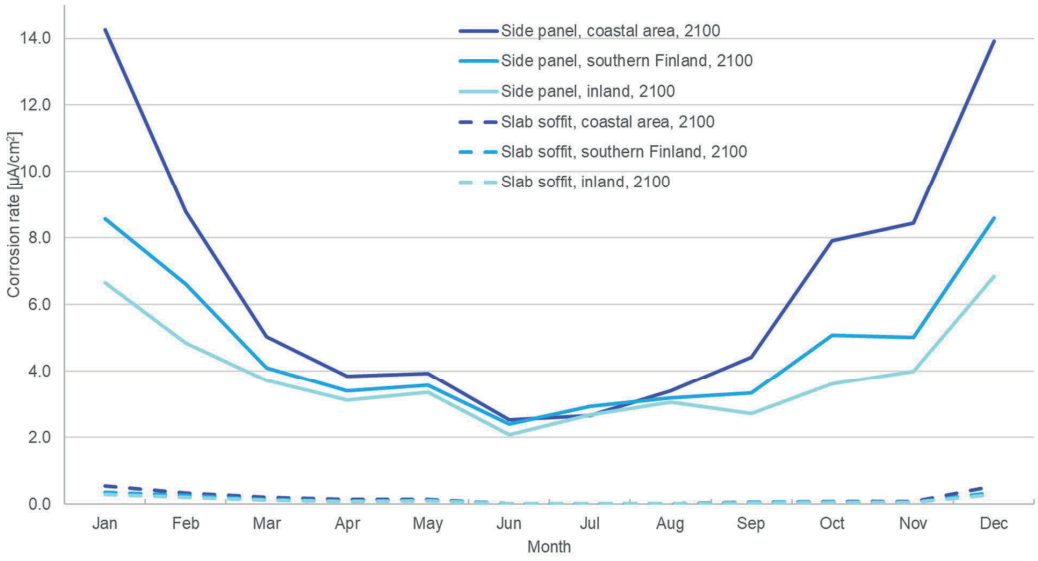

West-facing balcony structures, projected 2100 climate (**note:** the vertical axis)

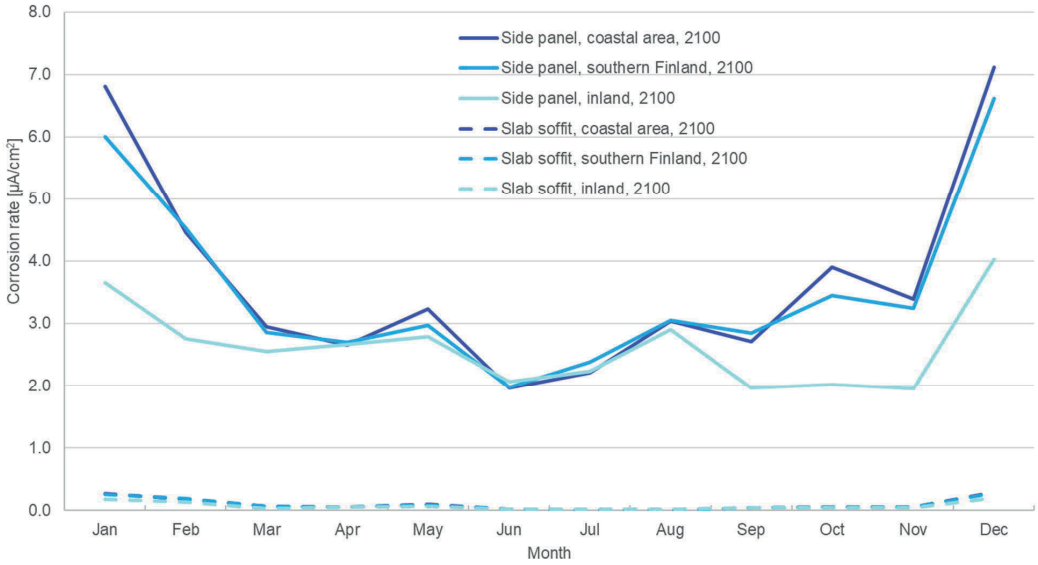

North-facing balcony structures, projected 2100 climate (**note:** the vertical axis)

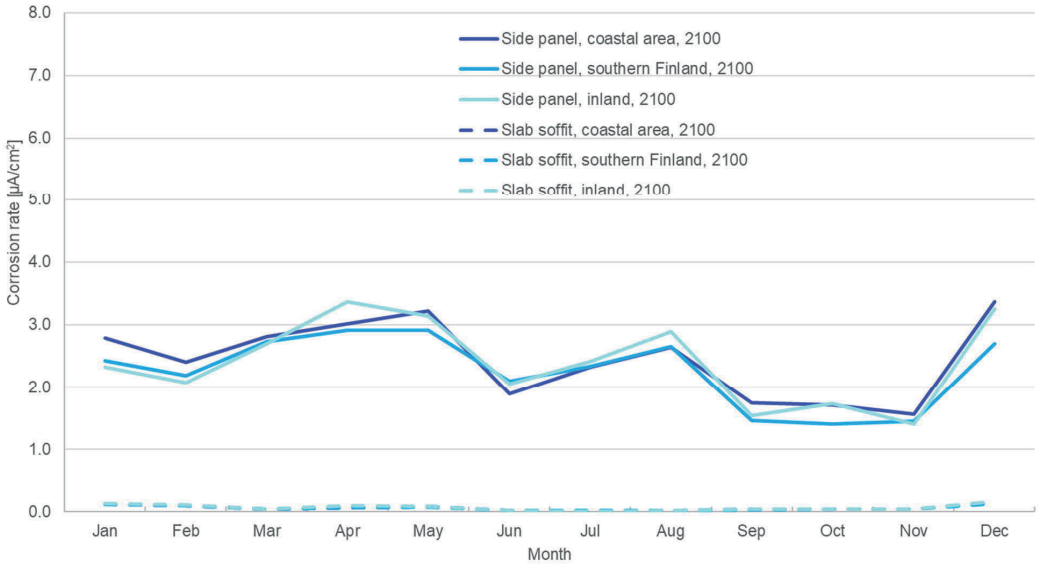

East-facing balcony structures, projected 2100 climate (**note:** the vertical axis)

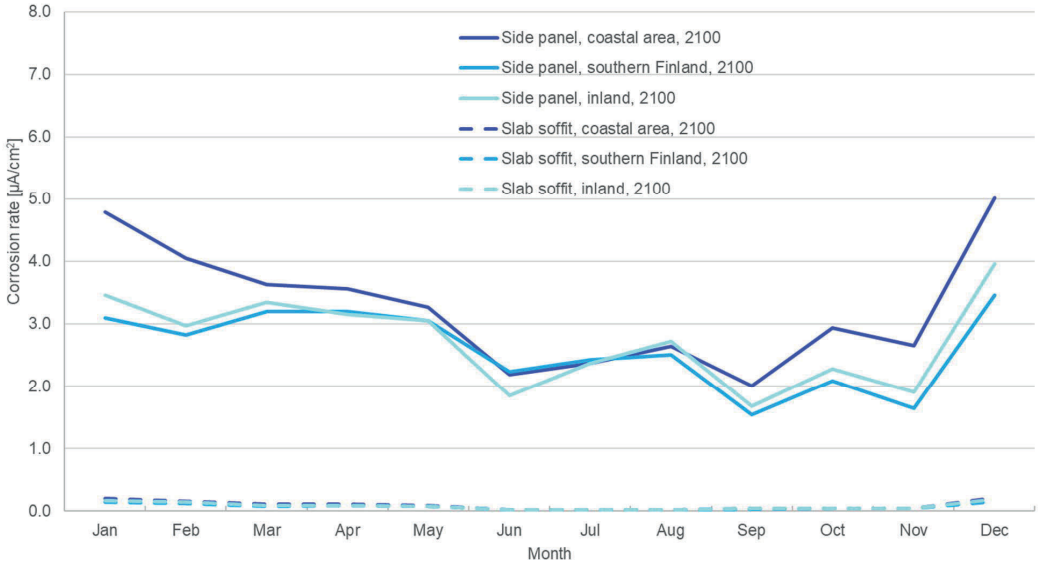

An average of the modelled corrosion rate [µA/cm²] in the carbonated concrete of facade reinforcements (C = coastal, S = southern Finland, I = inland, L = Lapland)

		North			East			South			West		
		Present	2050	2100	Present	2050	2100	Present	2050	2100	Present	2050	2100
Winter	C	1.24	1.32	1.72	1.44	1.94	2.48	2.42	4.02	5.28	1.73	2.23	2.85
	S	1.00	1.25	1.60	1.10	1.44	1.88	2.07	2.81	3.70	1.63	2.03	2.69
	I	0.87	1.15	1.55	0.94	1.41	1.98	1.29	2.01	2.96	1.04	1.39	1.88
	L	0.62	0.84	1.21	0.59	0.90	1.39	0.67	1.22	2.02	0.65	0.95	1.38
Spring	C	1.90	1.84	1.88	1.84	1.97	2.00	2.10	2.14	2.18	1.93	1.75	1.80
	S	1.89	1.84	1.87	1.81	1.91	1.93	2.02	2.04	2.07	1.87	1.73	1.77
	I	1.87	1.85	1.92	1.66	1.80	1.83	1.89	1.91	1.79	1.86	1.72	1.78
	L	1.79	1.83	1.91	1.66	1.82	1.91	1.79	1.84	1.90	1.70	1.60	1.66
Summer	C	1.50	1.47	1.48	1.62	1.67	1.56	2.29	2.35	2.38	1.64	1.60	1.77
	S	1.40	1.37	1.39	1.50	1.52	1.39	2.10	2.12	2.12	1.62	1.60	1.81
	I	1.44	1.42	1.44	1.45	1.50	1.42	1.78	1.81	1.83	1.45	1.39	1.49
	L	1.31	1.32	1.35	1.34	1.39	1.39	1.60	1.61	1.66	1.26	1.19	1.24
Autumn	C	0.71	0.98	1.28	1.64	2.12	2.13	4.31	5.23	6.30	1.84	2.19	2.92
	S	0.62	0.84	1.05	1.11	1.38	1.39	2.72	3.30	3.84	1.51	1.93	2.68
	I	0.53	0.83	1.22	0.90	1.27	1.59	1.60	2.20	2.93	0.77	1.09	1.56
	L	0.25	0.46	0.81	0.41	0.71	1.11	0.81	1.27	1.97	0.34	0.59	0.92

Colour highlights are used to classify values as follows: red as very high (≥ 3.00 µA/cm²), orange as high (2.00-2.99 µA/cm²), green as moderate (1.00-1.99 µA/cm²) and blue as low (< 1.00 µA/cm²) corrosion rate values.

An average of the modelled corrosion rate [µA/cm²] in the carbonated concrete of side panel reinforcements (C = coastal, S = southern Finland, I = inland, L = Lapland)

		North			East			South			West		
		Present	2050	2100	Present	2050	2100	Present	2050	2100	Present	2050	2100
Winter	C	1.63	1.95	2.67	2.16	3.19	4.15	4.24	7.12	9.35	2.63	3.68	4.74
	S	1.39	1.81	2.45	1.63	2.24	3.04	3.51	4.88	6.43	2.59	3.33	4.46
	I	1.18	1.66	2.36	1.39	2.22	3.26	2.09	3.38	5.07	1.52	2.15	2.98
	L	0.77	1.13	1.78	0.76	1.30	2.20	0.99	1.98	3.43	0.88	1.42	2.14
Spring	C	2.61	2.61	2.71	2.75	2.93	3.01	3.22	3.33	3.44	2.66	2.52	2.61
	S	2.56	2.57	2.64	2.64	2.79	2.83	3.02	3.07	3.12	2.57	2.46	2.55
	I	2.54	2.66	2.86	2.36	2.60	2.68	2.71	2.79	2.85	2.48	2.39	2.51
	L	2.29	2.48	2.64	2.26	2.54	2.77	2.39	2.55	2.73	2.10	2.08	2.18
Summer	C	2.28	2.24	2.24	2.47	2.51	2.34	3.39	3.45	3.48	2.48	2.43	2.65
	S	2.18	2.13	2.15	2.34	2.33	2.15	3.13	3.16	3.15	2.49	2.46	2.76
	I	2.27	2.23	2.28	2.32	2.35	2.26	2.75	2.78	2.81	2.29	2.22	2.36
	L	1.99	1.98	2.03	2.05	2.08	2.09	2.40	2.39	2.47	1.92	1.83	1.91
Autumn	C	1.31	1.73	2.21	2.73	3.49	3.54	6.92	8.39	10.09	3.11	3.66	4.80
	S	1.17	1.52	1.85	1.91	2.34	2.39	4.46	5.38	6.23	2.59	3.26	4.44
	I	1.04	1.50	2.13	1.59	2.18	2.71	2.70	3.65	4.82	1.43	1.93	2.66
	L	0.62	0.94	1.49	0.86	1.31	1.96	1.48	2.21	3.32	0.77	1.16	1.68

Colour highlights are used to classify values as follows: red as very high (≥ 3.00 µA/cm²), orange as high (2.00-2.99 µA/cm²), green as moderate (1.00-1.99 µA/cm²) and blue as low (< 1.00 µA/cm²) corrosion rate values.

An average of the modelled corrosion rate [µA/cm²] in the carbonated concrete of slab soffit reinforcements (C = coastal, S = southern Finland, I = inland, L = Lapland)

		North			East			South			West		
		Present	2050	2100	Present	2050	2100	Present	2050	2100	Present	2050	2100
Winter	C	0.03	0.06	0.09	0.06	0.11	0.15	0.16	0.27	0.36	0.07	0.13	0.17
	S	0.04	0.06	0.09	0.05	0.08	0.11	0.13	0.19	0.25	0.09	0.12	0.17
	I	0.03	0.06	0.09	0.05	0.09	0.13	0.08	0.14	0.21	0.05	0.08	0.12
	L	0.01	0.03	0.06	0.01	0.04	0.08	0.03	0.07	0.14	0.02	0.05	0.08
Spring	C	0.05	0.06	0.06	0.07	0.07	0.07	0.09	0.09	0.09	0.06	0.06	0.05
	S	0.05	0.05	0.05	0.06	0.06	0.06	0.08	0.08	0.08	0.05	0.05	0.05
	I	0.05	0.06	0.07	0.06	0.06	0.06	0.07	0.07	0.07	0.05	0.05	0.05
	L	0.05	0.05	0.05	0.06	0.06	0.07	0.06	0.06	0.07	0.04	0.04	0.04
Summer	C	0.02	0.02	0.02	0.02	0.02	0.02	0.02	0.02	0.02	0.02	0.02	0.02
	S	0.02	0.02	0.02	0.02	0.02	0.02	0.02	0.02	0.02	0.02	0.02	0.02
	I	0.02	0.02	0.02	0.02	0.02	0.02	0.02	0.02	0.02	0.02	0.02	0.02
	L	0.02	0.02	0.02	0.02	0.02	0.02	0.02	0.02	0.02	0.02	0.02	0.02
Autumn	C	0.04	0.05	0.07	0.06	0.08	0.10	0.15	0.19	0.24	0.08	0.10	0.13
	S	0.04	0.05	0.07	0.05	0.07	0.08	0.11	0.13	0.16	0.07	0.09	0.13
	I	0.04	0.06	0.08	0.04	0.07	0.09	0.07	0.10	0.14	0.05	0.07	0.09
	L	0.01	0.03	0.06	0.02	0.04	0.06	0.03	0.06	0.10	0.02	0.04	0.06

Colour highlights are used to classify values as follows: red as very high (≥ 3.00 µA/cm²), orange as high (2.00-2.99 µA/cm²), green as moderate (1.00-1.99 µA/cm²) and blue as low (< 1.00 µA/cm²) corrosion rate values.

Appendix IV: Airfield annual index from different directions in present and projected future climates

	Airfield annual index I_A [mm/year]								
Location	Climate	North	North-east	East	South-east	South	South-west	West	North-west
Coastal area	Present	70	81	115	170	247	212	123	70
	2050	82	94	134	201	289	244	140	83
	2100	96	101	137	214	335	296	174	102
Southern Finland	Present	63	73	93	128	183	166	105	66
	2050	73	83	104	144	209	194	125	79
	2100	85	87	103	145	235	235	163	100
Inland	Present	67	57	77	108	120	91	72	74
	2050	79	67	94	133	146	109	85	88
	2100	96	78	104	153	176	136	107	109

	Airfield annual index I_A [mm/year]								
Location	Cli-mate	North	North-east	East	South-east	South	South-west	West	North-west
Lapland	Present	54	56	61	73	79	60	41	44
	2050	63	65	72	89	99	75	50	53
	2100	78	78	90	116	130	96	64	67

Coastal area (Helsinki-Vantaa)

Southern Finland (Jokioinen)

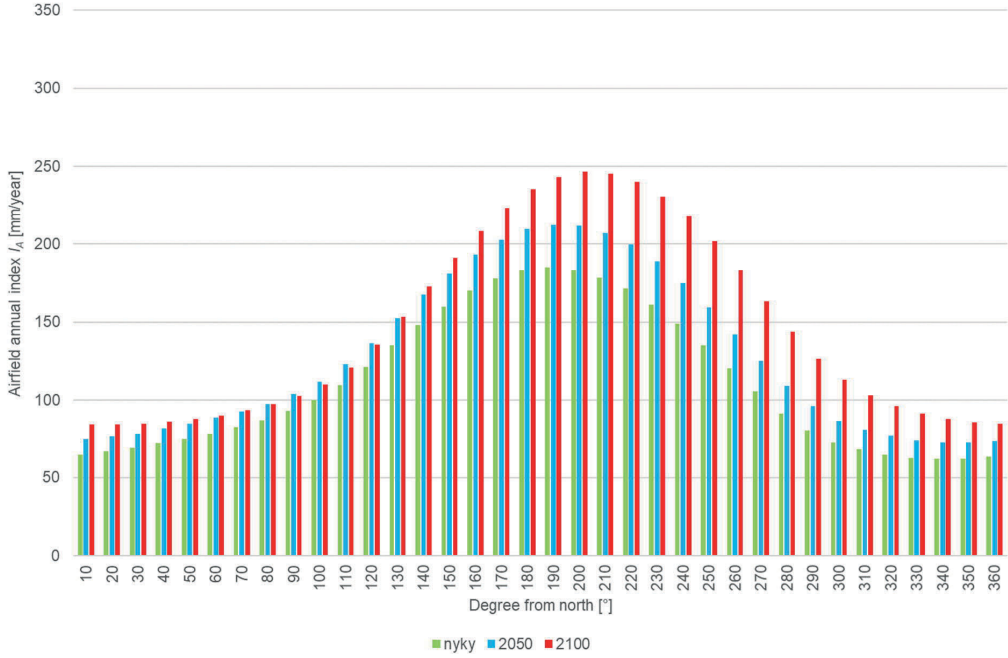

Inland (Jyväskylä)

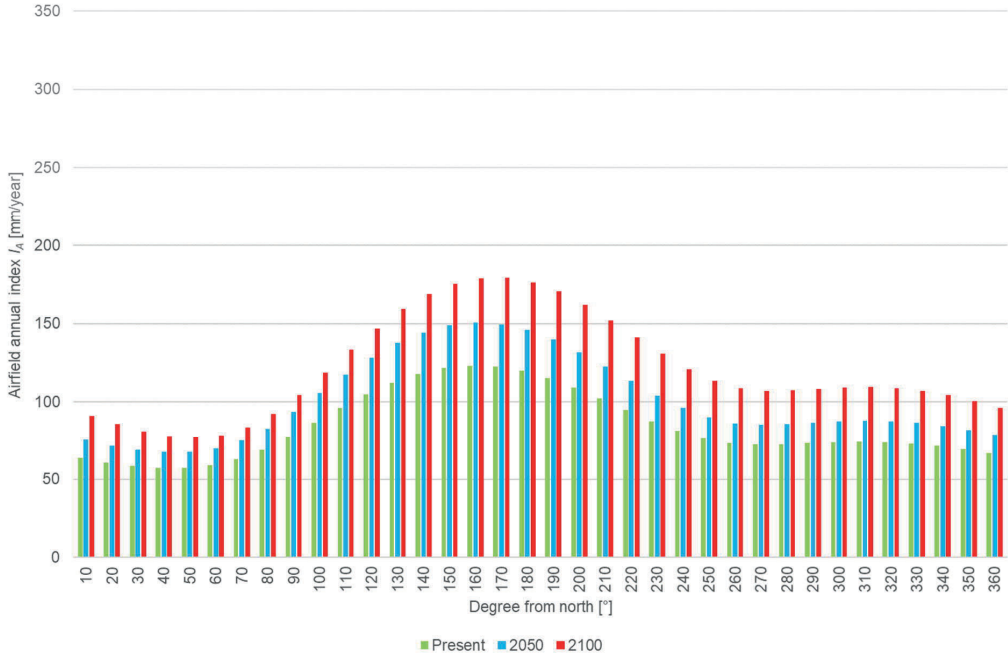

Lapland (Sodankylä)

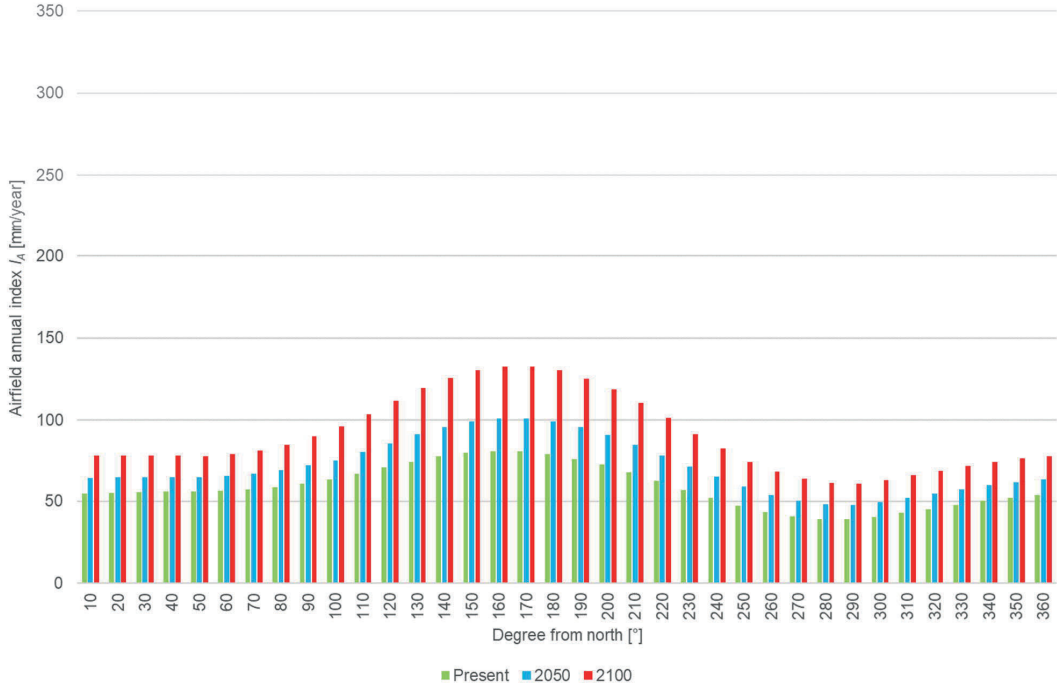

Appendix V: Monthly corrosion rates in the carbonated concrete of south- and north-facing facade and balcony structures in present and projected 2100 climates

South-facing facade, present climate

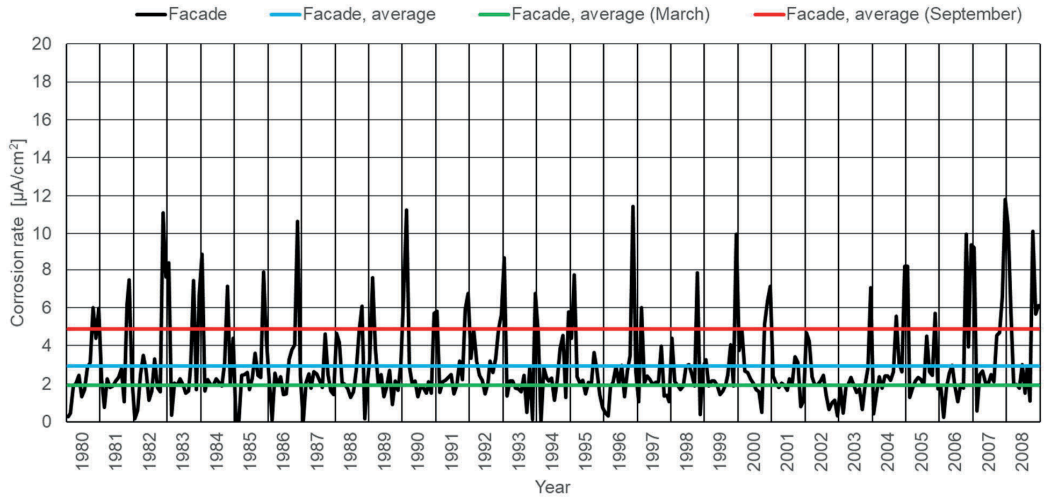

South-facing side panel, present climate

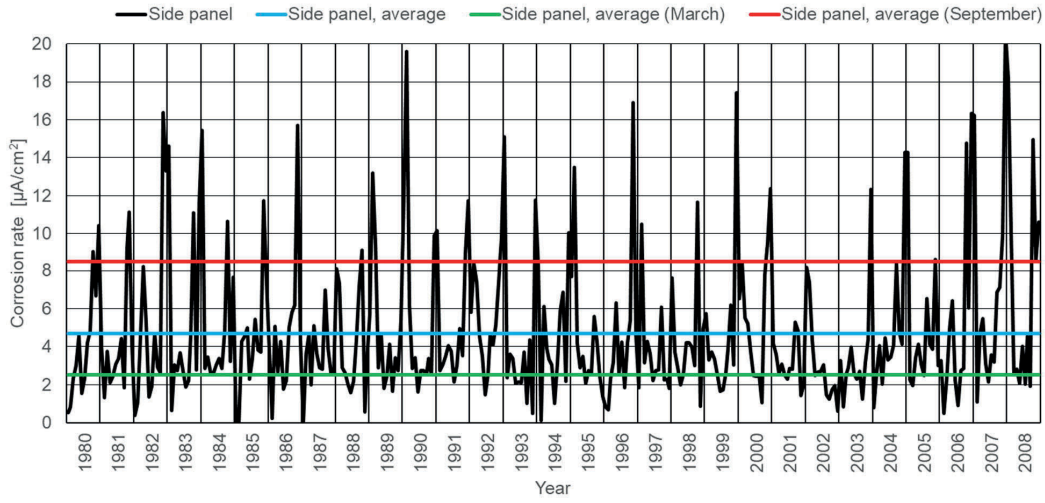

South-facing slab soffit, present climate (**note:** vertical axis)

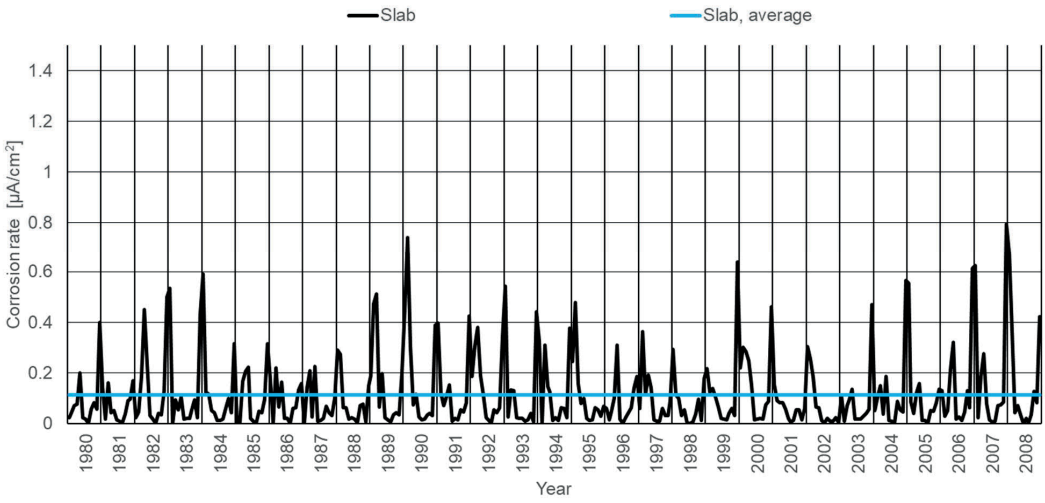

North-facing facade, side panel and slab soffit, present climate (**note:** vertical axis)

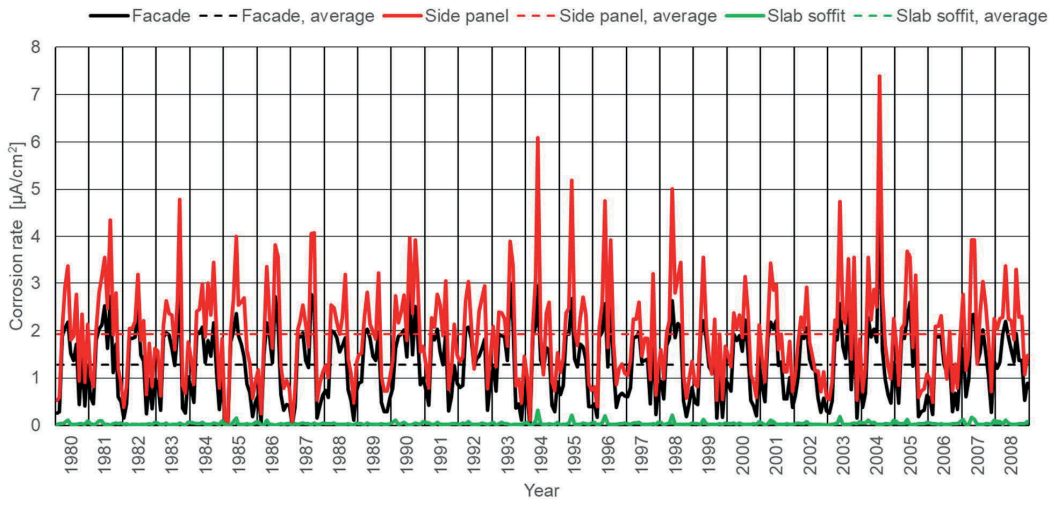

South-facing facade, 2100 climate

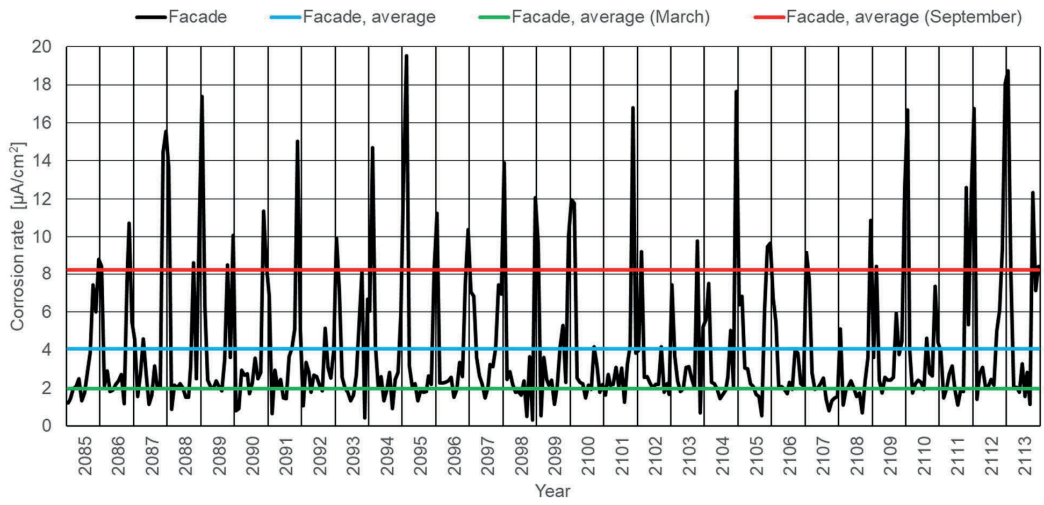

South-facing side panel, 2100 climate (**note:** the vertical axis)

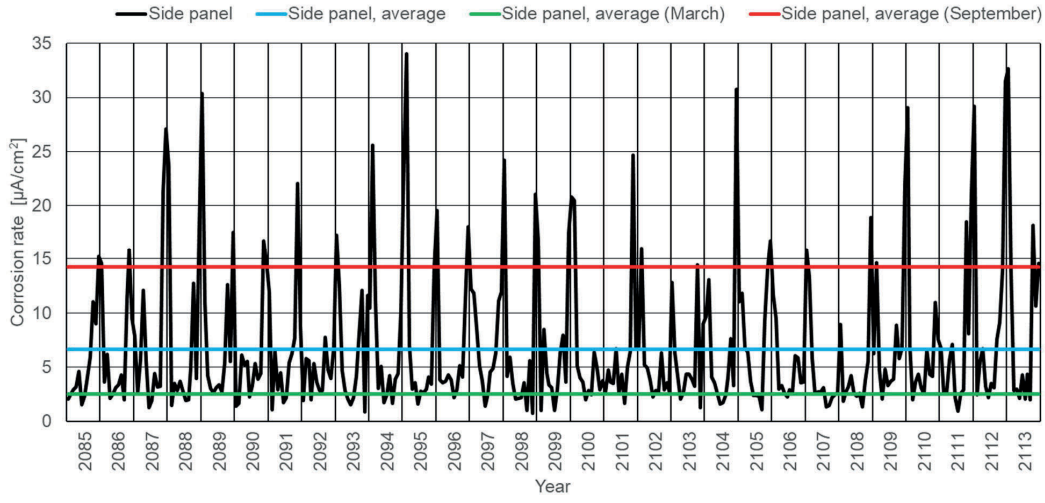

South-facing slab soffit, 2100 climate (**note:** vertical axis)

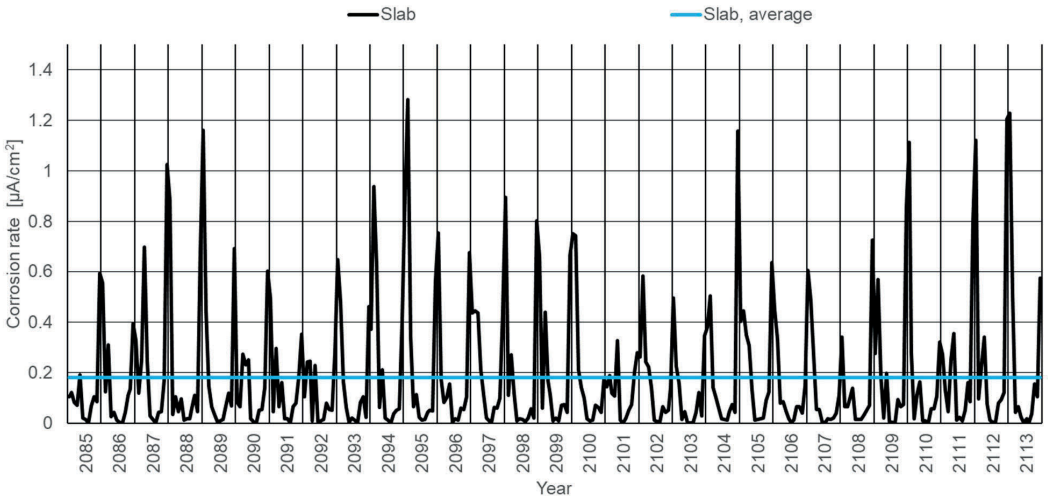

North-facing facade, side panel and slab soffit, 2100 climate (**note:** vertical axis)

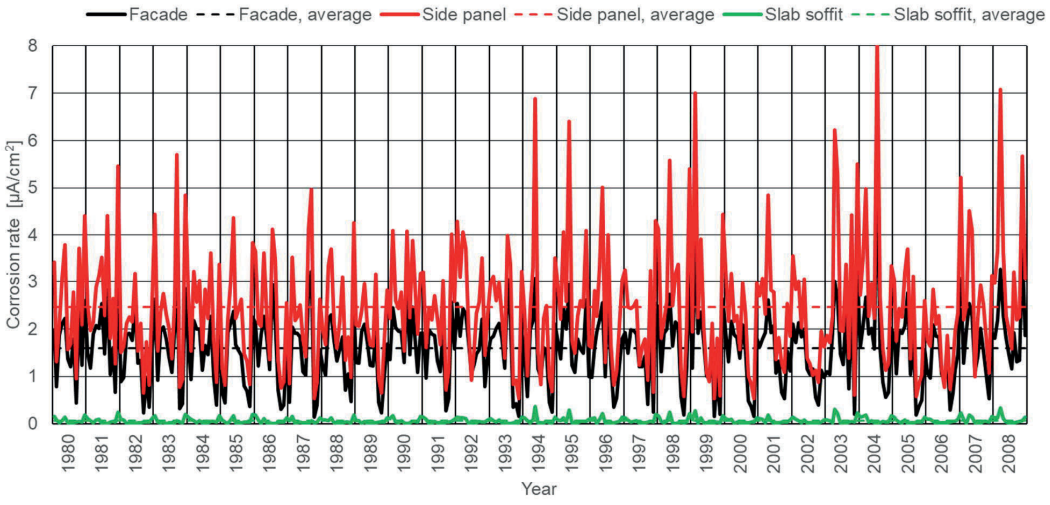

ORIGINAL PAPERS

I

DURABILITY DEMANDS RELATED TO CARBONATION INDUCED CORROSION FOR FINNISH CONCRETE BUILDINGS IN CHANGING CLIMATE

by

Köliö A., Pakkala T.A., Lahdensivu J. & Kiviste M. Mar 2014

Engineering Structures, Vol. 62–63, pp. 42–52

https://doi.org/10.1016/j.engstruct.2014.01.032

Engineering Structures 62–63 (2014) 42–52

Contents lists available at ScienceDirect

Engineering Structures

journal homepage: www.elsevier.com/locate/engstruct

Durability demands related to carbonation induced corrosion for Finnish concrete buildings in changing climate

Arto Köliö *, Toni A. Pakkala, Jukka Lahdensivu, Mihkel Kiviste

Tampere University of Technology, P.O. Box 600, FI-33101 Tampere, Finland

ARTICLE INFO

Article history:
Received 24 June 2013
Revised 17 December 2013
Accepted 20 January 2014

Keywords:
Concrete structure
Corrosion
Carbonation
Durability
Climate change
Modelling
Service life

ABSTRACT

The study is based on durability properties of concrete collected in condition assessments and climate change prediction. According to the prediction facades will face more driving rain in the future because of increasing precipitation and windiness. Outdoor circumstances in southern Finland will ease remarkably already 2030. Initiation by carbonation dominates service life of facades because active corrosion phase is only 5–8 years for surfaces exposed to rain. However, sheltered location will remarkably lengthen active corrosion. Properties that influence initiation time are highly important in ensuring eligible service life of the structure. Present requirements are enough also in the future climate but the required cover must always be achieved.

1. Introduction

During their service life new buildings are going to face more rapidly changing climate than before. The structures in the future have to be durable enough to cut unnecessarily frequent repairs that are not part of their maintenance plan. This does not only promote sustainable development but is also cost effective property management. Even today there are known cases where durability properties have not been met which indicates that the importance of durability design in construction and repair projects has not yet been fully recognized.

Climate change itself has been studied worldwide for a long time. In this context, climate change is referred to as a global-scale warming caused by an increase in greenhouse gases, especially carbon dioxide (CO_2). Climate change will affect the geographical and seasonal distribution of precipitation, wind conditions, cloudiness, air humidity and solar radiation. Modelling of future climate is based on alternative scenarios of greenhouse gas and aerosol particle emissions. In the scenarios, different assumptions are made about the future development of population growth, economic development, energy production modes, etc. The impact of climate change on the performance of structures is becoming an important research issue from an engineering point of view.

The future of European construction industry (under Horizon 2020) will involve the adaptation of current and future infrastructure towards climate-resilience (document SWD 137 [1]). Projected impacts of climate change and associated threats concerning the construction sector are as follows: (1) extreme precipitation, e.g. leading to water intrusion, damage to foundations and basements; (2) extreme summer heat events [2], e.g. leading to material fatigue and accelerated aging, high energy use for cooling; (3) exposure of structures to heavy snowfall; (4) rising sea and river levels that increase the risk of flooding, soil subsidence risks are likely to increase.

The Finnish Meteorological Institute (FMI) has examined in the ACCLIM project the different climate models, built models for Finnish climate conditions and adaptation to climate change. In all gas emission scenarios, based on three IPCC (2007) [3] scenarios for the evolution of greenhouse gas and aerosol particle emissions, the average temperature and the change of precipitation rises equally fast until 2040. Differences among the scenarios start to emerge only after the middle of the century [4]. The FMI has also made new calculations based on IPCC recently published new scenarios. In new scenarios differences in the average temperature and change of precipitation starts earlier but the values of the most severe scenario are not going to differ significantly from the values published in ACCLIM project which are used in this study.

Nowadays the estimated life cycle in building design is typically 50–100 years, and efforts are made to lengthen the service life of the older building stock by renovation. Thus, there is a great need

* Corresponding author. Tel.: +358 40 849 0837.
E-mail addresses: arto.kolio@tut.fi (A. Köliö), toni.pakkala@tut.fi (T.A. Pakkala), jukka.lahdensivu@tut.fi (J. Lahdensivu), mihkel.kiviste@tut.fi (M. Kiviste).

http://dx.doi.org/10.1016/j.engstruct.2014.01.032
0141-0296/

to study the performance of repaired structures and repair methods exposed to future climates. These studies are a major part of the FRAME project recently carried out at Tampere University of Technology (TUT). The project was based on data of the ACCLIM project [4]. However, the ACCLIM project is based only on a single future scenario of greenhouse gas emissions.

The ACCLIM and FRAME projects have shown that in the future climate conditions are likely to get worse in terms of durability of facades and other structures. It has been shown in the case of precast concrete buildings that presently deterioration of facades and balconies is faster in the coastal areas and southern Finland than inland and eastern and northern Finland [5]. According to the data of the ACCLIM project, precipitation during the winter season is also going to increase while the form of precipitation is going to be increasingly rain and sleet. At the same time, the conditions for drying are going to get worse. Thus, the degradation rate of structures will accelerate in most of Finland if maintenance and protection actions are neglected [6].

Research objective was to study whether the durability properties regulated by Finnish building codes are enough for the changing climate conditions. In this work a database of concrete material properties and observed degradation was combined with climate data projections from FMI.

2. Background

2.1. Corrosion of reinforcement due to carbonation

Because of its nature, corrosion of concrete reinforcement is in general depicted by a model with two distinct phases as in Fig. 1 [7].

2.1.1. Initiation phase and its modelling

Concrete reinforcement is protected from corrosion by high alkalinity of concrete pore water. This alkalinity is over time neutralized by carbon dioxide in the surrounding air or chlorides penetrating the concrete cover leaving the reinforcement susceptible to corrosion. Concerning concrete facades in a non-marine environment, the corrosion of reinforcement is mainly initiated by carbonation [5].

Although chloride-induced corrosion is considered to be worse than carbonation-induced corrosion, Parrott [8] and Jones et al. [9] states that 2/3 of all structural concrete is exposed to environmental conditions that favour carbonation-induced corrosion. Carbonation of concrete is a chemical reaction between alkaline hydroxides of concrete and carbon dioxide gas both dissolved in concrete pore water. The reaction product is calcium carbonate, which lowers the pH of the pore water (and concrete) gradually to a level where steel can corrode. As the alkaline hydroxide reservoir in concrete is limited, it is eventually used up leading to the neutralization of concrete.

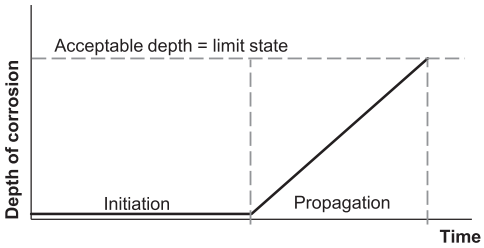

Fig. 1. The two-phase model of corrosion of reinforcement in concrete by Tuutti [7].

The evaluation of the service life of reinforced concrete structures has led to the development of several models to model carbonation evolution [7,10–17]. Carbonation has been found to involve a number of processes, from the aggressive environment of gas diffusion to the beginning of the corrosion itself, and there are several other parameters whose variability cannot be ignored. Neves et al. [18] provided a simple analytical model for the initiation period, calibrated with long-term carbonation results, which used the accelerated carbonation resistance and the environmental class as input parameters (semi-probabilistic approach). Recent work also focused on the assessment of climate change on the durability of concrete structures in specific locations. Wang et al. [19] studied the impact of climatic change on corrosion-induced damage in Australia. Talukdar et al. [20] estimated the effects of climate change on carbonation in Canadian cities. Based on those results Talukdar and Banthia [21] developed a model of carbonation in concrete infrastructure in the context of global climate change. The serviceable life, from construction through to cracking due to carbonation induced corrosion of concrete infrastructure is considered in all continents. It was concluded that global climate change will affect the progression and will result in much higher ultimate carbonation depths in the long term. Guiglia and Taliano [22] compared the carbonation measured on in-field exposed existing reinforced concrete structures with predictions made using fib-Model Code 2010. This comparison has highlighted the key role played not only by the environment, but also by the quality of the concrete through the inverse effective carbonation resistance of concrete on the evolution of the carbonation depth in time.

2.1.2. Propagation phase and its modelling

Corrosion of steel embedded in concrete is an electrochemical reaction where anode and cathode areas are formed on the steel surface as a result of differences in pH and moisture. Anode areas release positively charged hydrated ions in oxidation reaction into the pore water acting as an electrolyte. The excess electrons flow through metal from the anode to cathode where they are consumed in reduction reaction by hydrogen ions or by dissolved oxygen. The ions released in electrolyte react forming corrosion products. Corrosion, especially with shallow cover depths, leads to cracking or spalling of surrounding concrete as the reinforcing bar starts to rust forming residue greater in volume than the original bar [23]. To happen, electrochemical corrosion requires [24]:

- a reactive metal where anodic oxidation can take place,
- a reducible substance which acts as a cathodic reactant,
- electrolyte allowing the migration and movement of ions,
- an electron conduction between anodic and cathodic areas.

Therefore, amount of pore water is one of the critical preconditions for corrosion meaning that the moisture of reinforced concrete has a paramount effect on the rate of corrosion. The rise in temperature is considered to increase the solubility of chemical compounds thereby increasing also the rate of corrosion [7].

The corrosion propagation phase is now appreciated as a significant component in the service life of RC structures and a good understanding of the propagation process is paramount. Various models have been developed to simulate and/or predict the propagation phase. Empirical models are sub-divided into three types i.e.: (i) Expert Delphic oracle models, (ii) fuzzy logic models, (iii) models based on electrical resistivity and/or oxygen diffusion resistance of concrete. Three different approaches can be used to develop numerical models viz: (i) finite element method (FEM), (ii) Boundary element method (BEM) and (iii) resistor networks and transmission line method. Analytical models apply usually thick-walled cylinder approach. Division into cracked inner

cylinder and an uncracked outer have also been developed. Otieno et al. [25] presented a critical review of some of the available models for corrosion propagation, and proposed ways forward to overcome some of these problems.

The influence of the amount of precipitation to the behaviour of reinforcement corrosion was observed in research depicted in Refs. [26,27]. In his research Mattila measured the corrosion current in measurement devices embedded in existing concrete facades. High corrosion current was observed during a year when annual precipitation was exceptionally high. Vice versa, when annual precipitation was low also very low corrosion currents were observed. Refs. [28–30] establish a basis for estimating the relationships between aggressiveness of corrosion, corrosion rates and loss of cross section of reinforcing bar due to corrosion.

2.1.3. Limit state of reinforcement corrosion

Corrosion of reinforcement affects concrete structures basically either by cracking of concrete cover caused by corrosion products or by reduction of effective steel cross-section. Which one of these effects is more crucial depends on the functionality of the corroding structure. Cracking occurs in structures where the reinforcement is placed quite near the concrete surface and the pressure generated by corrosion products is sufficient. Cracking accelerates the penetration of harmful agents to concrete and causes visual defects in concrete facades ultimately leading to spalling of areas of concrete. In this context, the occurrence of cracks is not the ultimate limit for the life of the structure, but rather a limit based on the appearance and serviceability of the facade. There still exists an undefined residual life after this. As induced by carbonation, the corrosion of relatively small reinforcement with normal cover depths can go on for remarkably long time without showing any visual signs thus making it difficult to diagnose. Principles [7] and threshold values [28,31,32] for estimating the amount of corrosion needed to cause visual damage are discussed in literature for various corrosion cases.

2.2. Precast facade elements and balconies

Since 1970s almost all prefabricated concrete structures in Finland are based on the Concrete Element System [33]. That open system defines, for instance, the recommended floor-to-floor height and the types of prefabricated panels used. In principle, the system allows using the prefabricated panels made by all manufacturers in any single multi-storey building.

2.2.1. Facades

The concrete panels used in exterior walls of multi-storey residential buildings were, and still are, chiefly prefabricated sandwich-type panels with thermal insulation placed between two concrete layers. Facade panels are made up of two relatively thin reinforced concrete layers connected to each other by steel trusses. The thermal insulation between the layers is most often mineral wool of 240 mm nominal thickness according to the building regulations in force.

The usual nominal thickness of the outer layer is nowadays 80–85 mm. The layers are most typically reinforced with steel mesh of a wire diameter of 3 mm and spacing of 150 mm. Rebars 6–8 mm in diameter are typically used as so-called edge bars and often also diagonally at the corners of windows and other major openings in the layers. The bars are spliced by lap splices, which increase the overall thickness of the reinforcement, see Fig. 2.

The outer layer is generally supported by the inner layer. Sandwich facade panels are connected to the building frame by the inner layer, usually by means of cast concrete joints and reinforcement ties.

2.2.2. Balconies

The most common balcony type in Finland from the late 1960s until today consists of a floor slab, side panels and a parapet panel of precast concrete. These stacked balconies have their own foundations, and the whole stack is connected to the building frame only to brace it against horizontal loads. All structural members of a precast balcony are load-bearing. The cross-section of a typical balcony constructed of precast panels is presented in Fig. 3 [35].

The typical nominal thickness of a load-bearing wall panel is between 150 and 180 mm depending on the number of floors. In general, multi-storey residential buildings have no more than eight floors. This allows using plain concrete side panels as a bearing structure and rebars only 10–12 mm in diameter as so-called edge bars to take the forces caused by the shrinkage of concrete and the erection of the balcony.

The nominal thickness of a bearing concrete slab is between 140 and 200 mm. It varies a lot depending on the slope of the upper surface of the slab panel. The bearing reinforcement, typically 10–12 mm in diameter and with a spacing of 100–150 mm, is in the bottom section of the slab. Without exception there is not any waterproofing on the top of balcony slab.

The nominal thickness of parapets is from 70 to 85 mm. Parapets usually have quite heavy reinforcement near both surfaces, vertical rebars 6–8 mm in diameter spaced 150 mm apart. Parapets are most often joined to the slab by casting them together.

2.3. Climate projections in Finland

Although the climate is relatively steady for the latitudes and compared to size, it still varies considerably. However, the Finnish building stock is mainly focused on the few biggest cities and certain growth areas near them. Due to both the climate differences and the concentration areas of the population Finland can be divided to four main areas: coastal area, southern Finland, inland and Lapland. Coastal area includes 30 km wide sector of the coast from the city of Vaasa to Russian border. Southern Finland includes the rest of southern parts to the level of the Tampere city (150 km north from Helsinki). Inland area includes the rest of the country except Lapland.

The Finnish Meteorological Institute (FMI) has weather data since 1961 in digital form from several meteorological stations covering all of Finland. The data consist of temperature, relative humidity, rain intensity, wind speed and direction, solar radiation variables, etc. These observations have been collected at least daily and three times a day at best. In the REFI-B project [36], the FMI also forecast the climates of four localities (coastal area, southern Finland, inland, Lapland) in three periods (2030, 2050 and 2100). The forecasts are based on an average of 19 different models which are all based on greenhouse gas emission scenario A2. The A2 scenario involves a situation where greenhouse gases are assumed to increase significantly – it is a sort of worst-case scenario. The FMI also has other significant greenhouse gas emission scenarios: A1B (quite large emissions) and B1 (small emissions). The increase of the CO_2-level is depending highly on the scenario used. According to the IPCC [3], while using A2 scenario the CO_2-level can rise up to 840 ppm until the end of the century and about 540 when using B1 scenario. However, the increase is significant compared to present level (390 ppm) [36] (see Fig. 4).

The annual precipitation does not get evenly distributed over facades. The distribution depends on the height of the building and prevailing wind directions during rain. According to Jerling and Schechninger, the upper parts and corners of facades get more precipitation than lower and central parts [37]. Prevailing wind directions and wind speeds also have a strong influence on the distribution of precipitation across a building. In Finland most of the rain and sleet in wintertime comes with southerly to westerly

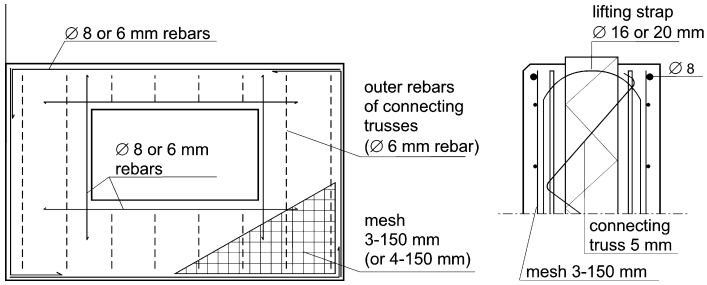

Fig. 2. Typical reinforcement of outer layer of a concrete facade panel [34].

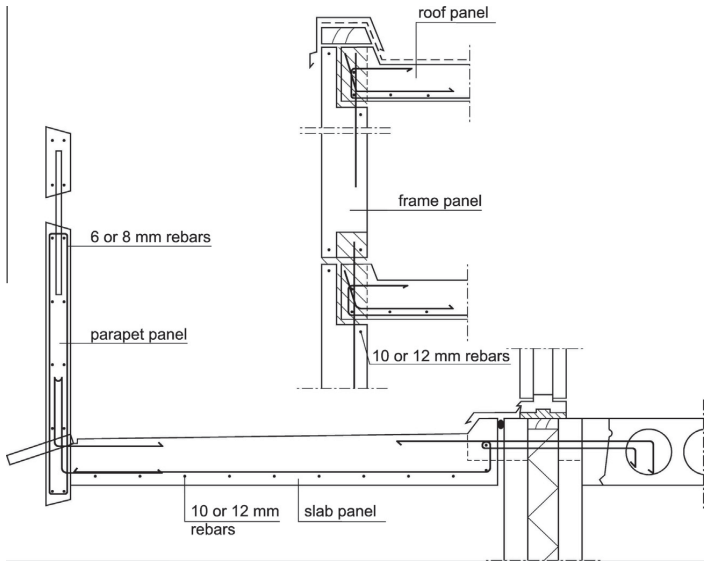

Fig. 3. Cross-section of a typical Finnish balcony made of precast structural members [35].

winds. Rain events with wind from other directions have been rare. Due to stronger winds, about 60% of the rain and sleet load in the coastal area hits the facades and balconies; the corresponding share inland is about 40%. Combined with the higher amount of precipitation in coastal areas, facades and balconies there are subject to considerably higher moisture stress than inland resulting in clearly more corrosion and frost damage. Winds are stronger at higher reaches of buildings than close to ground level which naturally leads to upper sections of high buildings receiving more rain and sleet stress than lower buildings, and lower sections of buildings in general [38].

3. Research methods and material

3.1. Research material

Research material for this study is composed of data on concrete durability assembled in condition assessments conducted on prefabricated concrete facades and balconies built in 1961–1996. As this study discusses the current concrete codes the data is delimited to 72 buildings built 1990 or after. The database withholds measurements of concrete pore structure, tensile strength, chloride content, carbonation depths as well as concrete cover depths of reinforcement. In addition it includes results from thin section analyses and visual observations made from the building facades and balconies.

Practical design of concrete structures is in Finland governed by national concrete codes [39]. Besides guidelines for structural design, it also gives recommendation on durability properties and service life design. These requirements are compared to the actual observed degradation processes and their progress in the future.

Future climate projections and their effects on weather conditions critical to concrete degradation have been prepared by the Finnish Meteorological Institute. This data is utilized in this study.

3.1.1. Quality of concrete

In Finland the concrete grade used in concrete facade panels as well as most structural members of balconies has been C30/37 since late 1980s by the guidelines for durability and service life of concrete [40]. The cement type used in those concrete panels is mostly CEM I (42.5 N) (ordinary Portland cement) because of good early age strength of concrete which allows rapid formwork rotation at precast concrete panel factory. White cement, CEM I (52.5 R) is also used in facade panels if necessary, but its share of total amount of used cement is small. In Nordic outdoor climate the concrete used for facades and balconies is always air-entrained.

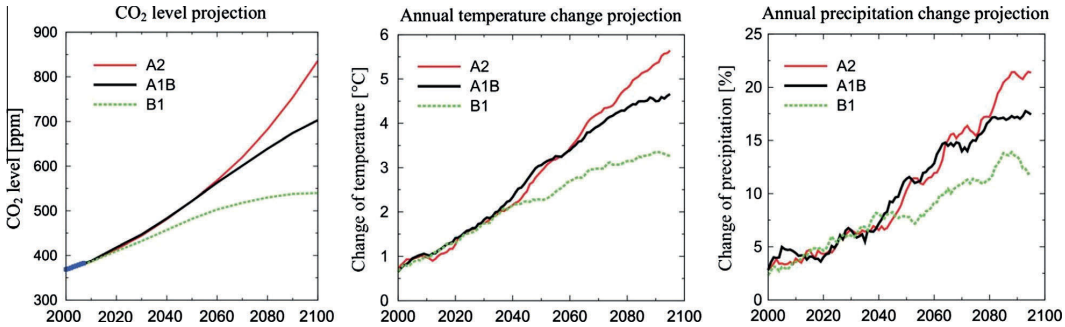

Fig. 4. Projections for CO_2 level increase, the annual mean temperature and the precipitation change for the period 2000–2100, relative to the mean of the reference period 1971–2000. The curves depict 11 year running means, averaged over Finland and the responses of 19 global climate models. Projections are given separately for the three greenhouse gas scenarios (A2, A1B and B1) [4].

3.2. Calculating the service life by reinforcement corrosion

3.2.1. Initiation phase

Corrosion of reinforcement in concrete facades and balconies is evaluated by a combined model for future climate in Finland by Finnish Meteorological Institute and carbonation initiated corrosion. Initiation is depicted with the square root model of carbonation (Eq. (1)), based on Fick's 2nd law on diffusion, using measured coefficients. The progression of carbonation inside the concrete is commonly acknowledged to follow a square root equation relationship with the time of exposure modified with a carbonation coefficient [7]. However, the square root model does not specify the influence of the rise in CO_2 in the environment due to climate change. For estimating the influence of CO_2 the model given in fib model code for service life design [41] was used (Eq. (2)). Propagation phase is estimated by combining future climate data and preset boundary conditions obtained through research and from literature. The service life of the reinforcement withholds the time of initiation and active corrosion to the limit state when first cracking occurs.

The demands in Finnish concrete codes for reinforcement cover depths are given in Table 1.

Carbonation time is calculated using the presumed square root dependence of carbonation depth x with time of exposure t to CO_2 in surrounding air [7]:

$$x = k \cdot \sqrt{t} \tag{1}$$

The carbonation coefficient k is highly dependent on (and includes the effect of all) type of structure, time of wetness, material properties, etc. These coefficients for different types of facade finishes and balcony units have been determined in facade condition assessments and thus, the values used in this study represent actual measured carbonation depths from existing buildings. The large amount of data enables statistical evaluation. The statistical numbers calculated were average, standard deviation (to the worse direction) and 95% percentile.

To study the effect of change in CO_2 in the environment and the amount of precipitation by climate change, the fib model for carbonation [41] was used with parameters given in Table 2:

Table 2
Parameters used in Eq. (2).

k_e	k_c	R_{NAC}^{-1}	t_0	w	C_s
0.466	1.00	28,500	0.0767	Varied	Varied

$$x_c = \sqrt{2 \cdot k_e \cdot k_c \cdot R_{NAC}^{-1} \cdot C_s} \cdot \sqrt{t} \cdot \left(\frac{t_0}{t}\right)^w \tag{2}$$

3.2.2. Propagation phase

As idealized in the model by Tuutti, corrosion of reinforcing steel in concrete is a phenomenon with two consecutive phases. It is also assumed here that active corrosion begins after the initiation phase has been completed. For a single point inside the structure this assumption is valid, but not for a whole structure resulting from the variations in structure's properties. The corrosion rate of a reinforcing bar varies depending greatly on the moisture of the surrounding concrete. Coarse boundary values for annual precipitation for very fast and very slow reinforcement corrosion have been established in an earlier study by Mattila [26]. According to Mattila corrosion is fast in Finnish climate conditions when the annual precipitation is over 480 mm/year. These results were combined with known corrosion rates obtained from literature. Rates at which corrosion penetrates reinforcing steel are presented by Andrade [29]. Negligible corrosion advances less than 1 μm/a and high corrosion over 10 μm/a. The respective corrosion rates are less than 0.1 μA/cm^2 and over 1 μA/cm^2.

Active corrosion phase was modelled as the penetration depth x_{corr} by the following rules:

$$x_{corr} = \sum_{i=1}^{t_{prop}} r_i \tag{3}$$

where x_{corr} = corrosion penetration depth, r_i = average annual corrosion rate during year i (1 μm/a if annual precipitation <480 mm and 10 μm/a if annual precipitation ⩾480 mm), and t_{prop} = the age in years when critical corrosion depth is achieved.

Table 1
Demands for concrete cover in different stress class when designed service life is 50 or 100 years [39].

Designed service life (a)	Stress class	Minimum concrete cover (mm)	Crack width (mm)
50	XC3/XC4	25	⩽0.2
100	XC3/XC4	30	⩽0.13

Table 3
Average annual change (%) in precipitation and temperature (°C) compared to present climate (2000) in four different observation station.

	Vantaa (south coastal area)			Jokioinen (south inland)			Jyväskylä (inland)			Sodankylä (Lapland)		
	2030	2050	2100	2030	2050	2100	2030	2050	2010	2030	2050	2100
Precipitation	3.8	7.1	17.7	3.1	6.1	15.2	3.6	7.1	18.2	3.9	7.9	21.3
Temperature	1.2	2.1	5.1	1.2	2.1	5.0	1.3	2.3	5.5	1.5	2.7	6.4

The average annual corrosion rate was chosen based on the amount of annual precipitation for each year *i*. For this data of measured annual precipitation from the period 1979–2009 was used to describe current climate. This data was then increased according to FMI predictions, see Table 3, to describe the change in 2030, 2050 and 2100. The change in the amount of precipitation will be higher during autumn and winter when drying of structures is slower in general. Again, according to FMI, the prevailing wind directions during rain events will stay same as present. It intends that facades faced from South-East to West will get more precipitation also in the future.

The fib model [41] for propagation phase until first cracking (Expert Delphic oracle based log–normal distribution with parameters $m = 4.5$ years and $s = 1.5$ years) was applied to study the effect of change in temperature in the environment by climate change.

3.2.3. Limit state of reinforcement corrosion

Alonso et al. [28] have presented estimates for the amount of corrosion in concrete reinforcement that can cause cracks and chipping of concrete cover. The critical amount is 15–50 μm presented as depth of corrosion or loss of bar diameter. The formation of cracks due to corrosion is, however, dependent on multiple factors including bar diameter and thickness of concrete cover, which can deviate considerably from the design value. In this study 50 μm was chosen as the critical depth of corrosion x_{limit} depicting the time of the first cracking of concrete.

4. Results and discussion

4.1. Initiation of corrosion of reinforcement in facades

The carbonation coefficients that have been used in the calculations of this study are presented in Fig. 5 as cumulative distribution functions. All of the carbonation coefficients have been determined from existing prefabricated concrete buildings constructed in 1990–1995 that have been subjected to a condition assessment.

Concrete facades with white concrete or brick tile finishing are generally less susceptible to carbonation that ordinary painted concrete facades. The difference of painted concrete is due to the brushing surface treatment that leaves the concrete surface more open to carbonation. Higher cement content of the white concrete and the compacting effect of the capillary suction of brick tiles while casting are influencing more slow carbonation in these facades [5]. Statistical numbers for carbonation coefficients used later in the assessment of carbonation depths by Eq. (1) are average and 95% percentile as shown in Table 4. The large standard deviation for both facades and balconies, in Tables 4 and 5, describes the large scatter in carbonation of these surfaces in practice.

Probable lengths of carbonation phase for different facades calculated using the above carbonation coefficients are shown in Fig. 6. Standard design service life of concrete facades (50 years) is marked with a horizontal line in the figure. The figures have been limited to illustrate more clearly the first 100 years. Very long estimates are also quite theoretical.

Fig. 6 indicates that by average the 50 year service life is always achieved by carbonation in facades with white concrete or brick tile finish. Painted concrete facade requires successful concrete cover to achieve 50 years. By the 95% percentile, painted concrete facades reach a service life of 20 years when reinforcement is placed according to the concrete codes (25 mm cover). With white concrete and brick tile finish a service life of 100 and 40, respectively, years are achieved.

As the service life by reinforcement corrosion is in Finnish guidelines managed only by the initiation phase, namely carbonation of the concrete cover, the ones to fill the requirement of 50 year service life with 5% safety margin are white concrete facades. As an average, it can be said that majority of facades fulfill the required service life. This is of course when the placing of the reinforcing bars/mesh has been successful according to the codes with sufficient concrete cover. The importance of sufficient concrete cover is clearly pointed out by Fig. 6. Even a decrease of 5 mm will shorten the service life through carbonation easily by 10 years.

4.2. Initiation of corrosion of reinforcement in balconies

The carbonation of prefabricated balcony units was analyzed with the same principle as with different facade types. Carbonation coefficients describing the aggressiveness of carbonation in different structure units are presented in Fig. 7 and the ones used in further studies are presented in Table 5.

The one balcony surface carbonating much faster than others is the lower surface of a balcony slab. This is affected mainly by the casting direction which is upside down. Therefore the lower surface has higher w/c ratio due to the effect of floating of fresh concrete surface. Secondly, the lower surface of the balcony slab is sheltered from the rain, which keeps the surface dry allowing easier carbonation [5]. That behaviour is illustrated in Fig. 8.

Probable lengths of carbonation phase for different balcony units are shown in Figs. 8–10. Standard design service life of concrete facades (50 years) is marked with a horizontal line in the figures.

According to Figs. 8–10, based on average carbonation rate the 50 year service life requirement is always fulfilled. Based on 95% percentile the 50 year service life is not certain with balcony parapet outer surface and balcony side panel inner surface. It is also questionable with parapet inner surface and side panel outer surface.

In balcony structures described in Fig. 2 the main reinforcement is located in the lower part of the prefabricated balcony slab. Thus the carbonation of the lower surface of a balcony slab is the most relevant in the question of service life. As an average, 50 years is achieved by initiation also in the case of the lower surface. However, based on 95% percentile the length of initiation is only 17 years.

4.3. The effect of climate change on initiation

In Nordic climate the climate change affects the carbonation of concrete by increasing the CO_2 concentration in air and by increasing raininess. The both have an opposite effect on carbonation. The effect of these factors have been presented in Fig. 11.

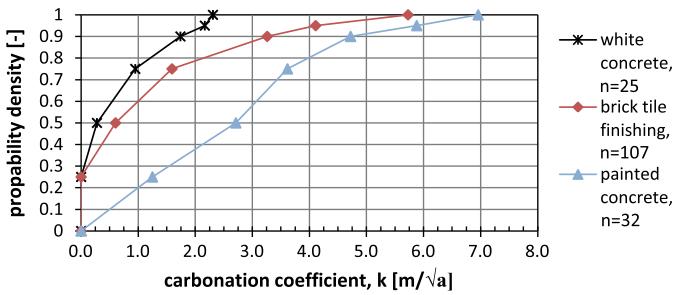

Fig. 5. Carbonation coefficients as cumulative graphs determined in facade condition assessments of buildings built in 1990–1995.

Table 4
Carbonation coefficients of concrete facades surfaces of different finishing (mm/√a).

	Brick tile finishing	Painted concrete	White concrete
Average	1.06	2.62	0.59
Std. deviation	1.31	1.64	0.70
95% percentile	4.11	5.88	2.17

Table 5
Carbonation coefficients in balcony units (mm/√a).

	Slab		Side panel		Parapet	
	Upper s	Lower s	Outer s	Inner s	Outer s	Inner s
Average	1.15	3.21	1.50	1.63	1.09	1.48
Std. deviation	0.90	1.42	1.02	1.24	1.13	1.02
95% percentile	2.82	6.02	3.47	4.14	3.95	3.49

The scenarios in Fig. 11 are based on the climate change scenario A2 (significant increase). According to the fib model [41] the increase in rain reduces the carbonation by 5.7% until 2050 and by 15.4% until 2100. The increase in carbonation by CO_2 level is 17.0% until 2050 and 48.2% until 2100. The results indicate that the influence of CO_2 level is dominating of these two factors in regard of concrete carbonation and, thus, the carbonation is likely to increase as the result of climate change. However, the weather function *w* in Eq. (2) is somewhat questionable for it takes into account only the number of rainy days and the probability of wind driven rain. The distribution and duration of rain events (seasonal rains or small amounts constantly) is also likely to have an effect on carbonation.

Fig. 12 shows the comparison between the average carbonation by the fib model [41] and the scatter in the carbonation coefficients measured from existing structures by the Tuutti's model.

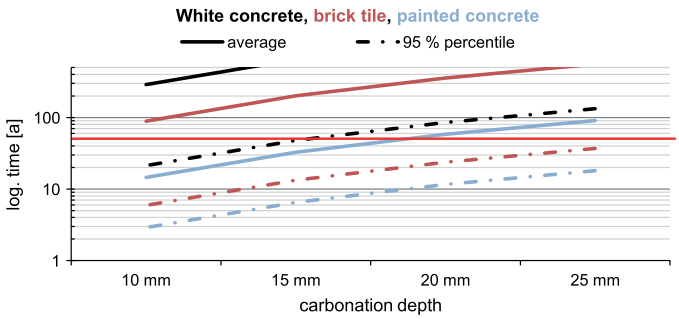

Fig. 6. Service life of reinforcement regarding the initiation phase (carbonation) for different cover depths and surface treatments of facades.

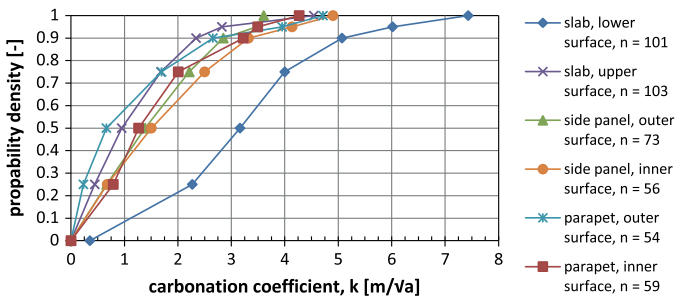

Fig. 7. Carbonation coefficients determined from prefabricated concrete balconies in facade condition assessments of buildings built in 1990–1995.

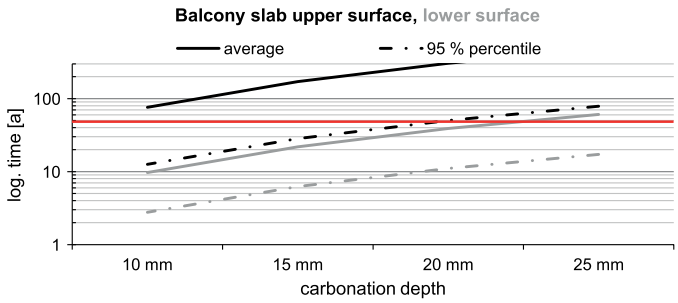

Fig. 8. Service life of reinforcement regarding the initiation phase (carbonation) for different cover depths in upper and lower surface of a balcony slab.

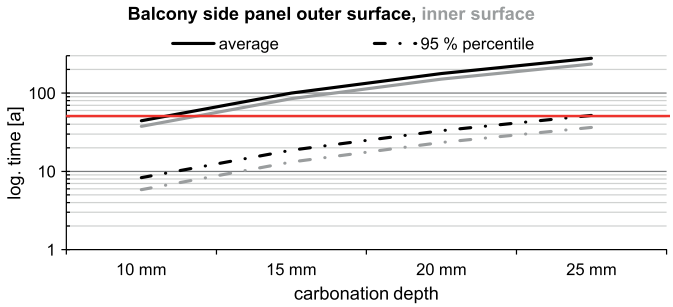

Fig. 9. Service life of reinforcement regarding the initiation phase (carbonation) for different cover depths in outer and inner surface of a balcony side panel.

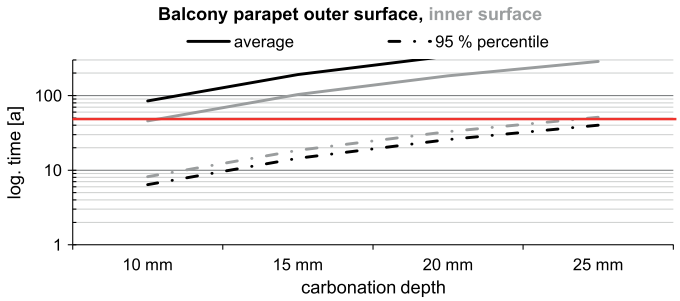

Fig. 10. Service life of reinforcement regarding the initiation phase (carbonation) for different cover depths in outer and inner surface of a balcony parapet.

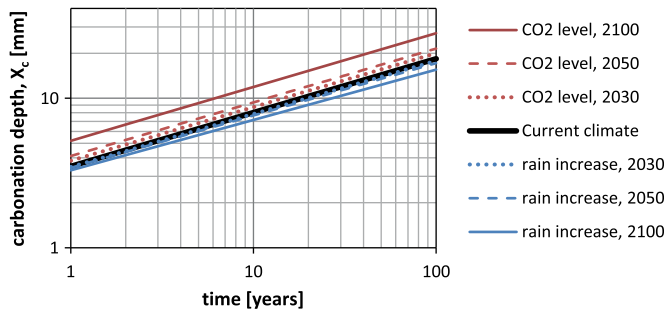

Fig. 11. The influence of CO_2 level and increase in raininess on corrosion initiation by carbonation.

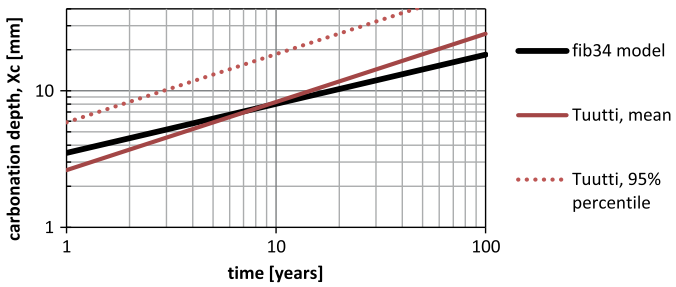

Fig. 12. Comparison between the carbonation coefficients of Tuutti model and the model by fib [41].

Table 6
The length (in years) of active corrosion phase in respect of crack initiation in different parts of Finland.

	Helsinki-Vantaa airport (coastal area)	Jokioinen observatory (southern Finland)	Jyväskylä-Tikkakoski airport (inland)	Sodankylä observatory (Lapland)
Current climate (1980–2009)	5.7	6.1	8.2	37.5
2030	5.5	5.7	7.8	37.5
2050	5.3	5.5	7.4	37.5
2100	5.3	5.1	6.1	19.7

Carbonation rate according to the fib model is slower than Tuutti's model based on measured carbonation depth of concrete. The fib model gives higher carbonation depth for young concrete but after 100 years fib model gives 8 mm lower carbonation depth than Tuutti's model in average. The difference is remarkable in case of service life of concrete structure. By extrapolating the fib model the difference of 8 mm equals 168 years in service life prediction.

The fib model is based on DuraCrete-project [17]. Concrete studied in that project has generally been of better quality than in existing Finnish concrete facades and balconies. For that reason Tuutti's model has been used in this study with measured coefficients leading to higher predictions in carbonation depth in 100 years.

4.4. The effect of increase in rain on propagation phase

The length of active corrosion phase to the initiation of cracks in concrete was estimated by using the background established in Refs. [26,28,29]. This knowledge was combined with future weather data by FMI in Table 2. Table 6 presents the calculated durations of active corrosion phase in respect to the weather conditions (annual raininess) of different locations in Finland.

Taking the active corrosion phase into consideration will lengthen the service life of reinforcement by 5–8 years in southern parts of Finland and up to 35 years in Lapland in current climate. Climate change will as a rule shorten the active corrosion phase by subjecting concrete structures to weather conditions more favourable to corrosion. The change is slow at first but will increase by the end of this century especially in northern parts of Finland.

Table 6 shows that the most severe conditions regarding active corrosion are in the coastal area and southern Finland. In these regions of Finland active corrosion phase is remarkably short. The climate change will not affect it significantly compared to Lapland. The active corrosion phase in Lapland will remain at the same level until 2050 and then drop dramatically. This change is due to much bigger precipitation prediction by FMI.

If the building is in Lapland combining initiation and active corrosion will easily give enough service life. However, the majority of Finnish building stock is located and construction activities are in the southern part of Finland. In the southern part of Finland initiation period dominates service life because active corrosion phase adds only 5–8 years. Therefore cover depth of reinforcement and the quality of concrete, that influence the initiation time, are highly important in ensuring the 50 year service life.

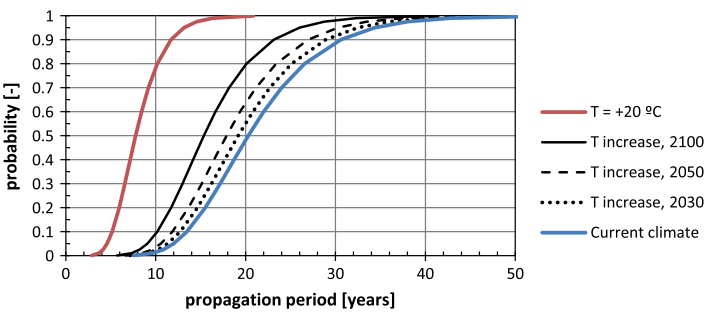

Fig. 13. The effect of increase in temperature on active corrosion of reinforcement in carbonated concrete according to fib 34 [41].

4.5. The effect of temperature change on propagation phase

Propagation model given in [41] represents a temperature relationship of active corrosion using a reference propagation time modified by a temperature related factor. This has been applied in Fig. 13 to predict the influence of increase in air temperature induced by climate change. According to FMI the annual average temperature in Finland varies from +5.9 °C (south coastal area) to −0.4 °C (Lapland). In calculations presented in Fig. 13 has been used +2.0 °C which is suitable for large areas in southern Finland.

Active corrosion phase takes 12 years in present climate when studying 95% percentile. The active corrosion phase decrease to 9.6 years by the end of century as a result of temperature increase caused by climate change. According to fib model, temperature has significant effect on corrosion rate; in 20 °C active corrosion phase takes 4.6 years. This is theoretically right and reasonable. However, according to field measurements made by TUT outdoor temperature does not have so significant influence on corrosion rate in practice. Corrosion rate remain approximately at the same level in temperature range of −5 to +25 °C, only very low rise was detected [27].

In current climate corrosion rate presented in Table 6 is rather close to 20 °C probability curve presented in Fig. 13. The raininess as well as properties of concrete (capillarity) are the crucial factors affecting on corrosion rate of reinforcement in carbonated concrete.

5. Conclusions

According to Finnish concrete codes the service life of reinforced concrete structure will end when carbonation achieves the reinforcement. In practice corrosion can start in that time if circumstances are favourable to corrosion (enough moisture, availability of oxygen, temperature, etc.). Active corrosion phase is not included to service life of concrete structure.

The carbonation rate of concrete varies a lot according to properties of concrete. Concrete is not a homogenous material, the durability properties varies due to e.g. compaction and curing of fresh concrete. Great difference might occur between patches due to e.g. moisture content of aggregate leading to different water–cement ratio. Concrete technology has a great influence on the capillarity of concrete. In general, the carbonation rate of concrete is slow in dense, low water–cement ratio concrete, where curing has been careful.

Regarding service life by reinforcement corrosion, for the majority of Finnish building stock the initiation period by carbonation dominates service life because active corrosion phase can add only 5–8 years. Therefore cover depth of reinforcement and the quality of concrete, that influence the initiation time, are highly important in ensuring the 50 year service life.

For buildings located in northern Finland the active corrosion phase can increase service life remarkably. Precipitation in northern Finland occurs mostly as snow. The above estimation of active corrosion time is valid for surfaces exposed to rain. Since the amount of rain has a paramount influence on active corrosion, also a sheltered location will remarkably lengthen the period of active corrosion. This is valid for the soffit surface of a balcony slab.

Visible corrosion damage in facades and balcony structures are rather unusual if the cover depth is in the level required in Finnish concrete codes (25 mm) even if the carbonation of concrete would achieve the reinforcement. Especially structures sheltered from the rain, like soffits of balcony slabs or inner surface of balcony parapets, the active corrosion of reinforcement is very slow.

Facades will get higher driving rain stress in the future because climate change will increase the amount of rain and sleet and also windiness. The increase of precipitation in the future will have only small effect to the corrosion rate during active corrosion period, because the active corrosion period is rather short even now, only 6–8 years which will accelerate to 5–6 year in the beginning of century in southern and middle Finland.

Visible corrosion damage will be noticed before designed service life has been achieved in the reinforced concrete structures where cover depths are low, e.g. less than 15 mm. During manufacturing of concrete structures sufficient cover depths should be ensured with spacers and careful installation of the reinforcement.

The fib 34 model gave a longer service life in both initiation and propagation phase than Tuutti's model and propagation phase studies conducted at TUT. The differences in initiation time were caused by different concrete quality and grade of research material. The increase of CO_2 dominates over the increase in precipitation during initiation. Thus, the initiation will be faster in future. Based on FMI predictions in Finnish climate the current study shows that the increase in precipitation affects the propagation phase more than the increase in temperature.

Acknowledgements

The authors would like to acknowledge the researchers in Finnish Meteorological Institute for preparing the future climate projections. This study was part of FRAME research project conducted at Tampere University of Technology in 2009–2012.

References

[1] SWD 137. Adapting infrastructure to climate change. Brussels; 2013.
[2] E.E.A. Report 12. Climate change, impacts and vulnerability in Europe 2012. European Environment Agency, Copenhagen; 2012.
[3] IPCC. Climate change 2007: the physical science basis. Contribution of working group I to the fourth assessment report of the intergovernmental panel on climate change. Cambridge University Press, Cambridge, UK; 2007. 996 p.
[4] Jylhä K, Ruosteenoja K, Räisänen J, Venäläinen A, Tuomenvirta H, Ruokolainen L, et al. The changing climate in Finland: estimates for adaption studies. ACCLIM project report 2009. Finnish Meteorological Institute. Reports 2009:4. Helsinki; 2009. 78 p. 36 app [in Finnish].
[5] Lahdensivu J. Durability properties and actual deterioration of Finnish facades and balconies. Tampere University of Technology, Faculty of Built Environment, Tampere. Publication 1028; 2012. 117 p. 37 app.
[6] Lahdensivu J. The durability of facades and balconies in a changing climate. Ministry of the Environment, Department of the Built Environment, The Finnish Environment 17/2010. Helsinki; 2010. 64 p. [in Finnish].
[7] Tuutti K. Corrosion of steel in concrete. Stockholm. Swedish Cement and Concrete Research Institute. CBI Research 4:82; 1982. 304 p.
[8] Parrott L. Some effects of cement and curing upon carbonation and reinforcement corrosion in concrete. Mater Struct 1996;29(3):164–73.
[9] Jones M, Dhir R, Newlands M, Abbas A. A study of the CEN test method for measurement of the carbonation depth of hardened concrete. Mater Struct 2000;33(2):135–42.
[10] Ho DWS, Lewis RK. Carbonation of concrete and its prediction. Cem Concr Res 1987;17(3):489–504.
[11] Bakker RFM. Initiation period. In: Schiessl P, editor. Corrosion of steel in concrete. RILEM; 1988.
[12] Papadakis VP, Vayenas CG, Fardis MN. Fundamental modelling and experimental investigation of concrete carbonation. ACI Mater J 1991;88(4):63–373.
[13] Parrott LJ. Design for avoiding damage due to carbonation-induced corrosion. TC104/WG1/Panel 1, CEN; 1992.
[14] Saetta A, Schreflerb BA, Vitaliani RV. 2-D model for carbonation and moisture/heat flows in porous materials. Cem Concr Res 1995;25(8):1703–12.
[15] RILEM Report 14 – durability design of concrete structures. London: E&FN Spon Press; 1996.
[16] CEB Bulletin d'information N° 238. New approach to durability design – an example for carbonation induced corrosion; 1997.
[17] DuraCrete. Probabilistic performance based durability design of concrete structures. The European Union – Brite EuRam III, DuraCrete. Final technical report of duracrete project, document BE95-1347/R17. CUR, Gouda, Nederland; 2000.
[18] Neves R, Branco FA, de Brito J. A method for the use of accelerated carbonation tests in durability design. Constr Build Mater 2012;36:585–91. http://dx.doi.org/10.1016/j.conbuildmat.2012.06.028. ISSN 0950-0618.
[19] Wang X, Stewart MG, Nguyen M. Impact of climate change on corrosion and damage to concrete infrastructure in Australia. Clim Change 2012;110:941–57.

[20] Talukdar S, Banthia N, Grace JR, Cohen S. Carbonation in concrete infrastructure in the context of global climate change: part 2. Canadian urban simulations. Cem Concr Compos 2012;34:931–5.
[21] Talukdar S, Banthia N. Carbonation in concrete infrastructure in the context of global climate change: development of a service lifespan model. Constr Build Mater 2013;40:775–82.
[22] Guiglia Matteo, Taliano Maurizio. Comparison of carbonation depths measured on in-field exposed existing r.c. structures with predictions made using fib-Model Code 2010. Cem Concr Compos 2013;38:92–108.
[23] Broomfield J. Corrosion of reinforcement in concrete. London: E&F Spon; 1997.
[24] Page CL. Basic principles of corrosion. In: Schiessl P, editor. Corrosion of steel in concrete. London: Chapman and Hall; 1988. p. 3–21.
[25] Otieno MB, Beushausen HD, Alexander MG. Modelling corrosion propagation in reinforced concrete structures – a critical review. Cem Concr Compos 2011;33(2):240–5.
[26] Mattila J. On the durability of cement-based patch repairs on Finnish concrete facades and balconies. Tampere, Tampere University of Technology. Publication 450; 2003. 111 p.
[27] Mattila J, Pentti M. Suojaustoimien tehokkuus suomalaisissa betonijulkisivuissa ja parvekkeissa. Tampere University of Technology, Research report 123; 2004 [in Finnish].
[28] Alonso C, Andrade C, Rodriguez J, Diez JM. Factors controlling cracking of concrete affected by reinforcement corrosion. Mater Struct 1998;31:435–41.
[29] Andrade C. Measurement of polarization resistance on-site. In: Corrosion of steel in reinforced concrete structures. Final report of COST action 521. Office for Official Publications of the European Communities, Luxembourg; 2003. p. 82–98.
[30] Andrade C, Castillo A. Evolution of reinforcement corrosion due to climatic variations. Mater Corros 2003;54(2003):379–86.
[31] Parrott L. Design for avoiding damage due to carbonation-induced corrosion. In: Proceedings of third international conference on durability of concrete, nice. Special Publication SP-145, American Concrete Institute. p. 283–98.
[32] Siemes AJM, Vrouwenvelder ACWM, van den Beukel A. Durability of buildings: a reliability analysis. Heron 1985;30:3–48.
[33] BES – Development of open concrete element system. Research report. Suomen Betoniteollisuuden Keskusjärjestöry; 1969 [in Finnish].
[34] Pentti M, Mattila J, Wahlman J. Repair of concrete facades and balconies. Part 1: structures, degradation and condition investigation. Tampere, Tampere University of Technology, Structural Engineering. Publication 87; 1998. 156 p. [in Finnish].
[35] Pentti M. Repair of building envelope. In: Kaivonen J-A, editor. Repair techniques and economy of buildings. Rakennustieto Oy: Saarijärvi; 1994. p. 287–358 [in Finnish].
[36] Jylhä K, Ruosteenoja K, Tietäväinen H, et al. Rakennusfysiikan ilmastollisten testivuosien sääaineistot nykyisessä ilmastossa ja arviot tulevaisuuden muutoksista. Väliraportti. Finnish Meteorological Institute, Helsinki; 2011. 6 p. 20 app. [in Finnish].
[37] Jerling A, Schechninger B. Fogars beständighet. Byggforskningrådet. Rapport R89:1083. Stockholm; 1983. 172 p. [in Swedish].
[38] Lahdensivu J, Mäkelä H, Pirinen P. Durability properties and deterioration of concrete balconies of inadequate frost resistance. J Sustain Build Urban Develop 2013;4(2):160–9.
[39] Concrete Association of Finland. Finnish concrete code BY 50. Helsinki, Concrete Association of Finland; 2012. 251 p.
[40] Guidelines for durability and service life of concrete structures. BY 32. Helsinki. Concrete Association of Finland; 1989. 60 p.
[41] fib Bulletin No. 34. Model code for service life design. International Federation for Structural Concrete, Lausanne; 2006. 116 p.

II

DURABILITY DEMANDS RELATED TO FROST ATTACK FOR FINNISH CONCRETE BUILDINGS IN CHANGING CLIMATE

by

Pakkala T.A., Köliö A., Lahdensivu J. & Kiviste M. Dec 2014

Building and Environment, Vol. 82, pp. 27–41

https://doi.org/10.1016/j.buildenv.2014.07.028

Building and Environment 82 (2014) 27–41

Contents lists available at ScienceDirect

Building and Environment

journal homepage: www.elsevier.com/locate/buildenv

Durability demands related to frost attack for Finnish concrete buildings in changing climate

Toni A. Pakkala*, Arto Köliö, Jukka Lahdensivu, Mihkel Kiviste

Tampere University of Technology, P.O. Box 600, FI-33101 Tampere, Finland

ARTICLE INFO

Article history:
Received 11 April 2014
Received in revised form
8 July 2014
Accepted 28 July 2014
Available online 14 August 2014

Keywords:
Concrete structure
Frost attack
Wind driven rain
Durability
Climate change

ABSTRACT

In this study a database of concrete material properties and observed degradation was combined with climate data projections. Due to the predicted increase in precipitation, facades will receive more driving rain in the future. Though the number of freeze-thaw cycles is about the same in the southern coastal and inland areas, the amount of rain is remarkably higher in the southern coastal areas which increases the risk of frost damage. South-facing facades will continue to be most susceptible to climate stress which should be taken into account in designing the details of concrete facades and balconies. As concerns frost durability, climatic conditions in southern Finland will ease remarkably already in 2030. In inland areas outdoor climate will remain the same as presently but in the southern coastal areas conditions will get more severe with the increasing amount of rain and sleet almost to the end of century. Properties that influence degradation initiation time are highly important in ensuring proper service life of a structure. Failure with air entraining fresh concrete results in early frost damage to concrete, i.e. air entrainment of fresh concrete must always be done. Present requirements are sufficient for the future climates.

1. Introduction

During their service life new buildings are going to face more rapidly changing climate than buildings did in the past. Future structures have to be so durable that they will not require unexpected repairs not included in their maintenance plan. That does not only promote sustainable development but is also necessary for cost-effective property management. Even today there are known cases where durability requirements have not been met which indicates that the importance of durability design in construction and repair projects has not yet been fully recognised.

Nowadays the estimated life cycle in building design is typically 50–100 years, while efforts are made to lengthen the service life of the older building stock by renovation. Thus, there is a great need to study the performance of repaired structures and their repair methods in relation to future climates. Such studies constituted a major part of the FRAME project recently carried out at Tampere University of Technology (TUT). The project was based on data of the ACCLIM project [1]. However, the ACCLIM project focussed only a single future scenario (A2) of greenhouse gas emissions published as part of a report by the Intergovernmental Panel on Climate Change (IPCC) in 2007 [2].

Climate change as such has been studied worldwide for a long time. In this context, climate change refers to global warming caused by an increase in greenhouse gases, especially carbon dioxide (CO_2). Climate change will affect the geographic and seasonal distribution of precipitation, wind conditions, cloudiness, air humidity and solar radiation. Modelling of future climate is based on alternative scenarios of greenhouse gas and aerosol particle emissions. In the scenarios, different assumptions are made about the future development of population growth, economic development, energy production modes, etc. The impact of climate change on the performance of structures is becoming an important research issue from an engineering point of view.

The future of the European construction industry (under Horizon 2020) will involve the adaptation of current and future infrastructure towards climate-resilience (document SWD 137 [3]). The projected impacts of climate change and associated threats concerning the construction sector are as follows: 1) extreme precipitation that may lead to water intrusion, damage to foundations and basements; 2) extreme summer heat events [4] that may lead to

* Corresponding author. Tel.: +358 40 198 1962.
E-mail addresses: toni.pakkala@tut.fi (T.A. Pakkala), arto.kolio@tut.fi (A. Köliö), jukka.lahdensivu@tut.fi (J. Lahdensivu), mihkel.kiviste@tut.fi (M. Kiviste).

http://dx.doi.org/10.1016/j.buildenv.2014.07.028
0360-1323/

material fatigue and accelerated aging, high energy use for cooling; 3) exposure of structures to heavy snowfall; 4) rising sea and river levels that increase the risk of flooding and are likely to increase soil subsidence risks.

The ACCLIM and FRAME projects have shown that future climate conditions are likely to get worse in terms of durability of facades and other structures. It has been shown in the case of precast concrete buildings that present deterioration of facades and balconies is faster in the coastal areas and southern Finland than inland and in eastern and northern Finland [5]. According to the data of the ACCLIM project, precipitation during the winter season is also going to increase while the form of precipitation is going to be increasingly water and sleet. At the same time, the conditions for drying are going to get worse. Thus, the degradation rate of structures will accelerate in most of Finland if maintenance and protection actions are neglected [6].

1.1. Precast façade panels and balcony elements

In 2008 the share of precast concrete elements in building production was 35%. In block of flats the precast concrete element was dominating frame material with 69% share; in the highest the share was 82% in mid-1990s [7]. Since the 1970's, almost all prefabricated concrete structures in Finland have been based on the Concrete Element System [8]. The above-mentioned open system defines, for instance, the recommended floor-to-floor height and the types of prefabricated panels used. In principle, the system allows using the prefabricated panels made by all manufacturers in any single multi-storey building.

The concrete facade panels used in exterior walls of multi-storey residential buildings were, and still are, chiefly prefabricated sandwich-type panels consisting of two relatively thin concrete layers with thermal insulation between them connected to each other by steel trusses. The thermal insulation between the layers is most often mineral wool of 240 mm nominal thickness according to the building regulations in force. The usual nominal thickness of the outer layer is 80–85 mm depending on the surface type of the panel.

All vertical and horizontal joints between the outer layers are elastic, made primarily with polymer sealants in order to allow thermal as well as other movement of the layers. It should also be noted that usually there is no ventilation gap behind the outer layers of precast exterior wall panels. Thus, if the thermal insulation gets wet e.g. due to leakage through the joints, the structure dries slowly. The drying of the outer layers is also slow because of the efficient thermal insulation that limits the drying heat flow through the wall. This means that the concrete may remain wet for long periods.

The most common balcony type in Finland from the late 1960's until today consists of a floor slab, side panels and a parapet panel of precast concrete. These stacked balconies have their own foundations, and the whole stack is connected to the building frame only to brace it against horizontal loads. All structural members of a precast balcony are load-bearing. The typical nominal thickness of a load-bearing wall panel is between 150 and 180 mm depending on the number of floors. The nominal thickness of a bearing concrete slab is between 140 and 200 mm. It varies a lot depending on the slope of the upper surface of the slab panel.

The water drainage systems of balconies vary a lot. Generally, the top surface of the slab has a slight slope, which leads rainwater to a drain pipe at the corner of the slab or outside through a spout pipe in the parapet. The water drainage system of some balconies consists of a gap between the slab and the parapet, which allows rainwater to exit the balcony. There is never waterproofing on top of balcony slabs.

1.2. Research objective

In this work a database of concrete material properties and observed degradation was combined with climate data projections from FMI. The research objective was to study whether the frost durability properties regulated by Finnish building codes are sufficient for the changing climate conditions. Although similar durability problems occur with concrete bridges and other concrete infrastructure in Finland, the current study focusses on concrete facades and balconies.

2. Background

2.1. Degradation of concrete

Concrete structures exposed to Nordic outdoor climate are subject to several parallel degradation mechanisms, whose progress depends on many factors related to the structure in question, type of exposure and materials. Frost attack is one of the most common deterioration mechanisms causing repair need of concrete [6]. Occurrence of degradation requires inadequate performance of structures, poor durability properties of materials and a harsh environment, see Fig. 1. In the absence of any one of them there will be no damage to the concrete structure.

The structures and material properties of a concrete building are defined during the design and building processes according to the design guidelines in force. The environmental load is then a variable factor. Even concrete of inadequate frost resistance will not suffer frost damage if the structure is sheltered from rain.

Degradation of concrete may limit the service life of structures and, therefore, the possibility of retaining the present or original appearance of structural members and buildings. Degradation may, for instance, have detrimental visual impacts or even reduce the bearing capacity of structures.

Cracking will decrease the strength of concrete and increase capillary water absorption. Continuing freeze-thaw cycles and a high moisture content of concrete finally lead to frost damage [9]. Detection of such inner cracking of concrete requires a sophisticated research method like thin-section analysis [10], see Fig. 2(a).

Far advanced frost damage is manifested as a reduction in strength of concrete, loss of adhesion, or crazing or chipping of the surface due to internal expansion, see Fig. 2(b). Disintegration of concrete also accelerates carbonation of concrete due to cracking and consequently also steel corrosion.

The behaviour of air-entrained concrete under compression with constant confined stress [11] after freeze-thaw cycles was studied by Shang and Song using triaxial tensile-compressive tests

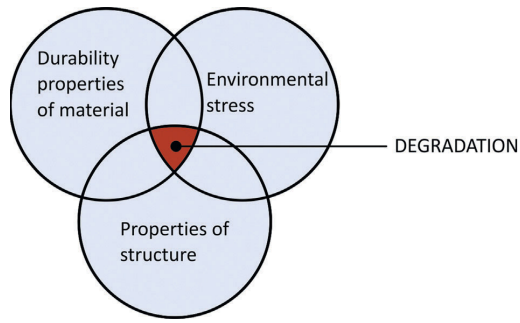

Fig. 1. Degradation of concrete occurs in a harsh environment when the performance of structures is inadequate and durability properties of materials are poor.

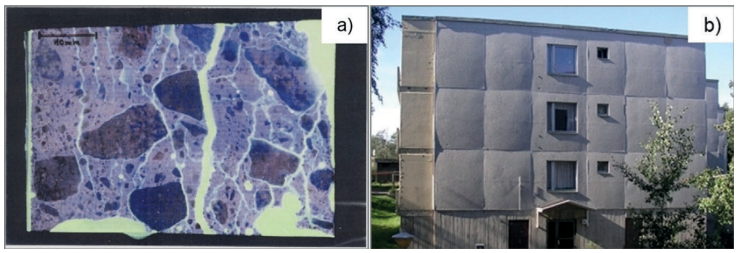

Fig. 2. (a) Severe frost damage in thin section analysis, the length of the dimension bar is 10 mm. (b) Far advanced and wide-spread frost damage in an exposed aggregate concrete facade (Photos Ins.tsto Lauri Mehto Oy).

[12]. Based on the test data, the influence of freeze-thaw cycles and the lateral compressive stress ratio on ultimate compressive strength was analysed. A unified failure criterion that takes into account the influence of freeze-thaw cycles and stress ratio was proposed [11]. The experimental results showed that dynamic modulus of elasticity and strength decreased as the freeze-thaw cycle was repeated. The influence of freeze-thaw cycles on mechanical properties, dynamic modulus of elasticity and weight loss was analysed based on the experimental results [13].

The pressures, stresses, and strains of wet concrete during freezing and thawing were calculated theoretically and compared with the test results by Penttala and Al-Neshawy [14]. The material and bond properties of frost-damaged concrete have been studied experimentally by Zandi Hanjari et al. [15]. The results showed the significant influence of freeze-thaw cycles on compressive strength and even bigger influence on modulus of elasticity and compressive strain at peak stress. Reduced tensile strength and increased fracture energy were also measured. Pull-out tests showed the influence of freeze-thaw cycles on bond strength and slip. The damage of concrete subjected to flexural fatigue load and closed freeze-thaw cycles simultaneously has been studied experimentally by Li et al. [16].

The degree of frost damage may vary in different parts of facades and balconies depending, for instance, on the moisture load and variation in material properties and thickness of the concrete structure. Frost damage due to a high local moisture load may affect only a very limited area. On the other hand, improper surface treatment of non-frost-resistant concrete may result in deterioration across most of the side wall surface and corners of buildings.

2.2. Quality and frost resistance of concrete

The concrete grade used for concrete facade panels and most structural members of balconies has been C30/37 since the late 1980's in Finland based on the guidelines for durability and service life of concrete [17]. The cement used for concrete panels is mostly CEM I (42.5 N) (ordinary Portland cement) because of the good early strength it gives to concrete which allows rapid formwork rotation at the precast panel plant. White cement, CEM I (52.5 R), is also used in facade panels if necessary, but its share of total use is marginal. The concrete used for facades and balconies in the Nordic countries is always air-entrained.

The frost resistance of the concrete used for facades and balconies is determined during concrete mixing. Air-entrainment of fresh concrete has been recommended since 1976 and demanded since 1980 by the Finnish Concrete Code.

Information related to used air entrainment and its success has been reported as a protective pore ratio (p_r), which was common practice in Finland until the year 2004. After 2004 the success of air-entrainment has been determined on the basis of the spacing factor which is the average of half the distance between protective pores and needs to be detected by microscope. According to the Concrete Code (1980), the protective pore ratio should be at least 0.20, which implies that at least 20% of all pores are never filled by capillary water. A protective pore ratio of 0.20 corresponds to a spacing factor of 0.25 mm [18]. The durability demands of different stress classes based on the Finnish Concrete Code in force [19] are shown in Table 1.

Facades and balcony side panels and parapets belong to stress class XF 1 and the balcony slab to stress class XF 3. The most common design service life of normal buildings is 50 years.

Koskiahde presented in 2004 a four-tier system for classifying cracking and protective pore spacing in concrete samples based on thin-section analyses, see Table 2 [18]. The classification is used to identify both the level of frost damage and the success of air-entrainment. All classes of frost damage indicated by cracking can only be detected by microscope.

2.3. Climatic stress on concrete structures

Lisø studied in his doctoral thesis the adaptation of building envelopes to the impacts of climate change in Norway [20]. He concentrated on wooden and brickwork structures, and studied also the effects of climate change but only in terms of the decay potential of wooden structures using a climate index based on changing temperatures. His thesis also produced a driving rain exposure index [21] and a frost decay exposure index [22] for geographically dependent design. The frost decay exposure index takes into account sums of rainfall prior to days with freezing events. The driving rain index presents the direction of rainfall in different locations. However, both indices show that Norwegian climate, especially the direction of wind during rainfall, varies significantly depending on location mainly due to differences in altitude.

The driving rain striking building facades has been the focus of several studies in the last decades as mentioned by Blocken & Carmeliet [23]. The moisture load resulting from driving rain depends not only on rainfall intensity and wind speed, but also on

Table 1
Requirements for frost-resistant hardened concrete of different stress classes when design service life is 50 or 100 years [19].

Designed service life [years]	Stress class	Spacing factor [mm]	Freeze-thaw test	
			Number of cycles	Requirement for residual bending strength after test [%]
50	XF 1	≤0.27	100	≥67
	XF 3	≤0.23	300	≥67
100	XF 1	≤0.25	300	≥67
	XF 3	≤0.22	–	–

Table 2
Classification of concrete degradation mechanisms observed in thin-section analysis [18].

	Class/designation			
	1	2	3	4
Frost damage	**No cracks**	**Initial** Crack widths <0.01 mm and lengths <10 mm.	**Frequent** Crack widths 0.01–0.1 mm and lengths ≥10 mm. Frequently <0.25 cracks/mm and 50% of aggregate loosened.	**Severe** Many cracks >0.1 mm wide and >25 mm long. Frequently ≥0.25 cracks/mm or 50% of aggregate loosened.
Air pores	**Frost resistant** Pore spacing ≤0.25 mm.	**Partially insufficient** Pore spacing 0.25–0.40 mm.	**Failed air-entrainment** Pore spacing ≥0.40 mm or no intentional air-entrainment but an abundance of small air pores (Ø 1 mm).	**No air-entrainment** Only occasional air pores detectable. Typical air content ≤2%.

raindrop trajectories around buildings. That increases the complexity of the phenomenon greatly. According to Jerling and Schechninger, the upper parts and corners of facades get more rainfall than lower and central parts [24]. Prevailing wind directions and wind speeds also have a strong influence on the distribution of rainfall across a building. In Finland most of the rain and sleet in wintertime arrives with southerly to westerly winds. Rain events with wind from other directions have been rare. If we calculate the simplified horizontal vector of rain, about 60% of the rain and sleet load in the coastal area hits the facades and balconies due to the stronger winds; the corresponding share inland is about 40%. In addition to the higher amount of precipitation in coastal areas, facades and balconies there are also subject to considerably higher moisture stress than inland resulting in clearly more corrosion and frost damage. Winds are stronger at higher levels of buildings than close to ground level which naturally leads to upper sections of high buildings receiving more rain and sleet stress than lower buildings, and lower sections of buildings in general [10].

Experimental, numerical and semi-empirical methods have been developed and employed for the estimation of parameters related to driving rain against building facades [25]. The annual driving rain index (aDRI) that is calculated on the basis of average annual wind speed and average amount of total annual rainfall is proportional to the amount of water on a windward vertical surface [26]. Based on the classification proposed by Lacy (sheltered areas, moderately exposed areas, severely exposed areas), driving rain maps have been produced for several countries including Sweden, United Kingdom, Canada [27], China [28], India [29], Nigeria [30], Turkey [31], Greece [32] and Spain [33].

Differences in the time resolutions of climatic data sets may result in large discrepancies in the calculated indices. In most cases hourly data are considered to have adequate time resolution. Given that in many cases hourly data covering adequate periods of time are not available, some methods for the derivation of directional driving rain indices on the basis of synoptic data have been formulated [21,34,35]. However, the driving rain indices cannot be used for direct estimation of the driving rain load on building components at site. Quantification of the amount and intensity of this load (formation of the wind pressure field around each building) is a complex task. The building's geometry and the position of the area under study on the building's vertical surface (height, middle part of the surface or near the edges) influence the resulting load [25,36–41]. Example calculations of quantitative parameters related to driving rain (e.g. intensity) for specific sites are found in several studies [e.g. Refs. [42–44]].

2.3.1. Frost decay exposure index

Lisø et al. [22] presented a frost decay exposure index for characterising the risk of frost or damage to a porous, mineral material in a given climate. The index takes into account the amounts of freeze-thaw cycles and precipitation. The weather data (from 1961 to 1990) consisted of daily air temperature measured three times a day (0600, 1200, 1800 UTC), daily maximum and minimum air temperatures and precipitation measured at 0600 covering the last 24 h. To divide the precipitation into snowfall and rainfall portions, the visual observations of present and past weather conditions, recorded three times a day, were used. The freeze-thaw cycles were considered as temperature crossings over freezing point (0 °C) and the number of cycles was defined as annual average number of days with freezing point crossings (FPC). The frost decay exposure index (FDEI) tells the amount of precipitation as rainfall from the day an FPC has occurred and the preceding 2, 3 and 4 days. The annual amount of precipitation is calculated subsequently. The FDEI does not take into account wind intensity or wind directions.

The frost decay exposure index (FDEI) links average annual freezing point crossings (FPC) to the amount of liquid precipitation recorded from the day an FPC has occurred and the preceding 2, 3 or 4 days. When the FDEI and FPC are presented in the same diagram, the risk of frost decay can be estimated by analysing their relation. For example, if the amount of freezing point crossings (FPC) is high but the amount of precipitation before the crossings is low, i.e. FDEI is low, the risk of frost decay is relatively low, but if they both are high, the risk is also considerable.

2.3.2. Driving rain exposure index

Rydock et al. [21] presented a method for estimating the amount of driving rain striking a vertical surface at a specific angle from north. They used synoptic weather observations made 3 to 4 times a day at different locations across Norway. They used the data to calculate a driving rain exposure index I_θ to compare driving rain exposures at different locations in Norway. To calculate the index I_θ for any direction θ (which represents the angle between north and a line normal to the wall), the following formula was used [21]:

$$I_\theta = 0.206 \sum_D v_D r_D \cos(D-\theta) \quad (1)$$

where I_θ is expressed in mm/year, 0.206 is the conversion factor [s/m] from Lacy [26], D is the wind direction [angle from north], v_D is the average annual wind speed [m/s] from direction D and r_D is the average annual rainfall [mm] with wind from direction D. The summation is taken over the angles D representing a wind blowing against the wall including the sector from $\theta - 80^\circ$ to $\theta + 80^\circ$.

The method is closely related to the airfield annual index I_A presented in standard ISO 15927-3 [45]:

$$I_A = \frac{2}{9} \frac{\sum v r^{\frac{8}{9}} \cos(D-\theta)}{N} \quad (2)$$

where v is hourly mean wind speed [m/s], r is hourly rainfall total [mm], D is hourly mean wind direction from north [°], N is number

of years for which data is available and the summation is taken over all hours for which $\cos(D-\theta)$ is positive. The main difference between the two methods is that the airfield annual index applies the exponent $8/9$ to r which reduces the estimated driving rain amount hitting the façade. The latter equation also requires hourly data which was not required by the equation of Rydock et al. [21].

2.4. Climate projections in Finland

Although Finnish climate is relatively steady considering the latitudes, it still varies significantly from the mild and relatively rainy coastal area to the drier inland. However, the Finnish building stock is mainly concentrated in the few biggest cities and surrounding growth areas. Finland can be divided into four main areas based on climatic differences and concentration of population: the coastal area, southern Finland, inland and Lapland. The coastal area consists of a 30 km wide sector along the coast from the City of Vaasa to the Russian border. Southern Finland includes the rest of the southern portion up to the City of Tampere (150 km north of Helsinki). The inland area includes the rest of the country except Lapland.

The Finnish Meteorological Institute (FMI) examined in the ACCLIM project the different climate models and built models for observing Finnish climatic conditions and adaptation to climate change. In all greenhouse gas emission scenarios, based on three IPCC (2007) [2] scenarios for the evolution of greenhouse gas and aerosol particle emissions, the average temperature rises at a constant rate until 2040. Differences between the scenarios start to emerge only after the middle of the century, see Fig. 3 [1].

The Finnish Meteorological Institute (FMI) has weather data since 1961 in digital form from several meteorological stations covering all of Finland. The data consist of temperature, relative humidity, rain intensity, wind speed and direction, solar radiation variables, etc. These observations have been collected at least daily and three times a day at best. In the REFI-B project, the FMI also forecast the climates of the four regions (coastal area, southern Finland, inland, Lapland) in three periods (2030, 2050 and 2100). The forecasts are based on an average of 19 different models which are all based on greenhouse gas emission scenario A2. The A2 scenario involves a situation where greenhouse gases are assumed to increase significantly – it is a sort of worst-case scenario. The FMI also has other significant greenhouse gas emission scenarios: A1B (quite large emissions) and B1 (small emissions) [46].

2.5. The nature and modelling of frost attack on concrete

Frost attack due to a high moisture load is a common reason for the deterioration of concrete structures in Nordic outdoor climate. Concrete is a porous material whose pore system may, depending on the conditions, hold varying amounts of water. As the water in the pore system freezes, it expands about 9% by volume creating hydraulic pressure in the system. If the level of water saturation of the system is high, the overpressure cannot escape into air-filled pores and therefore damages the internal structure of the concrete leading to its degradation.

More than 15 different theories or explanations for frost attack on porous materials have been presented [47]. That proves that frost attack is a complex process and frost damage can take many different forms [48].

Probably the most widely known frost damage theory is the hydraulic pressure theory by Powers published in 1949. Accordingly, damage occurs as freezing water expands creating hydraulic pressure within the pore structure of a porous material. The pressure is created when part of the water in a capillary pore freezes and expands forcing thereby the unfrozen water out of the pore. The migration of water causes localised internal tensions in the material whereby its strength may fail resulting in cracking [49].

The theory of volume changes in microscopic ice crystals was developed to complement the hydraulic pressure theory. During the freezing process, small ice crystals tend to grow in capillary pores. If there is not enough empty space for the growing ice crystals, they build pressure in the pore structure which may lead to its cracking. The growth of microscopic ice crystals will continue despite the lowering of temperature during the freezing phase [50].

The theory of osmotic pressure complements the two previous theories by taking into account also the migration of dissolved chemicals, mainly the alkalis Na_2O and K_2O, in pore water. These dissolved chemicals lower the freezing temperature of pore water and increase the concentration of salts in the water surrounding the ice. The concentration of dissolved chemicals tries to establish an equilibrium between different pore water solutions resulting in osmotic pressure in the pore structure [51].

Litvan noticed in the beginning of the 1970's that the water in the pore structure of a porous material does not freeze immediately as temperature drops below 0 °C. Freezing happens first in bigger capillary and gravitation pores. In smaller gel pores water begins to freeze when temperature is around −15 to −20 °C. The unfrozen pore water is thus supercooled, which tends to cause drying of the

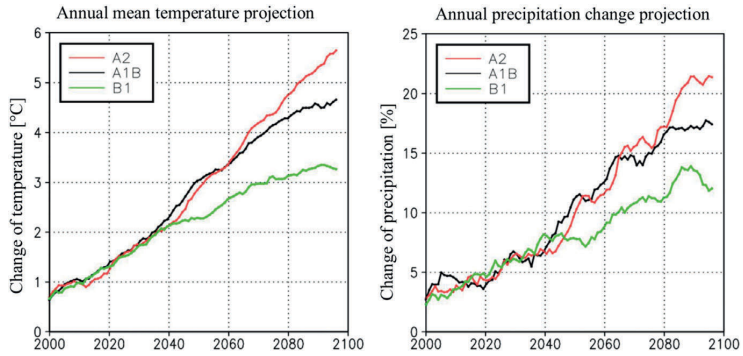

Fig. 3. Projections for (a) annual mean temperature and (b) precipitation change in 2000–2100, in relation to the mean of the reference period 1971–2000. The curves depict 11 year running means, averaged over Finland and the responses of 19 global climate models [46]. Projections are given separately for the three greenhouse gas scenarios (A2, A1B and B1) [1].

paste because the saturation pressure of supercooled water is higher than that of ice. According to Litvan, mechanical damage happens when moisture transfer cannot occur in an orderly manner, i.e. when the rate of freezing is too high, or the distance that water must travel to reach an external surface and freeze is too long [52].

The theory of critical degree of water saturation was developed in the early 1970's by Fagerlund. Its basic idea is that there is a critical degree of water saturation above which porous and brittle material gets damaged while freezing. If the actual water saturation is below the critical level, no damage occurs during freezing [48].

A design model for the service life of concrete structures based on the theory of critical degree of saturation [48,53] is proposed in the fib Model Code for Service Life Design [54]. The basis of the model is that there is a critical degree of saturation specific to each concrete type above which concrete is likely to be damaged by freezing. If the actual degree of saturation stays below the critical level, concrete is not harmed by freeze-thaw cycles based on the theory. According to this model, service life ends when this critical degree of saturation is achieved. It, however, does not specify whether a freezing event occurs at the same time and therefore has to be considered to be on the safe side.

The critical moisture content of concrete is influenced by material properties: (i) critical flow distance, (ii) the size distribution of the air pore system, (iii) total air content, and (iv) total porosity.

On the other hand, actual moisture content is influenced by (i) the diffusivity of dissolved air, (ii) the size distribution of the air pore system, (iii) total air content, and (iv) total porosity. Actual moisture content is not only influenced by material properties but also by the moisture load from the ambient environment of the structure in question.

The model requires special laboratory tests to be conducted on each specific concrete type in order to be able to calculate the critical degree of saturation. Therefore, the application of the model is limited in practice.

Increasing façade temperature also increases the temperature of the ice in the pore structure. When temperature decreases, the ice in the pore structure first shrinks allowing supercooled pore water to flow by capillary action to “new” empty spaces in pores where it freezes rapidly. When temperature increases, the ice requires more space than before. According to Penttala, this causes significant hydraulic pressure in the pore structure [55]. The thermal expansion coefficient of ice is 50×10^{-6} per K which is 3.5–10 times higher than the temperature expansion coefficient of concrete [56,57]. The temperature expansion coefficient of concrete varies a lot and is influenced by two main constituents of concrete: hydrated cement paste and aggregate [58].

3. Research methods and material

3.1. Research material

The research material of this study is composed of data on concrete durability and observed damage compiled in connection with condition assessments of prefabricated concrete facades and balconies built in 1961–1996 in Finland. The assessments consisted of a visual examination followed by field investigations and laboratory tests [6,59]. Both the condition assessment methodology [10,59] and the case studies on buildings, App. 1 in Ref. [6], have been described as part of earlier research at TUT. As this study discusses the current Concrete Code, the data is delimited to 72 buildings built in 1990 or thereafter. The database contains e.g. measurements of concrete pore structure and protective pore ratio and tensile strength tested from concrete core samples. It also includes results from thin-section analyses and visual observations of the existence and degree of frost damage on building facades and balconies.

Practical design of concrete structures in Finland is governed by the National Concrete Code [19]. Besides guidelines for structural design, they also give recommendations on durability properties and service life design as discussed in Chapter 2.2. These requirements are compared to the actual observed degradation processes and their progress in the future.

Present and future climate projections and their effects on weather conditions critical to concrete degradation have been prepared by the Finnish Meteorological Institute (FMI). The data used in this study are hourly interpolated observations of temperature, wind speed, wind direction and amount of precipitation over 30 years (1980–2009). The future climate projections, based on the A2 scenario, were calculated by FMI to represent hourly data for a similar period in 2030, 2050 and 2100.

Most of the calculations of this study focus on two locations, the southern coastal and the inland area, although both collected and forecast data are also available for other locations. The division is based on the distribution of the Finnish building stock as well as the locations of Finnish growth centres, both of which are concentrated in the southern coastal area and the area considered inland for the purposes of this study, see Fig. 4 [60].

3.2. Frost resistance of concrete and the observed frost damage

The success of air entrainment of concrete used in facades and balconies was studied from the thin section analysis results on samples in the database taken on the buildings built 1990 or afterwards. The classification [18] of frost damage and air entrainment, presented in Table 2, is used in the analysis of the data.

All of the classes in classification of frost damage indicated by cracking can be detected only by the microscope. That is why all possible cracking in this study is incipient and not visually detectable.

The observed frost damage was compared with the frost resistance parameter, namely success of air entrainment, and with the

Fig. 4. Finland can be divided into four main areas based on climate and concentrations of population.

climate parameters and indices produced from present and future climate data.

3.3. Number of annual freeze-thaw cycles

The number of annual freeze-thaw cycles at the Helsinki-Vantaa (southern coastal area) and Jyväskylä (inland) weather stations was recorded based on the following criteria [46]:

- Occurrence of rain or wet snow a maximum of 2 days before freezing
- The number of freeze-thaw cycles when temperature dropped under 0 °C, −2 °C, −5 °C and −10 °C
- The annual number of freeze-thaw cycles calculated for 2000, 2030, 2050 and 2100.

Table 3 shows the number of annual freeze-thaw cycles in 2000 based on the hourly interpolated observations during the reference period 1980–2009. The future scenarios are based on model estimations where observed data has been converted to represent future climate. The models are based on greenhouse gas emission scenario A2 which assumes the greenhouse gas emissions to increase significantly [46]. Because this study is an adaptation study, the scenario A2 was chosen for achieving adequate safety level for assessment of hygrothermal performance.

Based on research by FMI, annual rainfall will increase according to Table 4. The change in the amount of rainfall will be higher during autumn and winter when drying of structures is slower in general.

On the other hand, according to FMI, the prevailing wind directions during rain events will stay the same as presently. That implies that facades facing south-east to west will receive more rainfall also in the future.

3.4. Models for frost attack-related climate exposure indices

3.4.1. Frost decay exposure index

In this study, the amounts of freeze-thaw cycles and precipitation before freezing point crossings (FPC) are based on the FMI's observations for 12 h periods at 6 and 18 UTC over a time period of 50 years (1960–2009). In addition to temperature drops to 0 °C, drops to −5 °C were also considered because concrete has to freeze to −5 °C or below to start degrading [51].

The amount of precipitation on the day temperature dropped to freezing point and the preceding three days was determined for the frost decay exposure index (FDEI). The total amount of precipitation is that accumulated over a year.

Table 3
Number of annual freeze-thaw cycles at four different observation stations a maximum of 2 days after rain or sleet events. The calculations are by FMI [46].

Year and place	Temperature under (a max. of 2 days after rain or sleet)			
	0 °C	−2 °C	−5 °C	−10 °C
Helsinki-Vantaa (southern coastal area)				
2000	37.8	23.5	11.7	4.0
2030	25.9	15.2	7.7	2.3
2050	21.4	12.9	6.1	1.8
2100	14.5	9.4	3.9	0.4
Jyväskylä (inland)				
2000	30.4	20.2	10.4	4.2
2030	25.4	17.5	9.6	3.3
2050	24.8	17.0	9.4	3.2
2100	19.8	13.9	7.2	2.1

Table 4
Average change [%] in precipitation compared to present climate (2000) at four different observation station based on calculations of FMI [46].

Month	Helsinki-Vantaa (southern coastal area			Jyväskylä (inland)		
	2030	2050	2100	2030	2050	2010
1	4.1	9.9	29.6	3.8	9.7	32.6
2	6.4	9.5	29.3	6.3	10.8	30.5
3	3.9	6.5	20.6	3.9	6.6	21.5
4	3.4	6.5	19.1	2.3	5.8	16.4
5	3.5	5.9	16.6	3.9	5.3	14.9
6	−1.2	3.5	9.6	−0.6	3.8	12.3
7	2.6	4.4	11.3	2.1	5.1	11.1
8	3.8	4.9	5.7	3.5	4.5	5.8
9	3.5	5.8	9.5	4.4	6.7	11.0
10	3.1	8.4	18.6	2.8	8.0	20.1
11	7.1	10.9	24.4	7.9	10.6	27.6
12	5.4	9.0	28.7	6.5	12.0	34.0
Whole year	3.8	7.1	17.7	3.6	7.1	18.2

3.4.2. Driving rain index

The data used in this study is composed of hourly interpolated observations of temperature, wind speed, wind direction and amount of precipitation for the present (1980–2009) and future climate projections for 2050 and 2100.

The airfield annual index takes into account all precipitation but here we use the same method as Rydock et al. [21] and consider only wet precipitation. Precipitation in the form of snow and sleet has been excluded by including in calculations only precipitation when outdoor temperature was over 0 °C for two hours before measurement.

The airfield exposure index takes into account the hourly average amount of rain, wind direction and speed at the same time.

There are other more sophisticated methods and models for calculating the driving rain index which can take into account e.g. various obstacles near a building or the building's geometry. However, the frost decay exposure index and the airfield annual index are quite capable of clarifying the differences between various locations and present and future climates.

4. Results and discussion

4.1. Frost resistance of concrete

As indicated by Figs. 5 and 6, the air-entrainment of fresh concrete has been successful in varying degrees both with facades and balconies. The classification of the success of air-entrainment is based on Table 2. Only about 50% of precast panels meet the frost resistance requirements. Exposed aggregate concrete and brushed painted concrete have the best frost resistance with about 60% of the samples meeting the requirements. On the other hand, the share of ceramic and brick tile finishing concrete, white concrete and also exposed aggregate panels made of non-air-entrained concrete was high.

Non-air-entrained concrete is not frost resistant in high moisture content conditions, i.e. in normal Finnish outdoor climate in winter. Thus, concrete will suffer frost damage during the time discussed in Chapter 4.2.

Almost 60% of all concrete balcony panels are made of frost resistant concrete. However, 35% of the side panels are not of air-entrained concrete. The low frost resistance of balcony side panels can be considered a significant service-life limiting factor for the entire balcony stock since the side panels are bearing structures, which cannot be replaced without tearing apart the entire structure. The frost resistance of balcony slabs is also poor to a large extent (20%).

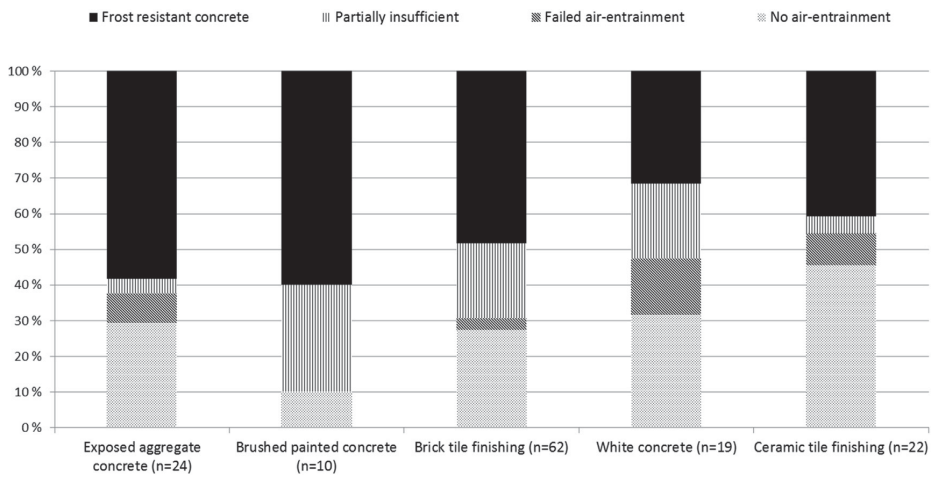

Fig. 5. Use of air-entrained concrete in different facade panel types according to database. The facades were built between 1990 and 1996. The total number of samples was 137. The success of air-entrainment is derived from Table 2.

4.2. Frost damage of concrete

As indicated by Fig. 1, poor durability properties by themselves are not enough to cause damage – inadequate performance of structures and a harsh environment are also needed for damage to occur. As shown by Figs. 7 and 8, the share of frost damage indicated by cracking of concrete is much lower than suggested by the inadequate air-entrainment, see Figs. 5 and 6.

The prerequisites for frost damage are that the pore structure of the concrete has been filled over the critical point by capillary action [48] and that the pore water freezes at a low enough temperature [51].Thus, even in the case of non-frost-resistant concrete, no frost damage will occur if the concrete is dry or the temperature does not drop low enough (−5 °C or lower).

The number of freeze-thaw cycles undergone by existing concrete facades and balconies built in 1960–1996 was studied using the following criteria [6]:

- Occurrence of rain or wet snow on a maximum of 3 days before freezing
- The number of freeze-thaw cycles when temperature drops under −5 °C
- The existence and state of frost damage is studied by thin-section analyses (245 samples)
- Samples are taken from exposed aggregate concrete facades (no paint or other disturbing surface treatment).

Based on the above-mentioned research, concrete can be very durable in the Nordic climate if it has been properly air-entrained,

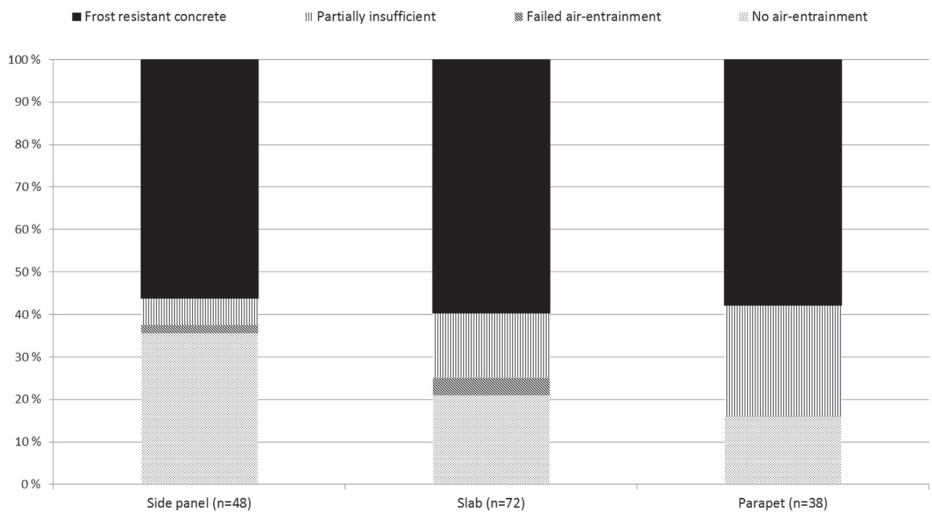

Fig. 6. Use of air-entrained concrete in different balcony panel types according to the thin-section analysis of the database. The balconies were made between 1990 and 1996. The total number of samples was 158.

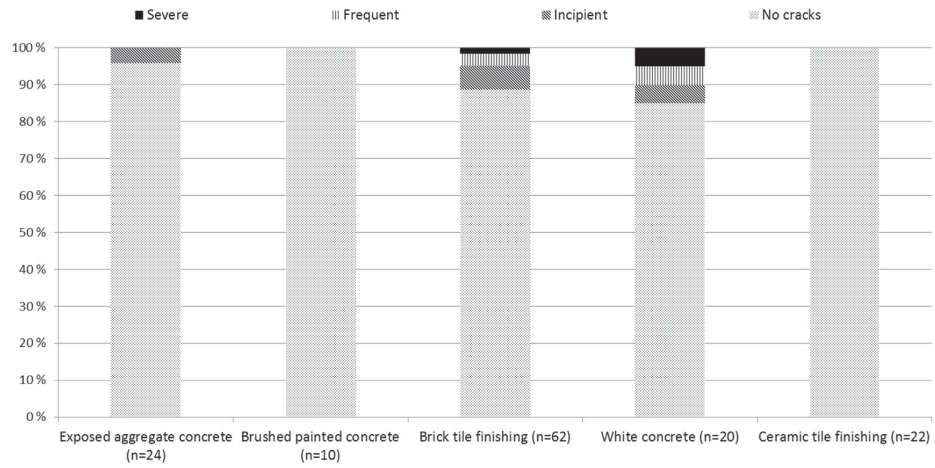

Fig. 7. Share of frost damage type indicated by cracking of concrete of different facade panel types according to thin-section analyses. The facades were made between 1990 and 1996. The total number of samples was 137.

see Fig. 9. The thin-section analyses on concrete samples of frost resistant concrete ($p_f \geq 0.20$) did not show any signs of frost damage after the structure had undergone over 500 freeze-thaw cycles in a real outdoor environment.

On the other hand, if the protective pore ratio measured from hardened concrete is less than 0.10, the air-entrainment of the concrete has failed. Yet, even insufficiently air-entrained concrete has a service life of some years as can be seen from Table 5.

In the southern coastal area the amount of cycles presented in the table would correspond to about 22 years and inland to about 24 years. With balconies, based on Table 5, the frequent frost damage revealed by thin sections begins to occur in the southern coastal area, on average, after 330 freeze-thaw cycles ($t \leq -5$ °C) and inland after 416 cycles which means that the frost attack-based service life of the two structures is similar [10].The number of freeze-thaw cycles inland is slightly higher than in Southern Finland, but the higher amount of rain and sleet in Southern Finland makes the number of freeze-thaw cycles needed to produce the same degree of frost damage much lower. The frequent frost damage in concrete samples revealed in thin-section analyses requires only about 20 more freeze-thaw cycles than incipient frost damage. Thus, frost damage will proceed quite fast if it ever begins.

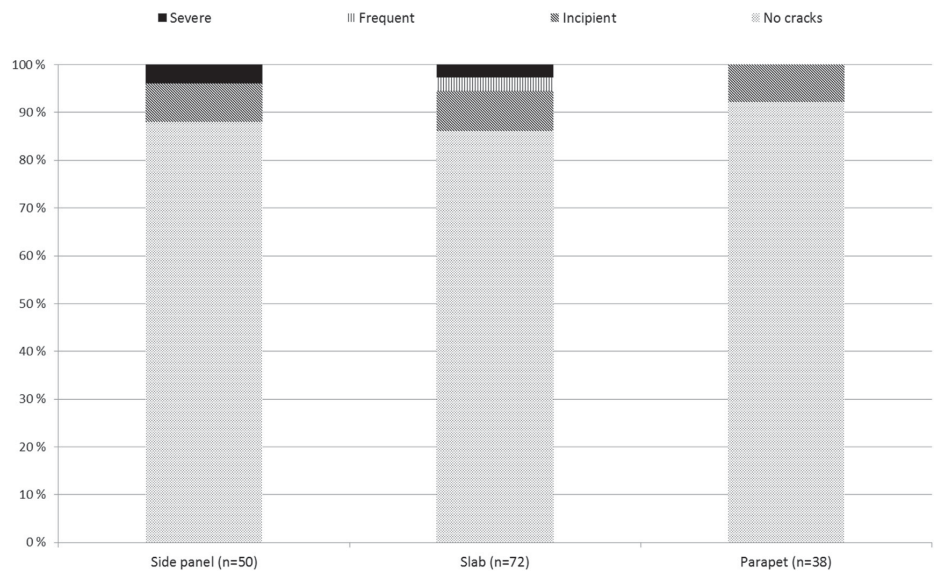

Fig. 8. Share of frost damage type indicated by cracking of concrete of different precast balcony panel types according to thin-section analyses. The balconies were made between 1990 and 1996. The total number of samples was 158.

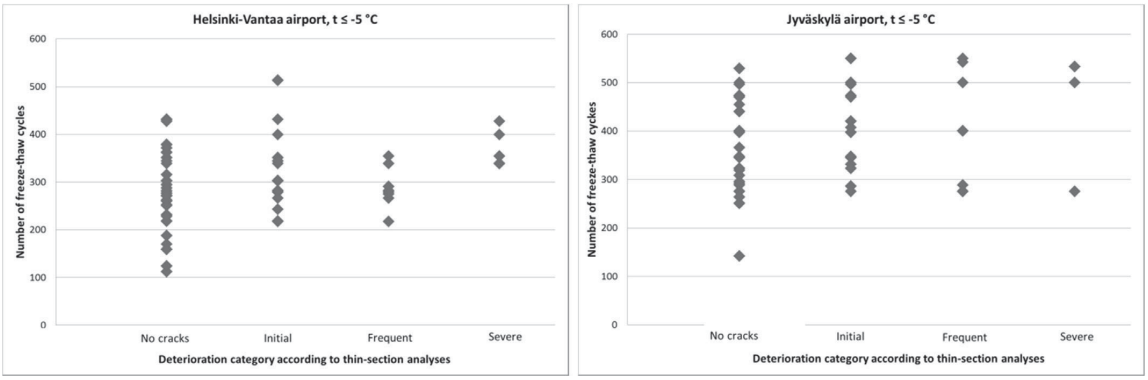

Fig. 9. Number of freeze-thaw cycles leading to different deterioration categories of exposed aggregate concrete facades at different locations according to thin-section analysis. The total number of samples was 245. The figure was reproduced from Ref. [6].

4.3. Climate exposure indices

4.3.1. Frost decay exposure index

The FDEI is presented in Fig. 10 as a line and the FPC as a column for three different locations: southern coastal area (Helsinki-Vantaa), inland (Jyväskylä) and Lapland (Rovaniemi). The number of times an FPC has occurred a maximum of 3 days after rain is also presented as a column because the number of freeze-thaw cycles is not relevant for frost damage occurrence if ambient conditions are dry.

Though the amount of freeze-thaw cycles is basically the same in both southern and inland areas, the amount of rain is remarkably higher in southern coastal areas, thus their FDEI is higher (Fig. 10). The figure also shows that even though Lapland is the northernmost part of Finland and its annual average temperature is much lower than in the rest of the country, both the amount of freeze-thaw cycles and the FDEI are also low there. The risk for frost attack in northern Finland is actually lower than in the southern parts.

The figure also shows that in the case of freeze-thaw cycles with a threshold of −5 °C a maximum of 3 days after rain, their amount is higher inland but the amount of precipitation, and thus the FDEI, is at the same level in both locations. That means that it rains more, on average, before every freezing event in the southern coastal area.

As can be noticed from Fig. 10, an FDEI does not describe well enough the actual risk of frost damage. The level of the index depends highly on the threshold temperature chosen for the FPC. The FPC with a threshold of 0 °C indicates a high risk but does not necessarily lead to frost damage. However, a comparison of FDEI calculations and the actual amount of freeze-thaw cycles needed for frost damage (Table 5) shows that the amount of precipitation before freezing has a larger impact on frost damage than the number of freezing events.

Table 5
Number of freeze-thaw cycles needed for incipient and frequent frost damage to start revealed by thin-section analyses of exposed aggregate concrete samples of insufficient air-entrainment ($p_t \leq 0.10$) at different temperatures when rain or sleet has fallen for a maximum of 2 days before freezing [5].

	Southern coastal area [number of freeze-thaw cycles]		Inland [number of freeze-thaw cycles]	
	$t \leq -5$ °C	$t \leq -10$ °C	$t \leq -5$ °C	$t \leq -10$ °C
Incipient frost damage	307	140	388	189
Frequent frost damage	320	146	400	200

4.3.2. Driving rain index

Figs. 11 and 12 show the average annual amount of driving rain from different wind directions in the southern coastal area and inland, respectively. The wind directions are given in degrees from north in 10° increments. The figures show the present amount of rain (30 year average, 1980–2009) and projections for future climates in 2050 and 2100.

As shown by Figs. 11 and 12, wind driven rain is carried in both locations mainly by southerly winds. In future wind driven rain will come increasingly from the southern or south-western direction and its amount will increase significantly in both areas.

Figs. 11 and 12 show the actual amount of rain from specific directions. Figs. 13 and 14 show the amount of wind driven rain hitting facades facing various directions. Therefore, the latter describe better the wind driven rain load of a façade than plain weather data. Figs. 13 and 14 use the driving rain index I_A (see Eq. (2)) for different wind directions in the southern coastal area and inland, respectively. The wind directions are given in degrees from north in 10° increments. The figures give the present indices (30 year average, 1980–2009) and projections for future climates in 2050 and 2100.

Compared to the amount of rain presented earlier, the driving rain index I_A presents higher differences between the two areas and also between the climate projections and present climate. The reason for the former is that the average wind speed during rainfall is higher in the southern coastal areas which increases the index. However, the wind speed of the future climate will not increase significantly in either area, which means that the differences between the indices are the result of an increase in the amount of wind driven rain. Actually, the inland wind speed during rainfall will even decrease.

Figs. 13 and 14 show clearly that south-facing facades will get significantly more wind driven rain. The same phenomenon has been noted in condition assessment studies where the most deterioration has been observed on south-facing facades and balconies. By the end of the century, wind driven rain will increase 30% in the southern coastal area and 40% inland. Although the calculations are based on greenhouse gas scenario A2, the most severe one, the possible increase should be taken into account in the design of the details of concrete facades and balconies.

4.4. Frost damage of concrete in future climate

Table 6 shows the estimated time needed for incipient frost damage to show in thin-section analyses of inadequately frost

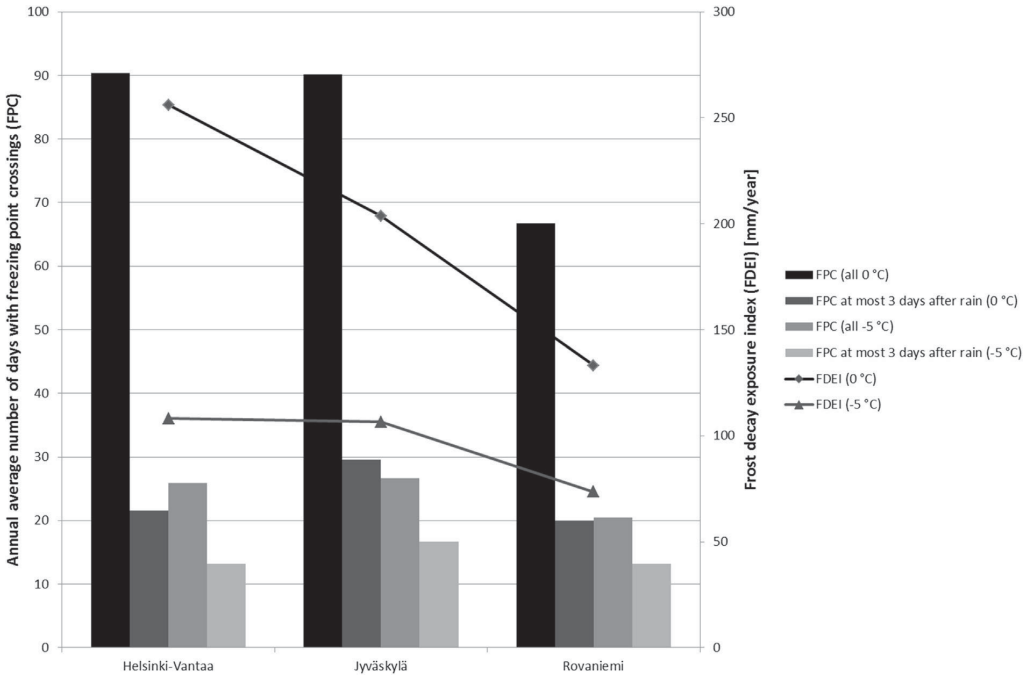

Fig. 10. Frost decay exposure index (FDEI) for three different locations in southern coastal area (Helsinki-Vantaa), inland (Jyväskylä) and Lapland (Rovaniemi) presented in a combination diagram as lines. The annual average number of freezing events with temperature crossings under 0 °C and −5 °C is indicated by the columns. FPCs are also presented as columns when it has rained within 3 days of freezing occurring.

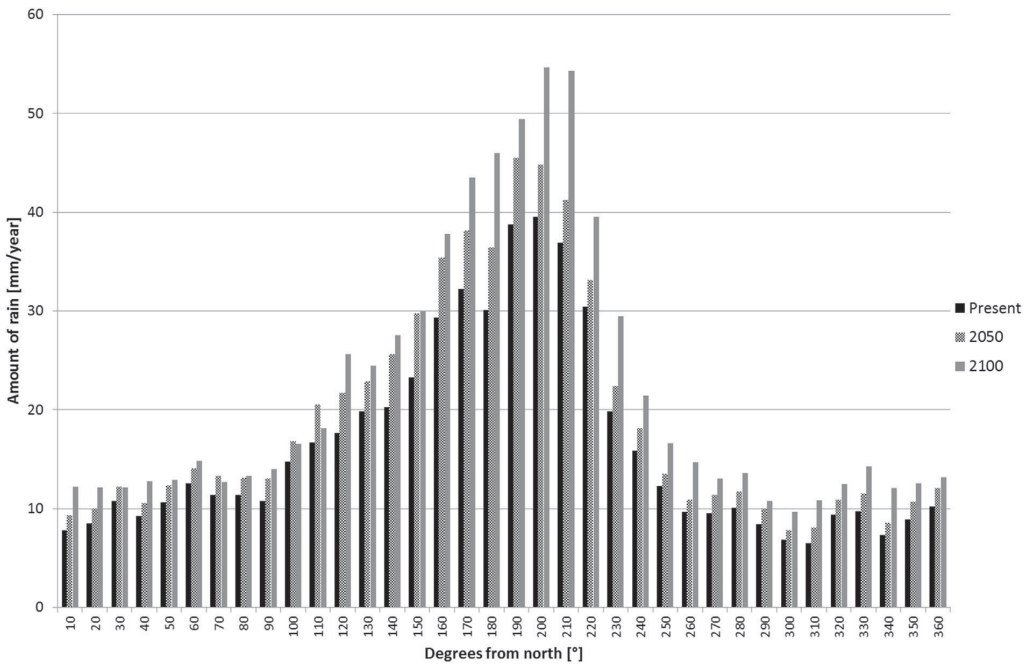

Fig. 11. Average annual amount of driving rain vs. wind direction for present and future (2050, 2100) climates in the southern coastal area.

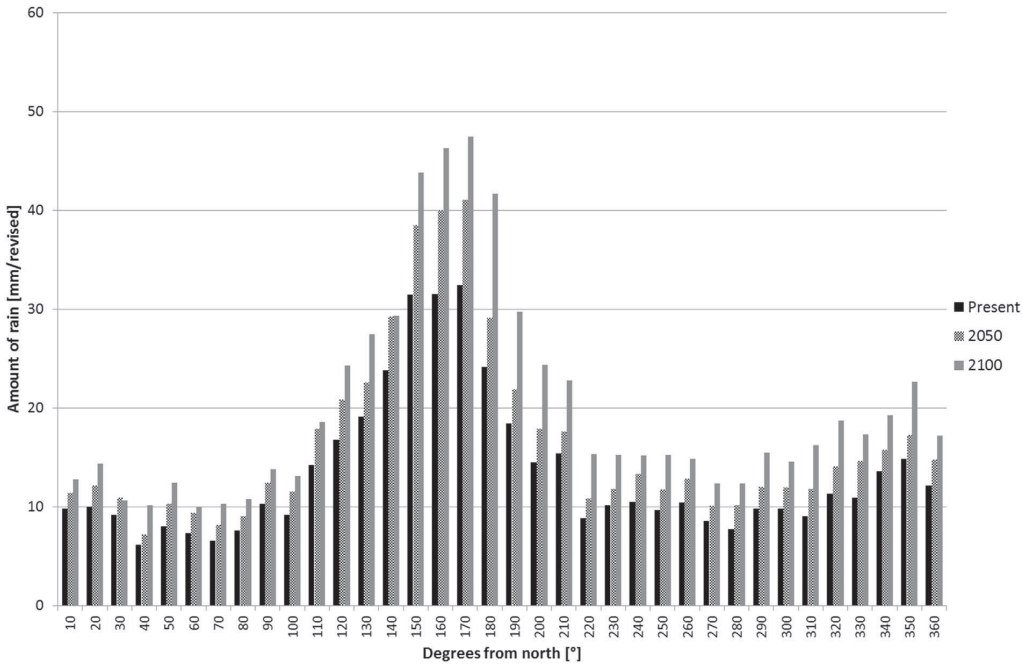

Fig. 12. Average annual amount of driving rain vs. wind direction for present and future (2050, 2100) climates inland.

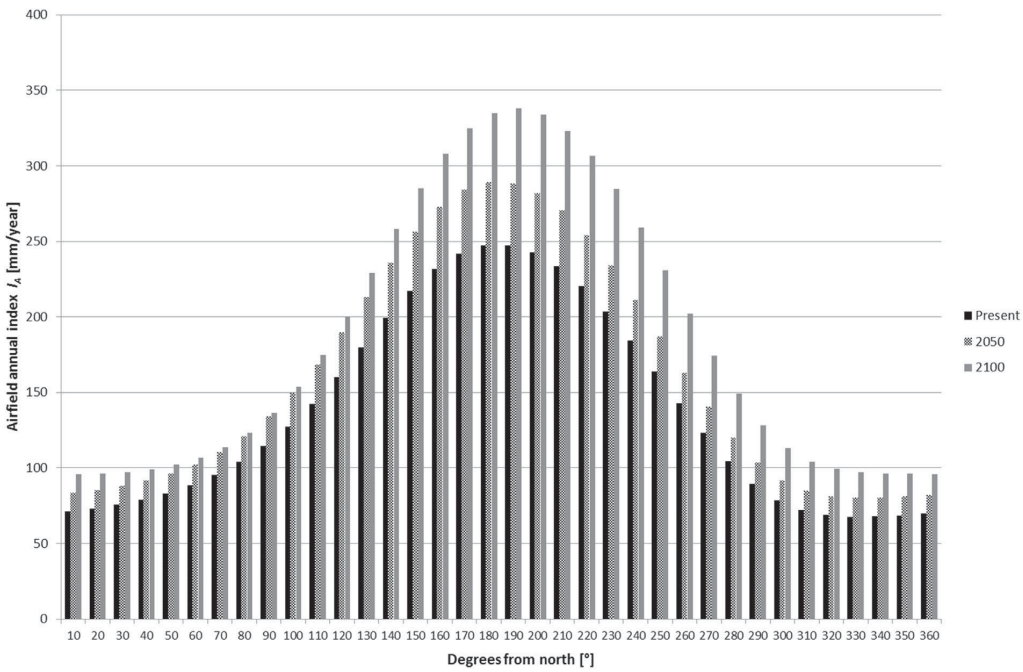

Fig. 13. Airfield annual index vs. wind direction of present and future (2050, 2100) climates in the southern coastal area.

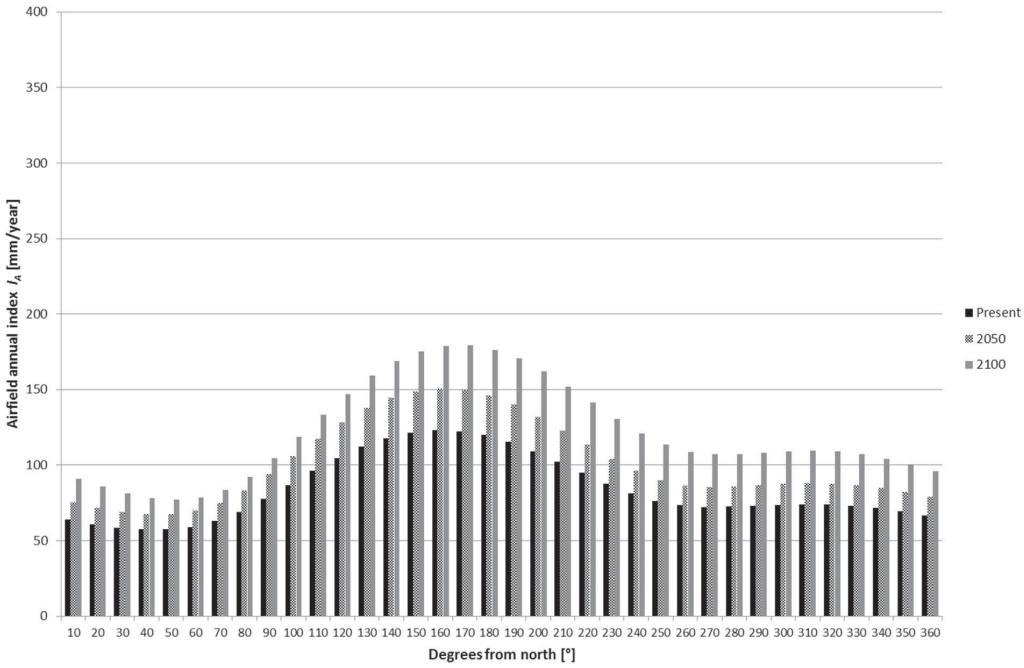

Fig. 14. Airfield annual index vs. wind direction of present and future (2050, 2100) inland climates.

resistant concrete both in the southern coastal area (Helsinki-Vantaa) and inland (Jyväskylä). The calculations are based on present and forecast weather data and the research referred to in Chapter 4.2. The time estimates have been calculated on the basis of the number of average annual freeze-thaw cycles (presented on Table 3) and the actual number of freeze-thaw cycles needed for incipient frost damage to show in thin-section analyses (see Table 5).

As a consequence of climate change, outdoor conditions where concrete freezes wet will ease remarkably already in 2030 in southern Finland. The inland outdoor climate will remain at the present level and the conditions will get even harder with increasing amounts of rain and sleet almost to the end of century. Complete failure to air-entrain fresh concrete ($p_r \leq 0.10$) will surely lead to frost damage in concrete structures before eligible service life of the structure (usually at least 50 years).

According to common theories, service lives of concrete structures can be divided into damage initiation and propagation periods. For instance, the authors of this study recently calculated, based on the same database, the length of the initiation and propagation phase of carbonation induced corrosion [61]. If we try to apply this model to frost attack, we find that there is no initiation time at all if frost resistance is inadequate, according to Fagerlund's theory [48] (no air-entrainment, critical moisture content of concrete has been achieved). In practice, concrete structures without frost resistance still have an initiation time of 388 (inland) and 307 (coastal area) freeze-thaw cycles.

Table 6
Time that it takes in the present and different future climates for incipient frost damage to show in thin-section analyses with different temperature thresholds and rain or sleet a maximum of 2 days before threshold exceedance (in the case of no air-entrainment).

Construction year	Southern coastal area [years]		Inland [years]	
	$t \leq -5$ °C	$t \leq -10$ °C	$t \leq -5$ °C	$t \leq -10$ °C
2000	26	35	37	45
2030	40	61	40	58
2050	50	78	41	59
2100	79	350	53	90

4.5. Sufficiency of the Concrete Code in force against frost attacks in future climates

The Finnish laboratory test for frost resistance is considerably harder than even the freeze-thaw cycles caused by the real outdoor climates of the future. According to the Concrete Code in force [19], the frost resistance of concrete should be tested in a laboratory with a freeze-thaw test of 100 cycles (XF 1, 50 years) or 300 cycles (XF 1, 100 years and XF 3, 50 years). In a laboratory test according to Finnish standard SFS 5447, a sample saturated by capillary action is exposed to a −20 °C to +20 °C temperature variation. The sample remains at −20 °C for one hour. The typical freeze-thaw cycle lasts approx. three hours [62]. Both the temperature and the time at a low temperature are more severe conditions than prescribed in e.g. ASTM C666 [63]. In laboratory freeze-thaw tests, the freezing rate is usually higher than in nature where it is typically 0.5–2 °C/h [51].

If the spacing factor is less than 0.20 mm, concrete can generally be considered frost resistant [51]. However, several tests have shown that concrete made of ordinary Portland cement is frost resistant if the spacing factor is less than 0.50 mm [51,64,65]. The Finnish Concrete Code always requires a spacing factor of 0.27 or less.

Concrete that is durable according to the present Concrete Code will also withstand the real outdoor climate for the expected service life.

5. Conclusions

The number of freeze-thaw cycles is slightly higher inland than in Southern Finland, but due to the higher amount of rain and sleet in Southern Finland the number of freeze-thaw cycles needed to cause the same degree of frost damage is much lower. In practice, concrete has to freeze to −5 °C or lower for frost damage to occur. Freezing events to −5 °C are significantly fewer than freezing events to just below 0 °C.

Though the amount of freeze-thaw cycles is basically the same in both southern and inland areas, the amount of rain is remarkable higher in the southern coastal areas, which is why the frost decay exposure index (FDEI) is higher there. Though Lapland is the northernmost part of Finland, and its annual average temperature is much lower than in the rest of the country, the amount of freeze-thaw cycles and the FDEI are also low. Thus, the risk for frost attack in northern Finland is actually lower than in the southern parts. However, the FDEI does not describe sufficiently well the actual risk of frost damage. The level of the index depends highly on the threshold temperature chosen for the freezing point crossing (FPC). An FPC with a threshold of 0 °C indicates a high risk but does not necessarily lead to frost damage. However, a comparison of FDEI calculations and the actual amount of freeze-thaw cycles needed for frost damage showed that the amount of precipitation before freezing has a larger impact on frost damage than the number of freezing events.

The driving rain index (airfield annual index I_A) shows that south-facing facades will get significantly more wind driven rain (30% in the southern coastal area and 40% inland by the end of the century), but its direction is not going to change significantly. Thus, south-facing facades will continue to be most susceptible to climate stress. That should be taken into account in the design of the details of concrete facades and balconies.

As a consequence of climate change, outdoor conditions where concrete freezes wet will ease remarkably already in 2030 in southern Finland, even though the amount of wind driven rain will increase significantly, because the number of freeze-thaw cycles will decrease at the same time. The inland outdoor climate will remain as it is and the exposure conditions will worsen with the increasing amount of rain and sleet almost to the end of century. Complete failure with air-entraining fresh concrete (no detectable protective air pores) is sure to lead to frost damage in a concrete structure before the end of the estimated service life, usually at least 50 years.

Concrete can be very durable in the Nordic climate if it is properly air-entrained. The present requirements for frost resistance of concrete are also sufficient in the future climates. However, attention must be paid to proper air entrainment of fresh concrete. It must always succeed.

Acknowledgements

The authors would like to thank the researchers at the Finnish Meteorological Institute for preparing the future climate projections. This study was part of the FRAME research project conducted at Tampere University of Technology in 2009–2012.

References

[1] Jylhä K, Ruosteenoja K, Räisänen J, Venäläinen A, Tuomenvirta H, Ruokolainen L, et al. The changing climate in Finland: estimates for adaption studies. ACCLIM project report. Finnish Meteorological Institute; 2009. Reports 2009:4. Helsinki. 78 p. 36 app. [in Finnish, extended English abstract].
[2] IPCC. Climate change 2007: the physical science basis. Contribution of Working Group I to the fourth assessment report of the Intergovernmental Panel on Climate Change. Cambridge, U.K.: Cambridge University Press; 2007. p. 996.
[3] SWD 137. Adapting infrastructure to climate change. Brussels; 2013.
[4] E.E.A. Report 12 climate change, impacts and vulnerability in Europe 2012. Copenhagen: European Environment Agency; 2012.
[5] Lahdensivu J. The durability of facades and balconies in a changing climate. Helsinki: Ministry of the Environment. Department of the Built Environment. The Finnish Environment 17/2010; 2010. p. 64 [in Finnish].
[6] Lahdensivu J. Durability properties and actual deterioration of Finnish Facades and Balconies. Tampere: Tampere University of Technology. Faculty of Built Environment; 2012. Publication 1028. 117 p. 37 app.
[7] Hytönen Y, Seppänen M. Let's prefabricate it: the history of Finnish precast concrete construction. Helsinki: SBK Foundation; 2009. p. 332 [in Finnish].
[8] BES. Development of open concrete element system. Research report. Suomen Betoniteollisuuden Keskusjärjestöry; 1969 [in Finnish].
[9] Fagerlund G. Mechanical damage and fatigue effects associated with freeze-thaw of materials. In: Setzer MJ, Auberg R, Keck H-J, editors. Frost resistance of concrete. Cachan Cedex. RILEM proceedings PRO24; 2002. p. 117–32.
[10] Lahdensivu J, Mäkelä H, Pirinen P. Durability properties and deterioration of concrete balconies of inadequate frost resistance. Int J Sustain Build Technol Urban Dev 2013;4(2):160–9.
[11] Shang H-S, Song Y. Behavior of air-entrained concrete under the compression with constant confined stress after freeze–thaw cycles. Cem Concr Compos 2008;30(9):854–60.
[12] Shang H-S. Triaxial T-C-C behavior of air-entrained concrete after freeze-thaw cycles. ISSN0165-232X. Cold Regions Science and Technology; 2013. http://dx.doi.org/10.1016/j.coldregions.2013.01.004 [Available online 23 January 2013].
[13] Shang H-S, Song Y, Ou J. Behavior of air-entrained concrete after freeze-thaw cycles. Acta Mech Solida Sin 2009;22(3):261–6.
[14] Penttala V, Al-Neshawy F. Stress and strain state of concrete during freezing and thawing cycles. Cem Concr Res 2002;32(9):1407–20.
[15] Zandi Hanjari K, Utgenannt P, Lundgren K. Experimental study of the material and bond properties of frost-damaged concrete. Cem Concr Res 2011;41(3):244–54.
[16] Li W, Sun W, Jiang J. Damage of concrete experiencing flexural fatigue load and closed freeze/thaw cycles simultaneously. Constr Build Mater 2011;25(5):2604–10.
[17] BY 32 Guidelines for durability and service life of concrete structures. Helsinki: Concrete Association of Finland; 1989. p. 60.
[18] Koskiahde A. An experimental petrographic classification scheme for the condition assessment of concrete in facade panels and balconies. Mater Charact 2004;53:327–34.
[19] Concrete Association of Finland. Finnish concrete code BY 50. Helsinki: Concrete Association of Finland; 2012. p. 251.
[20] Lisø KR. Building envelope performance assessments in harsh climates: methods for geographically dependent design [Doctoral theses at NTNU 185]. Trondheim: Norwegian University of Science and Technology; 2006. p. 187.
[21] Rydock JP, Lisø KR, Førland EJ, Nore K, Thue JV. A driving rain exposure index for Norway. Build Environ 2005;40(11):1450–8.
[22] Lisø KR, Kvande T, Hygen HO, Thue JV, Harstveit K. A frost decay exposure index for porous, mineral building materials. Build Environ 2007;42(10):3547–55.
[23] Blocken B, Carmeliet J. A review of wind-driven rain research in building science. J Wind Eng Ind Aerodyn 2004;92(13):1079–130.
[24] Jerling A, Schechninger B. Fogars beständighet. Rapport R89:1083. Stockholm: Byggforskningrådet; 1983. p. 172 [in Swedish].
[25] Blocken B, Carmeliet J. High-resolution wind-driven rain measurements on a low-rise building – experimental data for model development and model validation. J Wind Eng Ind Aerodyn 2005;93(12):905–28.
[26] Lacy RE, Shellard HC. An index of driving rain. Meteorol Mag 1962;91:177–84.
[27] Boyd DW. Driving rain map of Canada. Technical Note, vol. 398. Ottawa, Canada: National Research Council of Canada, Division of Building Research; 1963.
[28] Sauer P. An annual driven rain index for China. Build Environ 1987;22:239–40.
[29] Chand I, Bhargava PK. Estimation of driving rain index for India. Build Environ 2002;37:549–54.
[30] Akingbade FOA. Estimation of driving rain index for Nigeria. Archit Sci Rev 2004;47(2):103–6.
[31] Sahal N. Proposed approach for defining climate regions for Turkey based on annual driving rain index and heating degree-days for building envelope design. Build Environ 2006;41:520–6.
[32] Giarma C, Aravantinos D. Estimation of building components' exposure to moisture in Greece based on wind, rainfall and other climatic data. J Wind Eng Ind Aerodyn 2011;99:91–102.
[33] Pérez JM, Domínguez B, del Coz JJ, Cano E. Estimation of the exposure to driving rain in Spain from daily wind and rain data. Build Environ 2012;57:259–70.
[34] Rydock JP. A framework for using a present weather observation method to calculate a driving rain wall factor at any location. Build Environ 2007;42:1229–35.
[35] Pérez JM, Domínguez B, del Coz JJ, Cano E. Optimised method for estimating directional driving rain from synoptic observation data. J Wind Eng Ind Aerodyn 2013;113:1–11.

[36] Karagiozis A, Hadjisophocleous G, Cao S. Wind driven rain distributions on two buildings. J Wind Eng Ind Aerodyn 1997;67 and 68:559–72.
[37] Choi ECC. Parameters affecting the intensity of wind driven rain on the front face of a building. J Wind Eng Ind Aerodyn 1994;53:1–17.
[38] Choi ECC. Wind driven rain on building faces and the driving-rain index. J Wind Eng Ind Aerodyn 1999;79:105–22.
[39] Künzel HM. Bestimmung der Schlagregenbelastung von Fassadenfläschen. IBP Mitteilung 21, Nr. 263. Fraunhofer Institute für Bauphysik; 1994.
[40] van Mook FJR. Driving rain on building envelopes [PhD thesis]. Eindhoven, the Netherlands: Eindhoven University of Technology; 2003. p. 198.
[41] Nore K, Blocken B, Jelle BP, Thue JV, Carmeliet J. A data set of wind driven rain measurements on low-rise test building in Norway. Build Environ 2007;42: 2150–65.
[42] Zhu D, Mallidi SR, Fazio P. Quantitative driving rain exposure on vertical wall at various Canadian cities. Build Environ 1995;30:533–44.
[43] Fazio P, Mallidi SR, Zhu D. A quantitative study for the measurement of driving rain exposure in the Montreal region. Build Environ 1995;30:1–11.
[44] Rydock JP. A look at driving rain intensities at five cities. Build Environ 2006;41:1860–6.
[45] SFS-EN ISO 15927-3. Hygrothermal performance of buildings. Calculation and presentation of climatic data. Part 3: calculation of a driving rain index for vertical surfaces from hourly wind and rain data. Helsinki: Finnish Standards Association SFS; 2009.
[46] Ruosteenoja K, Jylhä K, Mäkelä H, Hyvönen R, Pirinen P, Lehtonen I. Weather data for building physics test years in the observed and projected future climate. Reports No. 2013:1. Helsinki: Finnish Meteorological Institute; 2013. p. 36. 9 app. [in Finnish].
[47] Kuosa H, Vesikari E. Ensuring of concrete frost resistance. Part 1: basic data and service life design. VTT Technical Research Centre of Finland; 2000. p. 141. Research notes 2056. [in Finnish].
[48] Fagerlund G. The critical degree of saturation method of assessing the freeze/thaw resistance of concrete. Tentative RILEM recommendation. Prepared on behalf of RILEM Committee 4 CDC. Materiaux et Constructions; 1977. p. 217–29. 1977 no 58.
[49] Powers TC. The air requirement of frost-resistant concrete. Chicago: Portland Cement Association, Research and Development laboratories, Development Department; 1949. Bulletin 33.
[50] Powers TC, Helmuth RA. Theory of volume changes in hardened Portland cement pastes during freezing. In: Proceedings of the Highway Research Board 32; 1953. p. 285–95.
[51] Pigeon M, Pleau R. Durability of concrete in cold climates. Suffolk: E & FN Spon; 1995. p. 244.
[52] Litvan G. Phase transitions of adsorbates IV – mechanism of frost action in hardened cement paste. J Am Ceram Soc 1972;55(1):38–42.
[53] Fagerlund G. A service life model for internal frost damage in concrete. Lund: Lund Institute of Technology, Division of Building Materials; 2004. p. 138. Report TVBM-3119.
[54] fib Bulletin No. 34. Model code for service life design. Lausanne: International Federation for Structural Concrete; 2006. p. 116.
[55] Penttala V. Freezing-induced strains and pressures in wet porous materials and especially in concrete mortars. Adv Cem Based Mater 1998;7:8–19.
[56] Hedlund H, Jonasson JE. Effect on stress development of restrained thermal and moisture deformation. In: Baroghel-Bouny V, Aïticin P-C, editors. Shrinkage of concrete, shrinkage 2000. CachanCedex. RILEM proceedings PRO17; 2000. p. 355–77.
[57] Mäkinen K. Strength and physical properties of materials. Builders calendar 2011. Hämeenlinna: Rakennustieto Oy; 2010. p. 375–8 [in Finnish].
[58] Neville A. Properties of concrete. Essex: Longman Group; 1995. p. 844.
[59] Concrete Association of Finland. BY 42, condition assessment manual of concrete facades and balconies. Helsinki: The Concrete Association of Finland; 2002. p. 178 [in Finnish].
[60] Official Statistics Finland (OSF). Population structure [e-publication]. Annual review. Helsinki: Statistics Finland; 2009 [referred: 28.3.2014]. Available at:, http://www.tilastokeskus.fi/til/vaerak/2009/01/vaerak_2009_01_2010-09-30_tie_001_en.html.
[61] Köliö A, Pakkala TA, Lahdensivu J, Kiviste M. Durability demands related to carbonation induced corrosion for Finnish concrete buildings in changing climate. Eng Struct 15 March 2014;62–63:42–52.
[62] SFS Standard 5447. Concrete. Durability. Freeze-thaw resistance. Helsinki: Finnish Standards Association SFS; 1988.
[63] ASTM Standard C666. Standard test method for resistance of concrete to rapid freezing and thawing. West Conshohocken, PA: ASTM International; 2008. http://dx.doi.org/10.1520/C0666_C0666M-03R08. www.astm.org.
[64] Pigeon M, Pleau R, Aitcin PC. Freeze-thaw durability of concrete with and without silica fume in ASTM C 666 (procedure A) test method: internal cracking versus scaling. Cem Concr Aggregates 1986;8(2):76–85.
[65] Aïtcin P-C, Mindess S. Sustainability of concrete. Oxon: Spon Press; 2011. p. 301.

III

CLIMATE CHANGE EFFECT ON WIND-DRIVEN RAIN ON FACADES

by

Pakkala T.A., Lemberg A.-M., Lahdensivu J. & Pentti M. Jun 2016

Nordic Concrete Research, Publ. 54, 1/2016, pp. 31–49

Climate change effect on wind-driven rain on facades

Toni A. Pakkala
M.Sc., PhD Student
Tampere University of Technology
P.O. Box 600
FI-33101 Tampere
E-mail: toni.pakkala@tut.fi

Antti-Matti Lemberg
B.Sc.
Tampere University of Technology
P.O. Box 600
FI-33101 Tampere
E-mail: antti-matti.lemberg@student.tut.fi

Jukka Lahdensivu
D.Sc., Adjunct Professor
Tampere University of Technology
P.O. Box 600
FI-33101 Tampere
E-mail: jukka.lahdensivu@tut.fi

Matti Pentti
D.Sc., Professor
Tampere University of Technology
P.O. Box 600
FI-33101 Tampere
E-mail: matti.pentti@tut.fi

ABSTRACT

It has been shown that the wind-driven rain has a major effect on all of the most significant concrete degradation mechanism in Finland and the degradation rate depends significantly on both location and orientation of outdoor concrete surface, e.g. façade. In this study, the amount of wind-driven rain and the effect of climate change on it has been studied at four different locations. As a result, it was found that at present the climatically most stressed façade orientations at the most stressed areas, the coastal and southern Finland areas, will face significantly more wind-driven rain in the future climate.

Keywords: concrete; wind-driven rain; durability; climate change

1 INTRODUCTION

More than 60 % of the Finnish building stock has been built in the 1960's or later. There are a total of 1.2 million apartments in the Finnish block of flat stock, of which 50% has been built during 1960-1979 [1]. Despite of young age of Finnish block of flats a considerable number of envelopes of the precast concrete buildings erected in that era have come near the end of the service life largely due to degradation.

Based on the latest research conducted at Tampere University of Technology (TUT), the durability properties of existing concrete façades and balconies have been found to be poor [2,3,4]. The material properties related to freeze-thaw resistance of concrete and cover depth of reinforcement rarely fulfil the requirements of national building codes. According to these studies, in 59.2% of Finnish concrete facades have been local corrosion damage and in 42.7% freeze-thaw damage. On the other hand, the protective pore ratio is less than 0.15 in about 70% of existing concrete facades and balconies. However, despite the insufficient durability properties of concrete, wide spread damage that can be seen visually are relative rare, less than 7%.

Moisture behaviour and environmental stress conditions have a strong impact on frost damage of concrete. For instance, the stress on concrete facade depends on the existence of proper waterproofing and prevailing wind direction during raining. Visual damage of concrete façades and balconies has a strong correlation with precipitation, wind directions during the rain and freeze-thaw cycles directly after the rain events [3,4,5].

The increasing amount of precipitation has been shown to have a strong correlation with the rate of the two most important deterioration mechanisms of Finnish outdoor concrete structures: freeze-thaw deterioration and carbonation induced corrosion of reinforcement [4,6]. In the present climate incipient freeze-thaw damage takes 22 years in average in non-frost resistant concrete [3]. Thus, it is important to explore the possible climate change scenarios considering their effect on critical outdoor conditions for deterioration of structures, for the repair need of existing building stock and for the timing of repair actions.

1.1 Research objective

Because it has been shown that the wind-driven rain (WDR) has a major effect on all of the most significant concrete degradation mechanism in Finland, in this paper the effect of climate change on the amount of the WDR on concrete facades is studied to assess the differences of climatic loads at variable locations and façade orientation. The climate data projections made by FMI are studied to estimate the possible changes on the amount of WDR on variable façade orientations at different locations in Finland.

2 BACKGROUND

2.1 Finnish concrete facades

Since 1970s almost all prefabricated concrete structures in Finland are based on the Concrete Element System [7]. That open system defines, for instance, the recommended floor-to-floor

height and the types of prefabricated panels used. In principle, the system allows using the prefabricated panels made by all manufacturers in any single multi-storey building.

Until 1980s dominant surface of the prefabricated concrete facades were exposed aggregate, brushed painted and painted form-finish concrete. Also brick tile and ceramic tile finishing were popular. Since 1990s white concrete and coloured white concrete have penetrated the market. [3]

2.2 Quality of concrete

The concrete grade used for concrete facade panels and most structural members of balconies has been C30/37 since the late 1980's in Finland based on the guidelines for durability and service life of concrete. Earlier the grade was C20/25. The cement used for concrete panels is mostly CEM I (42.5 N) (ordinary Portland cement) because of the good early strength it gives to concrete which allows rapid formwork rotation at the precast panel plant. White cement, CEM I (52.5 R), is also used in facade panels if necessary, but its share of total use is marginal.

The freeze-thaw resistance of the concrete is conducted by air-entrainment of fresh concrete and it can be determined by testing a protective pore ratio (p_r). In 1976 Concrete Codes started to recommend the protective pore ratio of 0.15 which means that at least 15 % of all pores are never filled by capillary water. At the Concrete Code 1989, the protective pore ratio was lifted to reach at least 0.20. Protective pore ratio $p_r < 0.10$ can be considered to make concrete non-freeze-thaw-resistant in Finnish outdoor climate [3].

The success of air-entrainment of concrete used in facades and balconies have been studied by Lahdensivu [3] from the thin section analysis results of the samples in the BeKo database (buildings built 1960-1995). Based on the study the freeze-thaw resistance differs considerably between various surface types of facades. Pakkala et al. [4] studied buildings built after the requirement of protective pore ratio of 0.20 has been demanded and presented that only approx. 50 % of the precast panels have met the freeze-thaw resistance requirements.

Lahdensivu [3] presented that visually observable reinforcement corrosion damage existed in 59% of the examined facades. 54 % of damage was local and extensive corrosion was found only in 5.7% of the facades. The corrosion damage was almost solely due to carbonation.

2.3 Deterioration rate of Finnish concrete facades

The deterioration rate and need for repair of existing outdoor concrete structures, especially concrete facades and balconies, have been monitored by systematic condition assessments over 20 years. Lahdensivu [3] studied in his doctoral thesis the deterioration of prefabricated concrete element buildings at present climate. His studies were based on 947 condition assessment reports made on buildings built 1960 – 1996 [2]. He studied the changes on quality requirements, dominating deterioration mechanisms, their progress on present climate based on climate data produced by the Finnish Meteorological Institute (FMI) and effect of a geographical distribution on them. The most essential results were:

- There is a significant lack of quality with concrete structures, also with structures made according to current concrete code,
- The most significant deterioration mechanisms have been carbonation induced corrosion and freeze-thaw weathering,
- The most significant climatic causes for damage have been wind-driven rain and freeze-thaw cycles within few days after the rain events,
- The deterioration rate has been faster in coastal areas than in inland.

Two recent studies by Pakkala et al. [4] and Köliö et al. [6] studied rates of freeze-thaw weathering of concrete facades and carbonation induced corrosion of concrete reinforcement, respectively, at the projected future climate. Köliö et al. presented that the increase of precipitation decelerates the carbonation rate and thus the initiation phase of reinforcement corrosion while the increase in CO2 level has a greater opposite impact. On the other hand, the increase of precipitation amount and temperature accelerate the active corrosion phase. Pakkala et al. concluded e.g.:

- Amount of precipitation will increase significantly until the end of the century and relatively more at inland than at coastal areas,
- Amount of freeze-thaw cycles after rain events will decrease significantly after 2050's at southern Finland but remains almost at the same level at inland,
- The amount of precipitation is almost the same at coastal areas and inland but at coastal areas the rate of freeze-thaw weathering is higher because of the annual average wind speed is higher, thus more of the precipitation will shower the vertical surfaces,
- The wind-driven rain load is both at present and at future significantly concentrated on south-west, south and south-east orientated facades and its relative increase is greater than the increase of precipitation because of the higher wind speed during the rain,
- Concrete can be durable in the Nordic climate if it has been properly air-entrained.

3 CLIMATIC STRESS ON OUTDOOR STRUCTURES

3.1 Modelling of wind-driven rain

The wind-driven rain (WDR) striking building facades has been the focus of several studies in the last decades as mentioned by Blocken & Carmeliet [8]. The moisture load resulting from driving rain depends not only on rainfall intensity and wind speed, but also on raindrop trajectories around buildings. That increases the complexity of the phenomenon greatly. According to Jerling and Schechninger [9], the upper parts and corners of facades get more rainfall than lower and central parts. Prevailing wind directions and wind speeds also have a strong influence on the distribution of rainfall across a building. Winds are stronger at higher levels of buildings than close to ground level which naturally leads to upper sections of high buildings receiving more rain and sleet stress than lower buildings, and lower sections of buildings in general. [10]

Experimental, numerical and semi-empirical methods have been developed and employed for the estimation of parameters related to driving rain against building facades [11]. The annual driving rain index (aDRI) that is calculated on the basis of average annual wind speed and average amount of total annual rainfall is proportional to the amount of water on a windward

vertical [12]. Based on the classification proposed by Lacy (sheltered areas, moderately exposed areas, severely exposed areas), driving rain maps have been produced for several countries including Sweden, United Kingdom, Canada, China, India, Nigeria, Turkey, Greece and Spain [11].

Differences in the time resolutions of climatic data sets may result in large discrepancies in the calculated indices. In most cases hourly data are considered to have adequate time resolution. Given that in many cases hourly data covering adequate periods of time are not available, some methods for the derivation of directional driving rain indices on the basis of synoptic data have been formulated [13,14,15]. However, the driving rain indices cannot be used for direct estimation of the driving rain load on building components at site. Quantification of the amount and intensity of this load (formation of the wind pressure field around each building) is a complex task. The building's geometry and the position of the area under study on the building's vertical surface (height, middle part of the surface or near the edges) influence the resulting load [11,16,17,18,19,20,21]. Example calculations of quantitative parameters related to driving rain (e.g. intensity) for specific sites are found in several studies, e.g. [22,23,24].

The standard SFS-EN ISO 15927-3 [25] presents a factor I_{WA} (Wall annual index) which can be used to estimate amount of precipitation collected by a free-standing driving-rain gauge in flat open country to present the amounts of precipitation that impacts on a real wall. The wall annual index is highly simplified simulation for assessing the WDR against building facades. There are other methods to model the WDR as is mentioned by Blocken and Carmeliet [8,26], e.g. CFD model. It takes into account more precisely the distribution of the WDR in different areas of the facades. Although the wall annual index is simplified method, it gives adequate results for e.g. comparing different locational effects on the amount of wind driven rain on facades. Compared to CFD modelling it underestimates the amount of wind driven rain near the top of the façade but overestimates the amount on the top 2.5 metres with high buildings and low rain intensity. The higher the rain intensity the more it underestimates the amount of wind driven rain. The underestimation increases near the edges of the building. With rain intensities from 10 mm/h to 30 mm/h the wall annual index gives adequately corresponding results with CFD modelling in the vertical middle line with high and low rise vertical buildings and tower buildings. [27]

3.2 Climate change projections

Climate change as such has been studied worldwide for a long time. In this context, climate change refers to global warming caused by an increase in greenhouse gases, especially carbon dioxide (CO_2). Climate change will affect the geographic and seasonal distribution of precipitation, wind conditions, cloudiness, air humidity and solar radiation. Modelling of future climate is based on alternative scenarios of greenhouse gas and aerosol particle emissions. In the scenarios, different assumptions are made about the future development of population growth, economic development, energy production modes, etc.

The ACCLIM [28] and FRAME [29] projects have shown that future climate conditions in Finland are likely to get worse in terms of durability of facades and other structures exposed to climate. According to the data of the ACCLIM project, precipitation during the winter season is also going to increase while the form of precipitation is going to be increasingly water and sleet. At the same time, the conditions for drying are going to get worse. Thus, the deterioration rate of structures will accelerate in most of Finland if maintenance and protection actions are neglected. [3]

The Finnish Meteorological Institute (FMI) examined in the ACCLIM project the different climate models and built models for observing Finnish climatic conditions and adaptation to climate change. In all greenhouse gas emission scenarios, based on three IPCC [30] scenarios for the evolution of greenhouse gas and aerosol particle emissions, the average temperature rises at a constant rate until 2040. Differences between the scenarios start to emerge only after the middle of the century, see figure 1. [31]

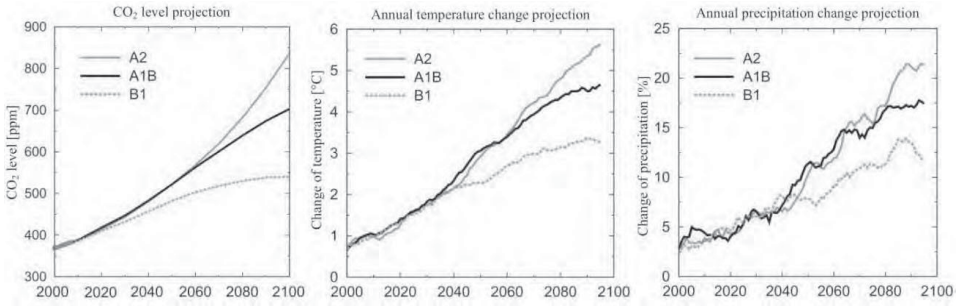

Figure 1 – Projections for (a) CO2 level, (b) annual mean temperature and (c) precipitation change in 2000–2100, in relation to the mean of the reference period 1971–2000. The curves depict 11 year running means, averaged over Finland and the responses of 19 global climate models [31]. Projections are given separately for the three greenhouse gas scenarios A2, A1B and B1 [30].

The FMI has extensive weather data since 1961 in digital form from several meteorological stations covering all of Finland. The data consist of temperature, relative humidity, rain intensity, wind speed and direction, solar radiation variables, etc. These observations have been collected at least daily and three times a day at best. In the REFI-B project [31] the FMI also forecast the climates of the four regions (coastal area, southern Finland, inland, Lapland) in three periods (2030, 2050 and 2100). The forecasts are based on an average of 19 different models which are all based on greenhouse gas emission scenario A2. The A2 scenario involves a situation where greenhouse gases are assumed to increase significantly − it is a sort of worst-case scenario. The FMI also has other significant greenhouse gas emission scenarios: A1B (quite large emissions) and B1 (small emissions). [31]

3.3 Climatic conditions in Finland

Although Finnish climate is relatively steady considering the latitudes, it still varies significantly from the mild and relatively rainy coastal area to the drier inland. However, the Finnish building stock is mainly concentrated in the few biggest cities and surrounding growth areas. Finland can be divided into four main areas based on climatic differences and concentration of population: the coastal area, southern Finland, inland and Lapland, see figure 2. [4]

Figure 2 – Finland can be divided into four main areas based on climate and concentrations of population. [4]

Pakkala et al. [4] presented that both the amount of precipitation and the amount of the WDR are highly concentrated on west to south-east directions and will be even more concentrated on future climate. The same phenomenon has been noted in condition assessment studies where the most deterioration has been observed on south-facing facades and balconies.

4 MATERIAL AND METHODS

4.1 Climate data

Present and future climate projections and their effects on weather conditions critical to concrete degradation have been prepared by the Finnish Meteorological Institute (FMI). The data used in this study are hourly interpolated observations of temperature, wind speed, wind direction and amount of precipitation over 30 years (1980–2009). The data of amount of precipitation, the wind speed and the wind direction were collected every three hours and interpolated to hourly data.

The future climate projections, based on the A2 scenario, were calculated by FMI to represent hourly data for a similar period in 2050 and 2100. The calculations of this study focus on all four locations presented in the Figure 2: coastal area, southern Finland, inland and Lapland.

4.2 Typical Finnish suburb

The locations of the buildings used in this study are set to the same areas as the climate data mentioned above. Imaginary Finnish suburban city blocks, shown in the figure 3, are located at

the coastal area, southern Finland, inland and Lapland. Two types of building were studied, both represented typical Finnish multi-storey residential building of 1970's with 2 staircases. The other one was 4- and the other 8-storey, see figures 4 and 5.

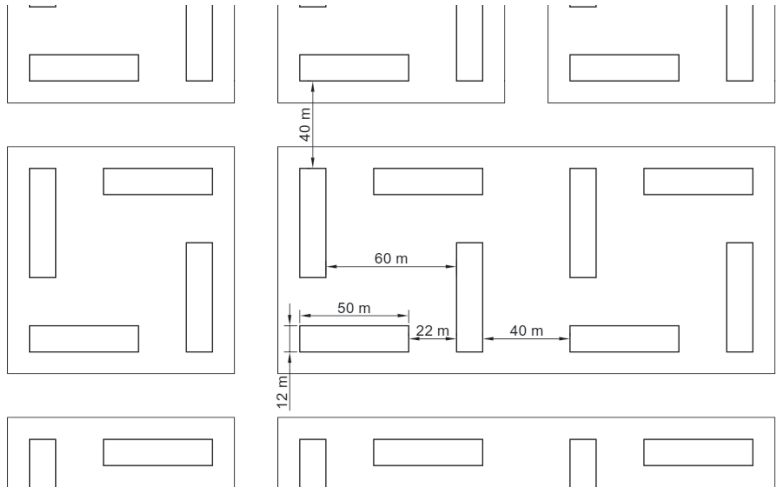

Figure 3 – Simplified Finnish suburban street plan with repetitive blocks.

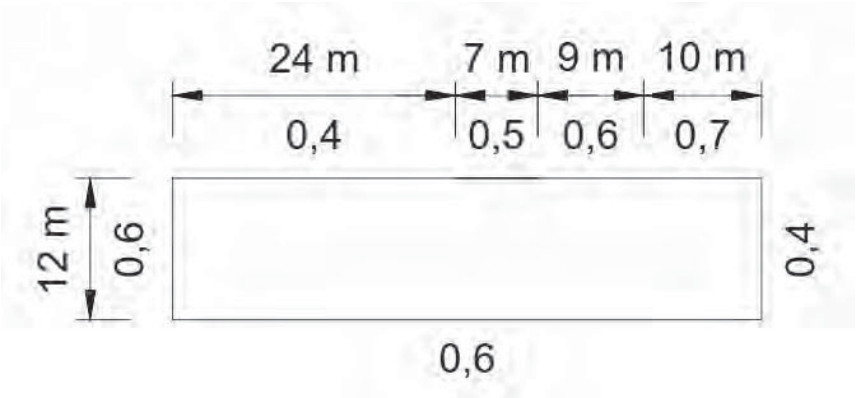

Figure 4 – The dimensions of studied building and the obstruction factor, see section 4.3, based on the suburban street plan presented at Figure 3.

Figure 5 Typical Finnish suburban precast concrete buildings.

4.3 Modelling of wind-driven rain

The Wall annual index I_{WA} is presented at the standard SFS-EN ISO 15927-3 [25] as follows:

$$I_{WA} = I_A C_R C_T O W \quad (1)$$

, where I_A is the airfield annual index, C_R is a terrain roughness coefficient, C_T is a topography coefficient, O is an obstruction factor and W is a wall factor. The airfield annual index I_A is defined as:

$$I_A = \frac{2}{9}\frac{\sum v r^{\frac{8}{9}} \cos(D-\theta)}{N} \quad (2)$$

, where v is an hourly mean wind speed [m/s], r is an hourly rainfall total [mm], D is an hourly mean wind direction from north [°], θ is a wall orientation relative to north [°], N is a number of years for which data is available and the summation is taken over all hours for which $\cos(D-\theta)$ is positive.

The roughness coefficient depends on the height above the ground and the roughness of the terrain in the direction from which the wind is coming, i.e. is there an open sea, a farm land, a suburban area or an urban area in the upwind direction. The coefficient C_R at height z is calculated as follows:

$$C_R(z) = K_R \ln(\frac{z}{z_0}) \qquad \text{for } z \geq z_{min} \quad (3)$$

$$C_R(z) = C_R(z_{min}) \qquad \text{for } z < z_{min} \quad (4)$$

This study uses only the terrain category *III*, see table 1, because typical Finnish suburban is usually located at considerably sheltered locations and is often surrounded by sector of forest.

Table 1 – Terrain categories and related parameters. [25]

Terrain category	Description	K_R	z_0	z_{min}
I	Rough open sea; lake shore with at least 5 km open water upwind and smooth flat country without obstacles	0.17	0.01	2
II	Farm land with boundary hedges, occasional small farm structures, houses or trees	0.19	0.05	4
III	Suburban or industrial areas and permanent forest	0.22	0.3	8
IV	Urban areas in which at least 15 % of the surface is covered with buildings of average height exceeding 15 m	0.24	1	16

The topography coefficient takes into account the increase of mean wind speed over isolated hills and escarpments near the building subjected to the study. In this research the studied buildings are consider to locate at flat surroundings when the topography coefficient $C_T = 1$.

The obstruction factor depends on the horizontal distance to the nearest obstacle which is at least as high as the wall subjected to the study, see table 2. The obstacle is taken into account when it is located at the line of sight from the horizontal view away from the wall, i.e. over a sector spanning 25° either side of the normal to the wall. The wall factor is, in the case of flat roof multi-storey building, 0.5 for the top 2.5 m of the wall and 0.2 for remainder.

Table 2 – Obstruction factor. [25]

Distance of obstruction from wall [m]	4 – 8	8 – 15	15 – 25	25 – 40	40 – 60	60 – 80	80 – 100	100 – 120	over 120
Obstruction factor O	0.2	0.3	0.4	0.5	0.6	0.7	0.8	0.9	1.0

Limitations of using the standard SFS-EN ISO 15927-3
Using the standard requires data from at least 10 years and preferably 30 years of hourly values of wind speed, wind direction and rainfall. The data, referred in this study as present, is collected from 1980 to 2009. The climate change projections are also made to represent 30 years' data and the studied periods are from 2035 to 2064 (referred in this study as 2050), and from 2085 to 2114 (referred in this study as 2100).

As mentioned before, the used data is collected in every three hours and interpolated to hourly values. The interpolation effects mostly on the rain intensity and mildly also the wind speed and direction during the rain event. However, it is considered to meet the aim of this study to compere different locations and climate change projections with each other.

In addition, there are three other limiting terms when the standard does not apply as mentioned in the standard: (1) mountainous areas, (2) areas in which 25% of the annual rainfall comes from severe storms and (3) areas and periods when a significant proportion of precipitation is made up of snow and hail.

The term (1) is met because Finnish landscape is flat except the most north-western part where the population is extremely low. The term (2) is also met because 6-7% (0-8 days) of the raining days in Finland are the ones when the rain intensity is thought to be quite severe, over 20 mm per day. [32]

Meeting the term (3) is the most questionable. At south-western part of Finland 30% of the precipitation is in the form of snow and on the other parts between 40-50%. The standard does not specify the "significant proportion" but it can be assumed that the kind of amounts are a significant proportion and thus, the data cannot be applied as it is. For meeting the term, in this study only the rain events when temperature is over 0 °C during and two hours before the events are taken into account.

5 RESULTS AND DISCUSSION

As has been noted before WDR is highly concentrated between west to south-east directions at every studied location in Finland. As a result of it and because of higher wind speeds during the rain events, at coastal area and southern Finland the Airfield annual index (I_A), see equation 2, is 3.5 and 2.9 times higher, respectively, from southern compared northern direction, see table 3 and figure 6. As a consequence of a more uniform distribution of wind direction and wind speed during the rain events the same figures are 1.8 and 1.5 at inland and Lapland, respectively.

Table 3 – Amount of average annual Airfield annual index I_A *from different wind directions at present climate and future climate projections.*

Wind direction	Coastal [mm/year]			Southern Finland [mm/year]			Inland [mm/year]			Lapland [mm/year]		
[° from north]	Present	2050	2100	Present	2050	2100	Present	2050	2100	Present	2050	2100
0	70	82	96	63	73	85	67	79	96	54	63	78
30	76	88	97	69	79	85	59	69	81	56	65	78
60	88	102	107	78	89	90	59	70	78	57	66	79
90	115	134	137	93	104	103	77	94	104	61	72	90
120	160	190	200	121	136	136	105	128	147	71	86	112
150	217	256	285	160	181	191	122	149	175	80	99	130
180	247	289	335	183	209	235	120	146	176	79	99	130
210	233	270	323	178	207	245	102	123	152	68	85	110
240	184	211	259	149	175	218	81	96	121	52	65	83
270	123	140	174	105	125	163	72	85	107	41	50	64
300	79	92	113	72	87	113	74	87	109	40	49	63
330	68	80	97	63	74	91	73	87	107	48	57	72

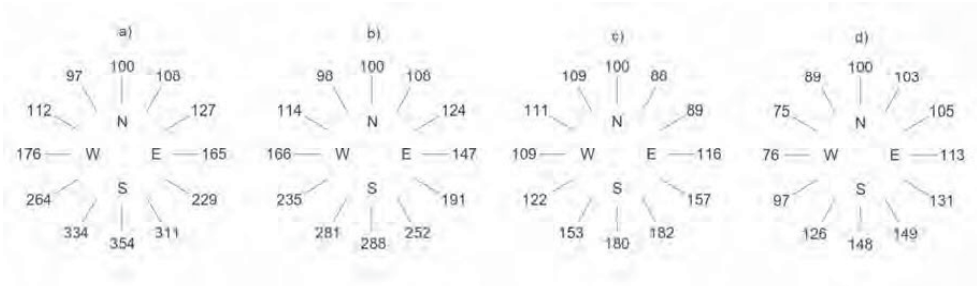

Figure 6 – Relative amount of I_A *compared to* I_A *from north direction at present climate from different wind directions at a) coastal area, b) southern Finland, c) inland and d) Lapland.*

At coastal area the I_A is at present climate on average 24%, 64%, 135% higher than at southern Finland, inland and Lapland, respectively, while the amount of precipitation is only 12%, 20% and 68% higher. The difference is a consequence of higher wind speed at coastal areas. At the coastal area 74% of precipitation hits a vertical wall while at inland the share is 66%, at southern Finland 54% and at Lapland 53%.

Depending of the façade orientation the I_A is at present climate 8 – 36% higher at the coastal area compared to southern Finland. The highest difference is from southern directions and the lowest from northern. At future climates the difference decreases from northern directions yet increases from southern directions, e.g. at 2100 climate I_A is 49% higher from south-east. At inland and Lapland, the I_A is significantly lower from southern directions at present climate, e.g. 2.3 and 3.5 times lower, respectively, from south-west direction. At future climates the

difference decreases at both locations, e.g. from south-west direction at 2100 climate the I_A is 2.1 and 3.0 times lower, respectively, compared to the coastal area.

Figure 7 shows wind direction related relative change of the I_A compared to present climate.

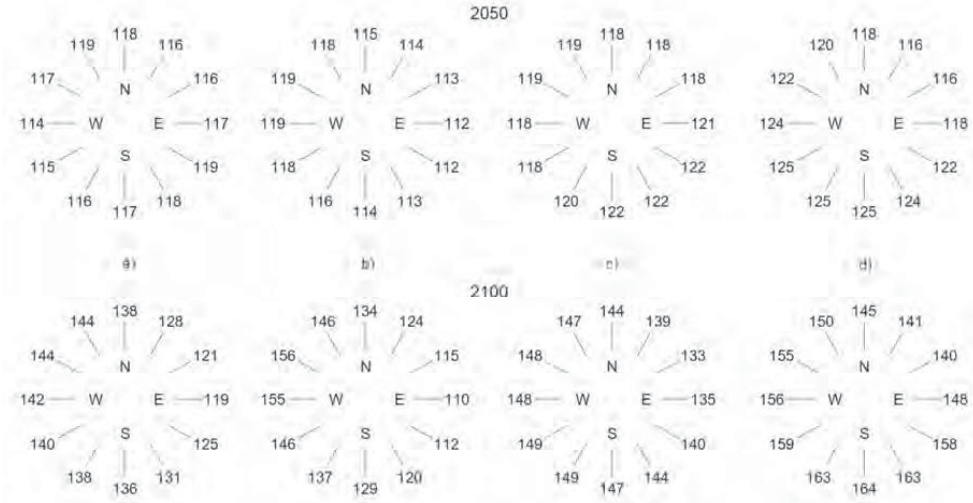

Figure 7 – Relative change of I_A *at 2050 and 2100 projected climate compared to the present climate from different wind directions at a) coastal area, b) southern Finland, c) inland and d) Lapland.*

The I_A will increase on average 34% at coastal area, 31% at southern Finland, at inland 44% and at Lapland 54% by the end of the century. At the same time the amount of precipitation increases 34%, 33%, 47% and 58%, respectively, which indicates that the wind speed during the rain events is not increasing significantly at any location. At coastal area and southern Finland, the increase of I_A concentrates southern, western and northern winds. At inland and Lapland, the I_A will increase quite evenly from all direction. As a result, south-west, south and south-east facing facades will face the most of the raining events still at future climate.

The study showed that the height of the building does not have significant impact on the amount of the Wall annual index (I_{WA}), see equation 1. At the top 2.5 m of 8-storey building an increase of the I_{WA} compared to 4-storey building is 19%. At the lower parts of the facades the I_{WA} is in practice the same.

The figures 8, 9, 10 and 11 present the I_{WA} on facades at typical Finnish suburban surroundings. The figure 8 presents the effect of variable locations on the I_{WA} on southern facades. As can be seen, at the most stressed point at the top corner of façade at Lapland, the I_{WA} level is almost at the same level (23 mm) as it is at the least stressed point at coastal area (15 mm). At coastal area, southern Finland and inland the most stressed points are facing annually WDR 70 mm, 52 mm and 34 mm, respectively. The figures also show that the lower parts of facades at inland and Lapland will face less than 10 mm of WDR annually.

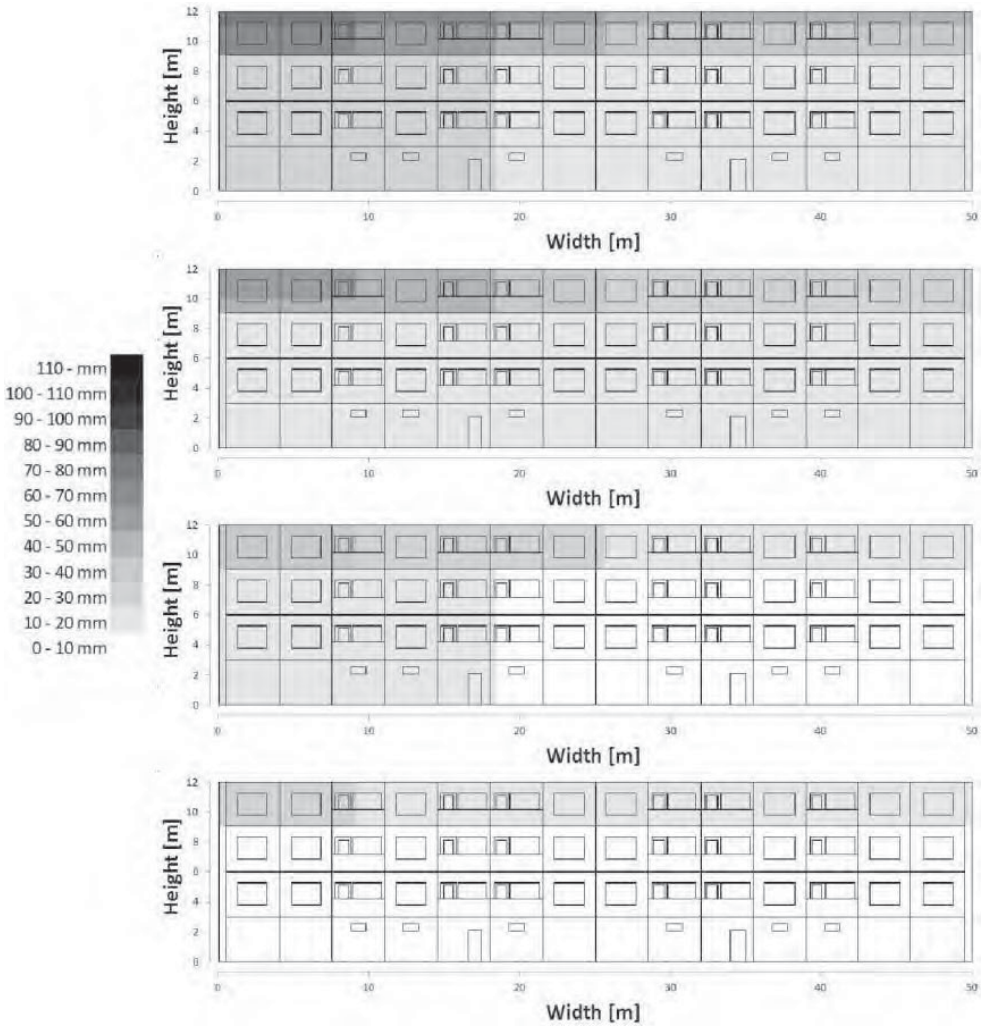

Figure 8 – The I_{WA} *on southern facades at current climate at coastal area, southern Finland, inland and Lapland.*

The figure 9 presents the effect of variable climate projections on the I_{WA}. As can be seen, at the most stressed point at the top corner of façade the I_{WA} is increasing while at the other parts of the façade the increase of the I_{WA} is not equally notable. The increase at the top part of the façade is 15 to 25 mm reaching maximum value of 95 mm while at lower parts the increase is 5 to 10 mm.

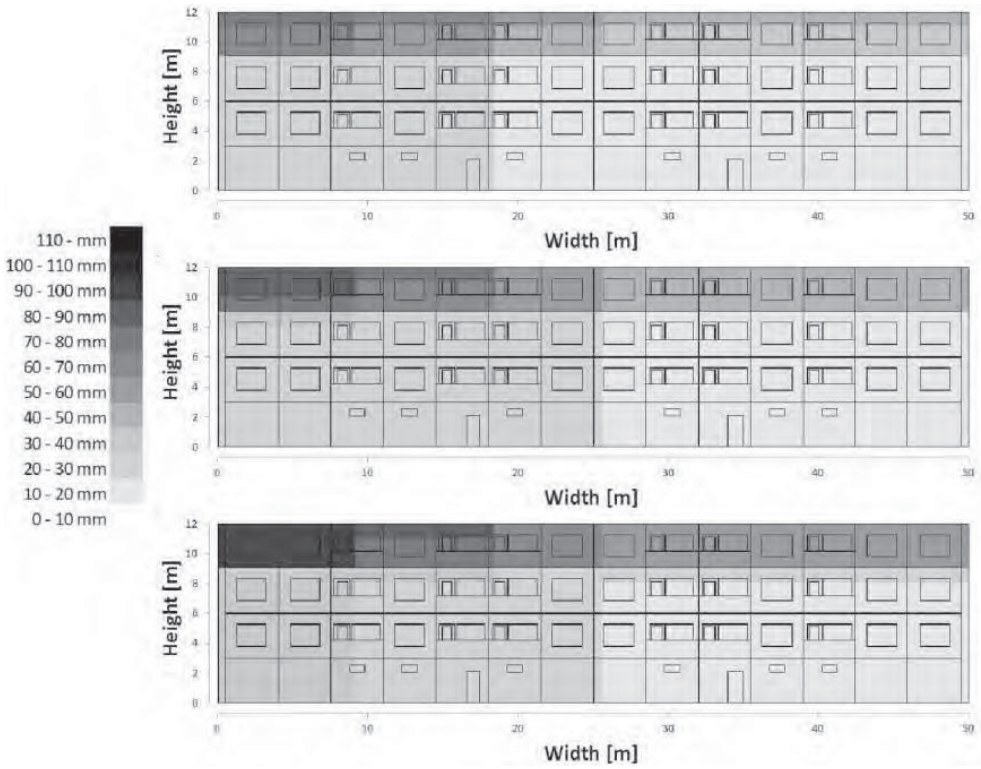

Figure 9 – The I_{WA} *on southern facades at coastal area at present, 2050 and 2100 climates.*

The figures 10 and 11 presents the effect of variable façade orientations on the I_{WA} at present and 2100 climates, respectively, at coastal area. As can be seen, even at coastal area the I_{WA} is at present almost negligible at lower parts of the northern façade and also most of the eastern and western facades. Still at 2100 the lower parts of the northern and eastern façades will face very small amounts of wind-driven rain. At the most stressed parts, i.e. at the top corners of all the facades, the I_{WA} stress level will increase quite evenly in the future climates.

At all studied climate projections the I_{WA} on the southern façade at Lapland and eastern and western facades at inland are quite similar to the northern façade at coastal area.

If the studied suburban area is thought to be by the sea or at lake shore and thus the terrain category, see table 1, is lifted to the category *I*, the increase of the I_{WA} is 48% at the top part of the façade, 57% at 8 metres from the ground and 25% at the lower parts of the facade.

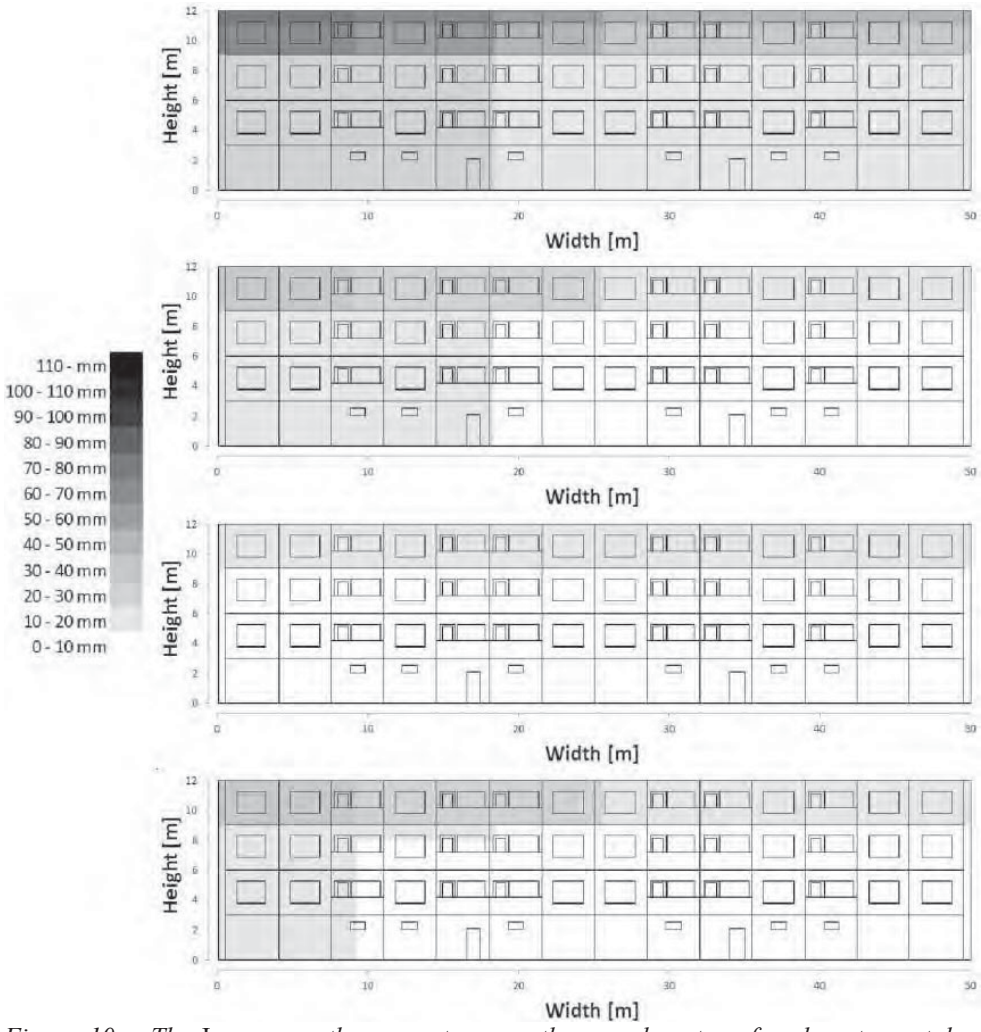

Figure 10 – The I_{WA} *on southern, western, northern and eastern facades at coastal area at present climate.*

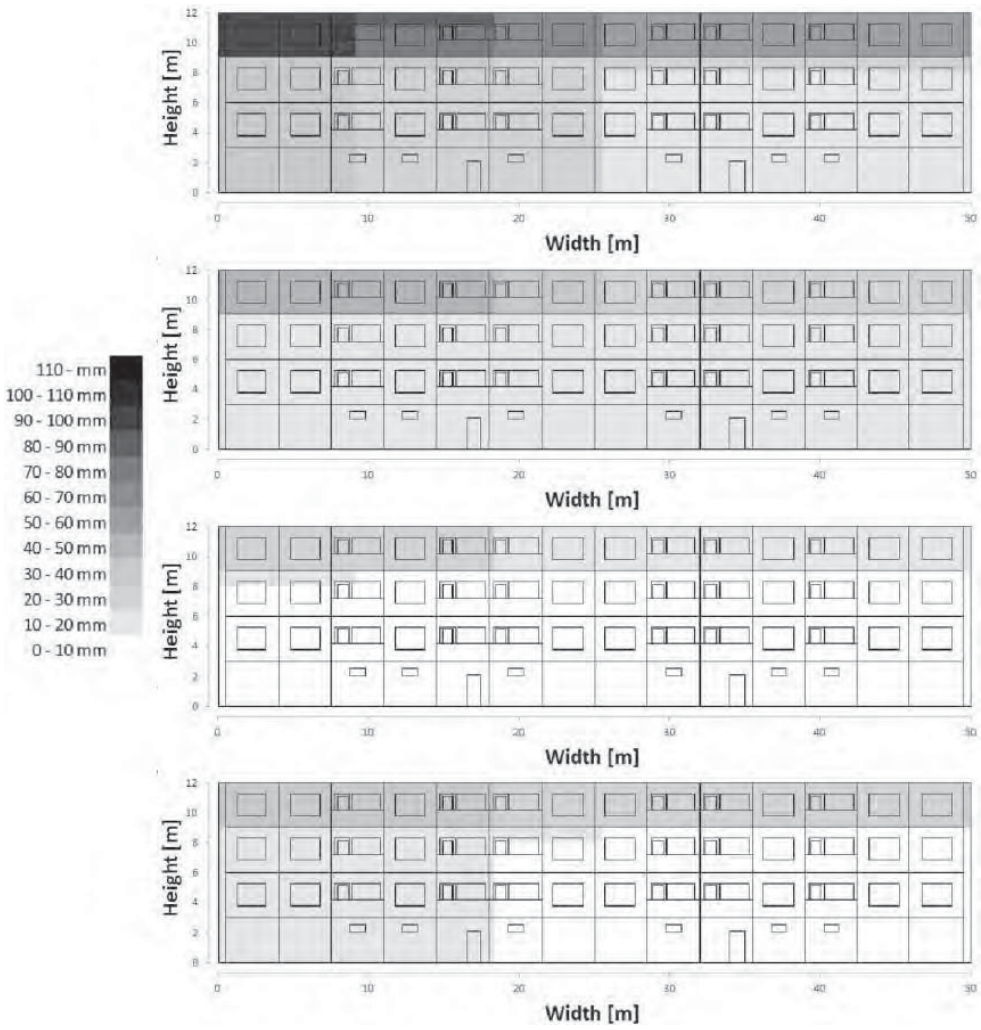

Figure 11 – The I_{WA} *on southern, western, northern and eastern facades at coastal area at 2100 climate.*

6 CONCLUSIONS

Wind-driven rain (WDR) has been noted to have a major effect on most of deterioration mechanisms of outdoor concrete structures. This study focused on determining the effect of location and climate change on the amount of the WDR on concrete façades at Finland. The calculations were based on the factors the Airfield annual index I_A and the Wall annual index I_{WA} presented at the standard SFS-EN ISO 15927 [25] at four different locations: coastal area, southern Finland, inland and Lapland. However, it should be noted that a substantial part of the Finnish building stock is located at coastal and southern Finland areas.

In Finland a direction of the WDR is highly orientated at southern wind directions depending only slightly on the location. However, a magnitude of the I_A and its dependence of the wind direction are highly connected to the location. The I_A at coastal area is 24% higher than at

southern Finland, 64% higher when compared to inland and 135% higher when compared to Lapland. At the same time the I_A is at coastal area is 354% higher from south than north while e.g. at Lapland the difference is 148%. The difference of amount of precipitation at different locations is not significantly differing but the higher wind speed during rain events causes considerable higher I_A at coastal area.

Based on the future climate projections, the I_A will increase significantly at every location and from every direction. At coastal area and southern Finland, the increase is the highest from already highly stressed directions from west to south. At inland and Lapland, the increase is quite even from every direction. By the end of the century, increase will be 34% at coastal area, 31% at southern Finland, 44% at inland and 54% at Lapland.

In addition to the I_A, the I_{WA} which takes into account also e.g. the surrounding terrain, topography and obstacles. When studying a type of a typical Finnish suburban multi-storey residential building at quite sheltered location, the I_{WA} is very low at northern facades at every location. Evidently most stressed parts of the facades are the top corners of the southern facades where the I_{WA} can be over 10 times higher than at the northern facades.

The wall annual index is highly simplified simulation for assessing the WDR against building facades. However, it gives adequate results for e.g. comparing different locational effects on the amount of wind driven rain on facades. Compared to e.g. CFD modelling it underestimates the amount of wind driven rain near the top of the façade and near the edges of the building but overestimates the amount on the top 2.5 metres with high buildings and low rain intensity.

The aim of this research was to study the orientation and location dependence of WDR and the effect of climate change on the amount of WDR. The results will be used to consider what are the possible actions to take the WDR and its orientation dependence into account at design process and whether the possible changes should be taken into account on Finnish building codes, e.g. increasing need for sheltering or better material properties.

7 ACKNOWLEDGEMENTS

The authors would like to thank the researchers at the Finnish Meteorological Institute for preparing the future climate projections.

REFERENCES

1. OSF, Official Statistics of Finland: www.tilastokeskus.fi (in Finnish), Reference date May 2nd 2016.
2. Lahdensivu, J., Varjonen, S and Köliö, A.: “Repair Strategies of Concrete Facades and Balconies” (in Finnish), Research report 148, Tampere University of Technology, Department of Civil Engineering, 2010.
3. Lahdensivu, J.: “Durability Properties and Actual Deterioration of Finnish Facades and Balconies”, Tampere University of Technology, Faculty of Built Environment, Tampere, Publication 1028, 2012, 117 p. 37 app.
4. Pakkala, T.A., Köliö, A., Lahdensivu, J. and Kiviste, M.: ”Durability demands related to frost attack for Finnish concrete buildings in changing climate”, *Building and Environment*, 82, (2014), Pp. 27–41.

5. Lahdensivu, J., Tietäväinen, H. and Pirinen, P.: ”Durability properties and deterioration of concrete facades made of insufficient frost resistant concrete”, *Nordic Concrete Research,* Publication no. 44, 2011, Pp. 175-188.
6. Köliö, A., Pakkala, T.A., Lahdensivu, J. and Kiviste, M.: “Durability demands related to carbonation induced corrosion for Finnish concrete buildings in changing climate”, *Engineering Structures* 62-63 (2014), Pp. 42–52.
7. Seppänen, M. and Koivu, T. (editors): ”BES – Development of open concrete element system” (in Finnish), Research report, Suomen Betoniteollisuuden Keskusjärjestö ry, 1970, 88 p.
8. Blocken, B. and Carmeliet, J.: “A review of wind-driven rain research in building science”, *Journal of Wind Engineering and Industrial Aerodynamics*, Volume 92, Issue 13 (2004), Pp. 1079–1130.
9. Jerling, A. and Schechninger, B.: “Fogars beständighet. Byggforskningrådet” (in Swedish), Rapport R89:1083, Stockholm, 1983, 172 p.
10. Lahdensivu, J., Mäkelä, H. and Pirinen, P.: ”Durability properties and deterioration of concrete balconies of inadequate frost resistance”, *International Journal of Sustainable Building Technology and Urban Development*, 4:2 (2013), Pp. 160–169.
11. Blocken, B. and Carmeliet, J.: “High-resolution wind-driven rain measurements on a low-rise building – experimental data for model development and model validation”, *Journal of Wind Engineering and Industrial Aerodynamics*, Volume 93, Issue 12 (2005), Pp. 905–928.
12. Lacy, R.E. and Shellard, H.C.: “An index of driving rain”, *Meteorological Magazine 91*, 1962, Pp. 177–184.
13. Rydock, J.P., Lisø, K.R., Førland, E.J., Nore, K. and Thue, J.V.: “A driving rain exposure index for Norway”, *Building and Environment* 40 (11), 2005, Pp. 1450–1458.
14. Rydock, J.P.: “A framework for using a present weather observation method to calculate a driving rain wall factor at any location”, *Building and Environment* 42 (2007), Pp. 1229–1235.
15. Pérez, J.M., Domínguez, B., del Coz, J.J. and Cano, E.: “Optimised method for estimating directional driving rain from synoptic observation data”, *Journal of Wind Engineering and Industrial Aerodynamics*, Volume 113, 2013, Pp. 1–11.
16. Choi, E.C.C.: “Parameters affecting the intensity of wind driven rain on the front face of a building”, *Journal of Wind Engineering and Industrial Aerodynamics*, Volume 53, 1994, Pp. 1–17.
17. Künzel, H.M.: “Bestimmung der Schlagregenbelastung von Fassadenfläschen” (in German), IBP Mitteilung 21, Nr. 263, 1994, Fraunhofer Institute für Bauphysik.
18. Karagiozis, A., Hadjisophocleous, G. and Cao, S.: “Wind driven rain distributions on two buildings”, *Journal of Wind Engineering and Industrial Aerodynamics*, Volume 67 and 68, 1997, Pp. 559–572.
19. Choi, E.C.C.: “Wind driven rain on building faces and the driving-rain index”, *Journal of Wind Engineering and Industrial Aerodynamics*, Volume 79, 1999, Pp. 105–122.
20. van Mook, F.J.R.: “Driving Rain on Building Envelopes”, Eindhoven University of Technology, Eindhoven, the Netherlands, PhD Thesis, 2003, 198 p.
21. Nore, K., Blocken, B., Jelle, B.P., Thue, J.V. and Carmeliet, J.: “A data set of wind driven rain measurements on low-rise test building in Norway”, *Building and Environment* 42 (2007), Pp. 2150–2165.
22. Zhu, D., Mallidi, S.R. and Fazio, P.: “Quantitative driving rain exposure on vertical wall at various Canadian cities”, *Building and Environment* 30 (1995), Pp. 533–544.
23. Fazio, P., Mallidi, S.R. and Zhu, D.: “A quantitative study for the measurement of driving rain exposure in the Montreal region”, *Building and Environment* 30 (1995), Pp. 1–11.

24. Rydock, J.P.: “A look at driving rain intensities at five cities”, *Building and Environment* 41 (2006), Pp. 1860–1866.
25. SFS-EN ISO 15927-3:2009: “Hygrothermal performance of buildings. Calculation and presentation of climatic data. Part 3: Calculation of a driving rain index for vertical surfaces from hourly wind and rain data”, Finnish Standards Association SFS, Helsinki.
26. Blocken, B. and Carmeliet, J.: “Overview of three state-of-the-art wind-driven rain assessment models and comparison based on model theory”, *Building and Environment*, Volume 45 (2010), Pp. 691–703.
27. Blocken, B., Dezsö, G., van Beeck, J. and Carmeliet, J.: “Comparison of calculation models for wind-driven rain deposition on building facades”, *Atmospheric Environment*, Volume 44 (2010). Pp. 1714–1725.
28. Jylhä, K., Ruosteenoja, K., Räisänen, J., Venäläinen, A., Tuomenvirta, H., Ruokolainen, L., Saku, S., Seitola, T.: ”The changing climate in Finland: estimates for adaption studies. ACCLIM project report 2009” (in Finnish, extended English abstract), Finnish Meteorological Institute, Reports 2009:4, Helsinki. 78 p. 36 app.
29. Vinha, J., Laukkarinen, A., Mäkitalo, M., Nurmi, S., Huttunen, P., Pakkanen, T., Kero, P., Manelius, E., Lahdensivu, J., Köliö, A., Lähdesmäki, K., Piironen, J., Kuhno, V., Pirinen, M., Aaltonen, A., Suonketo, J., Jokisalo, J., Teriö, O., Koskenvesa, A. and Palolahti, T.: ”Effects of Climate Change and Increasing of Thermal Insulation on Moisture Performance of Envelope Assemblies and Energy Consumption of Buildings” (in Finnish), Tampere University of Technology, Department of Civil Engineering, Research report 159, 2013, 354 p. + 43 app.
30. IPCC: “Climate Change 2007: The physical science basis. Contribution of Working Group I to the Fourth Assessment Report of the Intergovernmental Panel on Climate Change”. Cambridge University Press, Cambridge, U.K., 2007, 996 p.
31. Ruosteenoja, K., Jylhä, K., Mäkelä, H., Hyvönen, R., Pirinen, P. and Lehtonen, I.: “Weather data for building physics test years in the observed and projected future climate” (in Finnish), Reports No. 2013:1, Finnish Meteorological Institute, Helsinki, 2013, 36 p. 9 app.
32. Aaltonen, J., Hohti, H., Jylhä, K., Karvonen, T., Kilpeläinen, T., Koistinen, J., Kotro, J., Kuitunen, T., Ollila, M., Parvio, A., Pulkkinen, S., Silander, J., Tiihonen, T., Tuomenvirta, H. and Vajda, A.: ” Heavy rains and floods in urban areas” (in Finnish), Finnish Environment Institute 31/2008, Helsinki, 123 p.

IV

PREDICTED CORROSION RATE ON OUTDOOR EXPOSED CONCRETE STRUCTURES

by

Pakkala T.A., Köliö A., Lahdensivu J. & Pentti M. Feb 2019

International Journal of Building Pathology and Adaptation, Vol. 37 No. 5, pp. 679–698.

https://doi.org/10.1108/IJBPA-11-2018-0086

Predicted corrosion rate on outdoor exposed concrete structures

This is an Author accepted manuscript. The manuscript was accepted 6 February 2019 in International Journal of Building Pathology and Adaptation. Full version is available in: https://doi.org/10.1108/IJBPA-11-2018-0086

Toni A. Pakkala[a,b], Arto Köliö[a], Jukka Lahdensivu[a], Matti Pentti[a]

[a] *Tampere University, Civil Engineering, Tampere, Finland*

[b] *corresponding author: toni.pakkala@tuni.fi, tel. +358401981962*

Purpose

A significant part of Finnish concrete building stock is relatively young. Thus methods to adopt the existing building stock to climate change are needed. To plan and correctly timing service actions there is a need to study the rates of different deterioration mechanisms. The reinforcement corrosion in Finnish outdoor exposed concrete structures is almost solely carbonation-induced corrosion. In former studies, it has been shown that active corrosion phase can also have a major effect on the total service-life of the structure.

Design/methodology/approach

In this study, the effect of climate change on predicted corrosion rate of concrete reinforcement in projected 2050 and 2100 climates compared to present climate were studied to consider adaptation methods for the climate change. The calculations are based on a corrosion propagation model, which takes into account four different climatic factors: wind-driven rain, temperature, relative humidity and solar radiation.

Findings

A significantly higher corrosion rates and thus faster corrosion-induced damage can be expected in the future climate. The increase in corrosion rate is the highest

in the late autumn and winter because of the increasing amount of precipitation and weaker conditions for concrete structures to dry. In addition, the duration of high corrosion rate periods is increasing which may shorten the propagation phase. However, corrosion rate is highly dependent the direction of the greatest climate load and the grade of sheltering which can be taken into account in service life calculations and while planning service actions.

Research limitations/implications

There are different sources of error because of the uncertainties with both the used model and the climate change scenarios. That is why the results are discussed in more general way than comparing the actual numbers with each other.

Originality/value

The propagation model used in this study has not been used before in adaptation studies. The climate change effect on carbonation-induced corrosion has also been limited while the studies have focused on chloride-induced corrosion.

Keywords: concrete; reinforcement; corrosion; climate change; adaptation; service life

Acknowledgements

The authors would like to acknowledge the researchers at the Finnish Meteorological Institute for preparing the future climate projections as a part of the FRAME research project conducted at Tampere University of Technology in 2009–2012.

Introduction

Finnish building stock is relatively young. Almost 80% of all apartments in detached houses, row houses and apartment blocks are built after 1960. Private and public buildings built of concrete make up 34 % of the whole building stock in Finland of

which almost 40% is now 30-50 years old. (OSF, 2019). Because one third of the population lives in these aging apartment blocks, extending their service life by renovation and maintenance has been an increasing national concern. The maintenance and renovation have been a predominant method compared to demolition and re-building mainly because of the private ownership. (Huuhka, 2016) Thus, the significance of the adaptation to climate change of the existing building stock is increasing simultaneously with the aging of the buildings.

The field of adaptation studies is wide including both adaptation of the buildings and user adaptation to buildings as is presented in the state-of-art research by Heidrich et al. (2017). Many of the adaptation studies considering the buildings and their structures have concentrated mainly on building physical problems such as changes in energy need in cooling and warming of buildings and energy efficient performing of buildings (Gupta and Gregg, 2012; Li *et al.*, 2012; Nik *et al.* 2012; Williams *et al.* 2012, Wood and Muncaster, 2012; Botti and Ramos, 2017).

However, a fewer number of studies have focused on the effect of climate change on the outdoor exposed structures and the rate of their deterioration, especially in cold climates. Auld *et al.* (2006) presented extensive review of climate change effect on deterioration different structures and materials in Canada. In Norway Kvande and Lisø (2009) studied climate adapted design of masonry structure and Almås *et al.* (2011) climate change effect on wooden structures. When considering concrete structures, the main focus have been in possible changes both chloride and carbonation induced corrosion of the concrete reinforcement, however mostly in warm climate zones (e.g. Yoon *et al.*, 2007; Bastidas-Arteaga *et al.*, 2010; Stewart *et al.*, 2011; Stewart *et al.*, 2012; Bastidas-Arteaga and Stewart, 2015; Peng and Stewart, 2013; Peng and Stewart, 2014)

In Finnish climate conditions, the reinforcement corrosion in outdoor exposed concrete structures, such as facades and balconies, is almost solely carbonation-induced corrosion (Lahdensivu, 2012; Lahdensivu *et al.*, 2010). In his studies, Lahdensivu (2012) presented that the quality of construction, especially with prefabricated concrete sandwich panels built between 1960-80, has been low when considering possible service life of the structures. Compared to present knowledge, the requirements, for example, for concrete cover and freeze-thaw durability presented in Finnish Concrete Codes at the time were not sufficient for eligible service life. Although the requirements were tightened to almost the current level in 1989 and special attention was paid to durability properties, such aspects as the actual measured cover depths did not meet the requirements (Lahdensivu, 2012).

In recent studies (Lahdensivu, 2012; Pakkala *et al.*, 2014; Pakkala *et al.*, 2016) it has been shown that the deterioration rate of concrete structures exposed to the Finnish climate is highly dependent on geographical location and the direction in which the structure faces. The main factor affecting corrosion rate was the amount of wind-driven rain (WDR) on the structure. Pakkala *et al.* (2016) presented that the amount of WDR is significantly larger in coastal area than in inland ones and, in addition, the amount of WDR is significantly larger from westerly to south-easterly directions throughout Finland because of the concentrated wind directions during rain events. The studies based on actual condition assessment data (Lahdensivu, 2012; Pakkala *et al.*, 2014) have shown that the rate of different deterioration mechanisms has quite explicit correlation with the amounts of WDR. In addition, in his study Köliö *et al.* (2016b) presented that the level of corrosion rate was influenced by the geographical location and the direction in which the facade faced.

The effect of climate conditions on the deterioration rate of concrete structures, and in this context especially in Finnish concrete structures is studied quite extensively in current climate and in existing building stock as presented above. However, climate change studies are predicting major changes in the different climate factors which are known to have an effect on the deterioration rates. The Finnish Meteorological Institute (FMI) has predicted that during this century climate change will have a major impact e.g. on such things as temperature, cloudiness and the amount of WDR (Jylhä *et al.*, 2013). Annual average temperature is increasing, which has an effect on the amount of WDR because, during the winter, precipitation will be more in the form of rain than snow and sleet compared to the present climate. The relative humidity of outdoor air is increasing and solar radiation decreasing which, combined with increasing amount of precipitation, weakens the drying conditions of outdoor structures. The amount of precipitation is increasing, especially during autumn, winter and spring and, with a slight increase in wind speed during rain events, the amount of WDR is increasing significantly throughout Finland and from every direction (Pakkala *et al.*, 2016)

The effects of changing climate on freeze-thaw durability and initiation phase of the carbonation-induced corrosion on new construction have already been studied (Pakkala *et al.* 2014; Köliö *et al.* 2014b). In this study the focus is on estimating the effect of climate change on propagation phase of carbonation-induced corrosion. The objective of this study was to simulate the dependence of corrosion rate on varying climate conditions to which existing and already carbonated concrete facade panels and balcony structures are exposed. Different climatic factors are changing climate, geographical location and orientation of the facade.

Background

Corrosion in Finnish concrete facades and balconies

The corrosion of reinforcement in Finnish concrete facades and balconies is almost solely carbonation-induced (Lahdensivu, 2012), so the carbonation rate and thickness of the concrete cover are the main factors when considering the corrosion-dependent service life of those structures. The most vulnerable reinforcements for corrosion are the outer rebars of connecting trusses at facade panels and the rebars of the slab soffits and edge bars of the side panels (Pentti *et al.*, 1998; Pentti 1994). However, the most common reason for visible corrosion damage has been reinforcement misplaced close to the surface because of poor workmanship during prefabrication.

Lahdensivu (2012) presented an amount of visual damage and actual cover depths and carbonation rate at facade and balcony structures based on extensive condition assessment data from 947 concrete element buildings (Lahdensivu *et al.*, 2010) (see Table 1). The studies showed that visually observable reinforcement corrosion damage existed in 59% of the examined facades. The majority of damage was local (54% of facades and 66% of balconies) and extensive corrosion was found only in 5.7% of facades and 15% of balconies.

Table 1. The share of cover depths and carbonation coefficient of different façade surfaces and balcony structures (Lahdensivu, 2012).

Structure		Share by cover depth [%]					Carbonation coefficient, k [mm/a^{0,5}]		
		0…4 mm	5…9 mm	10…14 mm	15…19 mm	No.	Av.	Std. dev.	No.
Façade (edge bars)	Exposed aggregate	0.00	0.34	1.14	5.62	21,167	1.96	1.28	849
	Brushed painted	0.00	6.38	10.79	15.09	36,154	2.71	1.23	1,285
	Brick panel-clad	0.02	3.78	4.32	3.31	9,759	1.47	2.20	427
	White concrete	0.00	0.00	1.61	15.28	2,193	0.61	0.92	58
Balcony	Side panel (outer surf.)	0.06	3.84	5.47	15.10	32,540	2.61	1.52	901
	Slab (soffit)	0.04	3.69	5.65	14.41	42,628	3.08	1.40	884
	Parapet (outer surf.)	0.01	7.53	10.01	20.59	18,665	2.06	1.45	719

The carbonation rate of concrete varies greatly according to the properties of concrete and, naturally, the surface finishing. In a recent research paper by Köliö *et al.* (2016a), it was found by follow-up measurements that the carbonation of already aged concrete buildings in general follow the square root model quite accurately. The k-value

from Table 1 is used in Fig. 1 to present the correlation between carbonation depth and time in different studied surface structures.

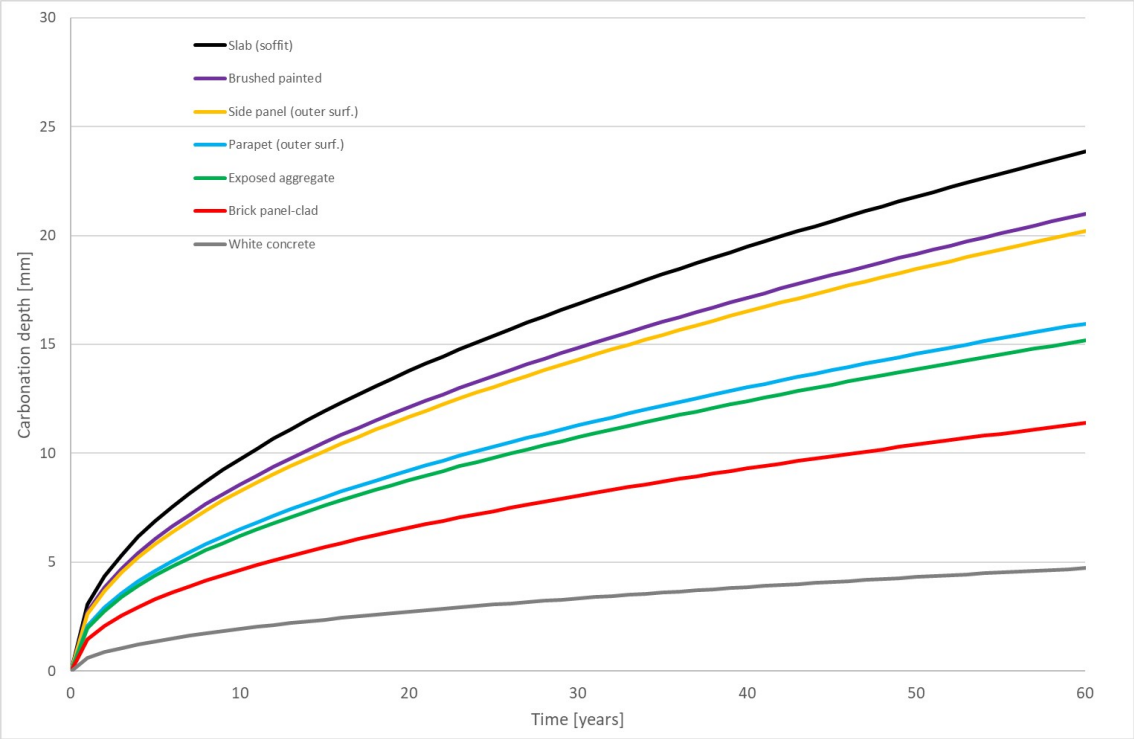

Figure 1. Average carbonation depth of concrete according to surface finishing or structure (reproduced from Lahdensivu, 2012 with permission from author).

Visible corrosion damage in facades and balcony structures is rather unusual if the cover depth is at the level required in Finnish concrete codes (25 mm) or the structure is sheltered from the rain even if the carbonation of concrete reaches the reinforcement due to the relatively small diameter of the reinforcement used (3-8 mm). There is evidence that the risk of cracking of the concrete due to corrosion is elevated when the ratio of cover depth to diameter is below approximately 1.5 (Köliö *et al.*, 2015; Hunkeler and Lammar, 2012). This relates to cover depths of 4.5-12 mm.

Modelling the corrosion of reinforcement

Universally, corrosion of concrete reinforcement is considered as a phenomenon with two consecutive phases of corrosion initiation and propagation (Tuutti 1982). The focus of this paper is set to the propagation phase where corrosion has already initiated via the carbonation of the surrounding concrete. Corrosion propagation models can be categorized into (i) empirical, (ii) numerical or (iii) analytical approaches (Otieno *et al.*, 2011). The empirical models are based on the experimentally achieved relationship between the degree of corrosion and the controlling parameters (e.g. DuraCrete, 2000) while numerical models rely on complex computation (FEM, BEM) (e.g. Gulikers and Raupach, 2006). In general, analytical models approach the problem from analytical mathematics often based on geometry such as the 'thick-walled cylinder' approach (e.g. Goltermann, 1994). Traditionally, corrosion propagation is modelled by modifying corrosion rate with the diameter of the reinforcement and the thickness of the concrete cover (Siemes *et al.*, 1985). The corrosion rate itself is related to the wetness and temperature of the structure, and this can be modelled by, for example, measuring the potential electrolytical resistivity of the concrete (DuraCrete, 2000).

Past advances in corrosion modelling have mainly concerned chloride-induced reinforcement corrosion, which has resulted in sophisticated ingress models in model codes (DuraCrete, 2000; fib34, 2006). Recent research has focused on modern mathematical modelling (Concha and Oreta, 2018) while less attention has been paid to carbonation induced corrosion. The effects of climate change on carbonation or carbonation induced corrosion has been studied based on model codes (DuraCrete, 2000) which take into account CO2 levels, temperature and relative humidity in Australia (Stewart *et al.*, 2011), Finland (Köliö *et al.*, 2014b) and Canada (Talukdar *et al.*, 2012). These studies, however, neglect wind-driven rain due to the limitations of the degradation models. Revert *et al.* (2018) have recently confirmed that the variability in

carbonation depth and partial carbonation has a major impact on the onset of reinforcement corrosion by carbonation.

Köliö (2016) presented a corrosion propagation model for carbonation-induced corrosion for concrete facades exposed to the Finnish climate. He studied the actual and modelled carbonation propagation during the initiation and active phases and also validation of the known models (Köliö, 2016; Köliö et al. 2014a; Köliö et al., 2014b; Köliö et al., 2015; Köliö et al., 2016a). In a study (Köliö et al., 2016b), measured long-term corrosion rate data was combined with actual climate data at different geographical locations to explore the individual and combined effect of weather parameters on the rate of reinforcement corrosion on already-carbonated concrete facade and balcony structures. Based on the studies, he presented a service life design model to correlate the critical weather parameters directly with corrosion rate inside the mentioned structures.

The service life design model presented by Köliö *et al.* (2016b) is based on a regression analysis of time series data on both the environmental conditions and field measurements of the corrosion rate of facade panels and balcony structures at two geographical locations (coastal area and southern Finland) in Finland. The study concluded that the scatter in the active corrosion rate in outdoor concrete structures could be explained by on-site weather parameters, especially by WDR. Model simulations conducted with 30-year current climate data showed that, despite the high temporal scatter due to weather changes, the long-term scale corrosion rate was relatively steady. The level of corrosion rate was influenced by the geographical location and the direction in which the facade faced (Köliö *et al.*, 2016b). For average critical corrosion penetration of 67.5 μm determined for this structure type (Köliö *et al.,* 2015), the length of the propagation phase differed from 2.0 years (south-facing balcony side panel in southern coastal Finland) to 8.0 years (north-facing facade in northern

Finland). With structures sheltered from WDR such as balcony slab soffits, the length of the phase was from 79.8 years in southern coastal Finland to 200 years in northern Finland.

Finnish climate

Finland can be geographically divided in four areas (coastal, southern Finland, inland and Lapland) based on the climate conditions and distribution of the building stock as presented by Pakkala *et al.* (2014), see Fig. 2. The same division is used in this research.

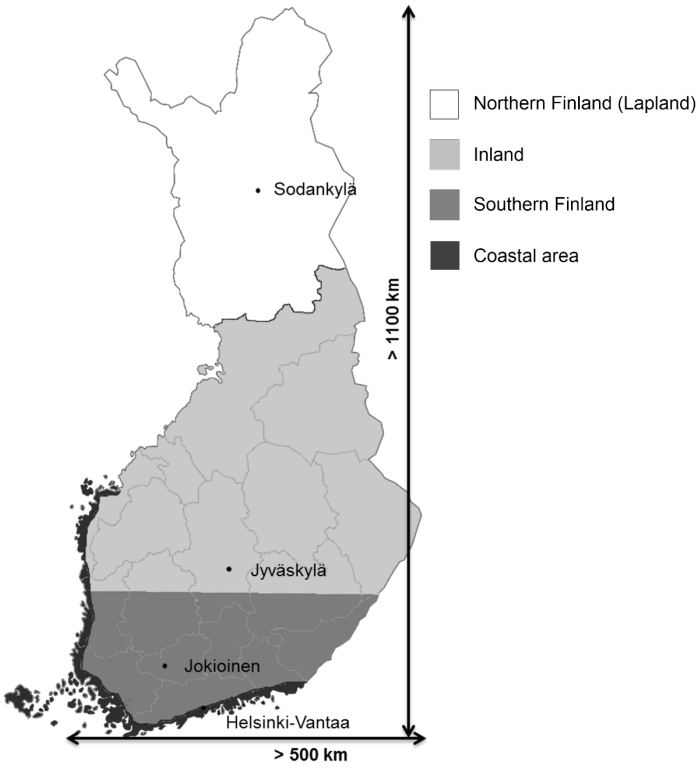

Figure 2. Finland can be divided into four main areas based on climate and concentrations of population. Reprinted from Building and Environment, Volume 82, Pakkala, T. A., Köliö, A., Lahdensivu, J. and Kiviste, M. Durability demands related to frost attack for Finnish concrete buildings in changing climate, Page 34, Copyright (2014), with permission from Elsevier.

In Finland, a direction of WDR is highly orientated towards the south depending only slightly on the location. However, the magnitude of WDR and its dependence of wind direction are highly connected to the location. Pakkala *et al.* (2016) presented that the Annual airfield index IA, excluding snow, is 24% higher in coastal area than at southern Finland, 64% higher compared to inland and 135% higher compared to Lapland. At the same time the IA in coastal area is 354% higher from the south than the north while, compared to Lapland for example, the difference is 148%. The difference in the amount of precipitation at different locations is not significantly wind direction-dependent but higher wind speed during rain events causes much higher IA in coastal area.

Because Finland is long country, approx. 1,100 km when latitudes are considered, the difference in temperatures is significant, especially in winter when comparing southern parts to northern parts of the country. In coastal area, southern Finland, inland and Lapland, the lowest monthly average temperatures are -5.7 °C (Feb.), -6.3 °C (Feb.), -8.5 °C (Feb.) and -13.6 °C (Jan.), respectively. In summer, the highest monthly average temperatures are 17.5 °C, 16.5 °C, 16.3 °C and 14.5 °C, respectively.

The changes in relative humidity are not significantly dependent on geographical location. Relative humidity is at its highest in late autumn and, in November for example, varies from 88.1% (Lapland) to 91.1% (inland). Relative humidity is at its lowest in late spring and, in May for example, from 64.2 (coastal area) to 66.9 (Lapland).

The amount of solar radiation is significantly dependent on both the orientation of the studied surface and the geographical location. In winter, solar radiation is very low at every geographical location, especially in Lapland where the sun stays below the

horizon. On the other hand, in summer the sun stays over the horizon for long periods, although the amount of solar radiation is not that great because the sun stays quite low over the horizon compared to more southerly locations.

Climate change

The climate change projections used in this study, were originally presented at REFI-B project by the Finnish Meteorological Institute (FMI) (Jylhä *et al.*, 2013). The projections are based on IPCC (2007) scenarios for the evolution of greenhouse gas and aerosol particle emissions. The projections are based on an average of 19 different models all based on greenhouse gas emission scenario A2, which assumes that the greenhouse gases are increasing significantly.

Based on the projections, in Finland the average temperature will increase ca. 2.1 to 2.7 °C until 2050 and 5 to 6.4 °C until 2100 depending on location. The amount of precipitation will increase significantly at every location and from every direction (Jylhä et al., 2013). In coastal area and southern Finland, the increase is the highest in the already highly stressed direction of west to south. Inland and in Lapland, the increase is quite even from every direction. By the end of the century, the increase will be 34% in coastal area, 31% in southern Finland, 44% inland and 54% in Lapland (Pakkala *et al.*, 2016).

Relative humidity will increase, especially in winter, until at the end of the century. The average increase in winter will be 3-8% depending on the location. In summer, relative humidity will remain at the same level except in southern Finland where it will decrease slightly. At the same time, total solar radiation will decrease by 20% in winter. However, the amount of radiation will be very low in winter, so the decrease is not significant. In summer, it will remain at the same level and in autumn even increase slightly (Jylhä *et al.*, 2013).

Research methods and material

Climate data

The FMI has extensive at least daily collected weather data since 1961 in digital form from several meteorological stations covering all of Finland. The data consists of temperature, relative humidity, rain intensity, wind speed and direction, solar radiation variables, etc. In the REFI-B project (Jylhä et al., 2013), the FMI also forecast the climates of the four regions (coastal area, southern Finland, inland, Lapland) in three 30 year periods (2030, 2050 and 2100).

In this study, three 30 year climate periods at four geographical locations (see Fig. 2) are used:

- present: collected weather data 1980–2009
- 2050: projected weather data 2035–2064
- 2100: projected weather data 2085-2114

Service-life modelling of carbonation-induced corrosion

Corrosion rates were simulated using a formerly generated model (Köliö *et al.*, 2016b) which relates the corrosion rate of reinforcement inside carbonated concrete to the weather exposure of the structure. The model is based on a multi-linear regression model based on the time-series analysis of long-term corrosion rate measurements and weather data. The corrosion rate was measured in façade panels and balcony structures at two geographical locations: coastal area and southern Finland. The regression equation and coefficients were determined by fitting the data with least squares method. Weather parameters taken into account are ambient temperature, ambient relative humidity, wind-driven rain and solar radiation. The background and the validation of

the model is introduced in detail in Köliö *et al.* (2016b).

The best performing combinations were judged by the coefficient of determination (R2) of the model from a relatively large number of analyses (525 analyses with different combinations of weather parameters, seasons, etc.). In cross-checking the models' functionality (using the coastal area model inland and vice versa), the models were found to have a fairly good fit (R2 of 0.49–0.53). Finally, a composite model was produced utilizing the spring, autumn and winter seasons from the inland data and the summer season from the coastal data, allowing a slightly better fit for both geographical locations (the R2 for inland was 0.71 and for the coastal area, 0.55) (Köliö, 2016).

Climate data representing future climate in 2050 and 2100 was formulated for the simulations. Climate was assumed to evolve by the IPCC (2007) scenario A2, which can be considered the "worst-case scenario". Also, comprehensive data on the current climate was prepared for comparison of the results. The weather data sets consisted of time series with 3-hour time resolution of air temperature (T), air relative humidity (RH), wind-driven rain (WDR) and solar radiation (RAD) at four geographical locations in Finland in facades facing in eight different directions. The factors for the multiple linear regression of weather exposure to corrosion rate are presented in table 2.

Table 2. The factors for the multiple linear regression of weather exposure to corrosion rate.

Season	Parameter	Coefficient, facades	Coefficient, balcony frames	Coefficient, balcony slab soffits
Spring	β_1, (T)	-	-	-0.0028
	β_2, (RH)	-	-	-0.0019
	β_3, (I_{WA})	0.0348	0.1260	0.0088
	β_4, (RAD)	-0.0008	-0.0007	
	β_0 (intercept)	1.9127	2.0909	0.1597
Summer	β_1, (T)	-	-	-0.0009
	β_2, (RH)	0.0107	0.0650	-0.0002
	β_3, (I_{WA})	0.0369	0.0470	-0.0006
	β_4, (RAD)	-0.0006	-0.0007	
	β_0 (intercept)	0.5620	-2.7485	0.0557
Autumn	β_1, (T)	-	-	0.0013
	β_2, (RH)	-	-	0.0012
	β_3, (I_{WA})	0.0842	0.1219	0.0008
	β_4, (RAD)	-	-	
	β_0 (intercept)	0.1121	0.4723	-0.0887
Winter	β_1, (T)	0.0682	0.1014	0.0017
	β_2, (RH)	-	-	0.0065
	β_3, (I_{WA})	0.1340	0.2349	0.0088
	β_4, (RAD)	-	-	
	β_0 (intercept)	0.8572	1.4196	-0.5239

Results and discussion

As mentioned in Research Method and Materials Section, calculations have been made for a large number of cases. In this Section, only selected results are presented to give an overview of the results focusing on differences between:

- geographical locations
- present climate and projected future climate data
- directions in which facades and balconies face.

Table 3 presents the average corrosion rates in carbonated facade concrete at all four studied locations, in directions of the cardinal points and collated as four seasons.

Winter consist of the months January, February and December, spring March, April and May, summer June, July and August and autumn September, October and November. Colour highlights are used to classify values as follows: red as very high (≥ 3.00 µA/cm²), orange as high (2.00-2.99 µA/cm²), green as moderate (1.00-1.99 µA/cm²) and blue as low (< 1.00 µA/cm²) corrosion rate values.

Table 3. An average of the modelled corrosion rate [µA/cm²] of façade reinforcement in four geographical locations (C = coastal, S = southern Finland, I = inland, L = Lapland) at present climate and in projected future climates.

		North			East			South			West		
		Present	2050	2100	Present	2050	2100	Present	2050	2100	Present	2050	2100
Winter	C	1.24	1.32	1.72	1.44	1.94	2.48	2.42	4.02	5.28	1.73	2.23	2.85
	S	1.00	1.25	1.60	1.10	1.44	1.88	2.07	2.81	3.70	1.63	2.03	2.69
	I	0.87	1.15	1.55	0.94	1.41	1.98	1.29	2.01	2.96	1.04	1.39	1.88
	L	0.62	0.84	1.21	0.59	0.90	1.39	0.67	1.22	2.02	0.65	0.95	1.38
Spring	C	1.90	1.84	1.88	1.84	1.97	2.00	2.10	2.14	2.18	1.93	1.75	1.80
	S	1.89	1.84	1.87	1.81	1.91	1.93	2.02	2.04	2.07	1.87	1.73	1.77
	I	1.87	1.85	1.92	1.66	1.80	1.83	1.89	1.91	1.79	1.86	1.72	1.78
	L	1.79	1.83	1.91	1.66	1.82	1.91	1.79	1.84	1.90	1.70	1.60	1.66
Summer	C	1.50	1.47	1.48	1.62	1.67	1.56	2.29	2.35	2.38	1.64	1.60	1.77
	S	1.40	1.37	1.39	1.50	1.52	1.39	2.10	2.12	2.12	1.62	1.60	1.81
	I	1.44	1.42	1.44	1.45	1.50	1.42	1.78	1.81	1.83	1.45	1.39	1.49
	L	1.31	1.32	1.35	1.34	1.39	1.39	1.60	1.61	1.66	1.26	1.19	1.24
Autumn	C	0.71	0.98	1.28	1.64	2.12	2.13	4.31	5.23	6.30	1.84	2.19	2.92
	S	0.62	0.84	1.05	1.11	1.38	1.39	2.72	3.30	3.84	1.51	1.93	2.68
	I	0.53	0.83	1.22	0.90	1.27	1.59	1.60	2.20	2.93	0.77	1.09	1.56
	L	0.25	0.46	0.81	0.41	0.71	1.11	0.81	1.27	1.97	0.34	0.59	0.92

For more visual view, the Figs. 3-6 present the monthly averages of the modelled corrosion rates in carbonated concrete on south-facing facades at all four studied locations. Figs. 7 and 8 present the same on north-facing facades at coastal area and Lapland.

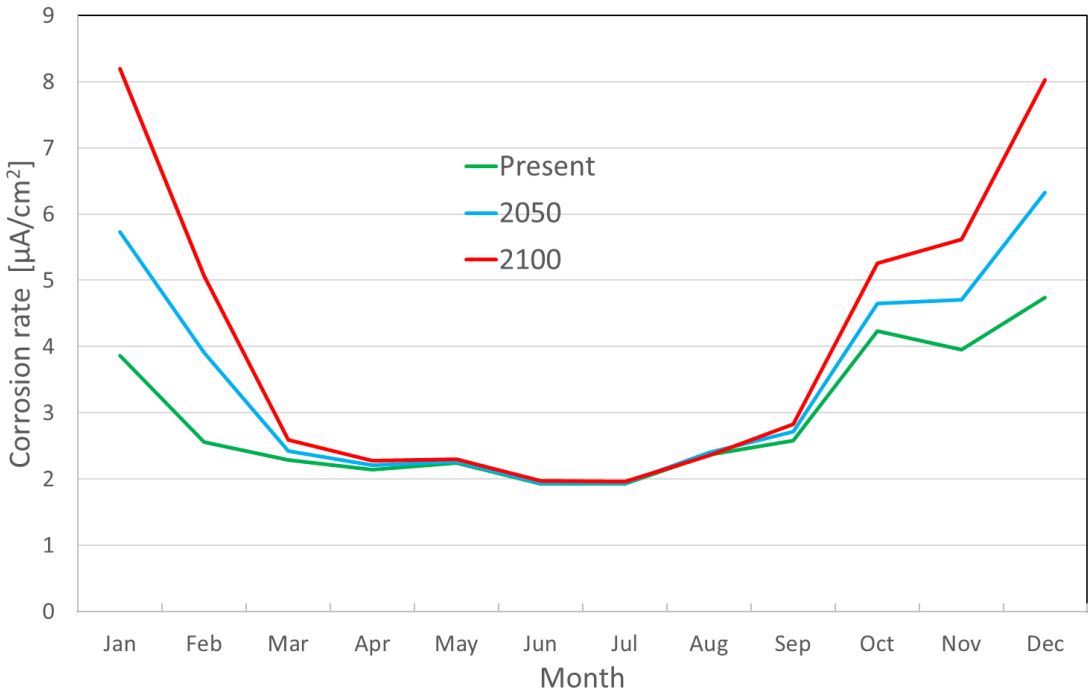

Figure 3. Monthly average of the modelled corrosion rate in carbonated concrete at coastal area on south-facing façade.

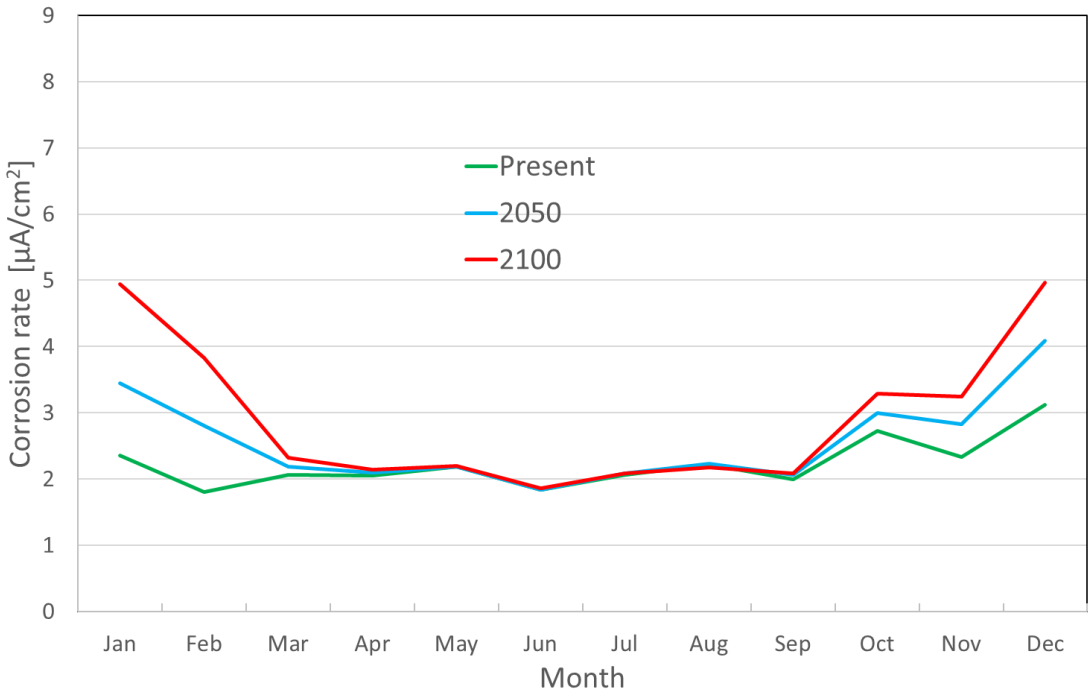

Figure 4. Monthly average of the modelled corrosion rate in carbonated concrete at southern Finland on south-facing façade.

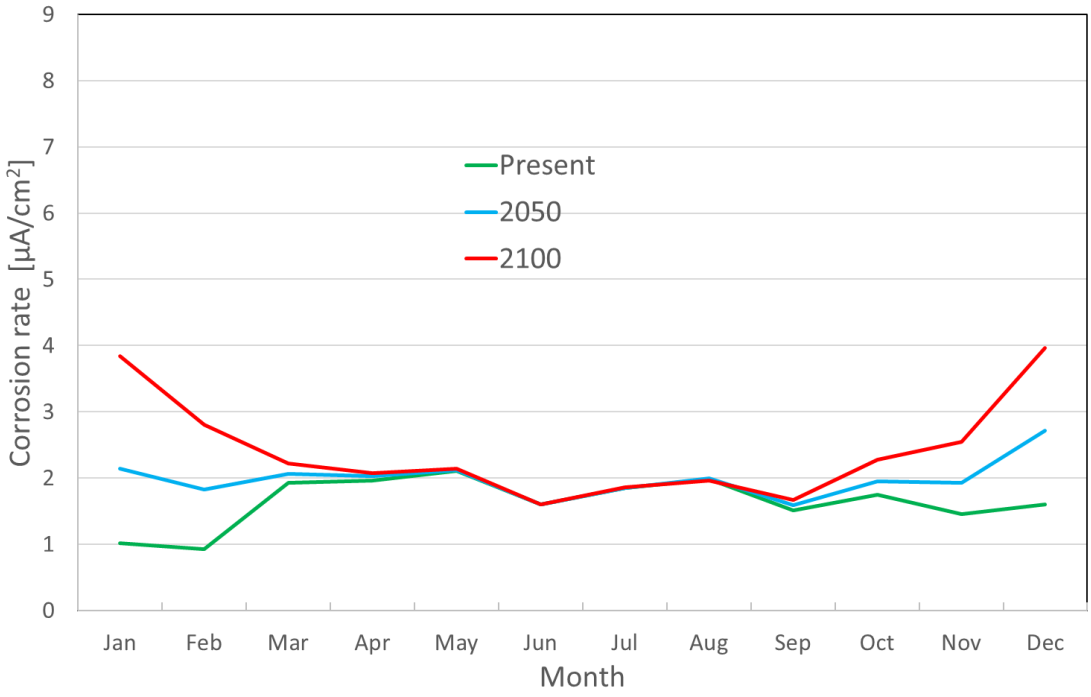

Figure 5. Monthly average of the modelled corrosion rate in carbonated concrete at inland on south-facing façade.

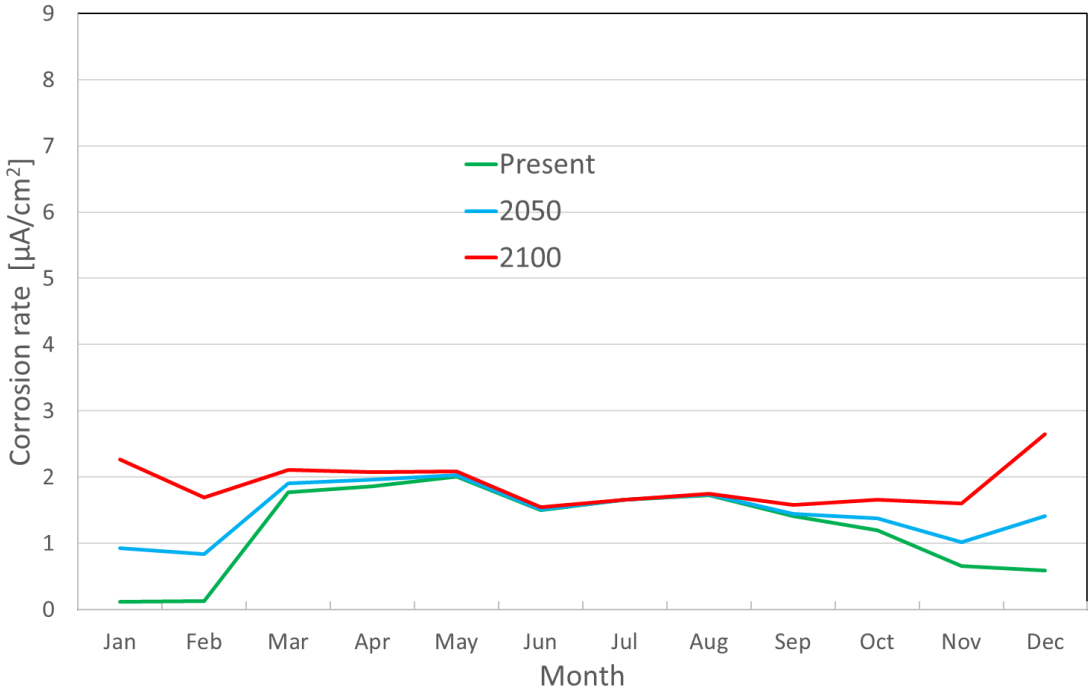

Figure 6. Monthly average of the modelled corrosion rate in carbonated concrete at Lapland on south-facing façade.

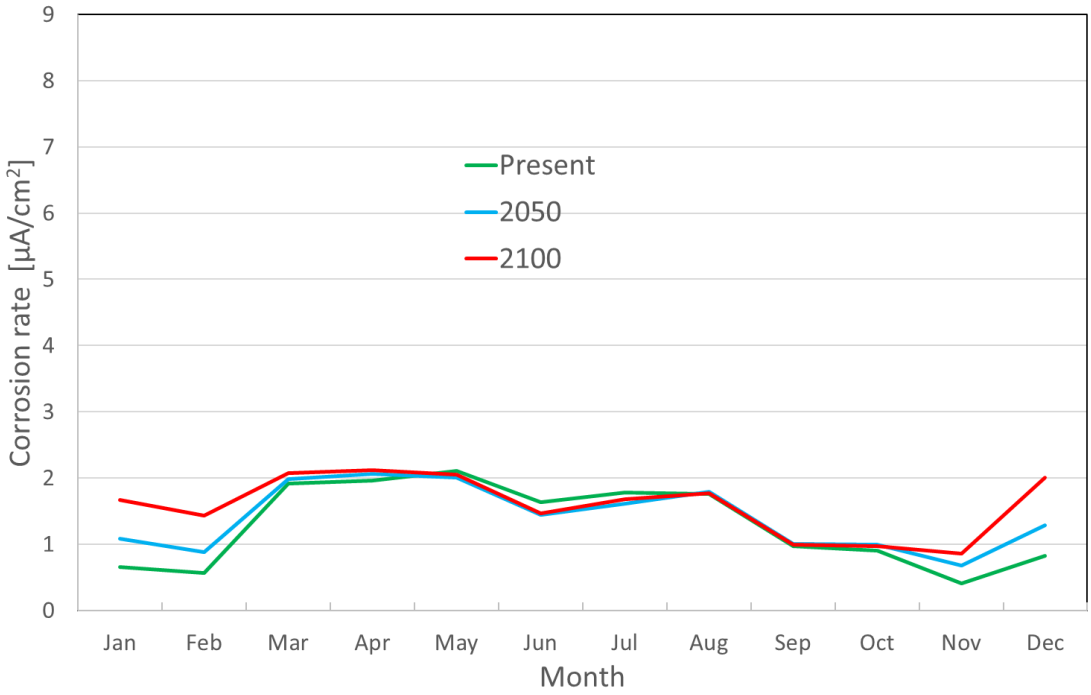

Figure 7. Monthly average of the modelled corrosion rate in carbonated concrete at coastal area on north-facing façade.

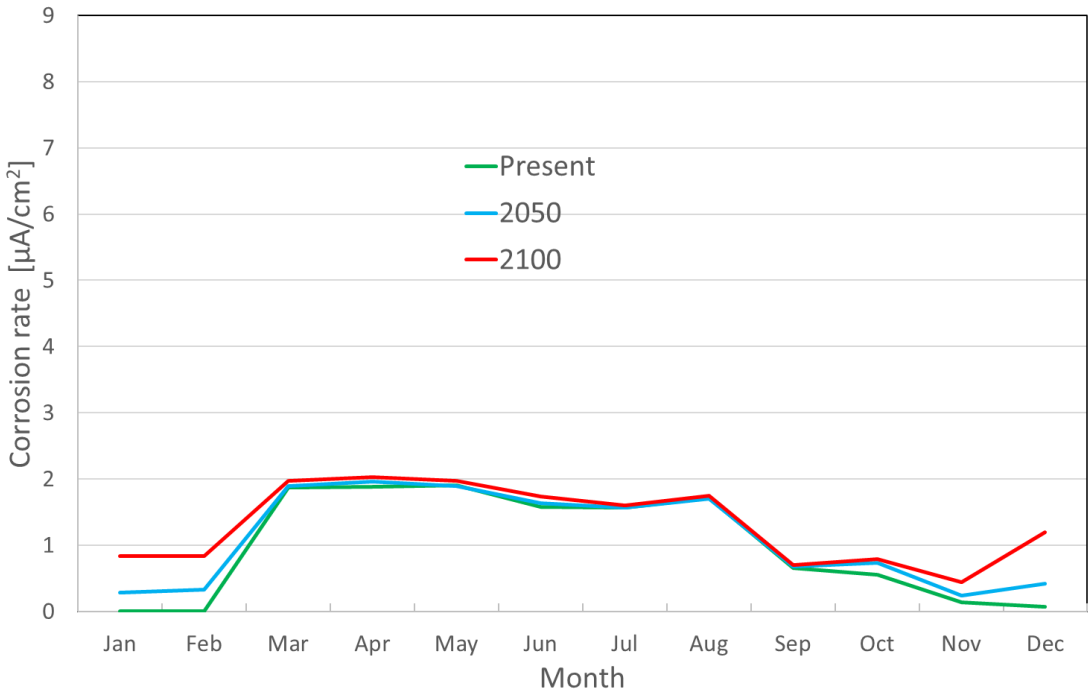

Figure 8. Monthly average of the modelled corrosion rate in carbonated concrete at Lapland on north-facing façade.

As can be seen, at spring and summer the corrosion rate in facades is quite constant regardless of geographical location, facade direction or climate projection. The main reason for this is that adequate solar radiation and outdoor temperature with fairly low relative humidity make it possible for concrete to dry after rain events. In fact, the greatest difference is a result of variations in the amount of WDR during the autumn and winter when it is difficult for facades to dry.

Winter and late autumn are the most critical times of year for corrosion rate, not just because of the amount of WDR but also because the amount of solar radiation is and will be low. Thus, conditions for structures to dry are weak, i.e. low solar radiation and high relative humidity. Based on the future climate scenarios, the relative amount of WDR is increasing the most in winter and late autumn because a greater share of precipitation will be in the form of rain and sleet instead of snow. The same observation

can be seen throughout the studied locations, but firstly in southern coastal area because the increasing average temperature reaches the 0 °C limit during winter sooner than in northern parts.

In the present climate in southern Finland and inland areas, the monthly changes in corrosion rate are minor. The reason for the low corrosion rate in winter compared to coastal area is the low temperature and the fact that the form of precipitation is mostly snow. In Lapland, no corrosion can occur in January and February because the temperature stays below 0°C the whole time. In the future climate, the average temperature in winter will rise and the form of precipitation will increasingly be rain and sleet.

On south-facing facades, the conditions for active corrosion will be quite similar to present conditions in coastal area in southern Finland in 2050 and inland in 2100. In Lapland, conditions will reach present conditions in inland in 2050 and present conditions in southern Finland in 2100.

On north-facing facades, the corrosion rate will remain almost at the present level at every location and be significantly lower than south-facing facades. The main reason for both is the significantly lower amount of the WDR from northerly directions, both at present and in future climates.

At every studied location, the corrosion rate is the highest for southwest-to-southeast-facing structures because the wind direction during the rain event is highly concentrated from these directions. At inland and Lapland the corrosion rate is slightly higher for east- than west-facing facades, at coastal area and southern Finland the opposite, again due to slightly varying wind direction during the rain event. The importance of these directions will be even greater in future climate because the increase is remarkable faster especially for south-faced facades.

Comparatively low average corrosion values, less than 1.00 µA/cm², occur in northern facades and in winter and autumn at inland and Lapland. Significantly high corrosion rates, more than 3.00 µA/cm², occur at coastal area and southern Finland in winter and autumn especially in future climate.

Tables 4 and 5 present the average corrosion rates in carbonated concrete similar to Table 3 in balcony side panel and slab soffit, respectively.

Table 4. An average of the modelled corrosion rate [µA/cm²] of balcony panel reinforcement in four geographical locations (C = coastal, S = southern Finland, I = inland, L = Lapland) at present climate and in projected future climates.

		North			East			South			West		
		Present	2050	2100	Present	2050	2100	Present	2050	2100	Present	2050	2100
Winter	C	1.63	1.95	2.67	2.16	3.19	4.15	4.24	7.12	9.35	2.63	3.68	4.74
	S	1.39	1.81	2.45	1.63	2.24	3.04	3.51	4.88	6.43	2.59	3.33	4.46
	I	1.18	1.66	2.36	1.39	2.22	3.26	2.09	3.38	5.07	1.52	2.15	2.98
	L	0.77	1.13	1.78	0.76	1.30	2.20	0.99	1.98	3.43	0.88	1.42	2.14
Spring	C	2.61	2.61	2.71	2.75	2.93	3.01	3.22	3.33	3.44	2.66	2.52	2.61
	S	2.56	2.57	2.64	2.64	2.79	2.83	3.02	3.07	3.12	2.57	2.46	2.55
	I	2.54	2.66	2.86	2.36	2.60	2.68	2.71	2.79	2.85	2.48	2.39	2.51
	L	2.29	2.48	2.64	2.26	2.54	2.77	2.39	2.55	2.73	2.10	2.08	2.18
Summer	C	2.28	2.24	2.24	2.47	2.51	2.34	3.39	3.45	3.48	2.48	2.43	2.65
	S	2.18	2.13	2.15	2.34	2.33	2.15	3.13	3.16	3.15	2.49	2.46	2.76
	I	2.27	2.23	2.28	2.32	2.35	2.26	2.75	2.78	2.81	2.29	2.22	2.36
	L	1.99	1.98	2.03	2.05	2.08	2.09	2.40	2.39	2.47	1.92	1.83	1.91
Autumn	C	1.31	1.73	2.21	2.73	3.49	3.54	6.92	8.39	10.09	3.11	3.66	4.80
	S	1.17	1.52	1.85	1.91	2.34	2.39	4.46	5.38	6.23	2.59	3.26	4.44
	I	1.04	1.50	2.13	1.59	2.18	2.71	2.70	3.65	4.82	1.43	1.93	2.66
	L	0.62	0.94	1.49	0.86	1.31	1.96	1.48	2.21	3.32	0.77	1.16	1.68

Table 5. An average of the modelled corrosion rate [µA/cm²] of balcony slab soffit reinforcement in four geographical locations (C = coastal, S = southern Finland, I = inland, L = Lapland) at present climate and in projected future climates.

		North			East			South			West		
		Present	2050	2100	Present	2050	2100	Present	2050	2100	Present	2050	2100
Winter	C	0.03	0.06	0.09	0.06	0.11	0.15	0.16	0.27	0.36	0.07	0.13	0.17
	S	0.04	0.06	0.09	0.05	0.08	0.11	0.13	0.19	0.25	0.09	0.12	0.17
	I	0.03	0.06	0.09	0.05	0.09	0.13	0.08	0.14	0.21	0.05	0.08	0.12
	L	0.01	0.03	0.06	0.01	0.04	0.08	0.03	0.07	0.14	0.02	0.05	0.08
Spring	C	0.05	0.06	0.06	0.07	0.07	0.07	0.09	0.09	0.09	0.06	0.06	0.05
	S	0.05	0.05	0.05	0.06	0.06	0.06	0.08	0.08	0.08	0.05	0.05	0.05
	I	0.05	0.06	0.07	0.06	0.06	0.06	0.07	0.07	0.07	0.05	0.05	0.05
	L	0.05	0.05	0.05	0.06	0.06	0.07	0.06	0.06	0.07	0.04	0.04	0.04
Summer	C	0.02	0.02	0.02	0.02	0.02	0.02	0.02	0.02	0.02	0.02	0.02	0.02
	S	0.02	0.02	0.02	0.02	0.02	0.02	0.02	0.02	0.02	0.02	0.02	0.02
	I	0.02	0.02	0.02	0.02	0.02	0.02	0.02	0.02	0.02	0.02	0.02	0.02
	L	0.02	0.02	0.02	0.02	0.02	0.02	0.02	0.02	0.02	0.02	0.02	0.02
Autumn	C	0.04	0.05	0.07	0.06	0.08	0.10	0.15	0.19	0.24	0.08	0.10	0.13
	S	0.04	0.05	0.07	0.05	0.07	0.08	0.11	0.13	0.16	0.07	0.09	0.13
	I	0.04	0.06	0.08	0.04	0.07	0.09	0.07	0.10	0.14	0.05	0.07	0.09
	L	0.01	0.03	0.06	0.02	0.04	0.06	0.03	0.06	0.10	0.02	0.04	0.06

The corrosion rates in side panels are in all cases higher than in facades. This is because they are as exposed to WDR as facades, while there is no drying effect of warm air from the other side of the structure. Even at Lapland in 2100 climate significantly high corrosion rates can occur in south-faced panels. In southern Finland the corrosion rates are already high in south-faced panels in every season and will be high in 2100

also in east- and west-faced panels. At coastal area in present climate the corrosion rates are relatively low in winter and autumn but will increase remarkably in 2100 climate. At coastal area in 2100 the corrosion rate in side panels will be significantly high throughout the year and in every direction faced panels.

The corrosion rates in balcony slab soffit are fractions of the values in facades and side panels in every studied case because the soffit is sheltered from WDR. In addition, this indicates the quite low effect of the relative humidity of outdoor air on reinforcement corrosion in carbonated concrete. Thus, the active corrosion phase of the reinforcements in balcony slabs can be much longer than for side panels and facades. There will be increase in corrosion rates until 2100, however, only the highest corrosion rates in coastal area are reaching the lowest rates in all studied façade cases.

Figs 9-14 present monthly corrosion rates in the carbonated concrete of south-facing facade panels, balcony side panels and balcony slabs in coastal area over 30-year climate periods. It should be noted that for explicit presentation of the graphs, the corrosion rate axis varies from comparatively high values in side panels to very low values in slabs.

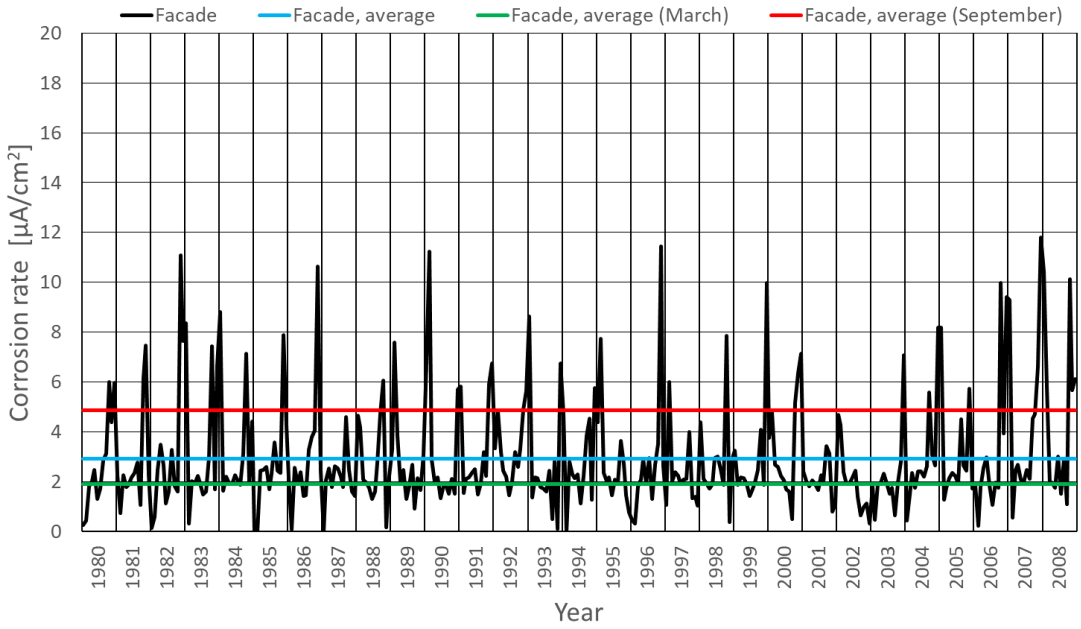

Figure 9. Monthly corrosion rates in the carbonated concrete of south-facing façade panel in coastal area at present climate.

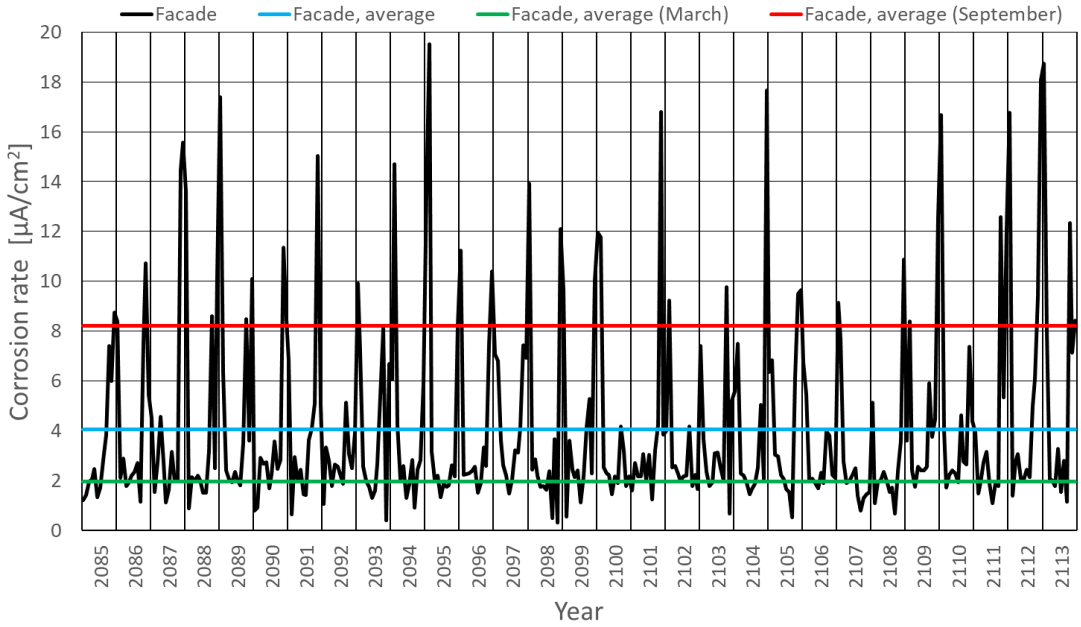

Figure 10. Monthly corrosion rates in the carbonated concrete of south-facing façade panel in coastal area in 2100 climate.

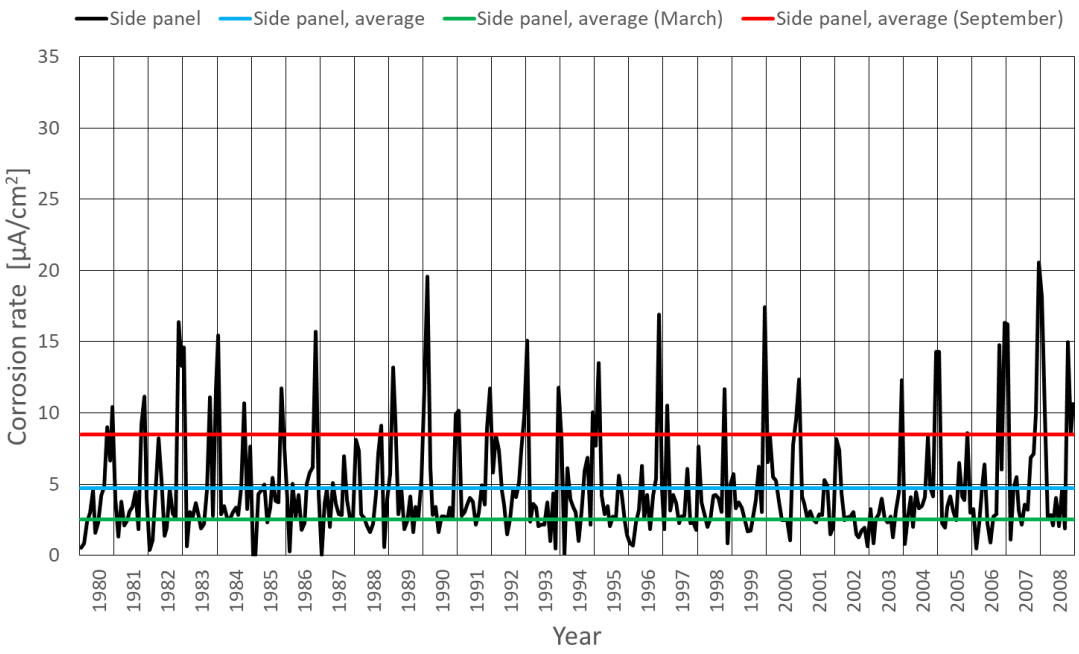

Figure 11. Monthly corrosion rates in the carbonated concrete of balcony side panel in coastal area at present climate.

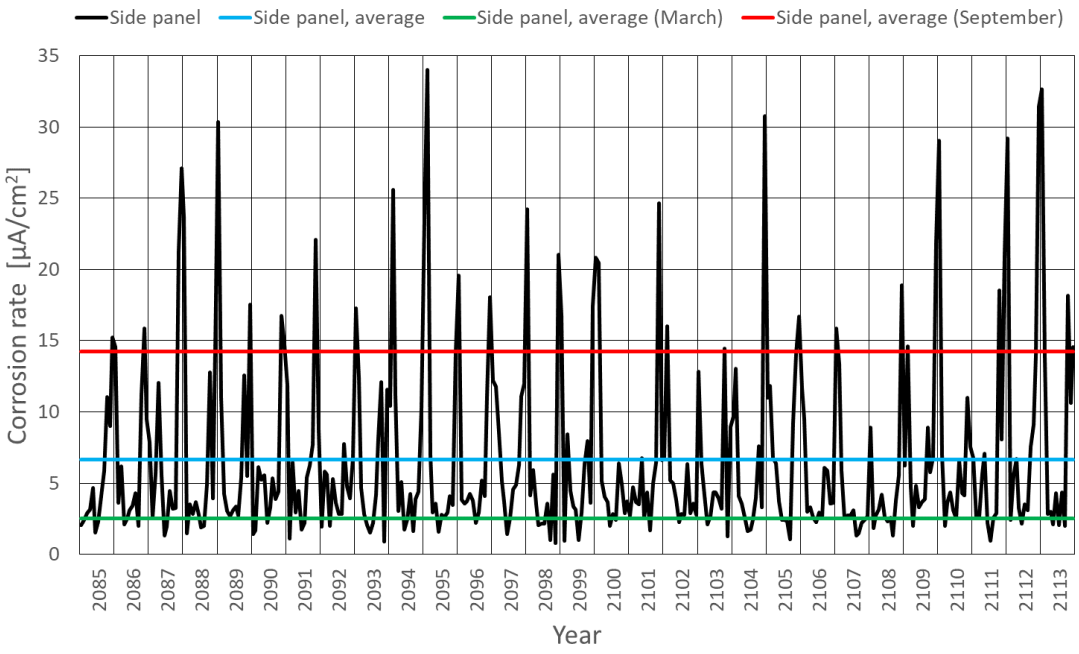

Figure 12. Monthly corrosion rates in the carbonated concrete of south-facing balcony side panel in coastal area in 2100 climate.

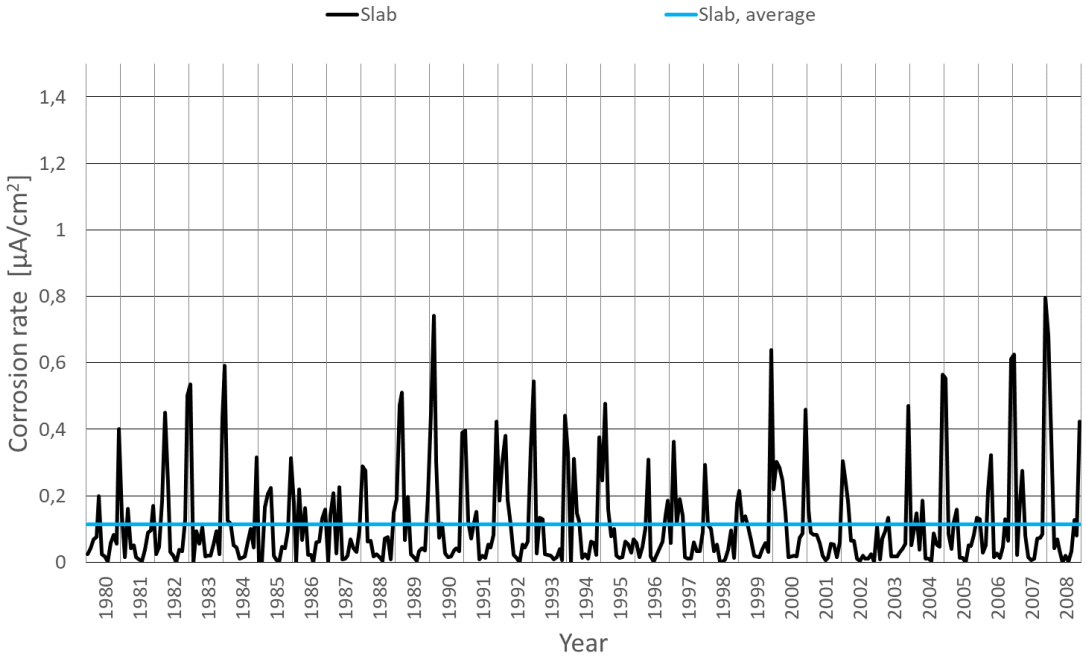

Figure 13. Monthly corrosion rates in the carbonated concrete of south-facing balcony slab soffit in coastal area at present climate.

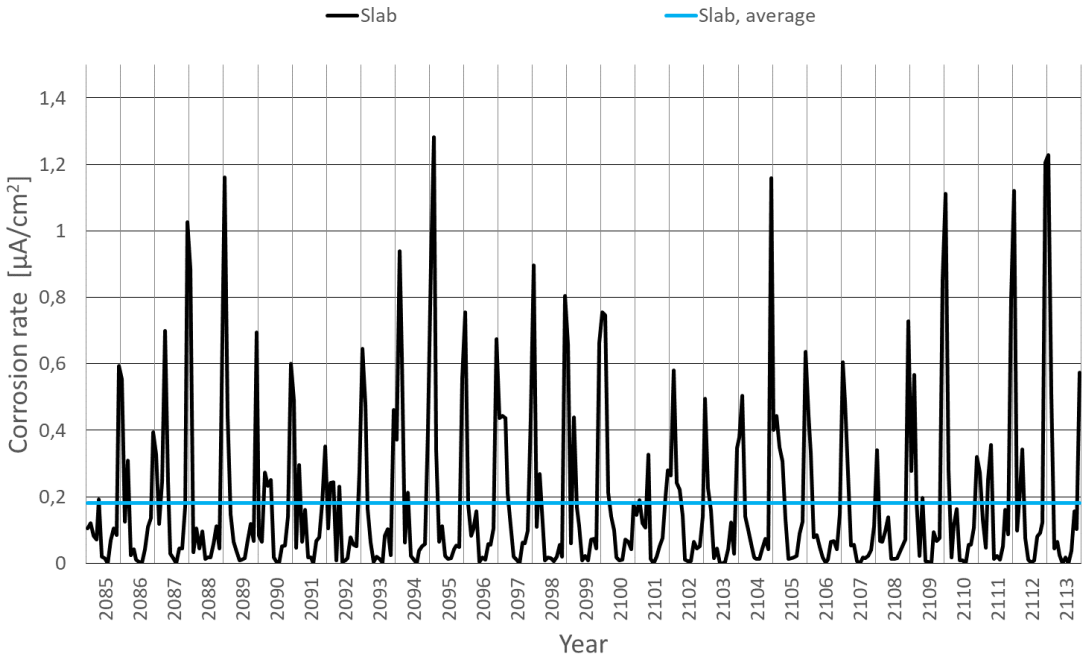

Figure 14. Monthly corrosion rates in the carbonated concrete of south-facing balcony

slab soffit in coastal area in 2100 climate.

The figures show that, on south-facing facades, the peaks will be significantly higher in the future climate for every studied structure. Contrary to the peaks, it can be noted that north-facing facades have more very low values of corrosion rate, although their number is decreasing.

The peaks may be high at present climate but most of the cases the time period of a peak not remarkable long. However, at the same time while the corrosion rate peaks will be significantly higher in future climate for façades and side panels, the time period of high corrosion rates is extending due to increase in the moderate corrosion rates of present climate in late winter and early autumn. The longer high corrosion rate periods may have a remarkable effect on the propagation phase of the reinforcement corrosion.

Conclusions

It has been shown that wind-driven rain (WDR) plays a major role in every significant deterioration mechanism of Finnish outdoor concrete structures. In that regard, it is alarming for outdoor exposed structures that the climate change projections forecast a significant increase in the amount of WDR and worse drying conditions. It is therefore important to model the possible effects of climate change on the deterioration mechanisms to estimate the remaining service life and to schedule possible service and renovation actions for existing structures. This study has predicted corrosion rates at four different locations based on climate change projections for 2050 and 2100. The model is based on actual corrosion measurement data combined with actual weather data. The regression-based model considers four main climate factors for corrosion: WDR, temperature, solar radiation and relative humidity. The corrosion rate is studied at three different outdoor exposed structures: facade, balcony side panel and balcony

slab.

At every studied location, the corrosion rate is much higher for southwest-to-southeast-facing structures because the wind direction during the rain event is highly concentrated from these directions varying only slightly depending on the geographical location. North-facing structures will still be protected from WDR, while south-facing facades will be exposed to even higher WDR loads, especially in winter and late autumn.

In coastal area at present climate, the highest corrosion rate is in winter and late autumn. In the future climate, the amount of precipitation will be more in the form of rain and sleet than snow, thus the corrosion rate will increase the most from December to February, i.e. in winter. The same phenomenon, though less intense, can be seen in every studied combination.

The level of corrosion rate from March to July is at present and in future climates quite the same at every location regardless of the direction in which the structure faces. This is because, in spring and summer, drying conditions after rain events are and will be quite good, even though the amount of WDR is increasing. On the other hand, compared to south-facing structures, north-facing ones are not exposed to a similar amount of WDR, while at the same time drying conditions are not that good either.

When comparing the different kind of structures, it can be seen that the greatest average corrosion rate and corrosion rate peaks are in the balcony side panels. This is because they are as exposed to WDR but their capacity to dry is not as good as facade panels. Instead, the balcony slab soffit is sheltered from WDR, so the corrosion rate is very low. Thus, the active corrosion phase of the reinforcements in balcony slabs can be much longer than for side panels and facades.

The study has factors of uncertainty such as climate change projections and validation of the used model, but it gives a perspective on where to focus with existing outdoor concrete structures and the corrosion of their reinforcements. The highlights are:

- faster active corrosion phase and thus corrosion-induced damage can be expected in the future as the temperature and amount of WDR increases
- the sheltering of structures can decrease corrosion rate significantly
- corrosion rate is highly dependent the direction of the greatest climate load, which can be taken into account while planning service actions
- the significantly lower corrosion rate of sheltered structures can be considered in service life calculations, which usually focus on the propagation phase of corrosion.

References

Almås, A.J., Lisø, K.R., Hygen, H.O., Øyen, C.F. and Thue, J.V. (2011), "An approach to impact assessments of buildings in a changing climate", *Building Research & Information*, 39(3), pp. 227–238.

Auld, H., Klaassen, J. and Comer, N. (2006), "Weathering of Building Infrastructure and the Changing Climate: Adaptation Options", in *2006 IEEE EIC Climate Change Technology Conference, EICCCC, 10-12 May 2006*, IEEE, pp. 1-11.

Bastidas-Arteaga, E., Chateauneuf, A., Sánchez-Silva, M., Bressolette, P. and Schoefs, F. (2010), "Influence of weather and global warming in chloride ingress into concrete: A stochastic approach", *Structural Safety* 32 (4), pp. 238–249.

Bastidas-Arteaga, E. and Stewart, M.G. (2015), "Damage risks and economic assessment of climate adaptation strategies for design of new concrete structures subject to chloride-induced corrosion", *Structural Safety* 52, Part A, pp. 40–53.

Botti, A. and Ramos, M. (2017), "Adapting the design of a new care home development for a changing climate", *International Journal of Building Pathology and Adaptation*, Vol. 35 Issue: 4, pp. 417-433.

Concha, N. and Oreta, A.W. (2018), “A model for time-to-cracking of concrete due to chloride induced corrosion using artificial neural network”, in *14th International Conference on Concrete Engineering and Technology, Kuala Lumpur, Malaysia, 8-9 August.*

DuraCrete (2000). *Probabilistic performance based durability design of concrete structures*, The European union – Brite EuRam III, DuraCrete, Final technical report of DuraCrete project, document BE95-1347/R17, CUR, Gouda, Nederland.

fib (2006), *fib Bulletin No.34: Model Code for Service Life Design*, International Federation for Structural Concrete, Lausanne.

Goltermann, P (1994), “Mechanical predictions on concrete deterioration. Part 1: Eigenstresses in concrete”, *ACI Materials Journal*, 91(6), pp. 543–550.

Gulikers, J. and Raupach, M. (2006), “Numerical models for the propagation period of reinforcement corrosion: comparison of a case study calculated by different researchers”, *Materials and Corrosion*, 57(8), pp. 618–627.

Gupta R. and Gregg, M. (2012), “Using UK climate change projections to adapt existing English homes for a warming climate”, *Building and Environment*, 55 (2012). Pp 20–42.

Heidrich, O., Kamara, J., Maltese, S., Re Cecconi, F. and Dejaco, M. C. (2017), "A critical review of the developments in building adaptability", *International Journal of Building Pathology and Adaptation*, Vol. 35 Issue: 4, pp. 284-303.

Hunkeler, F. and Lammar, L. (2012), *Anforderungen an den Karbonatisierungswiederstand von Betonen [Requirements for the carbonation resistance of concrete]*. TFB AG: Wildegg, Switzerland

Huuhka, S. (2016), *Building ‘Post-Growth’ – Quantifying and Characterizing Resources in the Building Stock*, Tampere University of Technology, TUT Publ. 1028, Tampere.

IPCC (2007), *Climate Change 2007: The physical science basis. Contribution of Working Group I to the Fourth Assessment Report of the Intergovernmental Panel on Climate Change*, Cambridge University Press, Cambridge, U.K.

Jylhä, K., Ruosteenoja, K., Mäkelä, H., Hyvönen, R., Pirinen, P. and Lehtonen, I. (2013), *Rakennusfysiikan testivuosien sääaineistot havaitussa ja arvioidussa tulevaisuuden ilmastossa - REFI-B-hankkeen tuloksia [Weather data for building physics test reference years in the observed and projected future*

climate - results from the REFI-B project], Finnish Meteorological Institute Reports 2013:1, Helsinki.

Köliö, A. (2016), *Propagation of Carbonation Induced Reinforcement Corrosion in Existing Concrete Facades Exposed to the Finnish Climate*, Tampere University of Technology, TUT Publ. 1399.

Köliö, A., Honkanen, M., Lahdensivu, J., Vippola, M. and Pentti, M. (2015), "Corrosion products of carbonation induced corrosion in existing reinforced concrete facades", *Cement and Concrete Research*, 78, Part B, pp. 200–207.

Köliö, A., Niemelä, P. J. and Lahdensivu, J. (2016a), "Evaluation of a carbonation model for existing concrete facades and balconies by consecutive field measurements", *Cement and Concrete Composites*, 65(2016), pp. 29–40.

Köliö, A., Pakkala, T. A., Annila, P. J., Lahdensivu, J. and Pentti, M. (2014a), "Possibilities to validate design models for corrosion in carbonated concrete using condition assessment data", *Engineering Structures*, Volume 75, 15 September 2014, pp. 539-549.

Köliö, A., Pakkala, T. A., Hohti, H., Laukkarinen, A., Lahdensivu, J., Mattila, J. and Pentti, M. (2016b), "The corrosion rate in reinforced concrete facades exposed to outdoor environment", *Materials and Structures*, 50(1), pp. 1–16.

Köliö, A., Pakkala, T. A., Lahdensivu, J. and Kiviste, M. (2014b), "Durability demands related to carbonation induced corrosion for Finnish concrete buildings in changing climate", *Engineering Structures*, 62-63(2014), pp. 42-52.

Kvande T. and Lisø K.R. (2009), "Climate adapted design of masonry structures", *Building and Environment* Vol. 44 No. 12, pp. 2442–2450.

Lahdensivu, J. (2012), *Durability Properties and Actual Deterioration of Finnish Concrete Facades and Balconies*, Tampere University of Technology, TUT Publ. 1028, Tampere.

Lahdensivu, J., Varjonen, S. and Köliö, A. (2010), *Betonijulkisivujen ja -parvekkeiden korjausstrategiat [Repair Strategies of Concrete Facades and Balconies]*, Tampere University of Technology, Department of Civil Engineering. Research report 148, Tampere.

Li D.H.W., Liu Y. and Lam J.C. (2012), "Impact of climate change on energy use in the built environment in different climate zones – A review", *Energy* 42 (2012), pp 103–112.

Nik, V.M., Kalagasidis, A.S. and Kjellström, E. (2012), "Assessment of hygrothermal performance and mould growth risk in ventilated attics in respect to possible climate changes in Sweden", *Building and Environment* 55 (2012), pp. 96–109.

OSF (2019), Official Statistics of Finland, available at: http://stat.fi/tup/statfin/index_en.html (accessed 6 February 2019).

Otieno, M., Beushausen, H. and Alexander, M. (2011), "Modelling corrosion propagation in reinforced concrete structures – a critical review", *Cement & Concrete Composites* 33:240–5.

Pakkala, T. A., Köliö, A., Lahdensivu, J. and Kiviste, M. (2014), "Durability demands related to frost attack for Finnish concrete buildings in changing climate", *Building and Environment*, Volume 82, December 2014, pp. 27-41.

Pakkala, T.A., Lemberg, A.-M., Lahdensivu, J. and Pentti, M. (2016), "Climate change effect on wind-driven rain on facades", *Nordic Concrete Research* 1/16, Publication NO. 54, pp. 31–49.

Peng, L. and Stewart M.G. (2013), "Deterioration of concrete structures in Australia under a changing climate", *in Materials to Structures: Advancement Through Innovation - Proceedings of the 22nd Australasian Conference on the Mechanics of Structures and Materials, ACMSM 2012*, pp. 1015–1020.

Peng, L. and Stewart M.G. (2014), "Climate change and corrosion damage risks for reinforced concrete infrastructure in China", *Structure and Infrastructure Engineering* 12(4), pp. 499–516.

Pentti, M., Mattila, J. and Wahlman, J. (1998), *Betonijulkisivujen ja parvekkeiden korjaus Osa 1: Rakenteet, vauriot ja kunnon tutkiminen [Repair of concrete facades and balconies, part I: structures, degradation and condition investigation]*, Tampere, Tampere University of Technology, Structural Engineering, Publication 87.

Pentti, M. (1994), Vaipparakenteiden korjaus [Repair of building envelope], In Kaivonen, J.-A. (Ed.), *Rakennusten korjaustekniikka ja talous [Repair techniques and economy of buildings]*, Saarijärvi: Rakennustieto Oy, pp. 287-358.

Revert, A. B., De Weerdt, K., Hornbostel, K. and Geiker, M.R. (2018), "Carbonation-induced corrosion: Investigation of the corrosion onset", *Construction and Building Materials*, 162 (2018), pp. 847–856.

Siemes, A.J.M., Vrouwenvelder, A.C.W.M. and van den Beukel, A. (1985), "Durability of buildings: a reliability analysis", *Heron*, 30(3), pp. 3–48.

Stewart, M. G., Wang, X. and Nguyen, M.N. (2011), "Climate change impact and risks of concrete infrastructure deterioration", *Engineering Structures*, Vol. 33 No. 4, pp. 1326–1337.

Stewart, M.G., Wang, X. and Nguyen, M.N. (2012)."Climate change adaptation for corrosion control of concrete infrastructure", *Structural Safety* 35, pp. 29–39.

Talukdar, S., Banthia, N., Grace, J.R. and Cohen, S. (2012), "Carbonation in concrete infrastructure in the context of global climate change: Part 2 – Canadian urban simulations", *Cement & Concrete Composites*, Vol. 34, No. 8 (2012), pp. 931–935.

Tuutti, K. (1982), *Corrosion of steel in concrete*, Swedish Cement and Concrete Research Institute, Stockholm, CBI Res 1982;4(82):304.

Williams K., Joynt J.L.R., Payne C., Hopkins D. and Smith I. (2012), "The conditions for, and challenges of, adapting England's suburbs for climate change", *Building and Environment* 55 (2012), pp. 131–140.

Wood, B. and Muncaster, M. (2012) "Adapting from glorious past to uncertain future", *Structural Survey*, Vol. 30 Issue: 3, pp. 219-231.

Yoon, I.-S., Çopuroğlu, O. and Park, K.-B. (2007). "Effect of global climatic change on carbonation progress of concrete", *Atmospheric Environment* 41 (34), pp. 7274–7285.

V

FREEZE-THAW DAMAGE DEPENDENCE ON WIND-DRIVEN RAIN OF OUTDOOR EXPOSED CONCRETE – A CASE STUDY

by

Pakkala T.A., Lahdensivu J., Huuhka, P., Kivioja, H. & Lemberg A.-M. Nov 2019

Nordic Concrete Research, Accepted manuscript 27th Nov 2019

sciendo

Nordic Concrete Federation

ISSN online 2545-2819
ISSN print 0800-6377

DOI: 10.2478/ncr-2019-xxxx

Received: xxxx
Revision received: yyyy
Accepted: zzzz

Freeze-thaw Damage Dependence on Wind-driven Rain of Outdoor Exposed Concrete – A Case Study

Toni A. Pakkala
M.Sc.
PhD student
Tampere University, Civil Engineering
P.O. Box 600, 33014 Tampere, Finland
toni.pakkala@tuni.fi

Jukka Lahdensivu
D.Sc.
Adjunct Professor
Tampere University, Civil Engineering
P.O. Box 600, 33014 Tampere, Finland
jukka.lahdensivu@tuni.fi

Petteri Huuhka
M.Sc.
Tampere University, Civil Engineering
P.O. Box 600, 33014 Tampere, Finland
petteri.huuhka@ramboll.fi

	Henna Kivioja M.Sc. Project Researcher Tampere University, Civil Engineering P.O. Box 600, 33014 Tampere, Finland henna.kivioja@tuni.fi
	Antti-Matti Lemberg B.Sc. Research Assistant Tampere University, Civil Engineering P.O. Box 600, 33014 Tampere, Finland antti-matti.lemberg@tuni.fi

ABSTRACT

It has been shown in previous studies that the existing precast concrete element building stock in Finland has quality issues, especially with freeze-thaw durability and reinforcement corrosion. In addition, it has been presented that deterioration rate is the fastest in coastal area and decreases towards north which has been supposed to be a reason of lower amount of wind-driven rain (WDR). The aim of this study was to examine the connection between the amount of WDR on structures and the freeze-thaw damage more comprehensively. Condition investigation reports of 472 precast concrete element buildings were reanalysed to study the relation and the results were compared to climate data of the same time period to study the correlation between condition investigation observations and the amount of WDR. In addition, the observations made in a condition investigations and their relation to climate load at the same building were studied as a case study. The results show that there is a significant connection between the WDR related climate load and the freeze-thaw damage occurrence. The results can be used to plan protective methods and be a base for service life estimations.

Key words: Concrete, climatic stress, freeze-thaw attack, service life, durability properties.

1. INTRODUCTION

1.1 General

Previous studies [1-3] have shown that the deterioration rate of outdoor exposed concrete structures in Finland is highly dependent on geographical location and the direction in which the structure faces. Pakkala et al. [2] presented that the severity of the freeze-thaw attack is heavier in coastal areas, leading to faster freeze-thaw damage. In a recent study, Pakkala et al. [3] presented that the corrosion rate in carbonated concrete is significantly higher in coastal areas than in other locations and for south-west-, south- and south-east-facing structures.

The deterioration itself and the rate of it are always linked to a combination of harsh environmental stress, inadequate structural properties and the poor durability properties and/or ageing of the used material. If one of them is excluded, there will be no deterioration. The Finnish climate is quite harsh for porous building materials such as concrete and masonry because of quite high wind-driven rain (WDR) amounts with almost perennial potential for freeze-thaw cycles while, especially during autumn, the possibilities for structures to dry are poor [2,3]. In addition, the existing concrete building stock has been shown to have large variation in quality because of lack of knowledge and regulation during its construction [1]. It has also been shown that, even since regulation based on current knowledge, the quality of concrete construction has not been up to standard [2].

Since the 1990s, the state of Finnish concrete facades and balconies has been followed extensively through systematic condition investigations. In addition, he connection between the deterioration of existing concrete structures and environmental stress has been studied quite comprehensively, especially the effect of climatic conditions on the corrosion of reinforcement [1, 3, 4].

Both globally and in Finland, studies connecting freeze-thaw deterioration and actual climatic stress have been rare and mostly focused on the annual number of freeze-thaw cycles. Lisø et al. [5] presented a combination of frost decay exposure index (FDEI) and freezing point crossings (FPC) to characterise the risk of freeze-thaw damage to a porous, mineral material in a given climate. In their studies, the freeze-thaw cycles were considered as temperature crossings over freezing point (0 °C) and the number of cycles was defined as annual average number of days with freezing point crossings.

The FDEI links average annual freezing point crossings (FPC) to the amount of liquid precipitation recorded from the day an FPC has occurred and the preceding two, three or four days. When the FDEI and FPC are shown in the same diagram, the risk of frost decay can be estimated by analysing their relation. For example, if the amount of FPCs is high but the amount of precipitation before the crossings is low, i.e. FDEI is low, the risk of frost decay is relatively low, but if they both are high, the risk is considerable. Later Pakkala et al. [2] made similar studies in Finnish climate with different freezing point temperatures (-5 °C and -10 °C).

1.2 Scope of the study

The mechanism of freeze-thaw damage of concrete and the role of the amount pore water is well known [1]. However, there has been lack of studies connecting the actual amount of WDR on structures and the freeze-thaw damage. The objective of this research was to study more deeply the known connection between the amount of WDR and freeze-thaw damage by assessing if it is possible to estimate the freeze-thaw stress level by the amount of WDR. The research includes

assessment of the results of condition investigation reports and a case study where the amount of WDR on the facades of an existing building is modelled.

2. BACKGROUND

2.1 Condition investigation of concrete structures

The condition of Finnish concrete facades and balconies is systemically investigated according to national guideline [6]. Lahdensivu et al. [7] have presented the methods based on this guideline. The aim of the investigation is to produce information about the state of the structures for owners to plan the timing of possible repairs.

As summarised, a condition investigation includes the study of preliminary information (design plans, site visit), the determination of potential degradation mechanisms, the planning of necessary sampling, the assembly of gathered information and its analysis and reporting. The gathering of information during the investigation includes both non-destructive (NDT) and destructive methods. The NDT methods usually include visual inspection and cover depth measurements of the reinforcement and hammering of the structures. The hammering is based on sound difference between the degraded and solid concrete. When hammered, the degraded concrete has a softer sound than solid concrete and can be detected easily, especially by comparing the sound to solid concrete, which is usually always available nearby. In addition to the overall view, the NDT methods are used to target the sampling. For example, if visual inspection or hammering indicate freeze-thaw damage, there is no need to take the sample directly from the deteriorated structure. Instead, the sampling should be conducted close to the damaged structure to investigate the extent of the damage. [6,7]

The destructive methods usually include an extensive amount of drilled concrete core samples and drill cuttings. The samples are inspected visually to determine the aggregate size and distribution, carbonation depth, compaction of the concrete, visible cracking or any other deterioration and the location and size of reinforcement. After the visual inspection, some of the samples are studied more thoroughly by thin-section analysis. The rest of the samples are used to determine the protective pore ratio and tensile strength, which both give inaccurate yet utilizable information about the quality of concrete and possible freeze-thaw damage. The drill cuttings are used to study the amount of chlorides in the cement paste. [6,7]

2.2 Freeze-thaw damage in Finnish concrete structures

According to Kuosa & Vesikari [8], there are more than 15 different theories or explanations for freeze-thaw attack on porous materials. However, in all of them the amounts of moisture and water play a key role. Probably the most widely known theory for freeze-thaw damage is the hydraulic pressure theory by Powers [9]. It suggests that freezing water expands creating pressure in the pore structure, forcing the unfrozen water out of the pore, and thus causing localised internal tensions in the material. Litvan [10] presented that the water in the pore structures of a porous material does not freeze immediately as the temperature drops below 0°C. Freezing happens first in larger capillary pores. In smaller gel pores, the water begins to freeze when the temperature is around -15 to -20°C. According to Pigeon & Pleau [11], -5°C can be considered the limiting temperature for a concrete pore structure to be exposed to freeze-thaw damage.

Freeze-thaw damage in outdoor exposed structures can be avoided using methods based on structural or material properties. Structural methods are based on sheltering or covering the material from moisture and direct water contact. In most cases, this is neither possible nor economical. The most effective methods by material properties are air-entrainment and increasing the strength of the concrete. Increasing the strength of the concrete prevents the freeze-thaw damage in two ways: the higher strength can tolerate the forces caused by the pressure of expanding water during freezing, and it usually results in a lower water-cement ratio, which leads to lower porosity, i.e. denser concrete.

Air-entrainment is based on protective pores where the pressure caused by freezing water can discharge. The protective pores achieved by the air-entrainment are round air voids with specific diameter and distribution. While the diameter of normal air voids occurring in cement paste differ from 10 µm to over 1 mm, an optimal diameter of protective pores are referred to be 50…300 µm and they should locate less than 400 µm of each other [11]. In Finland, it has been recommended in outdoor structures since 1976, and became mandatory in 1980 by virtue of the Finnish Concrete Code. The success of air-entrainment can be presented by a protective pore ratio p_r, see Equation 1, or more precisely by the spacing factor.

The protective pore ratio indicates the volumetric ratio of protective pores compared to all the pores without taking a stand on the distribution of the protective pores. In the protective pore ratio test, the concrete sample is first slowly immersed in water to fill the capillary pores. Then the sample is oven-dried. In the last step, a vacuum is used to fill also the protective pores, which do not fill up capillary. The protective pore ratio can be calculated by the ratio of the weight measurements as follows:

$$p_r = \frac{(m_v - m_c)}{(m_v - m_d)} \tag{1}$$

where m_v is the mass of a water saturated concrete sample after vacuum exposure, m_c is the mass of the sample after capillary suction and m_d is the dry mass of the sample after oven-drying.

Lahdensivu [1] presented that the porosity protection of Finnish concrete facades can be considered quite inadequate, both in facades and in the balcony structures of concrete-element buildings built between 1960 and 1997. For example, almost 50% of facades with exposed aggregate, clinker-clad, painted and plain concrete surfaces had a protective pore ratio of less than 0.10. In balconies, the numbers are even higher while 70% of side panels, 60% of slabs and 50% of parapets had a ratio under 0.10. In their study, Pakkala et al. [2] presented that, even in buildings built after 1990, i.e. the modern requirement for protective pore ratio, only approx. 50% of precast panels and less than 60% of balcony structures met the freeze-thaw resistance requirements.

The spacing factor indicates the average of half the distance between protective pores and can only be detected by microscope based on a standard ASTM C856-18A [12]. In the highest exposure class, the protective pore ratio of 0.15 was recommended in the Concrete Code in 1976 and regulated in 1980. The requirement of 0.20 was presented in the Concrete Code of 1989. Based on a number of thin-section analyses Koskiahde [13] presented that the protective pore ratio of 0.20 corresponds to a spacing factor of 0.25 mm if the protective pores are rather evenly distributed. In 2004, the spacing factor of 0.25 mm was made as a requirement because the spacing factor takes into account also the distribution of the pores. Nowadays the spacing factor requirement is related to exposure class where the lowest requirement is ≤ 0.27 mm in exposure class XF1 with a designed service life of 50 years. Lahdensivu [1] presented that a protective pore

ratio of < 0.10 can be considered to make concrete resistant to freeze-thaw in the Finnish outdoor climate.

Lahdensivu [1] presented that, in structures with inadequate air-entrainment, it has taken on average 307 freeze-thaw cycles (limiting temperature -5°C) for up to three days after a rain event in a coastal area and 388 cycles inland for incipient freeze-thaw damage to occur in thin-section analysis. The incipient freeze-thaw damage was classified based in classification by Koskiahde [13] as a cracking with width less than 0.01 mm and length less than 10 mm. The numbers were calculated by singling out each case where incipient freeze-thaw damage was detected in condition investigations and calculating the amount of freeze-thaw cycles after a rain event from climate data of the nearest weather station available in the study. The lowest numbers of freeze-thaw cycles where incipient freeze-thaw damage was detected were 210 and 270, respectively. Shang et al. [14] showed by laboratory freeze-thaw testing of concrete with similar entrained air content than used in Finland that even air-entrained concrete with a strength class of C50 eventually suffers from strength loss. In their studies, it was found that while C20 lost 50% of its compressive strength after 300 fast freeze-thaw cycles, C40 and C50 lost 10%. The non-air-entrained concrete degraded before 50 fast freeze-thaw cycles. However, the accelerated freeze-thaw testing in laboratory is more severe than exposure in outdoor conditions and thus is not directly comparable to actual deterioration rate.

3. RESEARCH METHODS AND MATERIAL

3.1 Condition investigation database

The research material is based on a BeKo (Repair strategies of concrete facades and balconies) research conducted by TUT between 2006-2009 [15]. The research collected a comprehensive database based on condition investigation reports of 947 concrete element buildings. The database consists of the degradation-related material properties of the structures including porosity, tensile strength, the carbonation depth of the concrete, the cover depths of reinforcement and the observed degradation in visual inspection and thin-section analysis done in a laboratory. However, the data based on freeze-thaw damage detected with hammering were not collected in the database to the same accuracy as other properties. The main reason was that the information based on freeze-thaw damage observations was not systemically or extensively presented in the reports. That has led to imprecise data about the far-advanced freeze-thaw damage lacking for example the facing directions of the observations.

In this study, 244 condition investigation reports from the BeKo database were reanalysed including the investigation of 472 concrete element buildings. Every mention of freeze-thaw damage in facades or balcony structures and the direction in which the structure was facing was recorded. Far-advanced freeze-thaw damage was mentioned in façade structures in 93 reports and in 68 of those cases, the facing direction could be identified. In balconies, the same figures were 101 and 74, respectively. In 13 cases in facades, far-advanced freeze-thaw damage was reported on two, and in two cases on three different facades, i.e. the total number of far-advanced freeze-thaw observations was 85. In balcony structures, far-advanced freeze-thaw damage was recorded in structures facing in two different directions in eight of the cases, resulting in a total of 82 observations.

The buildings were located geographically in four different areas based on climatic conditions and population concentration: a coastal area, southern Finland, inland and Lapland (northern

Finland). The background for dividing the buildings this way can be found in [16]. Far-advanced freeze-thaw damage was reported so that the direction of facing could be identified in facades in 42 cases in coastal area, 26 cases in southern Finland and 25 cases in inland. The same numbers with the balcony structures were 43, 42 and 15, respectively. Only one of the studied buildings where far-advanced freeze-thaw damage was reported was located at Lapland, so Lapland is not presented separately in the results.

The existence or success of air-entrainment was evaluated in 425 of the 472 studied buildings based on both the protective pore ratio and the spacing factor. In 11% of all measurements, the air-entrainment was stated as sufficient, in 81% insufficient and in 8% both. When considering only the cases where far-advanced freeze-thaw damage was observed, the share was 3%, 93% and 5%, respectively.

3.2 Weather data

A standard SFS-EN ISO 15927-3 [17] was used to estimate the WDR on different parts of the facades and balconies. The standard presents a wall annual index I_{WA} that takes into account the amount of rain, the effect of wind during the rain event, the roughness of the terrain near the studied building, topography, obstacles such as other buildings and the height level of the studied spot on the wall. The index is calculated as follows:

$$I_{WA} = I_A C_R C_T O W \tag{2}$$

where I_A is the airfield annual index, C_R is the terrain roughness coefficient, C_T is the topography coefficient, O the obstruction factor and W the wall factor. The airfield annual index I_A is defined as:

$$I_A = \frac{2}{9}\frac{\sum v r^{\frac{8}{9}} \cos(D-\theta)}{N} \tag{3}$$

where v is the hourly mean wind speed [m/s], r is the hourly rainfall total [mm], D the hourly mean wind direction from north [°], θ is the wall orientation relative to north [°], and N the number of years for which data are available, and the summation is taken over all hours for which $\cos(D-\theta)$ is positive. The roughness coefficient depends on the height above the ground and the roughness of the terrain in the direction from which the wind is coming. The coefficient C_R at height z is calculated as follows:

$$C_R(z) = K_R \ln\left(\frac{z}{z_0}\right), \text{ for } z \geq z_{min} \tag{4}$$

$$C_R(z) = C_R(z_{min}), \text{ for } z < z_{min} \tag{5}$$

where K_R is a terrain factor, z_o is roughness length and z_{min} minimum height. The parameters depend on the terrain category, which in this study is category III: suburban or industrial areas and permanent forests.

The climate data for the four regions are collected from coastal area (Helsinki-Vantaa Airport), southern Finland (Jokioinen), inland (Jyväskylä) and Lapland (Sodankylä).

3.3 Case building

A case study was made to examine if a basic climate load study could be used when planning the condition investigation and especially the sampling. The case study building was chosen from the investigation reports as a representative for a typical suburban concrete apartment building with insufficient freeze-thaw durability properties and extensive collected data. The case study

building is located in the city of Tampere, southern Finland. The 14-storey apartment building was built in 1977 and is made of precast concrete elements with exposed aggregate concrete surfaces. The building is located in an enclosed block surrounded by a low office building and multi-storey apartment buildings (see Figure 1). The balconies are located on southeast-, south-west- and north-east-facing facades.

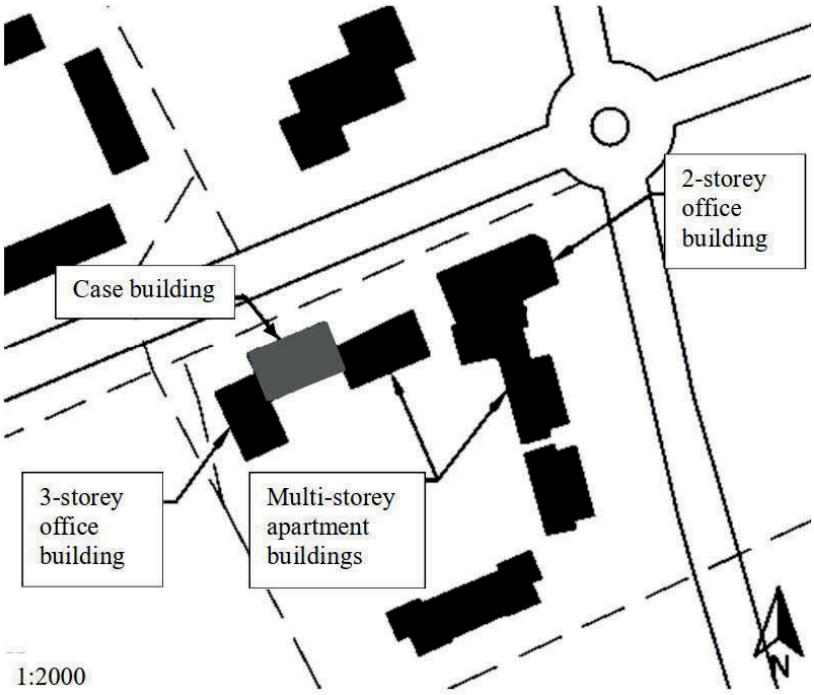

Figure 1 – Geography of case building in the block.

The condition investigation was made 1997 (when the building was 20 years old) and presented in 1998. The condition investigation included NDT methods (visual inspection and hammering), 10 concrete core samples from facades and 17 samples from balconies. Results from both the laboratory measurements and NDT methods are used in this study.

The weather data used in the case study are from Jokioinen, located approx. 70 km from the case building. The weather data includes data collected every 3 hours (converted to hourly data) from 1970 to 2009 including temperature, amount of rain, wind speed and solar radiation from 1980 to 2009. The data were used to estimate the total amount of WDR to facades and balconies from 1980 to 1997 (year of condition investigation). There was no access to weather data from 1977 to 1980, which is why data from the first years of the building are not included in calculations.

The parameters used are listed in Table 1.

Table 1 – Location- and orientation-dependent values used in this study.

Parameter	Value
C_T	1

W	Top 2.5 m: 0.5 Rest of the wall: 0.2			
K_R	0.22			
z_0	0.3			
z_{min}	8			
	Wall orientation			
	"North-west"	"North-east"	"South-east"	"South-west"
θ	340°	70°	160°	250°
O	0.7	0.2	0.7	1.0

In this case, N was chosen at 1 to sum up all the WDR, which has precipitated on the studied structures from the earliest available weather data to the time of the condition investigation. The wall annual index I_{WA} was then calculated at variable height z in all the facades. The summed amount of I_{WA} was then compared to the observations made in the condition investigation.

4. RESULTS AND DISCUSSION

4.1 Far-advanced freeze-thaw damage in database

Based on the condition investigation reports, 81% of far-advanced freeze-thaw damage was located in west-, south-west-, south- and south-east-facing facades. Based on the geographical location, the shares are 88%, 83% and 70% in the coastal area, southern Finland and inland, respectively. In balconies, the share is 84%. However, with balconies it must be taken into account that most of them are located on western and southern facades to maximise the daylight and evening sun. The distribution of observed far-advanced freeze-thaw damage in facades and balconies is presented in Figures 2 and 3, respectively.

Figure 4 shows Airfield annual index I_A to represent WDR from different directions, and Figure 5 shows I_A from different directions for up to three days before freeze-thaw cycles with a limiting temperature of -5 °C. The share of WDR from the west, south-west, south and south-east is 65% of all WDR. The share of WDR before freeze-thaw events is 78% and, when separated into coastal area, southern Finland and inland, it is 81%, 79% and 71%, respectively.

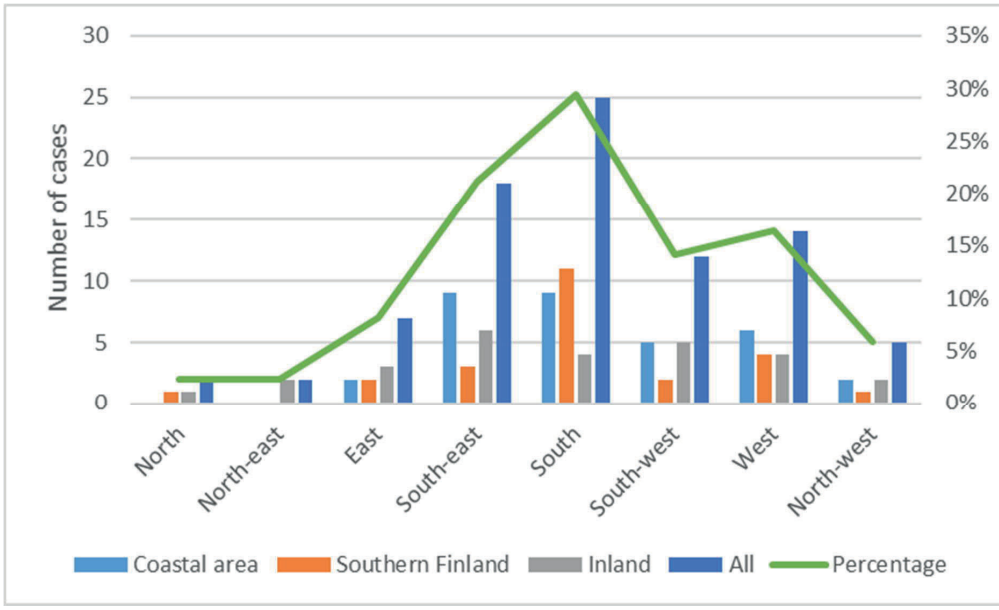

Figure 2 – Far-advanced freeze-thaw damage observed in facades based on the condition investigation data.

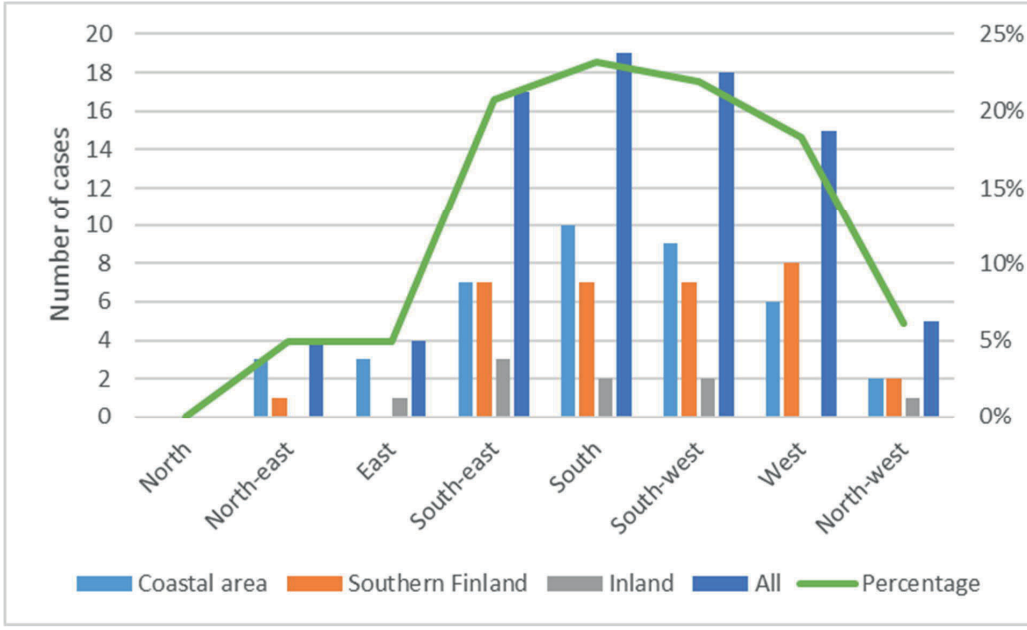

Figure 3 – Far-advanced freeze-thaw damage observed in balconies based on the condition investigation data.

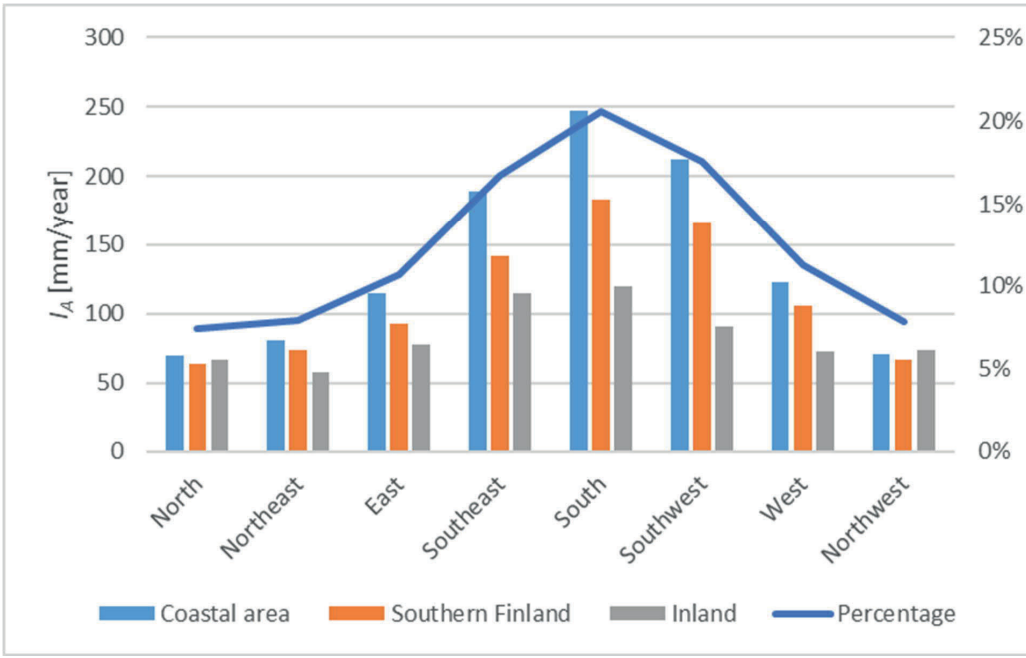

Figure 4 – Airfield annual index from different directions at the three locations studied.

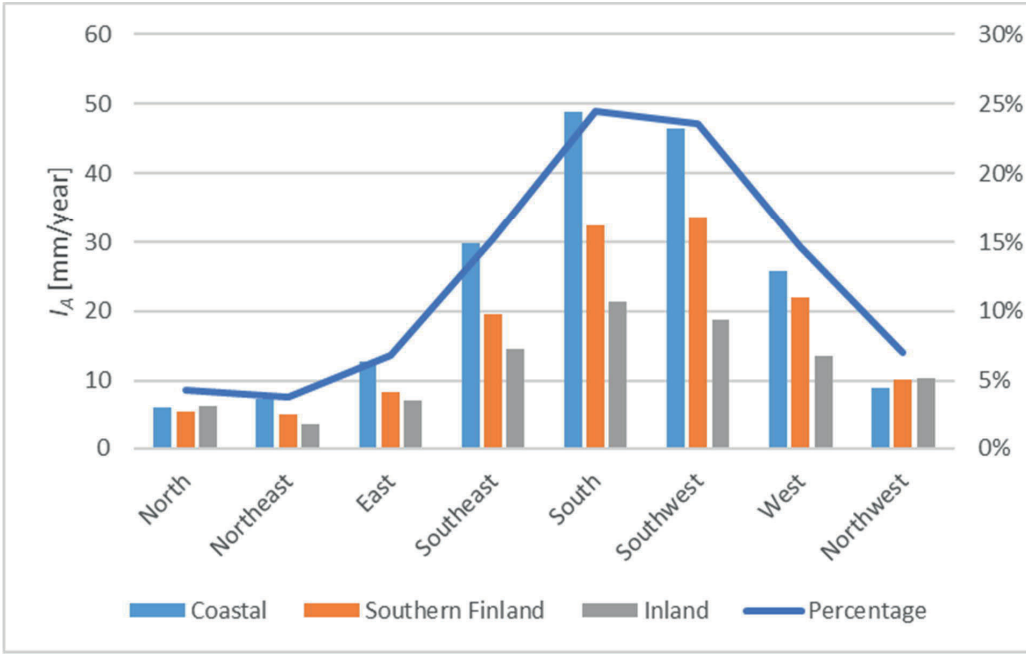

Figure 5 – Airfield annual index for up to three days before freeze-thaw cycles with a limit temperature of -5 °C from different directions at the three locations studied.

As the results show, the amount of WDR and especially the amount of WDR before freeze-thaw events has a significant relation to freeze-thaw damage observations.

4.2 Case building

Based on condition investigation, the concrete used in the case building was of poor quality. The average protective pore ratio was 0.09 in facades and 0.06 in balcony side panels, which indicates that either there was no air-entrainment or it was unsuccessful. According to laboratory tests, 20% of the concrete core samples had visible cracking parallel to the surface, indicating freeze-thaw damage. It should be noted, however, that 7% of the samples were taken from the elements where far-advanced freeze-thaw damage had already been detected using NDT methods. The tensile strength of the façade samples varied between 0.84 and 2.15 MPa and in samples taken from balcony structures between 0.61 and 2.77 MPa. Values under 1.00 MPa are considered to possibly indicate freeze-thaw damage. One sample from façade- and three from balcony structures were below the value.

Approx. 25% of the façade area and 10% of balcony structures were investigated with hammering. Far-advanced freeze-thaw damage was detected only in approx. 3% of the studied facade area but in almost half of the balcony structures studied, mainly side panels.

Figure 6 shows the amount of I_{WA} on different parts of the facades, the hammering areas and the locations of the samples taken. Signs of freeze-thaw damage were detected:

- visually in facade sample no. 24 and balcony side panel sample no. 2
- in thin-section analysis in facade sample no. 26
- in tensile strength tests in facade samples nos. 8 and 27 and in balcony side panel samples nos. 2, 10 and 23.

No signs of freeze-thaw damage were found in balcony slabs or parapets. Compared to facade and side panel samples, parapets and slabs had a slightly higher protective pore ratio, an average 0.11 and 0.13, respectively.

All the freeze-thaw damage indicated by visual observations, hammering or studies of the concrete core samples were located in areas where the total amount of I_{WA} was over 21 mm. The level of such WDR was achieved on north-west and north-east facades only on their top 2.5 meters. On south-east and south-west facades, the same level was reached already at the fourth floor, i.e. above 12 meters from the ground.

Almost all the freeze-thaw damage observations were made on the south-east- and south-west-facing facades or balconies. During the same 20-year time period, the total number of rain events followed by freeze-thaw cycles (-5°C) were 161 from north-west-, 101 from north-east-, 192 from south-east- and 207 from south-west-oriented rain events. When only the airfield annual index I_A (see Equation 3), i.e. the WDR in an open area, is calculated, the total amount of I_A during the same time period was 123 mm, 132 mm, 479 mm and 489 mm, respectively. Thus, the amount of WDR before a freeze-thaw cycle was significantly lower during the rain events from north-west and north-east directions while the number of cycles was lower.

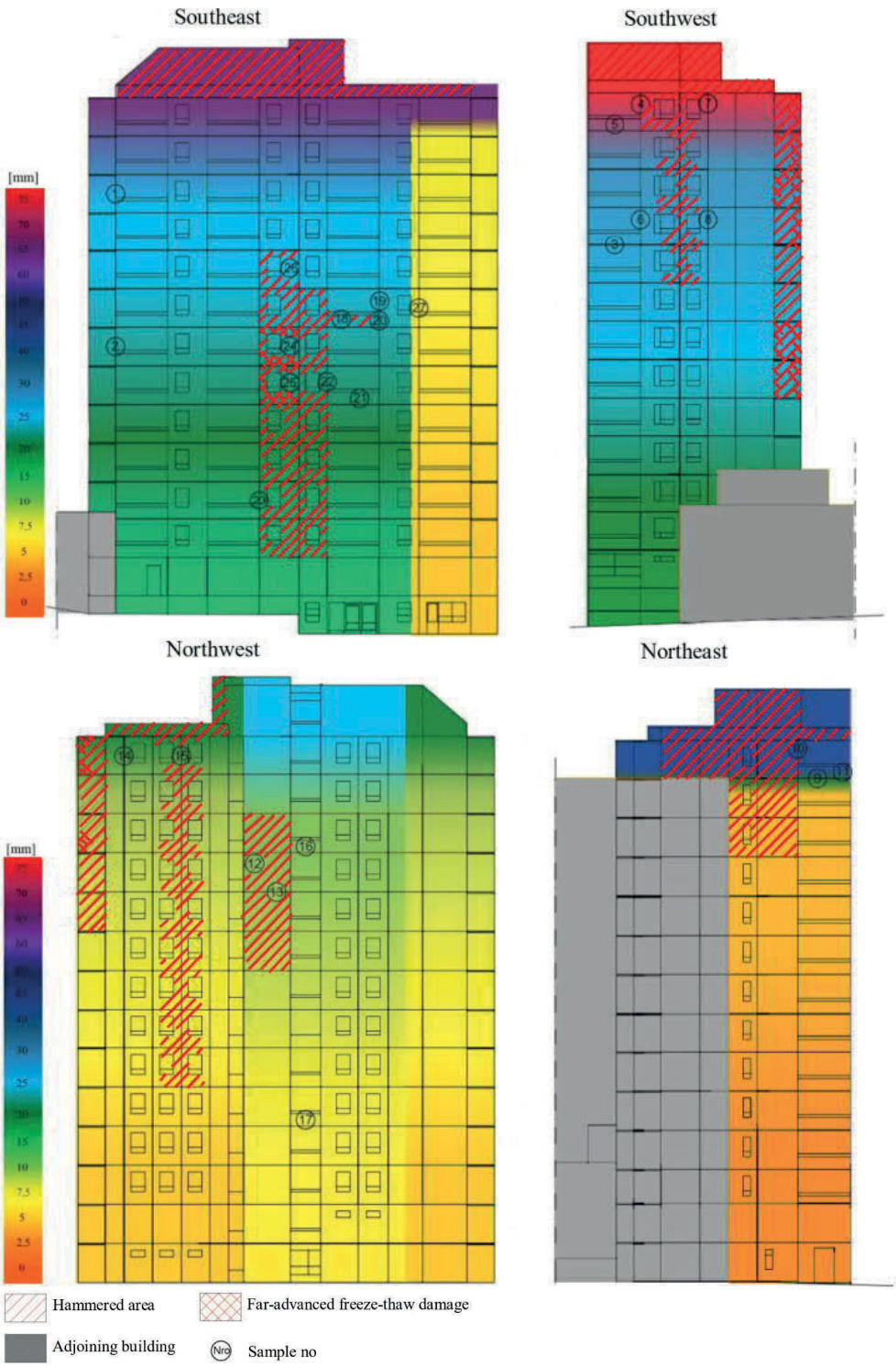

Figure 6 – Amount of I_{WA} on different parts of the facades, hammering areas and locations of the taken samples. The numbers and colour gradation on left present the amount of WDR.

The results indicate that both the amount of WDR itself and WDR before the freeze-thaw cycle have a major effect on the rate of detectable freeze-thaw damage. However, there were also facade and balcony structures with no detected freeze-thaw damage in the areas where the calculated amount of WDR was significantly high. There are many reasons explaining, such as:

- The quality difference with the used concrete and all the error sources related to the simplified calculation method.
- The location of the weather station beings quite far from the case building, though the used standard allows the distance to be less than 100 km.
- The used method underestimates the amount of wind-driven rain near the top and corner parts of the facade, but overestimates the amount on the top 2.5 metres with high buildings and low rain intensity [18].
- The method does not take into account the topography of the structures (e.g. offset of the facade) nor the effect of adjoining buildings.
- The quality of the used concrete may vary significantly within the same building.

5. CONCLUSIONS

In this study, a connection between the direction in which a concrete façade or balcony structures face, the amount of WDR on those structures and far-advanced freeze-thaw damage occurrence was studied by examining condition investigation reports more extensively than in previous studies. As an addition, a case building was studied in order to roughly observe the connection between WDR on different areas of the building and the observations made in the condition investigation of the building in question.

The first part of the study is based on condition investigation reports of 472 concrete-element buildings from which far-advanced freeze-thaw damage observations by hammering and visual inspection were gathered. A significant part of the observations in facades, 81%, were made from the facades facing west, south-west, south or south-east. In the coastal area, the percentage is even higher, 88%, and in inland lower, 71%. In balconies, the percentage is again higher, although it must be noted that most of the balconies traditionally face western to southern directions to maximise the amount of sunlight.

In addition, the amount of WDR calculated as a standard-based Airfield annual index (I_A) was studied. It shows that the connection between the orientation of freeze-thaw damage observations and the amount of WDR is clear. When the amount of WDR closely (up to three days) before a freeze-thaw cycle was studied, the connection is even more distinct.

With the case study building, the amount of WDR taking into account, for example, the close terrain and other buildings was calculated utilising the standard based Wall annual index (I_{WA}). The amount of I_{WA} on the different parts of the building erected in 1977 was calculated cumulatively starting from the year the data were available (1980) until the year of the condition investigation (1997). The results showed that almost all the freeze-thaw damage observations were made in the direction of the greatest climate load. The vertical level also has a great effect because the amount of WDR is higher at the top parts of the building.

The results of the study emphasise the significance of the orientation of outdoor exposed concrete structures when considering the freeze-thaw durability. The observation is even more significant

for existing concrete structures with poor freeze-thaw properties. In addition, the case study presents that even a basic study of climatic load on a specific building could be used to make the condition investigation sampling more specific. Together, the results show that climatic stress studies, especially with the condition investigation data, can be used to plan protective methods and be a base for service life estimations.

REFERENCES

1. Lahdensivu J: "Durability Properties and Actual Deterioration of Finnish Concrete Facades and Balconies". TUT Publ. 1028. (PhD Thesis), Tampere University of Technology. Tampere, Finland, 2012, 117 p.
2. Pakkala T A, Köliö A, Lahdensivu J & Kiviste M: "Durability demands related to frost attack for Finnish concrete buildings in changing climate", *Building and Environment*, Volume 82, December 2014, pp. 27-41.
3. Pakkala T A, Köliö A, Lahdensivu J & Pentti M: "Predicted corrosion rate on outdoor exposed concrete structures", *International Journal of Building Pathology and Adaptation*, accepted 6 February 2019.
4. Köliö A, Pakkala T A, Hohti H, Laukkarinen A, Lahdensivu J, Mattila J & Pentti M: "The corrosion rate in reinforced concrete facades exposed to outdoor environment", *Materials and Structures*, 50(1), 2016, pp. 1–16.
5. Lisø K R, Kvande T, Hygen H O, Thue J V, Harstveit K: "A frost decay exposure index for porous, mineral building materials", *Building and Environment*, 42(10), 2007, Pp. 3547–3555.
6. Finnish Concrete Association: "by 42 Condition investigation of concrete façade panels 2013". ("by 42 Betonijulkisivun kuntotutkimus 2013"). Helsinki, Finland. (In Finnish).
7. Lahdensivu J, Varjonen S, Pakkala T & Köliö A: "Systematic condition assessment of concrete facades and balconies exposed to outdoor climate", *International Journal of Sustainable Building Technology and Urban Development*, 4:3(2013), pp. 199-209.
8. Kuosa H & Vesikari E: "Ensuring of concrete frost resistance Part 1: Basic data and service life design". ("Betonin pakkasenkestävyyden varmistaminen. Osa 1. Perusteet ja käyttöikämitoitus"). VTT Technical Research Centre of Finland, Research notes 2056, 2000, 141 p. (In Finnish).
9. Powers T C: "The air requirement of frost-resistant concrete". Chicago: Portland Cement Association, Research and Development laboratories, Development Department, Bulletin 33, 1949.
10. Litvan G: "Phase transitions of adsorbates IV – Mechanism of frost action in hardened cement paste". *Journal of the American Ceramic Society* 55 (1), 1972, pp. 38–42.
11. Pigeon M & Pleau R: "Durability of concrete in cold climates". London. E & FN Spon, 1995, 244 p.
12. ASTM International: "ASTM C856-18a (2018) – Standard Practice for Petrographic Examination of Hardened Concrete". West Conshohocken, PA. 15 p.
13. Koskiahde A: "An experimental petrographic classification scheme for the condition assessment of concrete in facade panels and balconies". Materials Characterization, Vol. 53, 2014, pp. 327–334.
14. Shang H-S, Cao W-Q & Wang B: "Effect of Fast Freeze-thaw Cycles on Mechanical Properties of Ordinary-Air-Entrained Concrete". *The Scientific World Journal*, 2014, 7 p.

15. Lahdensivu J, Varjonen S & Köliö A: “Repair Strategies of Concrete Facades and Balconies”. (“Betonijulkisivujen ja -parvekkeiden korjausstrategiat”). Tampere University of Technology, Department of Civil Engineering. Research report 148, 2010. (In Finnish).
16. Pakkala T A, Lemberg A-M, Lahdensivu J & Pentti M: “Climate change effect on wind-driven rain on facades”. *Nordic Concrete Research*, Publication No. 54, 2016, pp. 31–49.
17. Finnish Standards Association SFS: “SFS-EN ISO 15927-3. 2009. Hygrothermal performance of buildings. Calculation and presentation of climatic data. Part 3: Calculation of a driving rain index for vertical surfaces from hourly wind and rain data”. Helsinki, Finland, 2009.
18. Blocken B. & Carmeliet J: “Overview of three state-of-the-art wind-driven rain assessment models and comparison based on model theory”. *Building and Environment*, Volume 45 (2010), pp. 691–703.

ERRATA OF THE PUBLISHED ARTICLES

Location	Is	Should be
Article II Caption of the Table 5	a maximum of 2 days before freezing	a maximum of 3 days before freezing
Article II Caption of the Table 6	a maximum of 2 days before freezing	a maximum of 3 days before freezing
Article III Page 44 First paragraph	at inland the share is 66%, at southern Finland 54%	in southern Finland the share is 66%, inland 54%
Article IV References	Jylhä, K., Ruosteenoja, K., Mäkelä, H., Hyvönen, R., Pirinen, P. and Lehtonen, I. (2013)	Ruosteenoja, K., Jylhä, K., Mäkelä, H., Hyvönen, R., Pirinen, P. and Lehtonen, I. (2013)
Article IV References	Köliö, A., Pakkala, T.A., Hohti, H., Laukkarinen, A., Lahdensivu, J., Mattila, J. and Pentti, M. (2016)	Köliö, A., Pakkala, T.A., Hohti, H., Laukkarinen, A., Lahdensivu, J., Mattila, J. and Pentti, M. (2017)